

1-1-2017

New Mechanism Based Approaches For Treating Prostate Cancer

Rayna Rosati
Wayne State University,

Follow this and additional works at: https://digitalcommons.wayne.edu/oa_dissertations

 Part of the [Oncology Commons](#)

Recommended Citation

Rosati, Rayna, "New Mechanism Based Approaches For Treating Prostate Cancer" (2017). *Wayne State University Dissertations*. 1865.
https://digitalcommons.wayne.edu/oa_dissertations/1865

This Open Access Dissertation is brought to you for free and open access by DigitalCommons@WayneState. It has been accepted for inclusion in Wayne State University Dissertations by an authorized administrator of DigitalCommons@WayneState.

NEW MECHANISM BASED APPROACHES FOR TREATING PROSTATE CANCER

by

RAYNA C. ROSATI

DISSERTATION

Submitted to the Graduate School

of Wayne State University,

Detroit, Michigan

in partial fulfillment of the requirements

for the degree of

DOCTOR OF PHILOSOPHY

2017

MAJOR: CANCER BIOLOGY

Approved By:

Advisor

Date

DEDICATION

This dissertation is dedicated to my family, who made me who I am today with all of their love and support.

To my grandmother, Lucy, who just recently lost her battle with lung cancer and who would send me newspaper clippings in the mail about new topics of prostate cancer research.

To my siblings, who have always been my best friends.

To my father, Daniel, who has been my greatest mentor in life.

To my mother, Nanci, who has been there for me through everything and who gave me my creative bone.

ACKNOWLEDGEMENTS

First off, I would like to thank my mentor, Dr. Manohar Ratnam, whose enthusiasm for science is undeniable. Thank you for always being so optimistic and believing I could accomplish this very challenging project. Thank you for teaching me how to ask the proper questions and how to be a good scientist. Thank you for your dedication to my project and your dedication in preparing me for my future.

I would like to thank my committee members, Dr. Larry Matherly, Dr. Izabela Podgorski, and Dr. Elisabeth Heath for all of their continued support and advice over the past five years and for being so accommodating for meetings. I would like to thank all of my lab members, both past and present, Dr. Mugdha Patki, Dr. Venkatesh Chari, Yanfang Huang, and especially Thomas McFall, for not only providing me with exceptional laboratory support but also for his friendship. I would like to thank the cancer biology graduate program, Drs. Matherly and Brush as well as Nadia Daniel. Thank you for taking a chance on me and accepting me into the program and for all of your guidance over the past few years.

Thank you to all of our collaborators, Dr. Zihui Qin from Wayne State University, Dr. Peter Shaw from Nottingham University, and Dr. Hiroki Kakuta from Okayama University. Thank you to Dr. Andrew Fribley and Martha Larsen for everything involving my small molecule screening optimization and help with performing the screen. Thank you to Dr. Lisa Polin for all of your contribution to the animal studies involved with my project, it truly would have not been possible without you. Thank you to Dr. Selvakumar Dakshnamurthy for performing the SPR studies over the past year that has contributed to this project. Thank you to Dr. Jing Li for all of the PK/PD support on this project.

Thank you to my funding, the 5T32CA009531 fellowship and the Thomas C. Rumble University Graduate Fellowship.

Lastly, thank you to everyone at Wayne State University School of Medicine that has contributed to my career and time here at the University.

TABLE OF CONTENTS

DEDICATION	ii
ACKNOWLEDGEMENTS	iii
LIST OF TABLES	xi
LIST OF FIGURES	xii
LIST OF ABBREVIATIONS	xiv
CHAPTER 1 – INTRODUCTION	1
1.1 Prostate Cancer –a 2017 overview.....	1
1.2 The normal prostate: structure and function.....	1
1.2.1 Prostate zones	2
1.2.2 Aspects of endocrine action, the androgen receptor and the prostate gland.....	4
1.3 Prostate Disease	9
1.3.1 Prostatitis	9
1.3.2 Benign Prostatic Hyperplasia	9
1.3.3 Prostate Cancer	10
1.4 Prostate Cancer-diagnosis	12
1.4.1 Prostate Cancer Grading	12
1.4.2 Prostate Cancer Staging	12
1.5 Prostate cancer treatment	13
1.5.1 Androgen deprivation therapy and anti-androgen therapy	13
1.5.2 Available Treatments for CRPC	14
1.6 Other Major Limitations of Testosterone Suppression in Prostate Cancer – Effects on Normal Tissues	15
1.6.1 Hot Flashes.....	16

1.6.2 Hyperlipidemia	16
1.6.3 Sexual Dysfunction	17
1.6.4 Anemia.....	17
1.6.5 Skeletal Complications.....	18
1.6.6 Effects on the cardiovascular system.....	19
1.6.7 Cognitive and Psychological Impairment	20
1.7 Mechanisms of restoration of AR signaling in CRPC.....	21
1.7.1 Intratumoral Androgen Synthesis.....	21
1.7.2 Overexpression of AR.....	22
1.7.3 Imbalance of AR co-regulator expression	22
1.7.4 Dysregulation of growth factors and crosstalk with other signaling pathways.....	23
1.7.5 Mutations in AR and Splice Variants of AR.....	23
1.8 Targeting the amino-terminal domain of AR	26
1.8.1 Bromodomain inhibitors	27
1.8.2 EPI family small molecules	28
1.8.3 Sintokamides	30
1.8.4 Bispecific antibodies to inhibit N-terminal AR activity.....	30
1.9 Targeting AR tethering proteins.....	31
1.9.1 HoxB13.....	32
1.9.2 C/EBP α	33
1.9.3 ELK1 and other TCF subfamily members	34
1.9.4 ELK1 as an AR tethering protein essential for PC/CRPC growth ...	35
1.10 The ELK1-AR complex as a critical and selective therapeutic target in prostate cancer.....	38

CHAPTER 2-THESIS OUTLINE	40
CHAPTER 3- THE AMINO-TERMINAL DOMAIN OF THE ANDROGEN RECEPTOR CO-OPTS ERK DOCKING SITES IN ELK1 TO INDUCE SUSTAINED GENE ACTIVATION THAT SUPPORTS PROSTATE CANCER CELL GROWTH	41
3.1 Introduction.....	41
3.2 Experimental Procedures	43
3.2.1 Cell culture and reagents	43
3.2.2 Purified proteins	45
3.2.3 Surface plasmon resonance	45
3.2.4 Plasmids	46
3.2.5 siRNA mediated gene knockdown	48
3.2.6 Co-Immunoprecipitation.....	48
3.2.7 Other experimental methods.....	49
3.2.8 Statistical analysis.....	49
3.3 Results.....	49
3.3.1 Role of the amino-terminal A/B domain of AR in functional interactions with ELK1	49
3.3.2 Mapping the region(s) in ELK1 required for association with AR(A/B)	54
3.3.3 ELK1 motifs required for association with the AR A/B domain participate in hormone-induced activation of ELK1 by full-length AR.....	65
3.3.4 Influence of SRF on the interaction of AR with ELK1	66
3.3.5 Influence of ERK1/2 on the interaction of AR with ELK1	69
3.3.6 Direct binding of AR and ELK1	73
3.3.7 Relevance of the physical association of ELK1 and AR to androgen- dependent cell growth.....	74

3.3.8 Synergy between the splice variant AR-V7 and ELK1 and AR-V7 dependent cell growth.....	77
3.4 Discussion	79
CHAPTER 4 – TUMOR SELECTIVE DISRUPTION OF ANDROGEN RECEPTOR FUNCTION IN PROSTATE CANCER.....	83
4.1 Introduction.....	83
4.2 Materials and Methods	87
4.2.1 Cell Culture and Reagents	87
4.2.2 Generation of recombinant cell lines for high throughput screening and counter screening of small molecule libraries	89
4.2.3 High Throughput Screening	91
4.2.4 Purified Proteins.....	92
4.2.5 Surface Plasmon Resonance	93
4.2.6 Transfections and Reporter Luciferase Assays	94
4.2.7 Lentivirus-mediated-Transduction.....	95
4.2.8 Colony Growth Assay	95
4.2.9 Cell Monolayer Growth Assay.....	96
4.2.10 Western Blot Analysis	96
4.2.11 RNA isolation, Reverse Transcription, and Real Time PCR.	97
4.2.12 Measurement of intracellular and serum levels of compounds	97
4.2.12.1 Chromatographic and mass-spectrometric conditions.....	97
4.2.12.2 Sample Preparation	99
4.2.13 Tumor xenograft model studies	101
4.3 Results.....	101
4.3.1 Discovery of the lead compound.....	101

4.3.2 Binding of KCI807 to AR and disruption of ELK1 binding	108
4.3.3 Narrow genotropic effects of KCI807 in AR-V7 expressing CRPC cells.....	113
4.3.4 Selective <i>in vitro</i> growth inhibition by KCI807 and comparison with enzalutamide	116
4.3.5 Suppression of CRPC growth <i>in vivo</i> by KCI807	120
4.4 Discussion	120
CHAPTER 5 – HYBRID ENZALUTAMIDE DERIVATIVE WITH HISTONE DEACETYLASE INHIBITOR ACTIVITY DECREASE HSP90 AND THE ANDROGEN RECEPTOR LEVELS AND INHIBIT VIABILITY IN ENZALUTAMIDE RESISTANT TC4-2 PROSTATE CANCER CELLS	
5.1 Introduction.....	125
5.2 Materials and Methods	129
5.2.1 Compound Synthesis.....	128
5.2.2 HDAC activity assay	128
5.2.3 Cell Culture and Reagents.....	129
5.2.4 Cell Viability Assay.....	130
5.2.5 Western Blot Analysis	130
5.2.6 RNA isolation, Reverse Transcription, and Real Time PCR	131
5.2.7 Chromatin Immunoprecipitation (ChIP).....	131
5.2.8 Statistical Analysis	132
5.3 Results.....	132
5.3.1 Design and synthesis of compounds 2-75 and 1005 with partial chemical scaffolds of Enz and SAHA.....	132
5.3.2 Compounds 2-75 and 1005 possess intrinsically weak inhibitor activity against nuclear HDACs and cytosolic HDAC6.....	134
5.3.3 The partial Enz chemical scaffold confers AR targeted antagonist	

activity without ligand-induced chromatin association of AR.....	135
5.3.4 Compounds 2-75 and 1005 induce enhanced degradation of AR and HSP90 and hyper-acetylation in a putative 55 KDa HSP90 fragment...	140
5.3.5 The hybrid molecules selectively inhibit cytosolic HDAC6 <i>in situ</i> ..	144
5.3.6 Compounds 2-75 and 1005 up-regulate p21 and inhibit viability of Enz-resistant prostate cancer cells	144
5.4 Discussion	149
CHAPTER 6-CONCLUSIONS.....	156
APPENDIX-INTELLECTUAL PROPERTY	158
REFERENCES.....	159
ABSTRACT	228
AUTOBIOGRAPHICAL STATEMENT.....	231

LIST OF TABLES

Table 4.1 Structure-activity relationships for inhibition of ELK1-dependent promoter activation by AR.	107
---	-----

LIST OF FIGURES

Figure 1.1 Zones of the prostate gland.....	3
Figure 1.2 Androgen Receptor Functional domains	5
Figure 1.3 Androgen receptor signaling in normal and malignant prostate cells	8
Figure 1.4 Schematic of the structural domains of ELK1, ELK4, and ELK3, the three TCF subfamily members	36
Figure 3.1 Adequacy of the A/B domain of AR for functional interactions of AR with ELK1	51
Figure 3.2 Mapping ELK1 polypeptide segments required for co-activation by AR(A/B) by amino-terminal deletion analysis	55
Figure 3.3 Mapping ELK1 polypeptide segments required for co-activation by AR(A/B) by carboxyl-terminal deletion analysis.....	58
Figure 3.4 Mapping ELK1 polypeptide segments required for co-activation by AR(A/B) by internal deletion analysis	61
Figure 3.5 Further refinement of the mapping of ELK1 motifs required for co-activation by AR(A/B)	63
Figure 3.6 ELK1 motifs required for co-activation by full-length AR	67
Figure 3.7 Effect of depleting SRF or ERK1/2 on the interactions of AR with ELK1.....	71
Figure 3.8 Direct binding of ELK1 and AR and the effect of disrupting docking sites in ELK1 on AR binding and androgen-dependent cell growth.....	75
Figure 3.9 Functional association of ELK1 and AR-V7 and effect on cell growth.....	78
Figure 4.1 Schematic of HTS screening system	103
Figure 4.2 Testing recombinant HeLa cells for HTS.....	104
Figure 4.3 Hit1 (5,7,3',4'-Tetrahydroxyflavone) selectively inhibits ELK1-dependent promoter activation by AR and the compound scaffold is obligatory.	106
Figure 4.4 Cellular uptake in HeLa cells for active compounds.....	109
Figure 4.5 KCI807 does not inhibit ERK1/2 activation of ELK1	110
Figure 4.6 KCI807 binds to purified AR and blocks ELK1 binding.....	112
Figure 4.7 Transcriptional targets of KCI807	116
Figure 4.8 Inhibition of AR-dependent PC/CRPC clonogenic survival and cell growth by KCI807 and comparison with enzalutamide.	117
Figure 4.9 Effect of KCI807 on in vitro growth of AR-negative cancer cell lines.....	119

Figure 4.10 Inhibition of in vivo CRPC tumor growth by KCI807.....	121
Figure 5.1 Compound structures and synthetic schemes.....	133
Figure 5.2 Measurement of intrinsic and in situ HDACI activities	136
Figure 5.3 Testing the ability of compounds to interact with AR and to induce chromatin association of AR.	139
Figure 5.4 Modulation of protein levels and hyperacetylation.....	141
Figure 5.5 Induction of AR degradation.....	143
Figure 5.6 Hyperacetylation of α -tubulin and histones H3 and H4.	145
Figure 5.7 Induction of p21 mRNA.	147
Figure 5.8 Effects on cell viability in Enz-resistant CRPC cells	148
Figure 5.9: Effects on cell viability in androgen-sensitive cells.....	150
Figure 5.10 Mechanistic model for the actions of compounds 1005 and 2-75.....	155

LIST OF ABBREVIATIONS

Abbreviation	Definition
1002	(E)-ethyl 3-(4-(3-(4-cyano-3-(trifluoromethyl)phenyl)-5,5-dimethyl-4-oxo-2-thioxoimidazolidin-1-yl)-2-fluorophenyl)acrylate
1005	(E)-3-(4-(3-(4-cyano-3-(trifluoromethyl)phenyl)-5,5-dimethyl-4-oxo-2-thioxoimidazolidin-1-yl)-2-fluorophenyl)-N-hydroxyacrylamide
2-75	<i>4-(3-(4-cyano-3-(trifluoromethyl)phenyl)-5,5-dimethyl-4-oxo-2-thioxoimidazolidin-1-yl)-2-fluoro-N-(7-(hydroxyamino)-7-oxoheptyl)benzamide</i>
3-52	methyl 7-(4-(3-(4-cyano-3-(trifluoromethyl)phenyl)-5,5-dimethyl-4-oxo-2-thioxoimidazolidin-1-yl)-2-fluorobenzamido)heptanoate
AF	activation function
AR	androgen receptor
ARE	androgen response element
AR-FL	androgen receptor full length
AR-V	AR splice variant
ASAP	atypical small acinar proliferation
BET	Bromodomain and Extra-terminal motif
beta-MSP	beta-microseminoprotein
BPH	benign prostatic hyperplasia
bsAb	bispecific antibody
C/EBP α	CCAAT enhancer binding protein
CA-MEK1	constitutively active mutant of MEK1
ChIP	chromatin immunoprecipitation
CRPC	castration resistant prostate cancer
DBD	DNA binding domain
DEF	Docking site for ERK, FXFP
DHEA	dehydroepiandrosterone
DHT	dihydrotestosterone
DLC1	deleted in liver cancer 1
DRE	digital rectal examination
ENZ	enzalutamide
ETS	E twenty six
FBS	fetal bovine serum

FK-228	cyclo[(2Z)-2-amino-2-butenoyl-l-valyl-(3S,4E)-3-hydroxy-7-mercapto-4-heptenoyl-d-valyl-d-cysteiny],cyclic(3-5)disulfide
GAPDH	glyceraldehyde-3-phosphate dehydrogenase
HDAC	histone deacetylase
HDACi	histone deacetylase inhibitor
HSP90	heat shock protein 90
HTS	High Throughput Screening
KLK3	kallikrein-related peptidase 3
LAQ-824	(2E)-N-hydroxy-3-[4-[(2-hydroxyethyl)[2-(1H-indol-3-yl)ethyl]amino]methyl]phenyl]-2-propenamide
LBD	ligand binding domain
LBH-589	(2E)-N-hydroxy-3-[4-([2-(2-methyl-1H-indol-3-yl)ethyl]amino)methyl]phenyl]acrylamide
LHRH	luteinizing hormone-releasing hormone
NR	nuclear receptor
NTD	N-terminal domain
PAP	prostatic acid phosphatase
PC	prostate cancer
PCa	prostate cancer
PCR	polymerase chain reaction
PDX-101	N-hydroxy-3-[3-(phenylamino)sulfonyl]phenyl]-2-propenamide
PIN	prostatic intraepithelial neoplasia
PSA	prostate specific antigen
P-TEFb	positive transcription elongation factor
R1881	17 β -17-hydroxy-17-methyl-estra-4,9,11-trien-3-one
RANKL	receptor activator for nuclear factor kB ligand
SAHA	suberoylanilide hydroxamic acid
SB-939	(E)-3-(2-butyl-1-(2-(diethylamino)ethyl)-1H-benzo[d]imidazol-5-yl)-N-hydroxyacrylamide
SINT1	Sintokamide A
SPR	surface plasmon resonance
SRE	serum response elements
SRF	serum response factor
SSRIs	serotonin reuptake inhibitors
TCF	ternary complex factors
TMPRSS2	transmembrane protease, serine 2
UBE2C	Ubiquitin-conjugating enzyme E2C

CHAPTER 1-INTRODUCTION

1.1 Prostate cancer- a 2017 review

It is estimated by the Prostate Cancer Foundation that there are 3 million American men currently living with prostate cancer (2). For the year 2017 it is estimated that over 160,000 individuals will be newly diagnosed with prostate cancer and there will be about 27,000 deaths associated with the disease (3). The prevalence and risk of prostate cancer, increases with age and the average age of diagnosis is about 66 years old (3). Despite decades of intensive efforts from researchers and clinicians to combat this disease, it is still the most common type of cancer in men and managing it remains a major challenge. Therefore, there is a pressing need for identification of novel therapeutic targets and development of new drugs to treat prostate cancer.

1.2 The normal prostate: structure and function

The human prostate is a glandular organ of the genitourinary system, located below the bladder (4, 5). Each one of 30-50 exocrine glands of the prostate comprises an epithelial bilayer of basal and luminal cells, supported by a fibromuscular stroma (6). The prostate gland is thus made up of gland cells, muscle cells, and fibrous cells. The prostate gland is part of both a man's reproductive system and urinary system. Testosterone is a master hormonal regulator of the prostate and plays a vital role in the embryonic development of the prostate and male accessory organs (7). Testosterone is also responsible for precisely regulating postnatal growth and maintenance of the adult prostate (7). The main function of the prostate is to produce and secrete from the glandular cells, an alkaline fluid which aids in protection, nourishment, and motility of

sperm (8-10). The prostate surrounds the urethra and also has a role in regulating urine flow and ejaculation, both which are controlled by muscle cells (11, 12). The urethra runs from the bladder and directly through the prostate, this is the same path urine is carried out of the penis (12). The fibrous cells are responsible for supporting the structure of the gland (13).

The prostate gland is surrounded by several other structures that also play key roles in the reproductive and urinary systems. They include (i) the seminal vesicles, which are glands located on both sides of the prostate and produce semen (14), (ii) the vas deferens, which are long muscular tubes that transport sperm to the urethra from the testicles (15) and (iii) nerve bundles that aid in bladder control and erectile function that surround the prostate (16).

1.2.1 Prostate zones

The prostate is made up of four zones: the peripheral zone, the transition zone, the central zone, and the anterior zone (17) (Figure 1.1). The peripheral zone makes up the majority of the prostate and is the area closest to the rectum that can be felt during a digital rectal examination (DRE) (18). Prostate tumors are predominantly found in this zone of the prostate(19). The transition zone is the area of the prostate that surrounds the urethra as it passes through the gland (20, 21). As a man ages this area of the prostate can enlarge and push the peripheral zone of the prostate towards the rectum and also cause narrowing of the urethra, leading to a bladder outlet obstruction (22, 23). This condition is known as benign prostatic hyperplasia or BPH. The central zone is between the peripheral zone and the transition zone of the prostate and is located furthest from the rectum. Therefore, tumors in this zone cannot be detected by DRE.

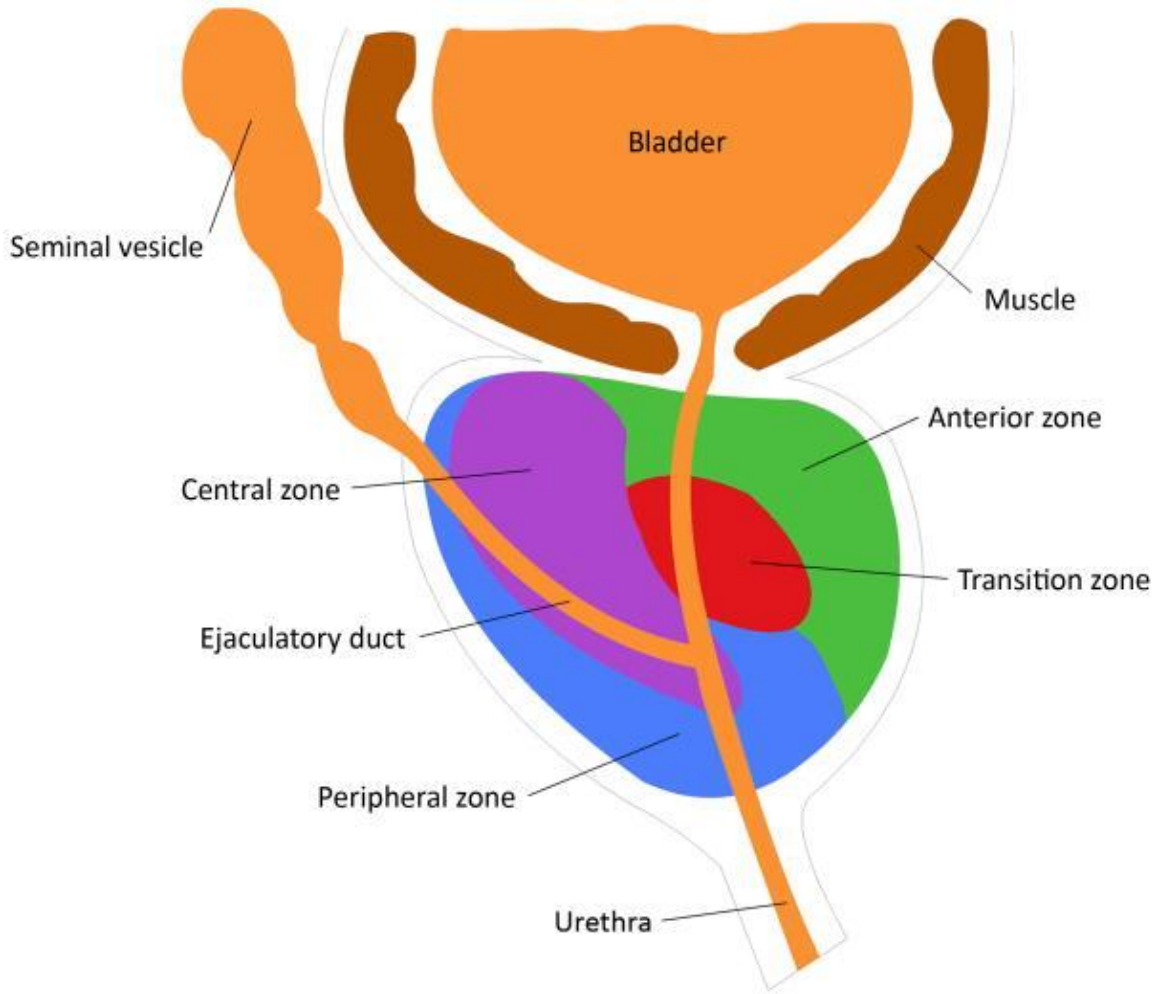


Figure 1.1 Zones of the prostate gland. The prostate gland can be divided into four zones: the anterior zone, transition zone, central zone, and peripheral zone out of which most carcinomas arise. *Reprinted from Molecular Aspects of Medicine, 34/2-3, M.C.Franz,P. Anderle,M. Bürzle,Y. Suzuki,M.R. Freeman,M.A.Hediger,G. Kovacs; Zinc transporters in prostate cancer:pages 735-741. Copyright (2013) with permission from Elsevier.*

The anterior portion of the prostate consists of fibromuscular stroma (24).

1.2.2 Aspects of endocrine action, the androgen receptor and the prostate gland

Prostate development, function and maintenance are all regulated by the steroid hormone androgen (25). The nuclear androgen receptor (AR) is the principal mediator of androgen action. AR is a member of the nuclear receptor transcription factor superfamily, categorized as a class I nuclear receptor, together with other steroid hormone receptors (26-29). The AR gene is located on the X chromosome and has eight exons that encode a 110kDa polypeptide (30, 31). The protein comprises four major domains: the N-terminal (A/B) domain (amino acids 1-538), the DNA binding domain (DBD, amino acids 539-628), the ligand binding domain (LBD, amino acids 671-920) and the hinge region (amino acids 629-670) (32) (Figure 1.2).

The N-terminal domain is essential for the transactivation function of the receptor (33). It is intrinsically disordered and presents a challenge in determining the solution structure and for X-ray crystallography of this protein domain (34-36). This region contains activation functional domain 1 (AF-1) with two functional entities - TAU-1 (residues 101 and 370 with a LKDIL core sequence) (37) and TAU-5 (residues 360 and 485 with a core sequence WHTLF) (38). TAU-1 has a critical role in ligand dependent transcriptional activity whereas TAU-5 has constitutive (ligand-independent) activity (39, 40). Within the N-terminal domain there is also an FxxLP motif (residues 23-27) (39) required for co-regulator binding and also for intermolecular interaction between N- and C-terminal regions during ligand-induced dimerization (41). There are two zinc finger regions within the DBD essential for dimerization and for binding to DNA at canonical androgen responsive elements (ARE) within promoter and enhancer regions of target

Androgen Receptor

A/B= N terminal Domain

C= DNA binding domain

D= Hinge region

E= Ligand binding domain

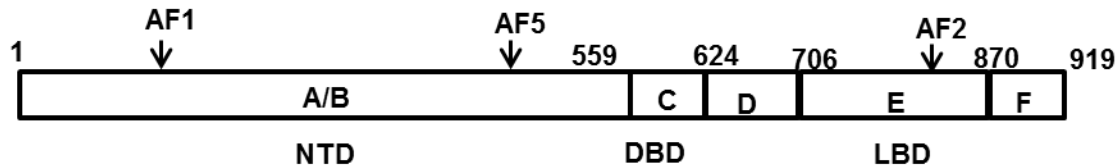


Figure 1.2 Androgen Receptor Functional domains. Schematic drawn roughly to scale indicating the structural organization of AR, including the positions of the major functional domains.

genes (42). There is a second ligand-dependent activation function domain (AF-2) in the LBD (residues 671-920) (43). This region also facilitates ligand-induced dimerization of AR (43). Both endogenous androgens and synthetic androgen antagonists bind to the LBD. A mutation in this region can result in androgen antagonists becoming agonists; an example is the T877A mutation in AR in the hormone-sensitive cell line LNCaP cells (44). In these cells the anti-androgen, bicalutamide activates transcription, rather than antagonizing it. The hinge region plays a critical role in AR activity (44). It is a flexible section on the receptor which contains a bipartite nuclear localization signal, RKLKLL between amino acids 629-634 (45). This region also contributes to intranuclear mobility of the receptor and is a target site for acetylation, ubiquitination, and methylation, which all have contributing roles in transactivation of AR target genes (45).

AR is the principal mediator of androgen action and regulates genes to support diverse physiological functions in various tissues (33, 46, 47). The classical mechanism of transcriptional signaling of AR requires the presence of androgen (48). Testosterone is the most abundant androgen in circulation and is produced in the testes. Testosterone is converted to dihydrotestosterone (DHT) by the enzyme 5 α reductase, located at the nuclear membrane of the endoplasmic reticulum, and in prostate tissue DHT is the primary agonist of AR (49, 50). The majority of testosterone is converted to DHT in the stromal cells and then is transported into the epithelial cells (51-53). The binding of DHT to AR induces a conformational change which releases the receptor from a chaperone protein complex in the cytoplasm and also exposes the nuclear localization signal within the receptor (54, 55). Ligand binding causes homodimerization and phosphorylation of the receptor. This results in stabilization of AR and translocation

of the receptor to the nucleus where it will bind to androgen-response elements (AREs) associated with its target genes (56). The AR-homodimer then recruits co-regulator proteins resulting in finely regulated transcription of target genes (57). The target genes may have a variety of cellular functions in normal and malignant tissues as well as expression of the prostate specific antigen (PSA), a well-known serum marker for prostate cancer (58-60).

The androgen signaling axis is critical for prostate development, proliferation, function, maintenance and oncogenesis. AR is expressed in both the stromal and epithelial cells of the prostate (61). The reciprocal relationship between these two cell types is responsible for ductal morphogenesis and homeostasis of the prostate (13, 62, 63). The normal development and maintenance of the prostate epithelium depends on paracrine signaling from the stromal cells through growth and survival factors known as andromedins, in response to androgen signaling through AR (64-66) (Figure 1.3). Secretions from the epithelial cells in turn signal to the stroma to maintain a supportive environment (67) This allows for a homeostatic balance between paracrine growth stimulation versus survival in adult prostate tissue. The development of prostate cancer is underpinned by a breakdown of this reciprocal paracrine interaction between the stromal and epithelial cells and an emergent autocrine mechanism within the epithelium (64, 68, 69). In this situation the epithelial cells are no longer dependent on stromal derived growth and survival factors but rather achieve proliferative functions due to self-stimulation. This mechanism paired with “gain of function” capability can lead to oncogenesis of the prostate (64, 70, 71).

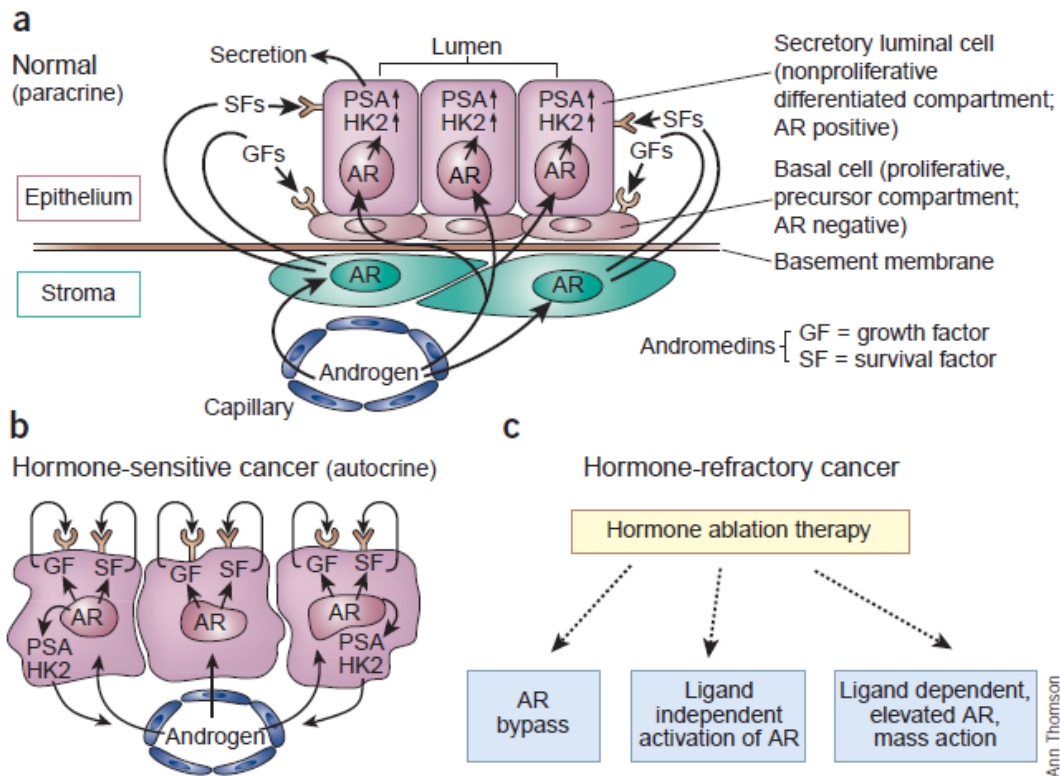


Figure 1.3 Androgen receptor signaling in normal and malignant prostate cells. (a) In normal prostate, growth and maintenance of prostate epithelium depends on andromedins—growth (GF) and survival (SF) factors produced by stromal cells (smooth muscle and fibroblasts). Andromedins are produced as a result of androgen signaling through androgen receptor (AR). Androgen signaling in prostate epithelium is required for production of secretory proteins such as PSA and human kallikrein-2 (HK2). Basal epithelial cells do not express AR. (b) During transformation to cancer, the paracrine mechanism of AR action is replaced by an emergent autocrine mechanism, whereby cancer cells are less dependent on stromal cell factors. Androgens acting through AR can directly stimulate production of growth and survival factors by cancer cells. (c) After hormone ablation therapy, progression to hormone-refractory cancer occurs. The study of Chen *et al.* supports a ligand-dependent, mass-action model resulting from elevated AR expression. Elevated levels of AR sensitize cells to residual amounts of androgen or, paradoxically, antiandrogens; cells become supersensitive to androgen rather than independent of it. *Reprinted by permission from Macmillan Publishers Ltd: Nature Medicine, (Isaacs and Isaacs 2004) copyright (2004)*

1.3 Prostate Disease

The precise regulation of the AR/androgen signaling axis enables maintenance of the normal prostate. However the prostate is prone to entering disease states. There are three major diseases that can develop in the prostate, prostatitis, BPH, and prostate cancer.

1.3.1 Prostatitis

Prostatitis is an inflammatory disease that can cause swelling of the prostate (72). The disease is quite common and affects about 50% of men during their lifetime (73). The disease can be caused by common strains of bacteria and is effectively treated with antibiotics; however the cause of infection is unknown in many cases. The symptoms of prostatitis include difficulty in urination, and discomfort and pain in the pelvic region. Prostatitis can be initially diagnosed using urine and blood samples that indicate signs of infection (74). Treatments for the disease include alpha blockers that can help relax the muscles surrounding the bladder and prostate, as well as nonsteroidal anti-inflammatory drugs(75).

1.3.2 Benign Prostatic Hyperplasia

Benign prostatic hyperplasia or BPH is a non-malignant enlargement of the prostate (76, 77). This condition generally occurs in older men (78). The cause of BPH is poorly understood. Some research has indicated that as males age they produce more dihydrotestosterone (DHT), because of an increased production of co-factors NAD and NADH (79). The accumulation of DHT stimulates the prostate cells to grow (80, 81). The majority of the hyperplastic cells are composed of the stroma cells while a minor portion is composed of epithelial cells (82). It has been noted that men who do not

produce DHT do not develop BPH (83). Since the prostate surrounds the urethra, enlargement of the prostate from BPH can cause urine retention and lower urinary tract symptoms. BPH is often diagnosed with a physical exam or a DRE and other medical tests such as a urinalysis, prostate specific antigen (PSA) blood test, or a biopsy. Often BPH is managed with alpha blockers which prevent the stimulation of adrenergic receptors that mediate prostate muscle contraction (84). This use of such molecules therefore relaxes the muscles and helps to improve urine flow and reduce bladder blockage (85). Medications like 5- α reductase inhibitors are also used to inhibit the production of DHT (86, 87).

1.3.3 Prostate Cancer

Prostate cancer is the most common cancer in American men. Prostate carcinomas occur when there is a disruption of epithelial differentiation of luminal cells within the gland and dysregulation of autocrine and/or paracrine mechanisms of growth control (88). Almost all prostate cancers are adenocarcinomas meaning that these cancers develop from glandular cells of the prostate. Certain conditions of the prostate have been recognized as a precancerous state. They include prostatic intraepithelial neoplasia (PIN) and atypical small acinar proliferation (ASAP) (89). These two types of lesions are restricted to the acini and ducts and the cells show a range of atypical morphologies (90, 91). PIN and ASAP may be identified in a biopsy of the prostate. In prostate cancer the abnormal cells disrupt the basal cell membrane and spread beyond these boundaries. PIN lesions are commonly found in the peripheral zone of the prostate and high-grade PIN have more pronounced abnormalities compared to low-grade PIN that are only slightly different compared to normal cells (92). Many studies

have shown that there is a strong correlation between the occurrence of high-grade PIN lesions and the diagnosis of prostate cancer (93).

The prostate gland synthesizes and secretes many unique proteins into the seminal fluid. Among them, prostatic acid phosphatase (PAP), prostate-specific antigen (PSA), and beta-microseminoprotein (beta-MSP) are predominant and are secreted by both normal and malignant prostate cells (94). PSA is a serine protease capable of cleaving peptide bonds and is responsible for regulating the liquefaction of semen (95). Serum PSA has historically been measured as an early detection method for prostate cancer but more recent studies have questioned its value in routine screening (96, 97). Nevertheless, the PSA test is very useful in monitoring treatment response in patients who have undergone surgical or chemical castration or who have been treated with systemic therapy for prostate cancer.

As mentioned earlier, androgens are the physiological ligands required for the transcriptional activity of AR. The AR/androgen signaling axis is necessary for the initial growth and development of the prostate and in the differentiated prostate this axis is required for maintenance of the differentiated state and for the secretory function of the prostate. In the normal differentiated prostate, the AR/androgen axis regulates both apoptosis and renewal of epithelial cells. In prostate cancer, cellular changes affecting this signaling pathway apparently cause the proliferative function of AR to become dominant with a simultaneous disruption of its differentiation program. As prostate oncogenesis typically relies on AR/androgen signaling, a major clinical approach to treating the disease is to target this axis.

1.4 Prostate cancer- diagnosis

In early stage prostate cancer, patients do not often experience clinical symptoms. The cancer may be found during routine screening by DRE or by detecting elevated serum PSA (98). The PSA test is used for early detection of a tumor and to monitor the patient's response to therapy throughout the course of their disease. It is generally well accepted that PSA levels below 4ng/mL are considered to be "normal" whereas levels over 10ng/mL are considered to be "high"; a PSA level between 4 and 10ng/mL can be considered to be "abnormal" (98). If the PSA level is higher than "normal" most likely the physician will repeat the test and follow up with confirmative tests including transrectal ultrasound imaging and a biopsy (98). Proteins such as PAP are not used for early detection but as biomarkers that provide information on response to therapy and progression of tumors if they have spread (99).

1.4.1 Prostate Cancer Grading

When there is a definite cancer diagnosis the tumor grade is defined by the Gleason score, which is based on histological evaluation of the tissue biopsy. This is a system of composite grading that ranges in value from 2 to 10. A low grade cancer grows slowly and has a lower tendency to spread. The higher scores indicate relatively poor differentiation and a more aggressive cancer.

1.4.2 Prostate Cancer Staging

Staging of the cancer describes the location of tumor lesions and extent of spread. Prostate cancer is staged using a system known as TNM staging (100, 101). The 'T' indicates how large the primary tumor is. The 'N' indicates whether the tumor is present in the lymph nodes, the location of the infiltrated lymph nodes and the number

infiltrated. The 'M' indicates the nature and extent of distal metastasis. The stage of the cancer, evaluated by combining these three different parameters, enables an appropriate treatment plan (102). The stages range from Stage I to Stage IV. In Stage I the tumor is slow growing and confined within the prostate gland (103). In Stage II the tumor is growing at a faster rate but is still confined. If a patient has been diagnosed with Stage III prostate cancer, the cells would have invaded outside of the prostate into proximal tissues (103). Stage IV is the most aggressive type of cancer and describes a tumor that has spread from the primary site; these new locations could include distant lymph nodes, the bladder, bone, liver, lungs, etc. (103). Recurrent prostate cancer is also categorized as Stage IV. **Thus there are many factors that contribute to a patient's prognosis of prostate cancer that help to guide treatment decisions.**

1.5 Prostate cancer treatment

Following diagnosis of localized prostate cancer most patients have several treatment options. The first line therapies comprise ablation of the prostate (104). This may be accomplished by radical prostatectomy where the entire prostate gland and some surrounding tissues including the seminal vesicles are surgically removed, external beam radiation, internal beam radiation (brachytherapy) and cryotherapy or the freezing of the prostate tumor (105, 106). These initial treatments could leave the patient with many undesirable genitourinary side effects including irritation and urinary retention (107). Moreover, prostate cancer may recur despite these treatments (108-110).

1.5.1 Androgen deprivation therapy and anti-androgen therapy

Advanced prostate cancer refers to local as well as systemic recurrence following first line therapy. Advanced disease is commonly treated with androgen deprivation therapy (ADT) by surgical castration or by chemical castration through the use of luteinizing hormone-releasing hormone (LHRH) agonists (110). The goal of ADT is to reduce the level of androgens in the body to prevent them from stimulating tumor growth. These powerful treatments can leave the patient with both acute and chronic side effects including fatigue, hot flashes, anemia, osteoporosis, changes in muscle and fat mass, sexual dysfunction, and cognitive defects (107, 111, 112). Response to ADT is generally temporary, with a median time to recurrence of 18-24 months (113).

Antagonists of AR or anti-androgens are taken orally every day and may also be included with LHRH agonists as first-line hormone therapy. These are drug molecules that bind to the ligand binding domain of AR, competing with androgen for binding to AR and interfering with the transcriptional activity of AR(114). Examples of anti-androgens currently used in the clinic are Flutamide (Eulexin), Bicalutamide (Casodex), and Nilutamide (Nilandron) (115-117).

Despite an initial favorable tumor response to testosterone suppression by means of ADT and the use of antiandrogens, prostate cancer frequently recurs by progressing to an apparently hormone refractory state. At this stage the advanced metastatic disease is referred to as castration resistant prostate cancer (CRPC).

1.5.2 Available Treatments for CRPC

It is unclear exactly how prostate cancer progresses to CRPC, although it is believed that ADT selects for cells that are able to grow and re-populate the tumor in the

absence of hormone or cells that are capable of synthesizing and restoring androgen intratumorally(118-120). CRPC is typically treated with docetaxel, an anti-mitotic chemotherapy, usually with prednisone, a synthetic corticosteroid drug (107, 118). However, at this point the disease is typically non-curative. Relatively new therapies have been developed which include cabazitaxel, a chemotherapeutic agent targeting microtubules (121) and alpharadin, which is used to treat metastatic bone cancer by relying on alpha radiation to kill the cancer cells (122). Abiraterone acetate, an oral androgen biosynthesis inhibitor which targets the androgen synthesis enzyme, CYP17 (123) extends the median survival to 14.8 months from 10.8 months. Enzalutamide, which is a high affinity AR antagonist that prevents nuclear localization and transcriptional activity of AR, extends median overall survival of CRPC patients by 5 months (124). Immunotherapies have also been FDA approved. These include denosumab, an antibody against RANKL (125) used as a treatment to increase bone mass in metastatic prostate cancer and also a vaccine called sipuleucel-T (126) for metastatic CRPC.

All of the current treatments for CRPC offer limited benefit in terms of extending median survival.

1.6 Other Major Limitations of Testosterone Suppression in Prostate Cancer – Effects on Normal Tissues

It is evident from the discussion above that targeting the AR signaling axis has proved to be the most effective form of treating advanced prostate cancer. However, the conventional approaches in this treatment are severely limited due to the relatively frequent and rapid development of drug resistance. Moreover, testosterone suppression

has a number of acute and chronic adverse side effects due to its effect on normal tissues, as discussed below.

1.6.1 Hot Flashes

Hot flashes are often described by patients as intense warmth and flushness of the skin and are one of the most common acute symptoms of ADT (127). They occur when the thermoregulatory centers in the hypothalamus are stimulated unnecessarily (128). This results in peripheral vasodilation and inapt heating throughout the patient's face and neck which can last from a few seconds to several minutes (129). This is the result of withdrawal of androgen leading to disruption of the equilibrium of neurotransmitters. This mechanism can also lead to the feeling of anxiousness. It is thought that selective serotonin reuptake inhibitors (SSRIs) can increase serotonin within these centers to alleviate the intense warmth and perspiration the patient experiences due to dysregulation of neurotransmitters within the thermoregulatory centers (130-132).

1.6.2 Hyperlipidemia

It is well known that sex hormones such as testosterone can influence the serum lipid profiles. Investigation in men with low testosterone levels from ADT has identified elevated levels of total cholesterol, low-density lipoprotein, and triglycerides (133, 134). Increasing duration of therapy has a positive correlation with further elevation of these lipids in the serum (135). Alteration of the lipid profile due to low testosterone levels can contribute to heart disease in prostate cancer patients (135, 136). To help manage this severe adverse effect, patients may adjust their nutrition plan to a low-cholesterol diet, or increase their physical activity to a manageable level without inducing intolerable

fatigue. In addition, statin based medications may be used to control cholesterol levels (137, 138).

1.6.3 Sexual Dysfunction

Testosterone is the major regulator for sexual function in males and therefore one of the major adverse effects of ADT is erectile dysfunction and loss of libido (139). This can also negatively impact quality of life. Testosterone is required to facilitate erection by acting as a vasodilator in the penis (140). Testosterone contributes to activation of nitric oxide synthase, which in turn activates a series of other enzymes and results in dilation of the blood vessels of the vascular beds within the penis leading to erection (141, 142). Therefore decreasing testosterone levels by ADT contributes to erectile dysfunction. ADT can drop testosterone levels to below 100ng/mL (143); it is believed that a minimum value of about 250ng/mL is needed for healthy erectile function. Another contributing factor to erectile dysfunction from ADT is the replacement of the muscle cells within the penis by fat tissue, leading to flaccidity (144). As a result collagen protein deposits arise and cause venous leakage (145). It has been reported that libido and sexual activity can improve when ADT is stopped and normal testosterone levels are restored (146, 147). Contributing factors to sexual dysfunction include the patient's age, duration of hormone depletion therapy and overall health (148, 149).

1.6.4 Anemia

Androgens have an important role in the hematopoietic system. Androgens regulate the production of red blood cells. Androgen induces the renal production of the protein erythropoietin, which promotes the formation of red blood cells by the bone

marrow and incorporates iron into these cells (150). The production of erythropoiesis-stimulating proteins can be induced specifically by testosterone (151, 152). Patients undergoing ADT experience a decline in hemoglobin levels and develop anemia as an indirect effect of inhibition of erythropoiesis (153). Symptoms include fatigue, loss of energy, dizziness, and difficulty in concentration (154). ADT-related anemia can be temporary and correlates with the duration of the treatment.

1.6.5 Skeletal Complications

Bone fractures, osteoporosis, bone pain, and bone metastases are all associated with men ADT (155-158). Androgens have a major role in skeletal homeostasis throughout life (159). The difference in the size of a male's skeleton and greater muscle mass compared to that of a woman can be explained in part by the increase levels of androgens in males (160). The androgen receptor is expressed in both osteoclasts (161) and osteoblasts (162), which are the cells that facilitate bone turnover and remodeling. Androgens stimulate osteoblast differentiation and decrease apoptosis of osteoblasts and osteoclasts (163). Androgens also regulate growth factors and cytokines to indirectly stimulate bone formation and downregulate factors involved in osteoclastogenesis (164). Because androgens are essential for bone turnover and development, several skeletal complications result from ADT. It is estimated that there is a six-fold increase in the rate of bone fracture in men undergoing ADT as well as a greater risk for development of osteoporosis (165-167). Both of these conditions are due to the bones becoming brittle and fragile as a result of withdrawal of androgens. Bone metastasis of prostate cancer also interferes with normal maintenance of the

healthy bone and strength of the bone, again leading to increase fracture rate and bone pain.

There are several lifestyle modifications, such as light exercise and calcium supplementation, to help manage skeletal complications due to ADT. In recent past years there has been much focus on supplemental therapies for patients experiencing skeletal-related events. Bisphosphonates such as zoledronic acid are the most commonly prescribed drug for osteoporosis as they induce osteoclasts to undergo apoptosis (168). Inhibition of osteoclast activity can help improve bone mineral density; this slows bone loss and reduces fracture and bone pain. Denosumab is a human monoclonal antibody which is a receptor activator for nuclear factor kB ligand (RANKL) inhibitor (169). RANKL is expressed on osteoclasts and is the key mediator for bone destruction (170). Denosumab neutralizes this activity to increase bone mineral density and reduce bone brittleness and fracture (171). Denosumab has also been shown to be effective in delaying bone metastasis and increased bone metastasis-free survival in men with non-metastatic advanced prostate cancer (125).

1.6.6 Effects on the cardiovascular system

ADT has been linked to major adverse effects related to cardiovascular disease (172-174). These effects can go unnoticed but can be fatal. Heart attacks, strokes, and peripheral vascular disease together can be categorized as cardiovascular disease. ADT can cause these cardiovascular events by causing metabolic changes. These changes can include an increase in high density lipoprotein cholesterol, development of hyperglycemia and obesity (136, 175, 176). These conditions are all risk factors that contribute to the progression of atherosclerosis, which leads to cardiovascular disease

(136). Androgens have also been shown to inhibit local inflammatory responses that contribute to atherosclerotic plaque development. The positive effects of androgens allow for normal blood flow and therefore have a role in promoting cardiovascular health (177). Due to the high risk of development of cardiovascular disease in patients on ADT, careful monitoring of the patient's overall health is essential. Precautions and certain alterations to the patient's lifestyle such as reducing caloric intake and increasing physical activity can contribute to lowering the risk of cardiovascular complications as a result of ADT.

1.6.7 Cognitive and Psychological Impairment

AR is endogenously expressed throughout the brain including the hippocampus, parietal lobe, and prefrontal cortex (178-180). These areas are critical for cognitive functions and memory (181). Processes involved in how people think, perceive, and remember can all be categorized as cognitive functions. Patients receiving ADT have reported memory problems while on therapy and cognitive side effects are almost immediate after initiation of treatment (182). Evidence from neuropathological studies has shown an association with low levels of testosterone in older men with depression (183). These symptoms have been shown to decrease with the use of testosterone replacement therapy. Depression is commonly reported in men with prostate cancer (184, 185). Depression reported by these patients is often linked with anxiety and is exacerbated by ADT(186).

As discussed above, adverse effects associated with ADT are both acute (fatigue, hot flashes, flares) and long-term (hyperlipidemia, cardiovascular disease, anemia, osteoporosis, sexual dysfunction and cognitive defects) and

include loss of the feeling of well-being (107, 111, 112). Although these effects are somewhat mitigated by routine monitoring, medications and changes in diet and lifestyle, the side effects of ADT remain a major challenge in the treatment of advanced prostate cancer.

1.7 Mechanisms of restoration of AR signaling in CRPC

It is clear from the cumulative pre-clinical and clinical evidence that the progression of prostate cancer is reliant on the AR/androgen signaling axis. Hormone-deprivation therapy has proven effective in patients; however a major limitation is that the cancer progresses to CRPC. An interesting aspect of CRPC is that the cancers typically remain dependent on AR for growth stimulation. Treatment-naive prostate cancer is typically dependent on androgen for growth and is therefore sensitive to ADT and anti-androgen drugs; however as the cancer progresses further, it still remains dependent on AR for growth but acts independent of androgen or could thrive on androgen produced within the tumor. Therefore these advanced cancers are insensitive to ADT and anti-androgen drugs. **Although it is difficult to elucidate the precise molecular mechanisms underlying clinical cases of CRPC, evidence based studies of *in vitro* and *in vivo* models, clinical response to newer drugs as well as well substantiated theoretical notions have indicated several possible molecular and cellular mechanisms driving CRPC. Notably, almost all of these mechanisms restore functional AR signaling.**

1.7.1 Intratumoral Androgen Synthesis

One adaptive response to ADT that restores AR signaling is the synthesis of intratumoral androgens from different androgen precursors such as cholesterol and

adrenal dehydroepiandrosterone (DHEA) (187). It has been reported that there is a correlation between the expression of cholesterol and the increase in the expression of an enzyme required for *de novo* androgen synthesis, CYP17A, in CRPC tumor tissue (137). Tumors may thus produce testosterone or DHT through the classical or a “backdoor” androgen biosynthesis pathway at levels thought to be sufficient to support progression of the disease (188). However, enzyme inhibitors to circumvent restoration of testosterone have only shown modest clinical benefit (189).

1.7.2 Overexpression of AR

One way in which prostate cancer can overcome the ability to grow in castrate levels of androgen is through the overexpression of AR (190). In these cells that overexpress the receptor, sensitivity to androgen or to hormone-independent autocrine/paracrine signaling may be enhanced (191). The overexpression of AR could be the result of selective pressure of the androgen depleted environment, causing the cells which express more AR to flourish (192).

1.7.3 Imbalance of AR co-regulator expression

The androgen/AR signaling axis is directed and finely regulated by many protein factors. Once AR is bound to the DNA, the composition of proteins that are co-recruited to that site determine if transcriptional activity will occur (193). These proteins are known as coregulators of AR and they could be either coactivators or corepressors (194). Coactivators are preferentially recruited by agonist-bound AR (195). Coactivators enhance transcription, through various mechanisms that either directly modulate the pre-initiation complex or do so indirectly through chromatin remodeling (193, 196). Corepressors are preferentially recruited by antagonist-bound AR and act through

similar mechanisms to repress transcription (197). Therefore the cellular complement of coactivators and corepressors can determine the biological response and functional activity of AR (198, 199). It has been shown that CRPC could be supported by an imbalance of AR co-regulator expression. In these situations there is a higher expression of coactivators in relation to corepressors(200). This disproportionality in the coregulator complement could enable AR to be activated by lower levels of androgen or even by anti-androgens (57, 201).

1.7.4 Dysregulation of growth factors and crosstalk with other signaling pathways

AR may support growth through activation of the receptor by crosstalk with other pathways resulting in the activation of the androgen receptor by ligand independent mechanisms. The dysregulation of growth factors in prostate cancer such as insulin-like growth factor and cytokine IL-6 contributes to an increase in the activation of MAPK pathways, PI3K/AKT pathways, and the PKC pathway (37, 202-204). This leads to direct phosphorylation of AR (205). Therefore the deregulation of multiple growth factors and the crosstalk between the nuclear receptor pathway and these MAPK signaling pathways can contribute to the development of androgen independent prostate cancer.

1.7.5 Mutations in AR and Splice Variants of AR

Increases in somatic mutations within AR have been reported in advanced prostate cancer samples (206, 207). As a result of these gain-of-function mutations, the malignant cells acquire a proliferative advantage. For example, the widely used hormone-sensitive prostate cancer cell line, LNCaP cells, contain a missense mutation at amino acid 877, converting the amino acid from threonine to alanine within the ligand

binding domain of the receptor(44). This mutation permits anti-androgens to bind as agonists and confers a growth-gain-of-function for the receptor (44).

More recent studies have established a role of the AR splice variants (AR-V) in acquired resistance to hormonal therapies in prostate cancer. AR splice variants are alternatively spliced variants of the androgen receptor and more than twenty different splice variants of AR have been identified (208). Almost all of the splice variants that have been identified have carboxyl-terminal truncations that eliminate the ligand binding domain of the receptor (208). The AR splice variants retain their amino-terminal domain which harbors two transactivation domains Tau-1 and Tau-5 which confer constitutive activity (209). This is significant because it allows for the activation of AR signaling in the absence of hormone ligand. Therefore ADT and antiandrogens, which both target the ligand binding domain of native AR are ineffective against AR-V expressing tumors (210-212). AR-V7 and AR^{v567es} are the most common and abundant AR variants found in clinical prostate tumors (213-215). Studies have shown that the expression of AR-V7 and AR^{v567es} correlates with disease progression to CRPC and are the most commonly found splice variants associated with tumor metastasis and decrease in patient survival (216, 217).

The binding of agonist is an essential event in the classical (ARE-mediated) mode of target gene activation by AR. Full length AR requires ligand binding to initiate homodimerization (33). In the process of dimerization, intramolecular interaction between the carboxyl- and amino-terminal regions of AR leads to a D-box-dimerization transition(218). The homodimer can then directly bind to ARE enriched DNA sequences and activate target gene transcription. It has been shown by studying D-box-D-box

interactions that dimerization of AR-V7 also must occur to transactivate target genes (219). Deletions or mutations in the D-box prevent dimerization in both the full length receptor and AR-V7 resulting in loss of their ability to activate target genes. This results in loss of their ability to support CRPC cell growth. Therefore it has been proposed that targeting the D-box interface might be an effective therapeutic approach to treating AR-V7 dependent tumors (219).

An important question is whether the splice variants of AR can activate the same set of canonical target genes as the full length receptor (AR-FL). It has been shown in several studies that AR-Vs localize to the nucleus in the absence of ligand to activate target genes. The AR-Vs can also facilitate AR-FL to localize in the nucleus in the absence of androgen (220, 221). When co-expressed, AR-V7 and AR-FL co-localize at the canonical ARE enhancer in the PSA gene promoter. Interestingly, in contrast to full length AR alone, co-occupancy of the full length and variant forms of AR at this site is not enhanced or diminished in the presence of androgen or in the presence of the potent anti-androgen, enzalutamide (220). Ubiquitin-conjugating enzyme E2C (UBE2C) is as an AR-V specific target gene; the promoter of this gene can only be occupied by an AR-V7 homodimer or by an AR-V7/ AR^{v567es} heterodimer but not by AR-FL (213, 215, 220). This indicates that most likely, there is a separate subset of direct target genes that are activated by AR-Vs alone. There is cumulative evidence to support the idea that there is a set of genes that are upregulated by AR-Vs alone and that they comprise genes that support CRPC cell growth (219, 222-224).

Following castration, the molecular changes in the tumor AR signaling axis discussed above overcome or minimize the need for systemic androgen to

activate AR. In these situations the tumors may themselves synthesize androgen to near pre-castration levels but, more often, AR is localized in the nucleus in the absence of androgen or in the presence of extremely low levels of androgen. Future studies may reveal additional mechanisms contributing to the development of CRPC. Presumably, even within a tumor, several mechanisms contribute to the ability of AR to activate transcriptional growth in the absence of hormone because of the heterogeneity of this type of cancer. Several newer approaches have attempted to disrupt ligand-independent activity of AR in prostate cancer.

1.8 Targeting the amino-terminal domain of AR

Despite the more recent development of enzalutamide and abiraterone acetate to treat CRPC, tumor escape and resistant mechanisms that restore AR signaling, as mentioned above, still remain a major challenge for treatment of the disease. Although there is a modest benefit and a gain in median overall survival of less than 6 months with these current agents for the treatment of CRPC, the majority of CRPC cases will develop resistance and the therapy will essentially become ineffective. As with all other current therapies, the functional action of these molecules targets the carboxyl ligand binding domain of AR. However, it is the amino-terminal domain of AR which harbors the region that drives constitutive hormone-independent transcriptional activity of AR or its splice variants in CRPC. It has been shown that deletions within this region of the receptor result in a transcriptionally inactive protein (40). Because the N-terminal domain of the receptor has not been crystallized due to the intrinsically disordered nature of the protein, it has made it difficult to develop targetable therapies to this

region by means of structure-based design. Despite these challenges, efforts have been made to use high-throughput screening methods to discover drug candidates that block recruitment of coactivators to the N-terminal domain. An advantage of such drugs is their expected ability to inactivate AR splice variants that pose a major problem in prostate cancer progression. Notable developments in studies of small molecules targeting interactions of the N-terminal domain of AR as well as very early conceptual studies of cell penetrating antibodies with similar effects are discussed below.

1.8.1 Bromodomain inhibitors

As mentioned earlier, the transcriptional activity of AR is precisely regulated by a complex network of proteins and epigenetic mechanisms that enable its entry into the nuclear compartment and localization to the chromatin. Therefore these mediators of transcription propose an alternative strategy for disrupting AR signaling in CRPC patients. Bromodomain and Extra-terminal motif (BET) proteins have a wide variety of functions in regulating transcription including histone acetyltransferase activity, chromatin remodeling and recruitment of co-regulators (225). BRD4 is a conserved BET family member that associates with acetylated chromatin and has a critical role in recruitment of the positive transcription elongation factor, P-TEFb, which in turn enhances the activity of RNA polymerase II by stimulating phosphorylation of its carboxyl-terminal domain (226-228). It was shown using co-immunoprecipitation studies that BRD4 directly interacts through its two conserved bromodomains, BD1 and BD2, with the N-terminal domain of AR to facilitate transcriptional activity (229). Inhibition of BRD4 decreases recruitment of full length AR and splice variants of AR to target loci in the chromatin to an extent that is comparable to the effect of enzalutamide on full length

AR (229). BRD4 inhibition is selective for AR-positive prostate cancer cell lines in promoting the induction of apoptosis and cell cycle arrest. Blockade of BRD4 *in vivo* resulted in inhibition of CRPC tumor growth (229). An interesting study that was done in parallel with the tumor xenograft models was observing the effect bromodomain inhibition of BRD4 had on metastasis. This was of interest because other studies have described enzalutamide to have a pro-metastatic effect in pre-clinical models (230) . There was evidence of metastases in the femur and liver of enzalutamide treated VCaP tumor-bearing mice in contrast to no evidence of metastasis in mice bearing the same tumors treated with BRD4 inhibitors(229). By functioning downstream in the AR signaling pathway, BET inhibitors are likely to circumvent resistance mechanisms that restore functional AR. There are at least four compounds currently being studied as BRD4 inhibitors. One of them, JQ1, is still in preclinical evaluation (231-233). BRD4 inhibitors currently in Phase 1 clinical trials are GSK525762 (NCT01587703), GS-5829(NCT0207228), and OTX015 (NCT02259114).

1.8.2 EPI family small molecules

The EPI family of small molecules compounds was initially discovered by screening a library of marine sponge extracts (234). The screen was performed to identify molecules that blocked the transactivation of the N-terminal domain of AR (234). This family of compounds binds to AF-1 of AR, specifically tau-5, blocking protein-protein interactions in this region (235). The binding of the EPI to this region also blocks the amino and carboxyl terminal interaction required for ligand activity of AR (234, 236). As a consequence they inhibit transactivation of the AR N-terminal domain. EPI seems to be specific for AR and does not inhibit transcriptional activities of the progesterone

and glucocorticoid receptors (234). EPI suppresses activation of the classical androgen responsive genes, PSA and TMPRSS2 (234). It does not compete for the ligand binding domain like other current AR targeted therapies and is effective in blocking transcriptional activity of the major AR splice variants. It has been demonstrated in a number of different prostate cancer cells lines that EPI is able to inhibit AR-dependent growth but has no effect on cells that do not rely on AR signaling for proliferation and survival (234). It was shown to be effective in blocking tumor growth in xenograft models that express full length AR and those that express splice variant AR in castrated male mice (234, 236, 237). There was no toxicity to internal organs of animals treated with EPI systemically; this along with the selective antitumor activity observed in preclinical models suggests potential for EPI as a new class of therapeutic drugs for CRPC (234, 236).

Further investigations of EPI compounds have led to the development of EPI-506. This is the first AR N-terminal domain inhibitor to enter into clinical trials. The original EPI compound that was discovered through screening was compound EPI-001. When detailed preclinical studies were conducted on this compound along with four of its isomers, EPI-002 was found to be the most potent (234, 236, 237). Compound EPI-506, which is the clinical drug candidate, is a prodrug form of EPI-002. Currently, EPI-506 is under investigation in Phase I/II clinical trials. Patients with metastatic CRPC who have failed on enzalutamide and abiraterone are eligible for this trial. The study is currently enrolling in both the United States and Canada (NCT02606123). EPI-506 has the potential to circumvent major AR-related resistance mechanisms and is the first

drug to enter clinical trials that has the ability to inhibit both the classical AR transcriptional signaling and also AR-V dependent signaling.

1.8.3 Sintokamides

Sintokamide A (SINT1) has also shown novel effects on the N-terminal domain of the androgen receptor. This is a natural compound (238) isolated from the marine sponge *Dysidea sp.* This natural product was able to block transactivation by the N-terminal domain and inhibit AR-dependent proliferation in prostate cancer cells *in vitro* and of CRPC xenografts *in vivo* (238). SINT1 was able to selectively block the transcriptional activity of both full length AR and AR splice variants by binding to AF-1, without interfering with other nuclear receptors with similar structures (239). SINT1 was unable to prevent the interaction between AR and STAT3, which is a necessary transcription factor in AR signaling, unlike EPI indicating that STINT1 binds to a different region of AF1 than EP1 (238, 239). These studies imply that most likely there are multiple regions within AF-1 that can be targeted independently. Further characterization of these sponge extracts may provide the foundation for further development of AR N-terminal targeted therapies.

1.8.4 Bispecific antibodies to inhibit N-terminal AR activity

Although still in the early stages of preclinical development, the synthesis and use of the bispecific antibody (bsAb), 3E10-AR44, to penetrate prostate cancer cells and simultaneously bind to the N-terminal domain of the AR is noteworthy. Treatment with the bsAb in the androgen sensitive PC cell line LNCaPs, resulted in accumulation in the nuclear compartment with AR (240). 3E10-AR44 was able to co-immunoprecipitate with AR as well as mutant AR or AR-V7, and inhibited AR activity in promoter-reporter

based assays (240). Data on 3E10-AR44 was presented in 2015 at the annual American Association for Cancer Research meeting and are currently unpublished. Data on the effects of 3E10-AR44 on tumor growth are unavailable. Nevertheless, 3E10-AR44 may represent an interesting alternative approach to inhibiting AR function in a manner that does not rely on the ligand binding domain of the receptor (240).

Clearly, drugs that inhibit the transcriptional activity of AR by preventing co-activator recruitment by the N-terminal domain of AR hold promise in overcoming the limitations of ADT and anti-androgens in that they are effective against AR splice variants that lack the ligand binding domain. Nevertheless, this approach is still limited by its lack of selectivity for androgen signaling in prostate cancer cells vs. normal tissues and may cause many of the side effects associated with ADT and androgen antagonists. In the following sections, this thesis advances a new concept to address this problem.

1.9 Targeting AR tethering proteins

Currently major efforts are underway to discover/develop new therapeutics for CRPC tumors including those resistant to enzalutamide and abiraterone. The idea of targeting the N-terminal transcriptionally active domain of AR is a novel approach that is suitable for disruption of canonical AR signaling pathways as well as AR-V transcriptional pathways. However, in all cases, the current clinical paradigm remains as total and ubiquitous attenuation of AR signaling. Disrupting the androgen signaling axis is clinically validated and the best available treatment for prostate cancer but is seriously limited by side effects of depriving the patient of testosterone or its receptor function in all tissues (107, 111, 112). It is therefore desirable to selectively disrupt a

functional arm of AR that is critical for prostate tumor growth at all stages but not for the normal role of androgen or AR in various normal tissues. Such an approach would obviate the need for testosterone suppression while enabling improved therapy outcome for the spectrum of prostate tumors including CRPC.

The precise mechanisms by which prostate cancer cells reprogram AR signaling to primarily support growth have not been well understood. Recent work from our lab and others [reviewed in (241)] has strongly supported the general premise that the pattern of expression of proteins that tether AR to chromatin during development, differentiation and malignant transformation of the prostate could redirect AR signaling according to the physiological context. This may be exemplified by the ability of several well established AR tethering proteins to profoundly influence the pattern of gene activation by androgen/AR. Those proteins include HoxB13 (involved in development) (242), C/EBPalpha (involved in terminal differentiation) shown in our lab (243-245) and ELK1 (required for growth signaling by AR) shown in our lab (246).

1.9.1 HoxB13

HoxB13 is a transcription factor that belongs to the homeodomain family of proteins and plays a vital role in prostate development (247, 248). HoxB13 can associate with the DNA binding domain of AR (242). It can associate with AR bound to a canonical ARE and act as a co-repressor of AR gene transcriptional activity (242, 249). HoxB13 can also act as a tether for AR at homeobox elements in the chromatin. In the presence of androgen, HoxB13 can recruit AR and support transcriptional activity at those sites (242). HoxB13 and AR may also interact by binding at adjacent sites on the chromatin (242). It has been suggested that in addition to supporting prostate

development, the cooperative actions of HoxB13 and AR may have a regulatory role in growth and migration of prostate cancer cells (242).

1.9.2 C/EBP α

The CCAAT enhancer binding protein, C/EBP α , is a member of dimeric basic leucine zipper family of transcription factors and is involved in differentiation of several different types of tissues (250). C/EBP α is also a tumor suppressor and exerts anti-proliferative effects through protein-protein interactions including stabilization of p21 and disruption of E2F complexes (251-253) (254, 255). Activation of the phosphatidylinositol 3 kinase/AKT pathway can lead to dephosphorylation, causing C/EBP α to stimulate proliferation by sequestering the tumor suppressor protein, retinoblastoma (256) (257).

Our lab has shown that coincident with differentiation of prostate epithelial cells, C/EBP α enters the nuclear compartment, suggesting a role for the protein in prostate differentiation(244) Previously it was reported that C/EBP α associates with AR bound to classical androgen response elements and acts as a co-repressor to suppress AR-mediated gene transcriptional activity (258). Studies from our laboratory following this finding revealed the action of C/EBP α as a tethering protein for AR at C/EBP-binding sites that could enable AR to activate a different set of genes possibly contributing to prostate differentiation and other functions of AR in the prostate (245). Although in the normal prostate, androgen is needed for nuclear localization of AR, the mechanism of recruitment of AR by C/EBP α per se was found to be ligand-independent and without a need for dimerization of AR (245). The interaction of C/EBP α with AR involves multiple domains of AR (245).

1.9.3 ELK1 and other TCF subfamily members

The E twenty six (ETS) domain transcription factors have distinct roles in differentiation, development, transformation, and cellular proliferation (259). Within this large family of proteins exists a subfamily of three members, the ternary complex factors (TCF), ELK1, ELK3 (Net), and ELK4 (Sap-1). The TCF subfamily members are characterized by the presence of the ETS DNA-binding domain of about 85 amino acids and like all ETS proteins; they bind to cis elements in the DNA containing a GGA core sequence. TCF proteins characteristically also interact with serum response factor (SRF) at serum response elements (SREs) as a ternary complex. The formation of this nuclear ternary complex is required for transient induction of immediate early genes such as c-fos and Egr-1 (260, 261) in response to hyperphosphorylation of ELK1 by activated mitogen-activated protein (MAP) kinase pathways (262).

The TCF subfamily polypeptides contain four domains (A, B, D, and C domains) that are conserved among ELK1, ELK3, and ELK4 (Figure 1.4). The N-terminal region comprises the A domain which encompasses the ets DNA binding domain (263). The B domain interacts with SRF and allows for the formation of the ternary complex (264). The C domain resides at the C-terminus of the protein and regulates activation through phosphorylation by MAPK. The D domain is a docking site (D box) for MAPK. There is an additional MAPK docking site within the C domain, known as the FXFP motif or F box. The three TCF subfamily members also contain domains that distinguish them from each other. ELK1 contains a repressor (R) domain that diminishes the activity of the C-terminal which has similar activity to the CID domain of ELK3. ELK3 contains an additional inhibitory domain, NID domain, which inhibits transactivation and DNA

binding. ELK4 also has an NID domain with similar function. ELK3 has an additional phosphorylation regulatory J domain (259).

ELK1 is primarily regulated through phosphorylation by the MAP kinase pathway protein ERK at serine 383; however it can also be phosphorylated by the MAP kinases JNK and p38. There have been several studies of ELK1's role in neuronal cell differentiation; however ELK1 knockout mice are viable and phenotypically normal (265) suggesting functional redundancy within the TCF subfamily members. ELK1 is expressed in the clinical spectrum of prostate tumors (266). ELK4 plays a role in regulating the proliferation of T cells after targeted activation by the ERK and p38 pathways. ERK and p38 target ELK3 through the D domain; in addition ELK3 can also be targeted through the JNK pathway at the J domain. ELK3 is expressed at sites of angiogenesis and vasculogenesis. Knockout of ELK3 results in the most severe phenotypic effect of all the TCF subfamily members. ELK3 most closely resembles ELK1 in structure and DNA binding specificity most likely causing a large part of the redundancy of ELK1 in normal tissues (259, 264).

1.9.4 ELK1 as an AR tethering protein essential for PC/CRPC growth

Our lab has reported that, in a PC cell line model capable of growing robustly in the complete absence of hormone, AR was localized in the nucleus without the need for hormone and that AR expression was obligatory for cell growth (267). In these same cells, replacement of endogenous AR with a DNA binding domain mutant of AR that could not bind directly to DNA, did not impair cell growth (267). The mutant AR was able to associate with the chromatin and activate the required genes to support cell growth (267). In the same cells, the direct binding of endogenous AR to DNA required

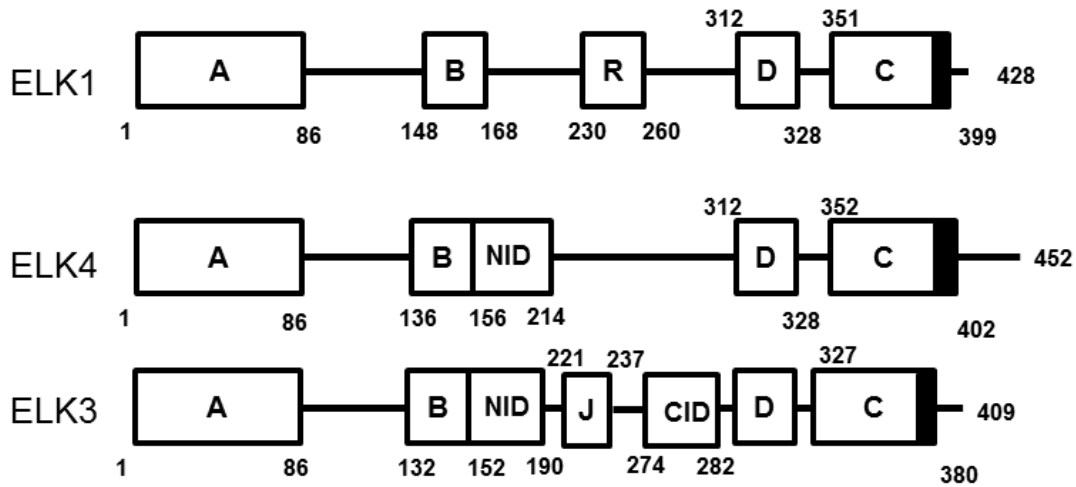


Figure 1.4 Schematic of the structural domains of ELK1, ELK4, and ELK3, the three TCF subfamily members. The A box represents the conserved ETS DNA binding domain. The B box is the SRF interaction domain. ELK4 contains one inhibitory domain and ELK3 contains two inhibitory domains represented by NID (net inhibitory domain) and CID (CtBP interaction domain). Docking sites for MAP kinases are represented by J, and D. The black box represents an additional secondary MAPK docking site known as the FXFP motif. The C box is responsible for transcriptional activation and contains phosphorylation sites targeted by MAPK.

androgen (267). These findings suggested that hormone-independent growth of prostate cancer cells could be supported by AR by associating with chromatin through DNA bound tethering proteins.

Systematic studies of a large number of candidate AR tethering proteins led our lab to the discovery that ELK1 is an AR tethering protein that is obligatory for androgen/AR-dependent malignant growth in a variety of the well-established PC/CRPC models (246). Both hormone sensitive PC and CRPC cell line models are absolutely addicted to ELK1 for AR-dependent growth, anchorage-dependent and –independent colony formation, and tumorigenicity (246, 268). ELK1 was at least partially required for activation by AR of approximately 27% of AR target genes in prostate cancer cells; these genes were primarily and heavily enriched for cell growth functions (246). The tethering of AR by ELK1 to ELK1 binding sites allows for constitutive activation of these genes. This dependence of prostate cancer cells on ELK1-dependent AR signaling is independent of known ets1-TMPRSS2 gene fusions (246). The cooperative action of ELK1 and AR is hormone-independent, unless hormone is needed for nuclear localization of AR and is mediated through the N-terminal A/B domain of AR. ELK1 is not required for growth of AR-negative cancer cell lines where it may be substituted by other proteins (e.g. ELK3) that do not interact with AR. In the normal differentiated prostate epithelium and in other normal differentiated AR+ tissues, where growth genes are not activated, it is possible that ELK1 is displaced in the chromatin by related members of the large ETS family that do not associate with AR. Alternatively, at the relatively low AR levels in normal tissues, the receptor could be sequestered by preferential binding to AREs associated with genes unrelated to growth. AR binding

sites in the chromatin are enriched for ELK1 binding elements (269) which are among the most enriched motifs at these sites (270).

1.10 The ELK1-AR complex as a critical and selective therapeutic target in prostate cancer

Both early stage and advanced prostate tumors are generally dependent on the androgen receptor (AR) for growth (271-274). Tumor growth could be driven by physiological levels of androgen, post ablation levels of androgen or by the androgen receptor (AR) acting completely independent of androgen. Hence, the disease is managed clinically by disrupting the AR signaling in the tumors via the use of androgen deprivation therapy (ADT) through androgen ablation and the use of androgen antagonists. However, these options present major drawbacks including limited efficacy in advanced disease, progression to castrate resistant prostate cancer (CRPC), and many undesirable acute and chronic side effects on non-target tissues including the central nervous system, cardiovascular system, bone, muscle, and adipose tissue. Therefore a more strategic approach is one that could disrupt a functional arm of AR signaling that is critical for prostate tumor growth at all stages but not for the essential roles of AR in normal adult tissues.

AR regulates genes to support diverse physiological functions in various tissues but in prostate cancer (PC) cells AR is redirected to gene targets that primarily support growth. The specificity of AR tethering interactions could be critical for AR-dependent growth signaling in both early stage prostate cancer and CRPC. If such tethering mechanisms are not required for the adult normal physiology they could then act as a functionally selective therapeutic target in prostate tumors. It has been previously shown

in our lab that ELK1, an ETS family transcription factor, tethers AR to the chromatin leading to the sustained activation of a critical set of growth genes in prostate cancer cells (246). ELK1 is genetically redundant in normal tissues (110). Moreover, our lab has shown that in a variety of prostate cancer cell lines both androgen and AR-dependent are addicted to ELK1 for cell growth, colony formation, and tumorigenicity (246).

The ELK1-AR synergy is independent of the classical mechanism of activation of ELK1 by ERK-dependent phosphorylation (246). The unique role of ELK1 in prostate cancer cells is underscored by the fact that ELK3, the closest functional substitute for ELK1, does not bind AR (246). Moreover, in contrast to ELK1, ELK3 is expressed at higher levels in normal prostate epithelial cells and tissues compared to standard models of both early stage PC and CRPC (266). Targeting the ELK1-AR complex for disruption would obviate the need for androgen ablation and reduce adverse effects associated with current AR targeted therapies. Because the synergy between the two proteins is a downstream event in the AR signaling axis, this approach would also evade resistance mechanisms to current therapies as these mechanisms typically restore functional AR. Therefore targeting the ELK1-AR complex should be effective against both hormone-dependent PC, as well as CRPC. The focus of this dissertation is to prove this concept and also discover a functional class of small molecules that could be developed as drugs that target the ELK1-AR complex.

CHAPTER 2-THESIS OUTLINE

This thesis describes our efforts to develop small molecule drugs using two different mechanistic approaches.

Chapters 3 and 4 describe the first approach. Here, the central premise was to avoid global attenuation of androgen/AR signaling, by only targeting a critical growth signaling arm of AR, specifically, the interaction of AR with ELK1 which has previously been reported by this laboratory. In order to accomplish this, we first mapped the docking sites for AR on ELK1 (Chapter 3). Next we designed and developed a high throughput small molecule screening system which we then used to discover and develop a lead drug candidate that would selectively disrupt the ELK1-AR complex (Chapter 4).

Chapter 5 describes the second approach. Here we developed hybrid molecules that incorporate scaffolds of a high affinity AR antagonist (enzalutamide) and a histone deacetylase (HDAC) inhibitor, suberoylanilide hydroxamic acid (SAHA). The hybrid molecules possess weak HDAC inhibitor activity compared with SAHA. Our premise was that the weak activity of the hybrid molecule would minimize the pan-HDAC inhibitor activity of SAHA. At the same time the enzalutamide moiety should redirect the HDAC inhibitor activity to client proteins of HDAC6 within the AR chaperone complex, resulting in cell growth inhibition in enzalutamide resistant cells expressing full length AR.

CHAPTER 3- THE AMINO-TERMINAL DOMAIN OF THE ANDROGEN RECEPTOR CO-OPTS ERK DOCKING SITES IN ELK1 TO INDUCE SUSTAINED GENE ACTIVATION THAT SUPPORTS PROSTATE CANCER CELL GROWTH

Reprinted by permission from Journal of Biological Chemistry Copyright 2016

3.1 Introduction

The androgen receptor (AR) and other members of the nuclear receptor (NR) superfamily mediate the transcriptional activities of their ligands as well as some of their non-genomic actions (60, 275-278). NRs in the cytosol, in the nucleus or in association with plasma membrane proteins are known to interact with a variety of signaling pathway proteins, either as protein kinase substrates or as regulators of transcription or signal transduction. Although some of the client proteins of NRs in these pathways have been identified, including those shared by different NRs, there is paucity of information on the structural elements that enable the mutual recognition of NRs and signaling proteins in both normal physiology and in pathogenesis.

Most early stage and advanced prostate tumors depend on AR for growth (272-274, 279-281). The human AR is a 919 amino acid polypeptide with a basic structural organization typical of NRs (282). In the classical model of gene regulation by AR, ligand binding is critical for several events including release of AR from a cytosolic chaperone complex as well as phosphorylation, stabilization, dimerization and nuclear import of AR (282-284). Ligand binding is also needed for optimal binding of AR to DNA at well-characterized response elements associated with target genes (267, 285). However, advanced prostate cancer (PCa) cells may acquire the ability to localize adequate AR to the nucleus where it is transcriptionally active through mechanisms that include AR amplification, hormone-independent phosphorylation of AR through hyper-activated signaling pathways or overexpression of ligand-independent AR splice

variants (221, 286-288). Splice variants of AR have carboxyl-terminal truncations that lack the ligand binding domain (289). The above cellular changes in advanced PCa cells, as well as intratumoral androgen biosynthesis, could render the tumors resistant to conventional AR-targeted therapies, including surgical or chemical castration and androgen antagonists (120, 192, 211, 214, 290, 291). Normal and malignant prostate epithelial cells appear to redirect androgen/AR signaling to regulate different sets of genes via tethering proteins that bind AR to chromatin (241, 242, 245, 246, 267). Therefore, developing drugs that disrupt interactions of AR with a tethering protein required exclusively for growth is an attractive approach to overcoming resistance to current AR-targeted therapies and would also obviate the need for androgen ablation.

We have previously reported that the ETS family transcription factor ELK1 is essential for growth in PCa cells that are either dependent on androgen or independent of hormone but still dependent on AR (246). In contrast, ELK1 was not required for growth in AR-negative PCa cells. In PCa cells, ELK1 is required wholly or in part for activation by androgen/AR of approximately 27 percent of target genes and these genes are enriched for clusters supporting cell cycle progression and mitosis (246). Promoter activation analyses, mammalian two-hybrid assays and chromatin immunoprecipitation studies have indicated that ELK1 recruits AR as a transcriptional co-activator (246). Other investigators have extended these studies to demonstrate that ELK1 is similarly required for androgen-dependent growth of bladder cancer (292, 293). Moreover, chromatin sites of AR binding are highly enriched for ELK1 binding DNA cis-elements (294).

ELK1 belongs to the ternary complex factor (TCF) sub-family of ETS proteins that characteristically bind to purine-rich GGA core sequences (295). ELK1 is activated through hyper-phosphorylation by ERK to transiently activate immediate early genes in association with the serum response factor (SRF) (261, 262, 295-297). Accordingly, ELK1 is one of many substrates of ERK1/2 that have variable types and combinations of recognition motifs for ERK (298-300). In the absence of hyper-phosphorylation, ELK1 is in a repressive association with many genes (301). However, ELK1 is expressed in the clinical spectrum of prostate tumors (266) and in PCa cells the activation of AR target growth genes through ELK1 was constitutive and did not entail hyper-phosphorylation or activation of immediate early genes (246). In this study, we now elucidate the physical basis for the interaction between ELK1 and AR in the context of growth dependency of PCa cells on ELK1.

3.2 Experimental Procedures

3.2.1 Cell culture and reagents

LNCaP, CWR22Rv1 cells and HeLa cell lines were from the American Type Culture Collection (Manassas, VA); 293FT cells were from Invitrogen. HeLa cells with a stably integrated minimal promoter-luciferase reporter containing five upstream Gal4 elements (Gal4-TATA-Luc) and expressing a Gal4-ELK1 fusion protein in which the Gal4 DNA binding domain was substituted for the ETS DNA binding domain of ELK1 were kindly provided by Dr. Johann Hofman (Innsbruck Medical University). These cells were then stably transduced with a vector expressing the full-length AR. Recombinant HeLa cells were also generated by stably transducing Gal4-TATA-Luc and a vector expressing the AR (A/B) domain fused to the VP16 transactivation domain [AR(A/B)-

VP16]. LNCaP cells were routinely grown at 37°C in 5% CO₂ in RPMI 1640 medium supplemented with 10% FBS (Invitrogen), 100 units/ml penicillin, 100 µg/ml streptomycin, 2mM L-glutamine mixture (Invitrogen); and sodium pyruvate (1mM) (Invitrogen). CWR22Rv1 cells were grown in phenol-red free RPMI 1640 medium supplemented with 10% FBS (Invitrogen), 100 units/ml penicillin, 100 µg/ml streptomycin, and 2mM L-glutamine mixture (Invitrogen). Parental and recombinant HeLa cells were grown in DMEM supplemented with 10% FBS and 100 units/ml penicillin, 100µg/ml streptomycin, 2mM L-glutamine mixture (Invitrogen). Additionally, the culture media for the recombinant HeLa cells included one or more of the following selection antibiotics: 100µg/ml Hygromycin (Invitrogen) (for Gal4-ELK1), 100µg /ml or 400ug/ml Geneticin (Invitrogen) (for Gal4-TATA-Luc) and 2 µg /ml Puromycin (Sigma-Aldrich) [for AR or AR(A/B)-VP16]. For hormone depletion, LNCaP cells were grown in phenol-red free RPMI 1640 medium supplemented with 10% heat-inactivated and charcoal-stripped FBS (Sigma) and 100 units/ml penicillin, 100µg/ml streptomycin, and 2mM L-glutamine mixture for 96 hours before each experiment. For hormone depletion, parental and recombinant HeLa cells were grown in phenol-red free DMEM supplemented with 5% heat-inactivated and charcoal-stripped FBS (Sigma) and 2mM L-glutamine for 48 hours before each experiment. Affinity-purified rabbit anti-human antibody to AR (sc-7305) and mouse antibodies to Gal4 (sc-510) and GAPDH (sc-47724) were purchased from Santa Cruz Biotechnology (Santa Cruz, CA). Rabbit monoclonal anti-human antibody to ERK1/ERK2 (ab17942), rabbit monoclonal anti-human to androgen receptor-ChIP grade antibody (ab74272), rabbit monoclonal anti-human antibody to ELK1 (ab32106) and Mouse monoclonal anti-human antibodies to

the Androgen Receptor (ab77557) and ELK1 (ab7712) were from Abcam (Cambridge, MA). R1881 was kindly provided by Dr. Steve Patrick (Wayne State University/Karmanos Cancer Institute, Detroit, MI). Testosterone was from Sigma-Aldrich. Lipofectamine™ 2000 was purchased from Thermo Scientific (product number 78410). Trametinib was purchased from Selleckchem. AKTi-1/2 was purchased from EMD Millipore (Darmstadt, Germany). esiRNAs were purchased from Sigma-Aldrich.

3.2.2 Purified proteins

Full length human AR expressed in insect cells and purified to >95% by affinity chromatography and FPLC chromatography (ab82609) was purchased from Abcam (Cambridge MA). Recombinant his-tagged ELK1 as well as his-tagged ELK1 mutated in both the D-box (Δ 308-321) and the DEF motif (F397L, P398A) expressed from baculovirus infected Sf9 cells were purified using nickel agarose affinity chromatography. The proteins were eluted with 200mM imidazole and dialysed against 20 mM HEPES, pH 7.9 containing 10% glycerol, 20mM KCl, 2mM MgCl₂, 0.2 mM EDTA, 0.5mM benzamidine and 0.5mM DTT. Purity of the proteins was estimated to be > 85% by SDS-polyacrylamide gel electrophoresis.

3.2.3 Surface plasmon resonance

Amine Coupling Kit, CM5 sensor chip and HBS-N buffer (GE Healthcare) were used for surface plasmon resonance (SPR) analysis. The rate and equilibrium binding constants of the interaction of AR with ELK1 or mutant ELK1 were determined using a Biacore 3000 (Biacore, Piscataway, NJ). Affinity-purified AR polypeptide (ligand) was immobilized on a CM5 research grade sensor chip by an amine coupling method (302). The immobilization involved activation of carboxymethyl groups on a dextran-coated

chip by reaction with *N*-hydroxysuccinimide, followed by covalent bonding of the ligand to the chip surface via amide linkages. Reference surfaces were prepared in the same manner but blocked with ethanolamine and thus contained no ligand. Kinetic binding analysis was carried out by injecting affinity-purified ELK1 polypeptide at different concentrations (0-160 nM) or mutant ELK1 (100 nM) into the flow cells (ligand and reference cell), and the interaction (response units, RU) between analyte and ligand was recorded as the ligand RU minus the reference RU. Kinetic values were determined using BIAevaluation software (Biacore), and the data were fitted with the model showing closest match (303, 304). A 1:1 Langmuir binding model was generally selected, in which all the sensorgrams representing the different analyte concentrations were fitted simultaneously with the wide window of association and dissociation phases. Individual concentration curves were also evaluated to confirm the fitting data. The equilibrium dissociation constant (K_d) was calculated by $K_d = k_{off}/k_{on}$.

3.2.4 Plasmids

The expression plasmid for human full length ELK1 in the pCMV plasmid was purchased from OriGene (Rockville, MD). The pLenti-GIII-CMV-hELK1 Lentiviral Vector was from Applied Biological Materials Inc. The Gal4-TATA-luc plasmid (pG5luc-Promega) and expression plasmid for VP16 and Gal4 were purchased from Promega (Madison, WI) (CheckMate Mammalian Two-hybrid System). The pRL plasmid encoding Renilla luciferase was purchased from Promega. The PatheDetect pFC-MEK1 *trans*-Reporter plasmid with a S218/222E point mutation and internal deletion between amino acid residues 32-51 rendering it constitutively active was from Stratagene. The pLVX-AR-V7 plasmid and pLVX control plasmid were a kind gift from Dr. Yan Dong from

Tulane University (New Orleans, LA). Construction of the (ELK1)₂-TATA-Luc plasmid and the ARE-TATA-Luc plasmid has been previously described (246). The Gal4-ELK1 fusion construct in which the DNA binding domain of ELK1 (amino acid residues 1-86) was deleted and replaced with the Gal4 DNA binding domain was constructed by PCR by using the ELK1-pCMV expression plasmid (Origene, Rockville, MD) as the template. The appropriate PCR primers were custom synthesized to generate the various amino-terminal and carboxyl-terminal deletion constructs of Gal4-ELK1 using the ELK1-pCMV expression plasmid as the PCR template and subcloned at *Bam*HI (upstream) and *Not*I (downstream) sites in the pBind vector expressing Gal4 fusions. The following ELK1 deletions reported previously (305) (i.e., pCMV5L ELK1 Δ31, pCMV5L ELK1 ΔD, pCMV5L ELK1 Δ32, pCMV5L ELK1 Δ32, pCMV5L ELK1 Δ24, pCMV5L ELK1 Δ19, pCMV5L ELK1 FxLa) were subcloned into the appropriate vectors. PCR primers were designed to subclone each of the ELK1 deletions into the pBind vector at *Bam*HI (upstream) and *Not*I (downstream) sites. All other ELK1 internal deletion and mutant constructs were generated using the The QuickChange II XL Site-Directed Mutagenesis kit (Agilent Technologies) according to the manufacturer's protocol. They include: Lentiviral ELK1 Δ308-321 and Lentiviral ELK1 FxLa, Gal4-ELK1Δ287-306, Gal4-ELK1Δ307-313, Gal4-ELK1Δ307-315, Gal4ELK1Δ400-407, Gal4-ELK1Δ331-340, and Gal4-ELK1Δ340-350.

The AR(A/B)-VP16 fusion construct was initially constructed using the VP16 expression plasmid from Promega. Using this plasmid as the PCR template, custom synthesized PCR primers were then used to amplify the AR(A/B)-VP16 sequence which was cloned into the pCDH-CMV-MCS-EF1-Puro cDNA Cloning and Expression Vector

(System Biosciences) at *NheI* (upstream) and *BamHI* (downstream) sites. The full length AR was subcloned from the pCMV expression vector (Origene) into the pCDH-CMV-MCS-EF1-Puro cDNA Cloning and Expression Vector (System Biosciences) at *NheI* (upstream) and *BamHI* (downstream) sites. Generation of the AR(A/B) expression plasmid in the pCDH vector has been described (246). Custom synthesized PCR primers were used to amplify and clone the five tandem Gal4 elements from the pG5luc vector into the pGreenFire1TM-mCMV-EF1-Neo (Plasmid) at *SpeI* (upstream) and *BamHI* (downstream) sites.

All of the plasmid constructs generated above were sent to either the Plant-Microbe Genomics Facility for DNA Sequencing at The Ohio State University (Columbus, OH) or to Genewiz (South Plainfield, NJ) to verify DNA sequences before the constructs were used in the studies.

3.2.5 siRNA mediated gene knockdown

The appropriate recombinant HeLa cells were plated in a 6-well plate (CytoOne, from USA Scientific) in DMEM media supplemented with 10% FBS and 2mM L-glutamine 24 hours before transfection. The following day cells were transfected with esiRNAs against ERK1 (MAPK3, 1ug) and ERK2 (MAPK1, 1ug) or 2µg of control siRNA using LipofectamineTM 2000.

3.2.6 Co-Immunoprecipitation

HeLa cells were transfected with the expression plasmid for AR and co-transfected with expression plasmid for wtELK1, ELK1 Δ 308-321 or ELK1 FxLa. Cells were harvested in radioimmune precipitation assay lysis buffer and 1X protease inhibitor mixture 48h post-transfection. Whole cell lysates (500µg) were pre-cleared for 2h using

protein A-agarose beads (Calbiochem). Immunoprecipitation was performed by first incubating 100 μ l of the protein A-agarose beads with 20 μ g of the anti-rabbit androgen receptor antibody (ab74272) or negative control for 4h. After washing the antibody bound beads three times, 500 μ g of the cell lysate was added and incubated at 4°C overnight under rotary agitation. At the end of the incubation, the complexes were washed five times with the radioimmune precipitation assay buffer. The western blot was probed with mouse monoclonal AR antibody (ab77557) and mouse monoclonal ELK1 antibody (ab7712).

3.2.7 Other experimental methods

Transient transfection and luciferase reporter assays, Checkmate mammalian two hybrid assay, Lentivirus mediated gene knockdown and gene expression, cell proliferation assay, western blot analysis, RNA isolation, reverse transcription, and real time PCR have been described in (246).

3.2.8 Statistical analysis

All experiments were performed in triplicate and repeated at least three times. The error bars in all graphs represent the standard deviation. Statistical analysis was performed using one-way ANOVA with post-hoc and LSD (Least Square Differences) and/or T-test using GraphPad v.6.0 software. The *P* values are indicated in the figure legends.

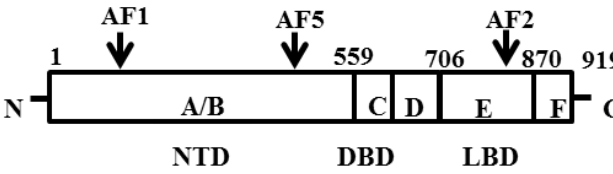
3.3 Results

3.3.1 Role of the amino-terminal A/B domain of AR in functional interactions with ELK1

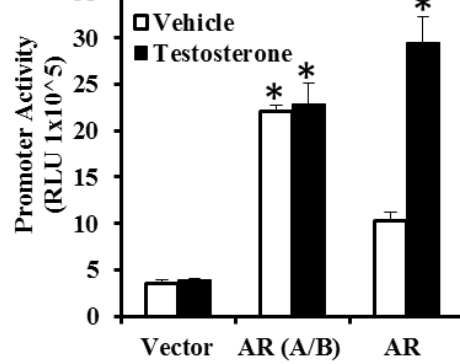
AR includes (i) an amino-terminal A/B domain containing ligand-independent transcriptional activation functions (AF1 and AF5), (ii) a carboxyl-terminal region (E and F domains) containing the ligand binding pocket and a ligand-dependent activation function (AF2) and (iii) internal DNA-binding and hinge domains (C and D domains) (Figure 3.1A). Typically, (e.g., in LNCaP cells) the binding of androgen is necessary for AR to localize in the nucleus, to associate with classical androgen response elements (AREs) and activate its gene targets. However AR has splice variants with carboxyl-terminal truncations that remove the ligand binding pocket; such variants are known to activate growth genes and support growth of PCa cells in a hormone-independent manner. Therefore we tested the ability of the A/B domain of AR to induce ELK1-dependent gene activation. In contrast to full-length AR the AR A/B domain does not require bound hormone for nuclear localization.

We first used a minimal TATA-dependent promoter luciferase construct in which two ELK1 binding cis-elements were placed upstream of the TATA box [(ELK1)₂-TATA-luc]. This construct was transfected along with an expression plasmid for either the full-length AR or the N-terminal A/B domain of AR into AR-negative HeLa cells. The full-length AR was able to activate the promoter in an androgen-dependent manner (Figure 3.1B). In contrast, the A/B domain activated the promoter to a comparable extent both in the presence and in the absence of hormone (Figure 3.1B). On the other hand, when the cells were transfected with the minimal promoter construct in which the ELK1 binding elements were substituted with a canonical androgen response element (ARE), promoter activation only occurred through the full-length AR and in the presence of

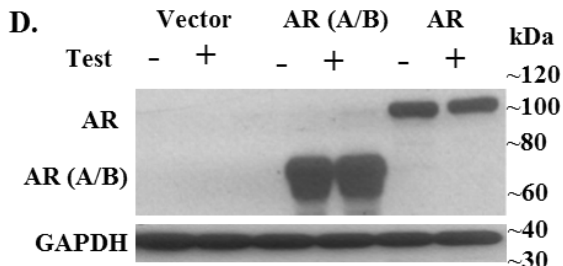
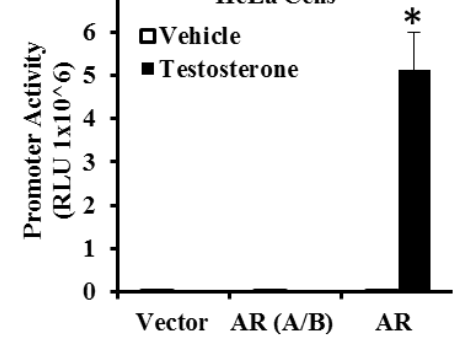
A.
Androgen Receptor



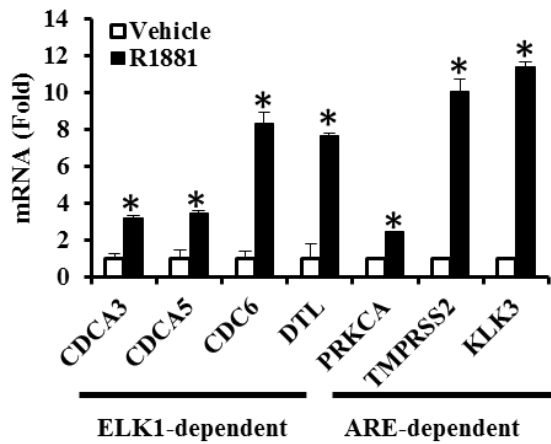
B. (ELK1)₂-TATA-Luc
HeLa Cells



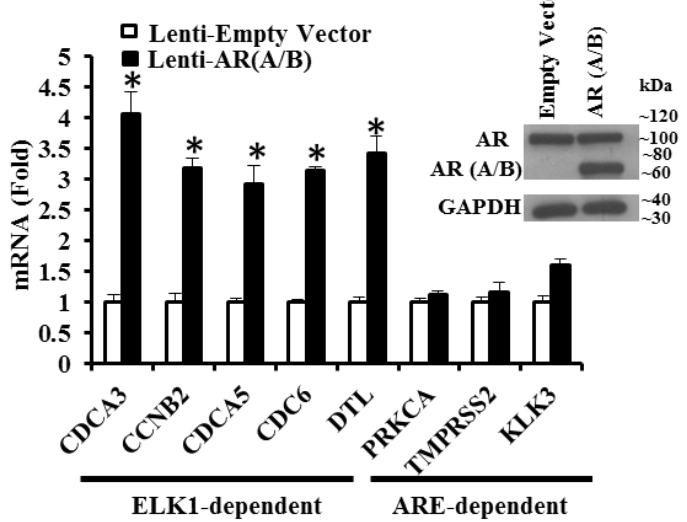
C. ARE-TATA-Luc
HeLa Cells



E. LNCaP Cells



F. LNCaP Cells



G. LNCaP Cells

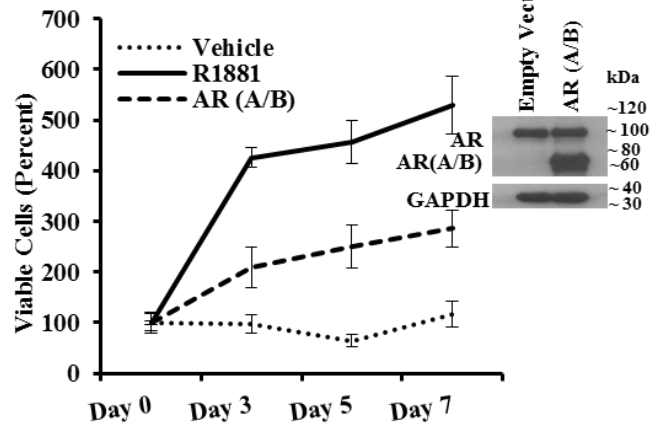


Figure 3.1 Adequacy of the A/B domain of AR for functional interactions of AR with ELK1. A shows a schematic for the organization of functional domains in AR. The A/B domain is the amino-terminal domain (NTD), which contains the ligand-independent activation functions AF1 and AF5. The C domain comprises the DNA binding domain (DBD) adjacent to a hinge region (D). The E domain encompasses the ligand binding domain (LBD) and the ligand-dependent activation function, AF2. The F domain represents the carboxyl-terminal domain. B and C, hormone-depleted HeLa cells were transfected with an ELK1-driven minimal promoter-luciferase reporter ((ELK1)₂-TATA-LUC) (B) or with an androgen-response element-driven minimal promoter-luciferase reporter (ARE-TATA-Luc) (C) and co-transfected with expression plasmids for the AR A/B domain, full-length AR, or the plasmid vector control. The cells were treated with either testosterone (10 nM) or vehicle at the time of transfection. Luciferase activity was measured in the cell lysates 48 h post-transfection. D shows a Western blot of lysates from cells transfected with expression plasmids for either the full-length AR or the AR A/B domain and treated with either testosterone (10 nM) or vehicle for 48 h and probed using an antibody to the amino-terminal domain of AR or with antibody to GAPDH (loading control). E, hormone-depleted LNCaP cells were treated with R1881 (1 nM) or vehicle for 48 h. Total RNA from the cells was used to quantify mRNA levels for the indicated genes that were known to be either ELK1-dependent or ARE-dependent for activation by AR. F, hormone-depleted LNCaP cells transduced using lentivirus expressing either the AR A/B domain or with control lentivirus. Cells were harvested 72 h after infection. Total RNA from the cells was used to quantify mRNA levels for the indicated genes that were known to be either ELK1-dependent or ARE-dependent for activation by AR. The inset shows cell lysates probed by Western blotting using an antibody to the amino-terminal domain of AR or with antibody to GAPDH (loading control). G, hormone-depleted LNCaP cells transduced using lentivirus expressing either the AR A/B domain or with control lentivirus. After 72 h, cells were plated in 96-well plates, and cell growth was monitored by the MTT assay. The vector control cells were treated with R1881 (1 nM) or vehicle 24 h after plating. The inset shows Western blotting analysis of cell lysates, 72 h post-infection, using antibody to the amino-terminal domain of AR or with antibody to GAPDH (loading control). For all transfections, a Renilla luciferase reporter was used as the control for transfection efficiency. In all panels, the error bars represent standard deviation of experimental triplicates. *, $p < 0.001$. *Reprinted by permission from Journal of Biological Chemistry Copyright 2016 (1).*

androgen (Figure 3.1C). Western blot analysis confirmed expression of both the full-length AR and AR(A/B) in the transfected cells (Figure 3.1D).

Next, we compared the abilities of AR(A/B) and the full-length AR to activate genes (CDCA3, CDCA5, CDC6 and DTL) previously shown to be activated by AR in an ELK1-dependent manner (246). We also tested for activation of genes (PRKCA, TMPRSS2 and KLK3) known to be activated by androgen (R1881) in an ARE-dependent manner. Androgen activated both classes of target genes in LNCaP cells, which express full-length AR (Figure 3.1E). However, when AR(A/B) was ectopically expressed in LNCaP cells in the absence of androgen (Figure 3.1F, inset), only the ELK1-dependent target genes were activated (Figure 3.1F). This result demonstrates that the A/B domain of AR is able to recapitulate ELK1-dependent gene activation by androgen plus AR.

Next, we tested whether the A/B domain of AR could support hormone-independent growth in LNCaP cells. AR(A/B) was ectopically expressed in LNCaP cells by lentiviral transduction and control cells were infected with non-expressing lentivirus (Figure 3.1G, inset). Growth of the control cells was dependent on androgen (Figure 3.1G). The A/B domain of AR was capable of supporting androgen-independent cell growth, albeit less robustly than androgen (Figure 3.1G).

Collectively, the data in Figure 3.1 demonstrate that the amino-terminal A/B Domain of AR is adequate for cooperation with ELK1 and for ELK1-dependent transcriptional activation. This hormone-independent action of the A/B domain is associated with partial recapitulation of androgen-dependent growth induced by full-

length AR. The A/B domain may represent the minimal structural unit of AR that is required for synergizing with ELK1.

3.3.2 Mapping the region(s) in ELK1 required for association with AR(A/B)

ELK1 consists of several functional domains. The amino-terminus comprises the A domain, encompassing the ETS DNA binding domain (263). The B domain interacts with SRF and directs ternary complex formation (264). The C domain resides at the C-terminus of the protein and regulates activation through phosphorylation by mitogen-activated protein kinases (MAPKs). The D domain is a docking site for MAPKs. There is also an additional MAPK docking site within the C domain, known as the DEF (Docking site for ERK, FXFP) motif (259, 306, 307). Segments of ELK1 that are required for association with the AR A/B domain were mapped using a mammalian two-hybrid assay. For the two-hybrid assay, we used HeLa cells in which a minimal promoter-luciferase reporter construct with Gal4 elements upstream of the TATA box (Gal4-TATA-Luc) was stably integrated. These cells also stably expressed the AR(A/B)-VP16 fusion protein. The recombinant HeLa cells were transfected with Gal4-ELK1 fusion constructs in which the DNA binding domain (amino acids 1-86) was replaced by that of Gal4. The reporter readout was used to assess the ability of the Gal4-ELK1 fusion proteins to associate with AR(A/B)-VP16. In parallel, HeLa cells stably expressing Gal4-TATA-Luc alone were co-transfected with each one of the Gal4-ELK1 constructs and an expression plasmid for a constitutively active mutant of MEK1 (CA-MEK1). Activation of Gal4-TATA-Luc by CA-MEK1 entails phosphorylation and functional association of ERK1/2 with Gal4-ELK1; therefore this parallel test probes the ability of each Gal4-ELK1 deletion/mutation construct to associate with and become activated by ERK1/2.

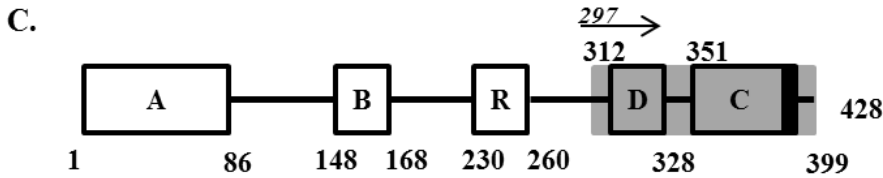
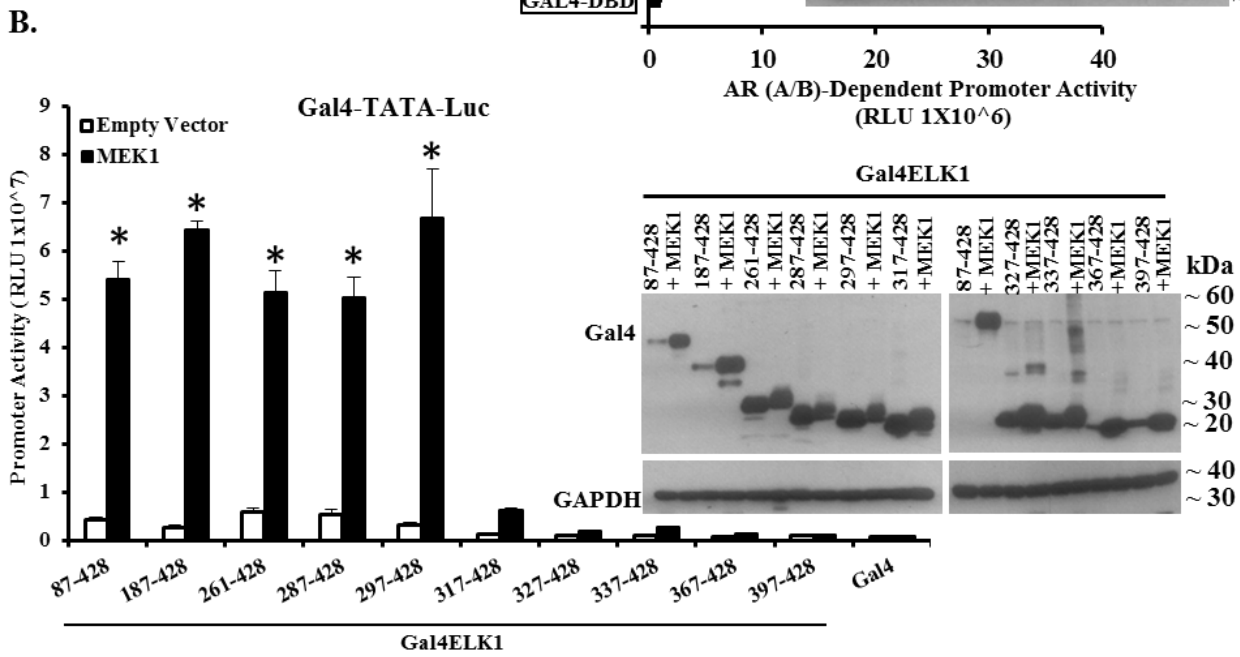
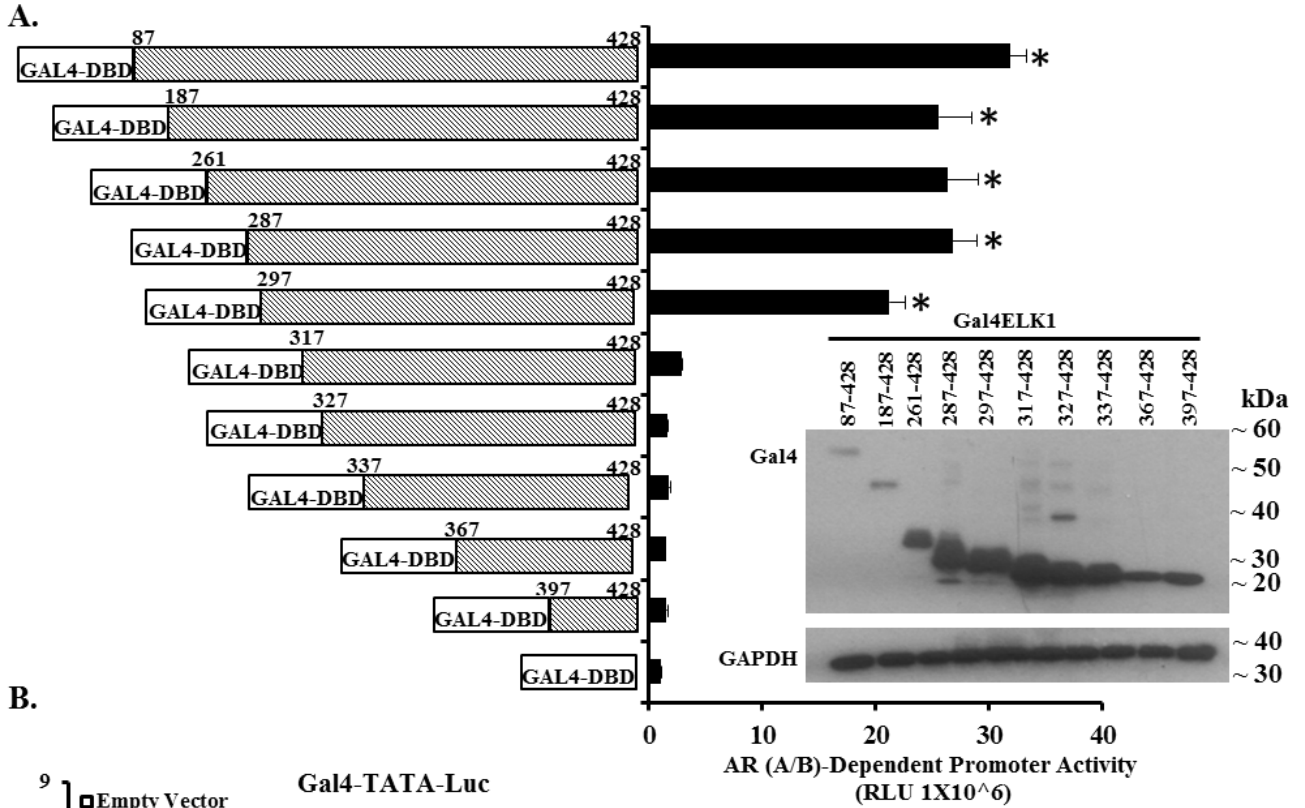


Figure 3.2 Mapping ELK1 polypeptide segments required for co-activation by AR(A/B) by amino-terminal deletion analysis. A shows data obtained using recombinant HeLa cells generated by stably transducing a minimal promoter-luciferase reporter containing upstream Gal4 elements (GAL4-TATA-LUC) and also with a vector expressing the AR A/B domain fused to the VP16 transactivation domain. Cells were transfected with plasmids expressing Gal4 fusion proteins of ELK1. The fusion constructs substituted the Gal4 DNA binding domain (Gal4-DBD) for the ETS DNA binding domain of ELK1. Within this fusion construct, a series of amino-terminal deletions were made, as indicated in the schematic in A. Forty eight hours after transfection with the various Gal4-ELK1 fusion constructs, cells were harvested by preparing lysates for measurement of luciferase activity. The promoter activity shown on the y axis required the presence of the AR A/B domain as knocking down AR(A/B) expression in the same cells transfected with full-length Gal4-ELK1 decreased the promoter activity to the basal value shown in the figure for Gal4-DBD alone. The inset shows cell lysates probed by Western blotting with antibodies against Gal4 or GAPDH (loading control). B shows data obtained using recombinant HeLa cells generated by stably transducing only GAL4-TATA-LUC. The cells were transfected with each of the Gal4-ELK1 fusion constructs used in A and co-transfected with an expression plasmid for a constitutively active mutant of MEK1 or with the vector control. Forty eight hours after transfection with the various Gal4-ELK1 fusion constructs, cells were harvested by preparing lysates for measurement of luciferase activity. The inset shows cell lysates probed by Western blotting with antibodies against Gal4 or GAPDH (loading control). C shows a schematic of the domain organization of ELK1; here, the amino-terminal deletion mapping of an ELK1 polypeptide segment encompassing residues required for association with AR(A/B) (data from A) is represented by gray shading. For all transfections, a Renilla luciferase reporter was used as the control for transfection efficiency. In all panels, the error bars represent standard deviation of experimental triplicates. *, $p < 0.001$. *Reprinted by permission from Journal of Biological Chemistry Copyright 2016 (1)*

First, Gal4-ELK1 constructs containing progressive deletions beginning from the amino-terminus were tested in the two-hybrid assay (Figure 3.2A). Expression of the transfected constructs was confirmed by western blot, using antibody to the Gal4 DNA binding domain (Figure 3.2A, inset). The reporter assay values were similar to the full length construct for deletions to positions 187, 261, 287 and 297. However, there was virtually a complete loss of reporter activity for deletions to positions 317, 327, 337, 367 and 397. These results map an element required for association of AR(A/B) to the region downstream of amino acid residue 297 of ELK1 (Figure 3.2A and schematic in Figure 3.2C). The parallel experiment testing activation of the Gal4-ELK1 constructs by CA-MEK1, showed a virtually identical pattern of activity (Figure 3.2B and inset), a result that is consistent with the position of the D-box region beginning at residue 312 (schematic in Figure 3.2C).

Next, Gal4-ELK1 constructs containing progressive deletions beginning from the carboxyl-terminus were tested in the two-hybrid assay (Figure 3.3A). Again, expression of the transfected constructs was confirmed by western blot (Figure 3.3A, inset). The reporter assay values were similar to the full length construct for the deletion made at position 397, but was lost for deletions to positions 387, 377 and 367. These results map an element required for association of AR(A/B) to the region upstream of amino acid residue 397 of ELK1 (Figure 3.3A and schematic in Figure 3.3C). The parallel experiment testing activation of the Gal4-ELK1 constructs by CA-MEK1 again showed the same pattern (Figure 3.3B and inset). This result is consistent with the position of the DEF motif, which serves as an additional ERK docking site (schematic in Figure 3.3C).

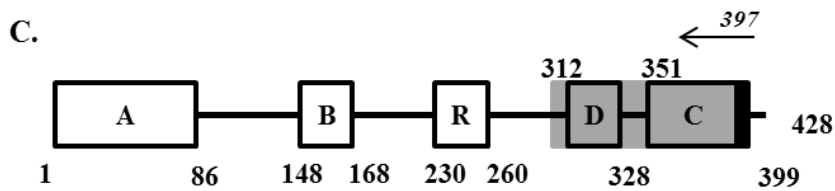
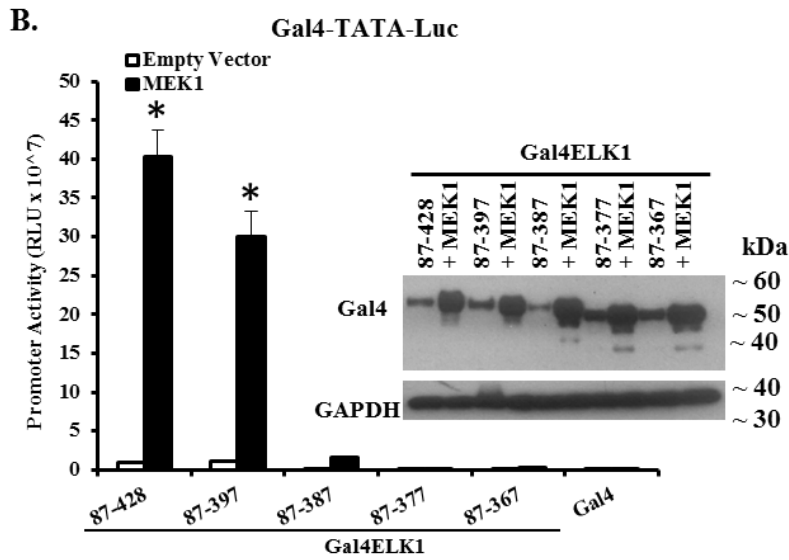
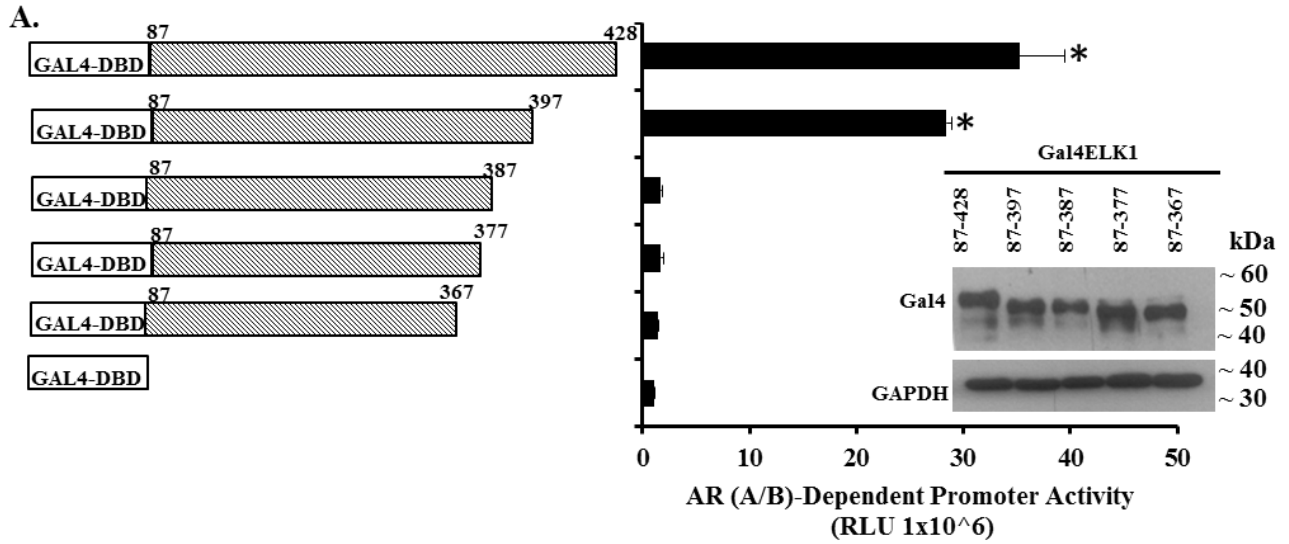
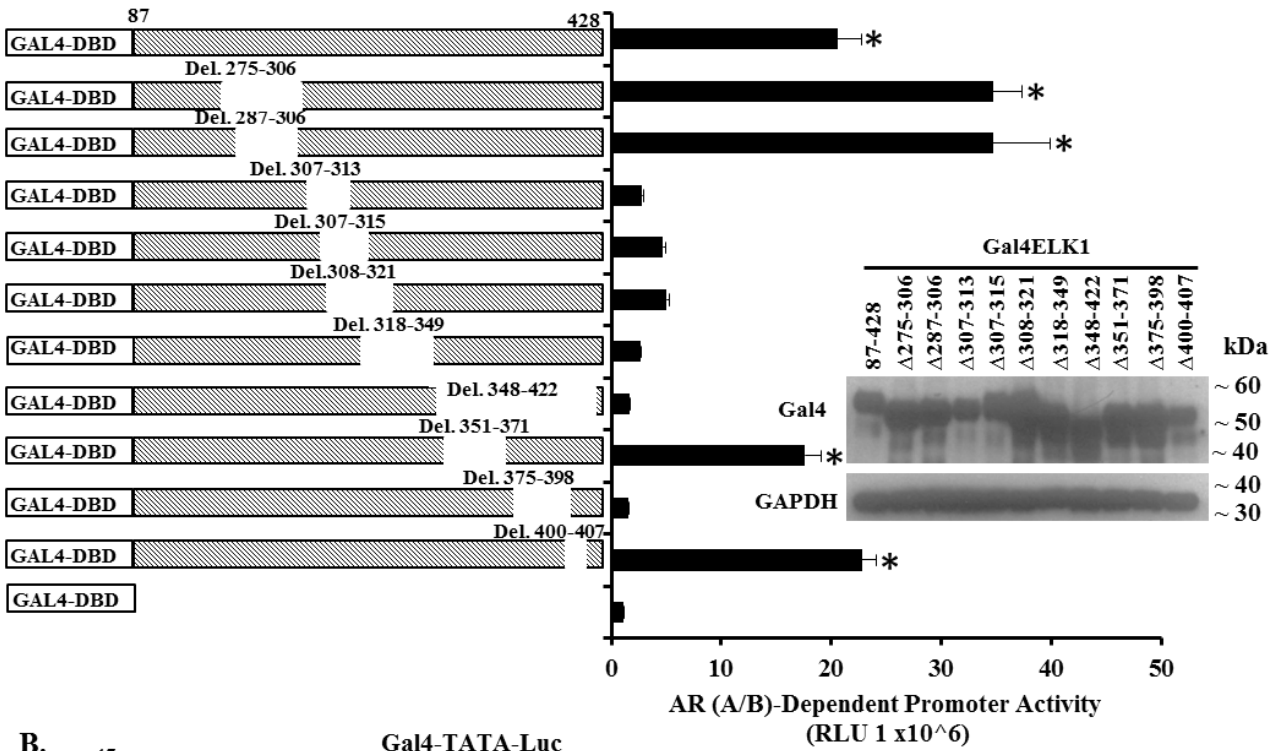


Figure 3.3 Mapping ELK1 polypeptide segments required for co-activation by AR(A/B) by carboxyl-terminal deletion analysis. A shows data obtained using recombinant HeLa cells generated by stably transducing a minimal promoter-luciferase reporter containing upstream Gal4 elements (*GAL4-TATA-LUC*) and also with a vector expressing the AR A/B domain fused to the VP16 transactivation domain. Cells were transfected with plasmids expressing Gal4 fusion proteins of ELK1. The fusion constructs substituted the Gal4 DNA binding domain (*Gal4-DBD*) for the ETS DNA binding domain of ELK1. Within this fusion construct, a series of carboxyl-terminal deletions were made, as indicated in the schematic in A. Forty eight hours after transfection with the various Gal4-ELK1 fusion constructs, cells were harvested by preparing lysates for measurement of luciferase activity. The promoter activity shown on the y axis required the presence of the AR A/B domain because knocking down AR(A/B) expression in the same cells transfected with full-length Gal4-ELK1 decreased the promoter activity to the basal value shown in the figure for Gal4-DBD alone. The *inset* shows cell lysates probed by Western blotting with antibodies against Gal4 or GAPDH (loading control). B shows data obtained using recombinant HeLa cells generated by stably transducing only *GAL4-TATA-LUC*. The cells were transfected with each of the Gal4-ELK1 fusion constructs used in A and co-transfected with an expression plasmid for a constitutively active mutant of MEK1 or with the vector control. Forty eight hours after transfection with the various Gal4-ELK1 fusion constructs, cells were harvested by preparing lysates for measurement of luciferase activity. The *inset* shows cell lysates probed by Western blotting with antibodies against Gal4 or GAPDH (loading control). C shows a schematic of the domain organization of ELK1; here, the carboxyl-terminal deletion mapping of an ELK1 polypeptide segment encompassing residues required for association with AR(A/B) (data from A) is represented by *gray shading*. For all transfections, a *Renilla* luciferase reporter was used as the control for transfection efficiency. In all panels, the *error bars* represent standard deviation of experimental triplicates. *, $p < 0.001$. Reprinted by permission from *Journal of Biological Chemistry* Copyright 2016 (1).

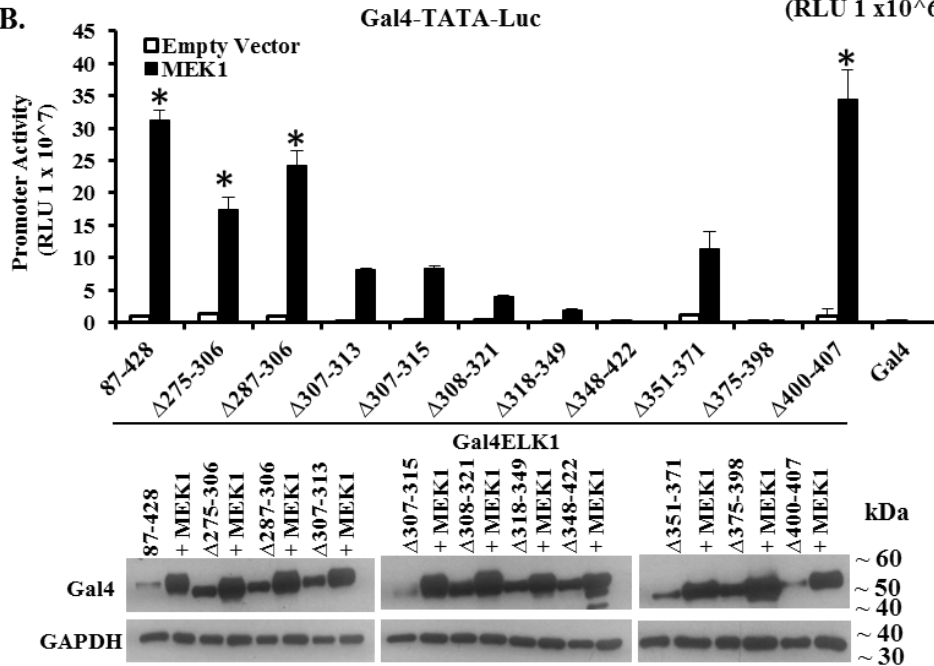
Additionally, we made and tested the effects of a series of short, overlapping internal deletions within Gal4-ELK1 (Figure 3.4A) using the two-hybrid assay. The internal deletions covered segments flanking and within the region mapped above by amino- and carboxyl-terminal deletion analyses. Expression of the Gal4-ELK1 constructs was confirmed by western blotting (Figure 3.4A, inset). As shown in Figure 3.4A, the reporter assay values for the constructs clearly fell into two groups – those corresponding to the activity of the full length construct and those approaching the background value obtained by transfecting the Gal4 DNA binding domain alone. Based on this data, we were able to confirm and further bracket peptide motifs required for association of AR(A/B) to within the amino acid sequences 307-350 and 372-397. Activation of the Gal4-ELK1 internal deletion constructs by CA-MEK1 followed a similar pattern except for the deletion 351-371 which reduced activation by CA-MEK1 but not association with AR(A/B)-VP16 (Figure 3.4B and inset). These results are again consistent with the locations of the ERK docking sites in ELK1 (D box and DEF motif) (schematic in Figure 3.4C). As residues 351-371 lie within the transactivation domain (domain C, residues 351-399) of ELK1 (schematic in Figure 4C) and includes two ERK phosphorylation sites (297) its requirement for optimal activation of ELK1 by CA-MEK1 was anticipated.

To further refine the mapping data for the motif required for association of AR(A/B) within the ELK1 polypeptide segment 307-350, we made additional deletions of residues 331-340 and 341-350 (Figure 3. 5A). Western blotting confirmed expression of the constructs (Figure 3.5B, inset). Neither deletion reduced the reporter activity in the two-hybrid assay (Figure 3. 5B), thus further bracketing the upstream element required

A.



B.



C.

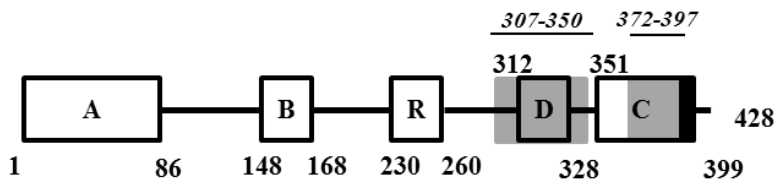
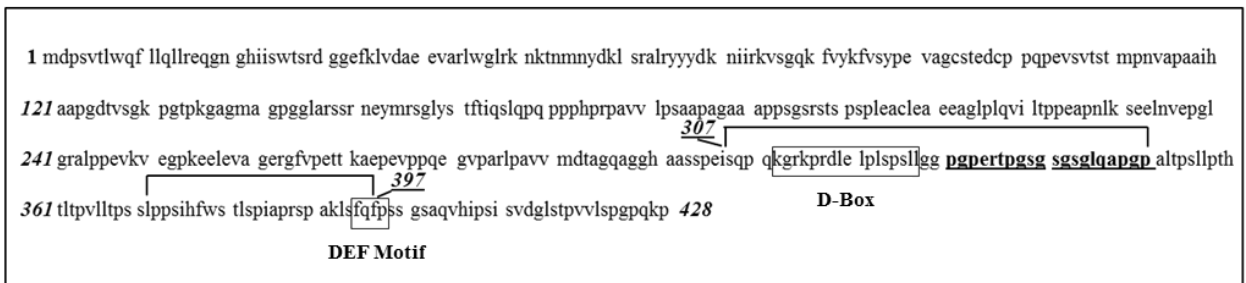
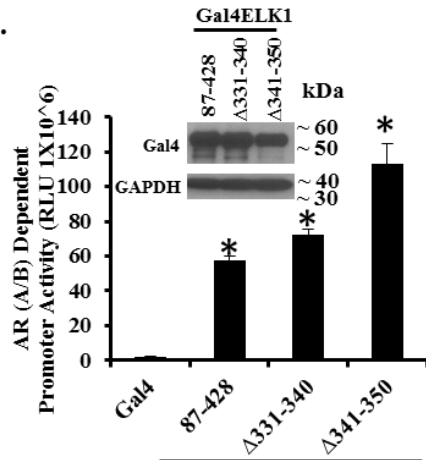


Figure 3.4 Mapping ELK1 polypeptide segments required for co-activation by AR(A/B) by internal deletion analysis. A shows data obtained using recombinant HeLa cells generated by stably transducing a minimal promoter-luciferase reporter containing upstream Gal4 elements (GAL4-TATA-LUC) and also with a vector expressing the AR A/B domain fused to the VP16 transactivation domain. Cells were transfected with plasmids expressing Gal4 fusion proteins of ELK1. The fusion constructs substituted the Gal4 DNA binding domain (Gal4-DBD) for the ETS DNA binding domain of ELK1. Within this fusion construct, a series of internal deletions were made, as indicated in the schematic in A. Forty eight hours after transfection with the various Gal4-ELK1 fusion constructs, cells were harvested by preparing lysates for measurement of luciferase activity. The promoter activity shown on the y axis required the presence of the AR A/B domain because knocking down AR(A/B) expression in the same cells transfected with full-length Gal4-ELK1 decreased the promoter activity to the basal value shown in the figure for Gal4-DBD alone. The inset shows cell lysates probed by Western blotting with antibodies against Gal4 or GAPDH (loading control). B shows data obtained using recombinant HeLa cells generated by stably transducing only GAL4-TATA-LUC. The cells were transfected with each of the Gal4-ELK1 fusion constructs used in A and co-transfected with an expression plasmid for a constitutively active mutant of MEK1 or with the vector control. Forty eight hours after transfection with the various Gal4-ELK1 fusion constructs, cells were harvested by preparing lysates for measurement of luciferase activity. The inset shows cell lysates probed by Western blotting with antibodies against Gal4 or GAPDH (loading control). C shows a schematic of the domain organization of ELK1; here, the deletion mapping of two ELK1 polypeptide segments encompassing residues required for association with AR(A/B) (data from Figs. 3A, ,44A, and and55A) is represented by gray shading of the two segments. For all transfections, a Renilla luciferase reporter was used as the control for transfection efficiency. In all panels, the error bars represent standard deviation of experimental triplicates. *, $p < 0.001$. *Reprinted by permission from Journal of Biological Chemistry Copyright 2016 (1)*

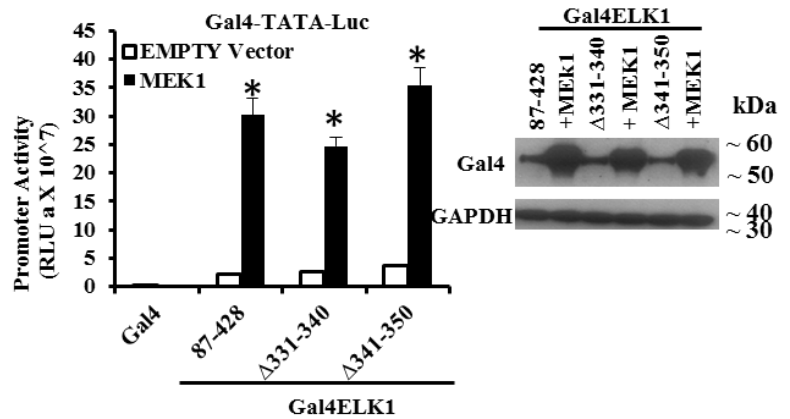
A.



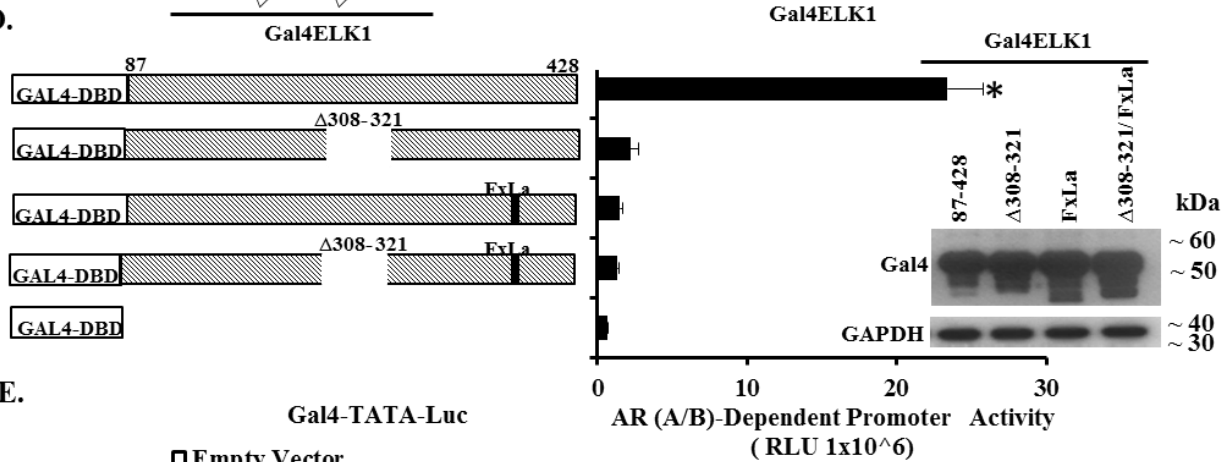
B.



C.



D.



E.

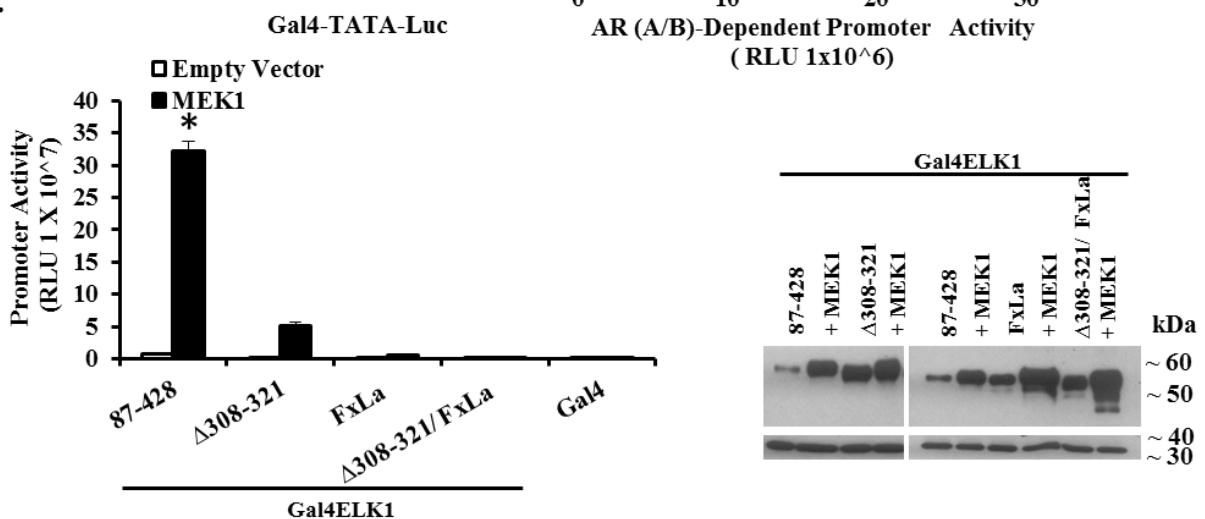


Figure 3.5 Further refinement of the mapping of ELK1 motifs required for co-activation by AR(A/B). A shows the ELK1 polypeptide sequence. The bracketed segments indicate the two segments that were mapped from the deletion analyses in Figs. 33–5 as regions containing residues essential for the association of ELK1 with AR(A/B). The boxed segments denote the D-domain of ELK1 and the FXFP motif of ELK1. The segments in bold font represent peptides that were deleted for further mapping in B and C. B and D show data obtained using recombinant HeLa cells generated by stably transducing a minimal promoter-luciferase reporter containing upstream Gal4 elements (GAL4-TATA-LUC) and also with a vector expressing the AR A/B domain fused to the VP16 transactivation domain. Cells were transfected with plasmids expressing Gal4 fusion proteins of ELK1. The fusion constructs substituted the Gal4 DNA binding domain (Gal4-DBD) for the ETS DNA binding domain of ELK1. Within this fusion construct, the indicated internal deletions or mutations were made, as indicated in the schematics in B and D. Forty eight hours after transfection with the various Gal4-ELK1 fusion constructs, cells were harvested by preparing lysates for measurement of luciferase activity. The promoter activity shown on the y axis required the presence of the AR A/B domain as knocking down AR(A/B) expression in the same cells transfected with full-length Gal4-ELK1 decreased the promoter activity to the basal value shown in the figure for Gal4-DBD alone. The insets in B and D show cell lysates probed by Western blotting with antibodies against Gal4 or GAPDH (loading control). C and E show data obtained using recombinant HeLa cells generated by stably transducing only GAL4-TATA-LUC. The cells were transfected with each of the Gal4-ELK1 fusion constructs used in B and D, respectively, and co-transfected with an expression plasmid for a constitutively active mutant of MEK1 or with the vector control. Forty eight hours after transfection with the various Gal4-ELK1 fusion constructs, cells were harvested by preparing lysates for measurement of luciferase activity. The insets in C and E show cell lysates probed by Western blotting with antibodies against Gal4 or GAPDH (loading control). For all transfections, a Renilla luciferase reporter was used as the control for transfection efficiency. In all panels, the error bars represent standard deviation of experimental triplicates. *, $p < 0.001$. *Reprinted by permission from Journal of Biological Chemistry Copyright 2016 (1)*

for association of AR(A/B) to within amino acid residues 307-330. These internal deletions also had no effect on activation of Gal4-ELK1 by CA-MEK1 (Figure 3.5C and inset). Finally, we tested whether the FQFP motif (FXFP motif) and the D-box region (residues 308-321), both of which direct ERK docking to ELK1, were also required for the association of AR(A/B) to ELK1. We tested a Gal4-ELK1 construct in which the FQFP motif was mutated to FQLA, a Gal4-ELK1 construct in which the D-box region (ELK1 residues 308-321) was deleted and a Gal4-ELK1 construct with both lesions. All three resulted in loss of function of AR(A/B)-VP16 in the two-hybrid assay (Figure 3.5D and inset), mirroring the loss of activation by CA-MEK1 (Figure 3.5E left and right).

Collectively, the data from Figures 3.2-3.5 identify two peptide motifs in ELK1 that are both essential for its association with the A/B domain of AR. The pattern of retention or loss of association with AR(A/B) due to the various deletions/mutations in ELK1 mirrored the pattern for activation by ERK with one exception, i.e., a deletion within the transactivation domain of ELK1, which disrupted activation by ERK but did not affect association with AR(A/B). The two ELK1 motifs required for association with AR(A/B) equate to the two ERK docking sites in ELK1.

3.3.3 ELK1 motifs required for association with the AR A/B domain participate in hormone-induced activation of ELK1 by full-length AR

To further validate the mapping of ELK1 motifs required for association with AR, it was necessary to confirm that the mapping data obtained above by the mammalian two-hybrid assay using AR(A/B)-VP16 applies to the full-length AR. For this purpose we tested Gal4-ELK1 fusion constructs with deletions and mutations that were indicative for

bracketing the binding sites for AR(A/B) (Figure 3.6A). Each of these constructs, as well as control constructs, were co-transfected with full-length AR into recombinant HeLa cells in which the Gal4-TATA-Luc promoter-reporter was stably integrated. The cells were treated with testosterone or the vehicle control beginning at the time of transfection. Androgen activated the promoter only in cells transfected with Gal4-ELK1 constructs that were found in the preceding sections to have the ability to bind AR(A/B) (Figure 3.6A). It was confirmed that both AR and the appropriate Gal4-ELK1 construct were expressed in the transfected cells, as observed by western blot using antibody to either Gal4 or AR (Figure 3.6B).

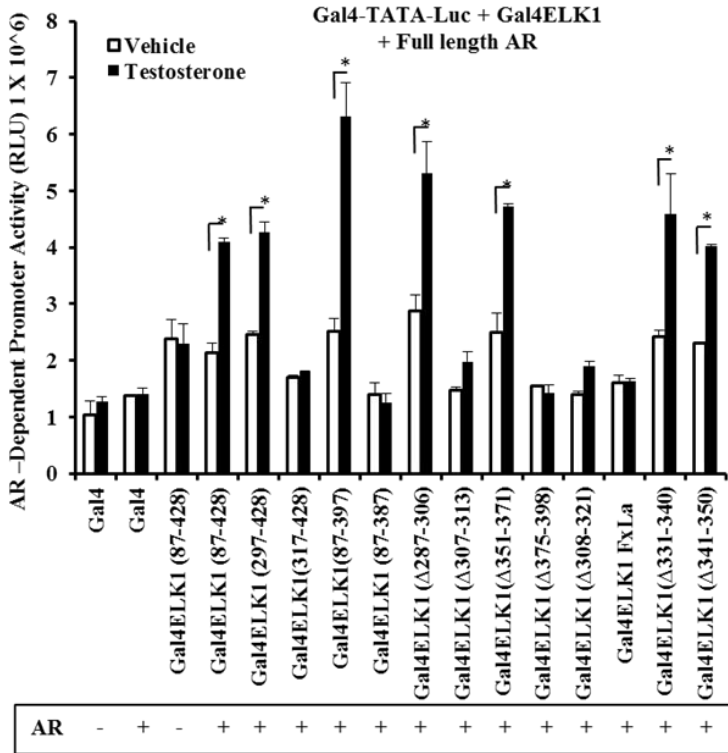
To complement the above data we co-expressed in HeLa cells, AR and wtELK1 or AR and a mutant of ELK1 in which either one of the two ERK docking sites was disrupted. AR and wtELK1 co-immunoprecipitated in these cells; however, when ELK1 was mutated at either one of its two ERK docking sites, it was unable to co-immunoprecipitate with AR (Figure 3.6C).

These results demonstrate that functional association of the full-length AR with ELK1 (or transcriptional co-activation of ELK1 by AR) requires the same ELK1 motifs as those mapped for the binding of AR(A/B) to ELK1.

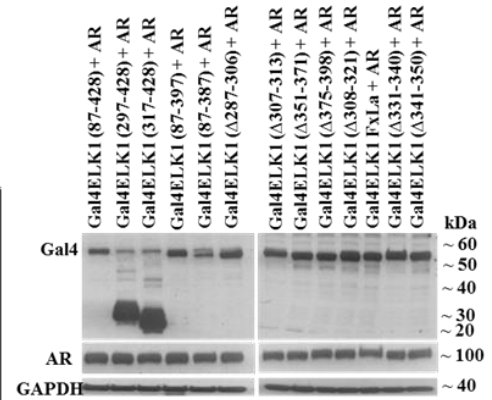
3.3.4 Influence of SRF on the interaction of AR with ELK1

Functional interactions between AR and ELK1 could be influenced by the association of ELK1 with its DNA binding partner, SRF. To explore this possibility we first used recombinant HeLa cells in which a minimal promoter-luciferase reporter construct with Gal4 elements upstream of the TATA box (Gal4-TATA-Luc) was stably integrated in the chromatin. The cells also stably expressed full-length AR and the Gal4-

A.



B.



C.

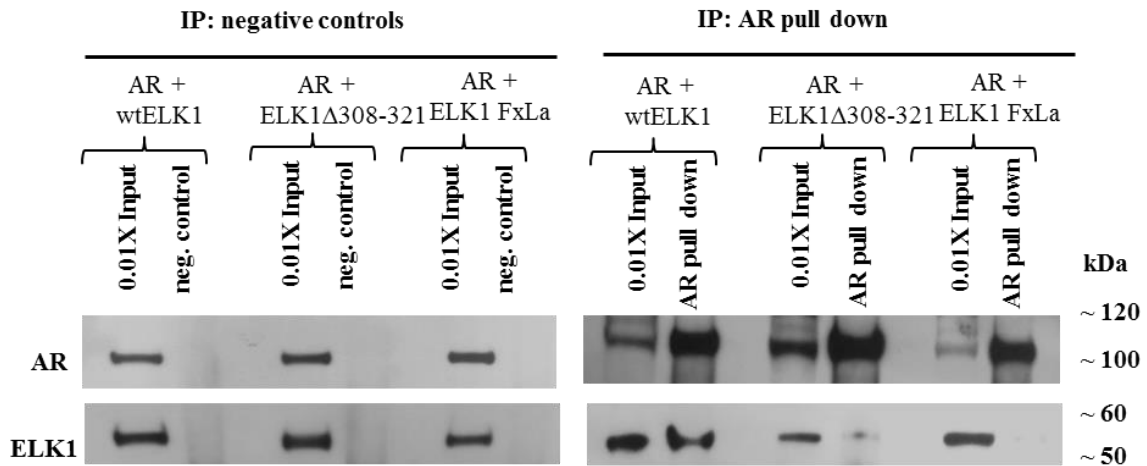


Figure 3.6 ELK1 motifs required for co-activation by full-length AR. A shows data obtained using recombinant HeLa cells generated by stably transducing a minimal promoter-luciferase reporter containing upstream Gal4 elements (GAL4-TATA-LUC). Cells were plated in hormone-depleted media and co-transfected with expression plasmids for the indicated Gal4-ELK1 fusion proteins and an expression plasmid for full-length AR. The fusion constructs substituted the Gal4 DNA binding domain (Gal4-DBD) for the ETS DNA binding domain of ELK1. At the time of transfection, the cells were treated with testosterone (10 nM) or vehicle control. Forty eight hours after transfection, cells were harvested by preparing lysates for measurement of luciferase activity. B shows cell lysates probed by Western blotting with antibodies against Gal4, AR, or GAPDH (loading control). C shows data on co-immunoprecipitation of ectopic AR and ectopic ELK1 or ELK1 mutants from HeLa cell lysates. HeLa cells were transfected with the expression plasmid for AR and co-transfected with an expression plasmid for WTELK1 or one of two ELK1 mutants, ELK1 Δ 308–321 and ELK1 FxLa. The lysates were immunoprecipitated (IP) using either antibody to AR or a negative control. The immunoprecipitates were probed by Western blotting using antibody to either AR or ELK1 as indicated. *, $p < 0.01$. . *Reprinted by permission from Journal of Biological Chemistry Copyright 2016 (1)*

ELK1 (87-428) fusion protein. Induction of reporter luciferase activity by testosterone was measured to quantify the binding of AR to ELK1. In these cells, lentiviral transduction with shRNA against SRF resulted in knocking down SRF at both the mRNA and protein levels compared to control shRNA (Figure 3.7A and inset). Knockdown of SRF significantly increased testosterone-induced luciferase activity (Figure 3.7B).

As a complementary approach, we used recombinant HeLa cells that stably expressed the AR(A/B) domain fused to the VP16 transactivation domain [AR(A/B)-VP16]. Additionally, the Gal4-TATA-Luc promoter-reporter was stably integrated in the chromatin. In these cells, we examined the effect of SRF knockdown on the hormone-independent activation of ELK1 by AR(A/B)-VP16. Cells were transduced with shRNA against SRF or with control shRNA followed by transfection with the Gal4-ELK1 fusion construct or with the Gal4 control vector. SRF shRNA substantially decreased both SRF mRNA and protein (Figure 3.7C and inset) and increased the luciferase reporter activity three-fold compared to cells transduced with control shRNA (Figure 3.7D). Taken together, these results demonstrate that SRF is not required for activation of ELK1 by AR; rather, SRF may hinder optimal ELK1-dependent transcriptional activation by AR.

3.3.5 Influence of ERK1/2 on the interaction of AR with ELK1

The requirement for MAPK docking motifs in ELK1 suggested the possibility that the functional association of AR with ELK1 could involve ERKs, the classical ELK1 activating protein kinases, as an essential component of the ELK1-AR complex. As a first test we used recombinant HeLa cells stably expressing AR(A/B)-VP16 in which the Gal4-TATA-Luc promoter-reporter was also stably integrated. These cells were co-

transfected with siRNAs against ERK1 and ERK2 or transfected with control siRNA. ERK mRNAs and proteins were depleted within 48 hours of siRNA transfection compared with the control siRNA (Figure 3.7E, top and bottom). Following knockdown of ERKs, the cells were transfected again, this time with expression plasmid for the Gal4-ELK1 fusion protein or the control Gal4 vector. In parallel, cells were also co-transfected with Gal4-ELK1 and the expression plasmid for CA-MEK1. The reporter luciferase activity was measured 24 hours following the second transfection (72 hours following the first transfection) while the knockdown of ERKs persisted (Figure 3.7E, top and bottom). The synergistic activation of the promoter-reporter by AR and ELK1 was unaffected by the combined depletion of ERK1 and ERK2 (Figure 3.7F). In contrast, the CA-MEK-induced hyper-activation of the promoter was abrogated by depletion of ERK1 and ERK2, decreasing the promoter activation to the level observed for cells only expressing AR(A/B) and Gal4-ELK1 (Figure 3.7F).

Next we tested whether AR(A/B) would compete with ERKs as activators of ELK1. We used recombinant HeLa cells in which the Gal4-TATA-Luc promoter-reporter was stably integrated and which also stably expressed the Gal4-ELK1 fusion protein. As expected, in these cells ectopic expression of CA-MEK1 strongly stimulated expression of the luciferase reporter (Figure 3.7G). However, co-expression of AR(A/B) decreased the promoter activation (Figure 3.7G), indicating that AR interferes with hyper-activation of ELK1 by ERKs.

In a third approach, the effect of ERK activity on the interaction ELK1 and AR was tested using HeLa cells co-transfected with the (ELK1)₂-TATA-luc reporter and an expression plasmid for either AR(A/B) or CA-MEK1. The (ELK1)₂-TATA-luc promoter is

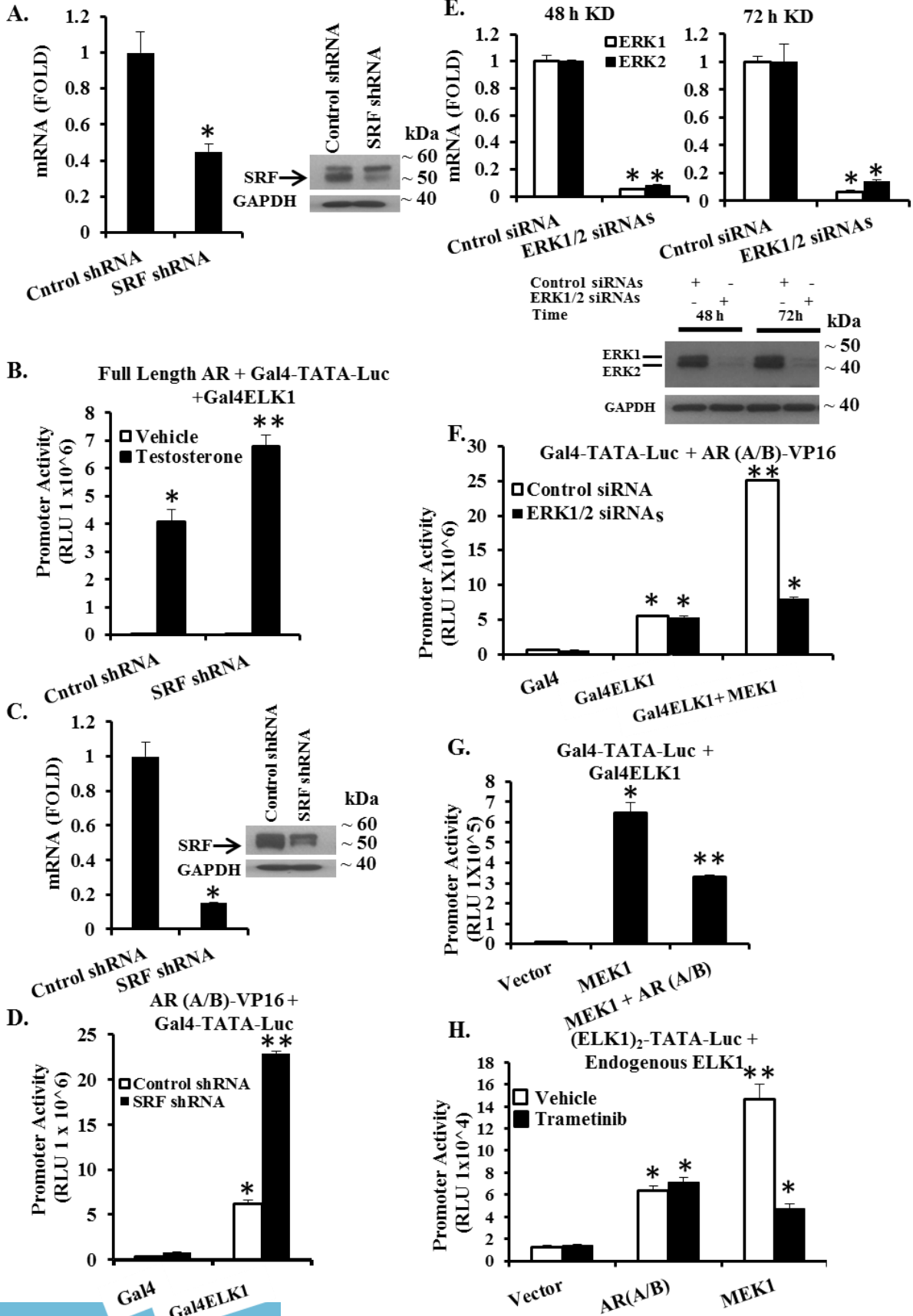


Figure 3.7 Effect of depleting SRF or ERK1/2 on the interactions of AR with ELK1.

A and B show data obtained using recombinant HeLa cells generated by stably transducing a minimal promoter-luciferase reporter containing upstream Gal4 elements (GAL4-TATA-LUC) and also with vectors expressing AR and a Gal4-ELK1 fusion construct in which the Gal4 DNA binding domain was substituted for the ETS DNA binding domain of ELK1. The cells were depleted of hormone and then transduced with shRNA against SRF or a non-targeted control shRNA using lentivirus. Seventy two hours after infection, cells were treated with testosterone (10 nm) or vehicle for a further 48 h. The cells were then harvested to quantify SRF mRNA (A) or for Western blotting analysis using antibody to SRF or to GAPDH (loading control) (A, inset) or for luciferase activity (B). C and D show data obtained using recombinant HeLa cells generated by stably transducing GAL4-TATA-LUC and also a vector expressing the AR A/B domain fused to the VP16 transactivation domain (AR(A/B)-VP16). The cells were transduced with shRNA against SRF or a non-targeted control shRNA using lentivirus. Seventy two hours after infection, the cells were transfected with expression plasmid for the Gal4-ELK1 fusion protein. Forty eight hours later, the cells were harvested to quantify SRF mRNA (C) or for Western blotting analysis using antibody to SRF or to GAPDH (loading control) (C, inset) or to measure luciferase activity (D). E–G show data obtained using the recombinant HeLa cells with stably incorporated GAL4-TATA-LUC and stably expressing the AR(A/B)-VP16 fusion protein. Cells were transfected with a mixture of siRNA against ERK1 and ERK2 or with control non-targeted siRNA. After 48 h of transfection, the cells were harvested to quantify mRNAs for ERK1 and ERK2 (E) or for Western blotting analysis using antibody to ERK1/2 or to GAPDH (loading control) (E, below); the remaining cells were transfected for a second time with the Gal-4ELK1 expression plasmid or the control vector plasmid or the plasmid for constitutively active mutant of MEK1 (F). After a further 24 h, the cells were harvested to quantify mRNAs for ERK1 and ERK2 (E) or for Western blotting analysis using antibody to ERK1/2 or to GAPDH (loading control) (E, below) or to measure luciferase activity (F). H, HeLa cells were co-transfected with an ELK1-driven minimal promoter-luciferase reporter ((ELK1)²-TATA-LUC) and expression plasmid for either AR(A/B) or constitutively active MEK1 or control vector plasmid. The cells were treated with trametinib (1 μm) or vehicle for 48 h beginning with the time of transfection. Luciferase activity was measured in the cell lysates. For all transfections, a Renilla luciferase reporter was used as the control for transfection efficiency. In all panels, the error bars represent standard deviation of experimental triplicates. *, p < 0.001; **, p < 0.001. *Reprinted by permission from Journal of Biological Chemistry Copyright 2016 (1)*

responsive to the endogenous ELK1 in the cells. Following the transfections, the cells were treated with the MEK inhibitor, trametinib. As expected, MEK-induced activation of the promoter was inhibited by trametinib (Figure 3.7H). In contrast, trametinib did not affect activation of the promoter by AR(A/B). The results from the complementary approaches of depletion and inhibition of ERK1/2 and competition between MEK1 and AR(A/B) as activators of ELK1 all demonstrate that the functional interaction of AR and ELK1 is insensitive to the expression or activation status of ERKs. The data indicates that the association of AR with ELK1 occurs independently of ERK1 and ERK2.

3.3.6 Direct binding of AR and ELK1

The studies above indicate that the classical binding partners of ELK1, i.e. SRF and ERK1/2, interfere with rather facilitate functional association of AR with ELK1. Therefore, to test whether the association of AR with ELK1 could be due to direct binding, we used surface plasmon resonance (SPR). Purified AR (Abcam, Cambridge, MA) was immobilized as the “ligand”. His-tagged ELK1 and his-tagged mutant ELK1 in which both the D-box and the DEF motif were disrupted (Δ 308-321, F397L, P398A) were affinity purified to >85% percent (Figure 3.8A) and used as the analyte. The binding kinetics for ELK1 was determined at concentrations of 0, 5, 10, 20, 40, 80, and 160 nM (Figure 3.8B). Bovine serum albumin was used as the negative control. Kinetic constants were evaluated using the BIAevaluation software. The equilibrium dissociation constant for the AR-ELK1 interaction was determined to be 1.9×10^{-8} M. When the mutant ELK1 was used as the analyte at a concentration of 100nM the average response from triplicate measurements was reduced by ~90 percent compared with 100nM ELK1 (Figure 3.8C). The relatively high affinity of binding of purified

preparations of AR and ELK1 strongly supports the concept that the *in situ* interactions of the two proteins are due to direct binding. Moreover, loss of this binding due to disruption of the ERK docking sites in ELK1, strongly indicate that these are also the docking sites for AR.

3.3.7 Relevance of the physical association of ELK1 and AR to androgen-dependent cell growth

Previous studies using ELK1 depletion methods have demonstrated that both prostate and bladder cancer cells require ELK1 for androgen-dependent growth (246, 292, 293). However, they did not test the physiological effect of disrupting the association of ELK1 with AR. To disrupt the hormone-dependent association of AR and ELK1 *in situ* without disrupting the ability of ELK1 to bind to DNA, we used an ELK1 mutant lacking the D-box region (amino acids 308-321) that should compete with endogenous ELK1 for binding to chromatin. We tested whether the mutant ELK1 would produce a dominant-negative effect on androgen-dependent growth. LNCaP cells were transduced with lentiviral expression vectors for either ELK1 or the ELK1 Δ 308-321 mutant (Figure 3.8D, inset). Ectopic overexpression of ELK1 did not appreciably influence androgen (R1881)-dependent growth compared with the vector-transduced control (Figure 3.8D). In contrast, ectopic overexpression of the ELK1 Δ 308-321 mutant showed a dominant-negative effect by inhibiting hormone-dependent growth. To confirm that the dominant-negative effect of this ELK1 Δ 308-321 on androgen-dependent growth was not due to dependence on activation of ELK1 by ERK, we demonstrate that LNCaP growth is insensitive to inhibition of MEK by trametinab (Figure 3.8E); as a control in Figure 3.8E, the AKT inhibitor AKTi-1/2 completely inhibited

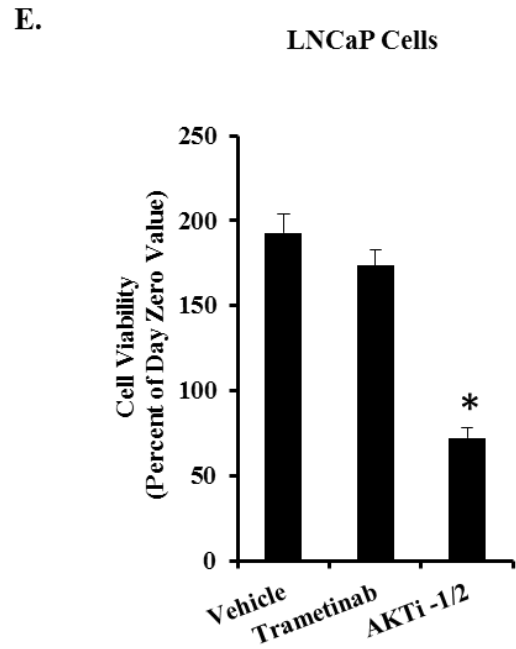
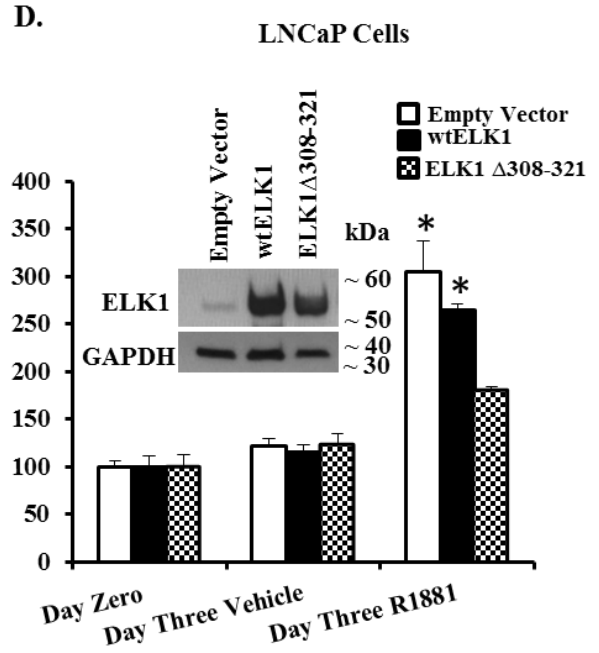
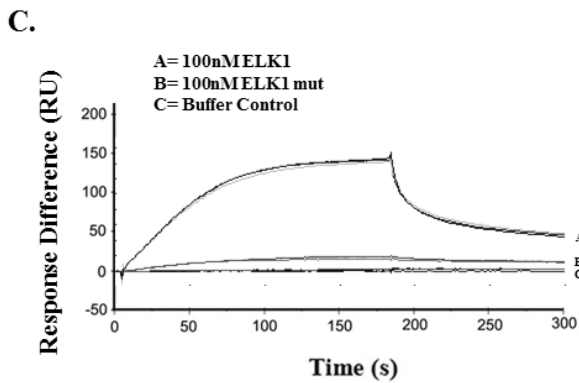
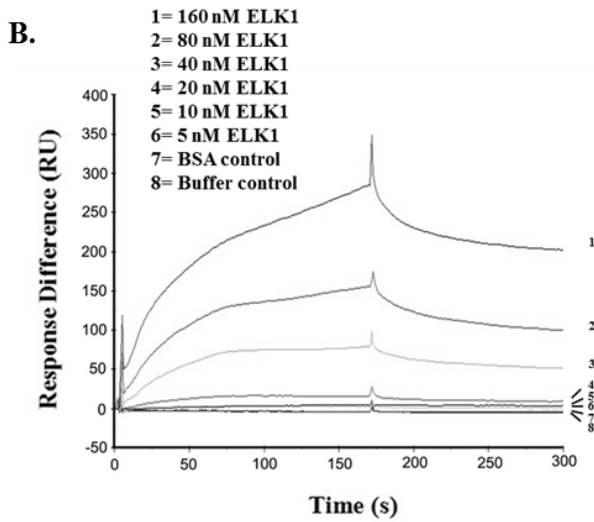
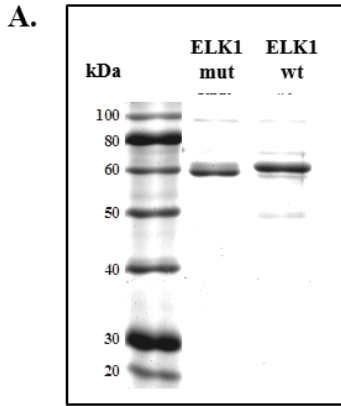


Figure 3.8 Direct binding of ELK1 and AR and the effect of disrupting docking sites in ELK1 on AR binding and androgen-dependent cell growth. A shows SDS-PAGE of purified His-tagged ELK1 protein and His-tagged ELK1 protein mutated (ELK1 mut) in both D-box ($\Delta 308-321$) and DEF motif. The protein bands were visualized by Coomassie Blue staining and estimated to be >85% pure and used in the SPR experiments below together with purified AR obtained commercially. B shows SPR kinetic curves for quantitative analyses of AR binding to His-tagged ELK1. AR was immobilized on a CM5 sensor chip, and ELK1 was diluted in a series of concentrations (0, 5, 10, 20, 40, 80, and 160 nM). The results were normalized by subtracting the SPR response (RU) for buffer alone or BSA and performed in duplicate. C shows SPR kinetic curves for quantitative analyses of AR binding to His-tagged mutant ELK1. AR was immobilized as in B, and ELK1 or mutant ELK1 was used at 100 nM. The kinetic curves for triplicate determinations are shown. D, hormone-depleted LNCaP cells were transduced using lentivirus expressing either the WTELK1, or ELK1($\Delta 308-321$), or with control lentivirus. After 72 h, cells were plated in 96-well plates, and cell growth was monitored by the MTT assay. Twenty four hours after plating, the cells were treated with R1881 (1 nM) or vehicle for a further 72 h. The inset in D shows Western blotting analysis of cell lysates, 72 h post-infection, using antibody to ELK1 or with antibody to GAPDH (loading control). The error bars represent standard deviation of experimental triplicates. *, $p < 0.001$. E, hormone-depleted LNCaP cells were plated in 96-well plates in the presence of R1881 (1 nM) together with vehicle, trametinib (1 μM), or AKTi-1/2 (2 μM). MTT assay was performed 72 h later. The error bars represent standard deviation of experimental triplicates. *, $p < 0.001$. *Reprinted by permission from Journal of Biological Chemistry Copyright 2016 (1)*

androgen-dependent growth. These results further validate the model that docking of AR on ELK1 is an essential component of growth signaling by androgen/AR in prostate cancer cells.

3.3.8 Synergy between the splice variant AR-V7 and ELK1 and AR-V7 dependent cell growth

The ability of the amino-terminal A/B domain of AR to synergize with ELK1 suggested that AR-V7, the major splice variant of AR, would most likely also synergize with ELK1. To test this possibility we co-transfected the (ELK1)₂-TATA-luc promoter-reporter construct with an expression plasmid for AR-V7 and wtELK1 into the AR-negative HeLa cells. Ectopic AR-V7 activated the promoter driven luciferase activity well above the basal level presumably associated with endogenous ELK1 (Figure 3.9A). Similarly, when the Gal4-TATA-luc promoter was co-transfected with Gal4-ELK1 and AR-V7, there was strong induction of promoter activity (Figure 3.9B). Western blot analysis confirmed expression of the AR-V7 construct in both cases (Figure 3.9C).

We have previously demonstrated that ELK1 is necessary for androgen/AR-dependent growth of prostate cancer cells. To test whether prostate cancer cells that are dependent on AR-V7 also depend on ELK1, we used shRNA to deplete ELK1 in CWR22Rv1 cells, which depend on endogenous AR-V7. Partial depletion of ELK1 prevented the growth of these cells (Figure 3.9D, top and bottom panels).

These results confirm that the AR-V7 splice variant cooperates with ELK1 as a transcriptional co-activator in the same manner as AR(A/B) and that ELK1 is also necessary for AR-V7 dependent growth of prostate cancer cells.

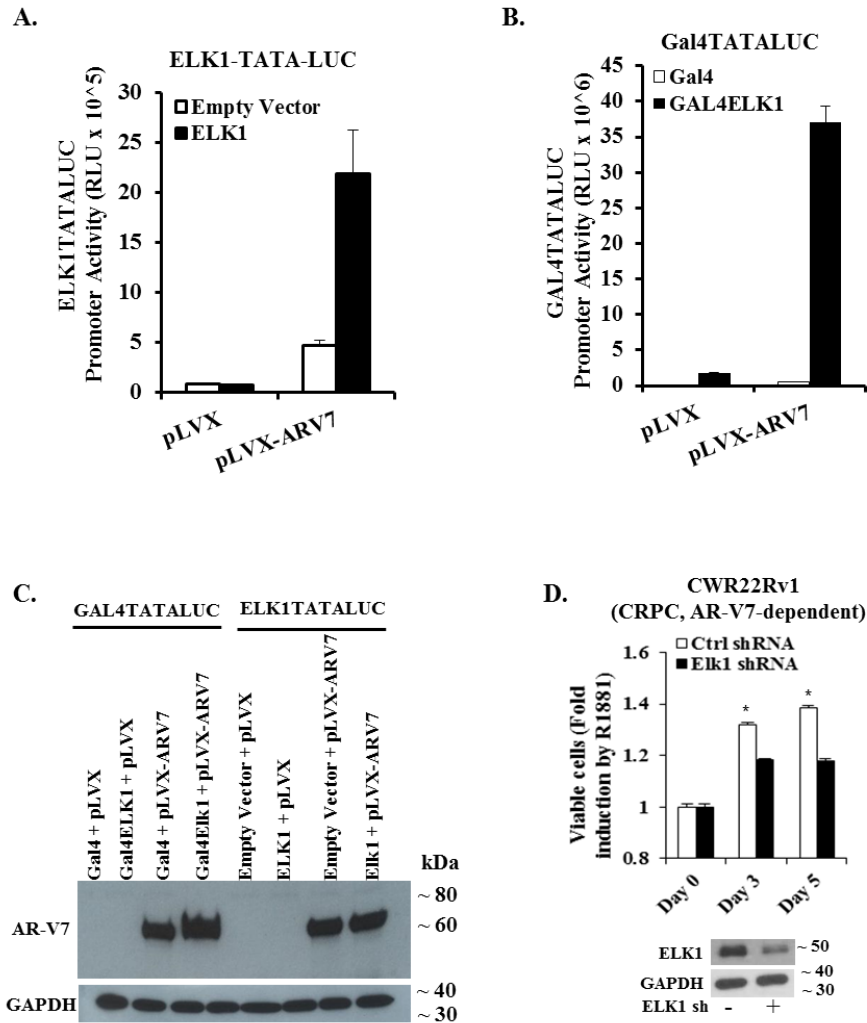


Figure 3.9 Functional association of ELK1 and AR-V7 and effect on cell growth. A, HeLa cells were co-transfected with an ELK1-driven minimal promoter-luciferase reporter ((ELK1)₂-TATA-LUC) and expression plasmid for either AR-V7 or WTELK1 or control vector plasmid for 48 h. Luciferase activity was measured in the cell lysates. For all transfections, a Renilla luciferase reporter was used as the control for transfection efficiency. B, HeLa cells were co-transfected with a Gal4-driven minimal promoter-luciferase reporter (Gal4-TATA-Luc) and expression plasmid for either AR-V7 or Gal4-ELK1 or control vector plasmid for 48 h. Luciferase activity was measured in the cell lysates. For all transfections, a Renilla luciferase reporter was used as the control for transfection efficiency. C shows a Western blot of HeLa cell lysates corresponding to all of the transfections in A and B, which was probed using an antibody to the amino-terminal domain of AR or with antibody to GAPDH (loading control). D, top panel shows the effect of depleting ELK1 by lentiviral shRNA transduction on the growth of CWR22Rv1 cells monitored by the MTT assay compared with control shRNA. The Western blot in the bottom panel shows ELK1 shRNA-induced depletion of ELK1 compared with control shRNA; GAPDH was probed as the loading control. *Reprinted by permission from Journal of Biological Chemistry Copyright 2016 (1)*

3.4 Discussion

The results of this study elucidate the nature of the interaction of the ligand-independent A/B domain of AR with ELK1 that accounts for the ELK1-dependent transcriptional activity of AR in PCa cells. Systematic mapping using a mammalian two-hybrid assay and an extensive series of ELK1 deletion and point mutants, and confirmatory co-immunoprecipitation experiments, identified the two ERK docking motifs (D-box and DEF motif) in ELK1 as the elements essential for co-activation by AR. Nonetheless, the AR synergy with ELK1 is independent of ERKs and involves AR binding directly to ELK1. Interactions with ELK1 are required for hormone-dependent growth of PCa cells and also account for the ability of the AR A/B domain, as well as the major AR splice variant AR-V7, to support their hormone-independent growth. Indeed the results strongly support the view that synergy with ELK1, via AR docking on ELK1, is a critical component of growth signaling by AR and AR-V7.

The mammalian two-hybrid mapping data with Gal4ELK1 mutants were clear-cut. Parallel studies using a constitutively active form of MEK to activate ELK1 demonstrated that the regions required for co-activation by AR(A/B) precisely coincided with the D-box and DEF motifs in ELK1 (298-300). Activation was hormone independent as, in contrast to full length AR, the A/B domain is not constrained by the need for ligand binding to enter the nuclear compartment. Importantly, mapping data for the sites of interaction of the AR A/B domain with ELK1 were entirely recapitulated with full length AR and confirmed by co-immunoprecipitation. There were two notable differences between co-activation of ELK1 by AR and activation by MEK. First, the level of ELK1 transcriptional activity induced by MEK was substantially higher than that induced by AR. This

difference in magnitude is associated with the transient nature of ELK1 activation through the MAPK pathway in contrast to the constitutive ELK1-dependent activation of growth genes by AR (246). Second, an intact ELK1 transactivation domain was essential for activation by MEK but not for co-activation of ELK1 by AR. This finding indicates that AR only utilizes ELK1 for recruitment to regulatory sites in chromatin to activate growth genes and that the transcriptional activity per se of ELK1 is unimportant for the ELK1-AR synergy.

Complementary approaches, including one- and two-hybrid assays, promoter assays, gene knockdown, MEK inhibition and competition assays demonstrated that the classical binding partners of ELK1 in the TCF complex, i.e. SRF and ERKs (307), are not required for co-activation of ELK1 by AR. Indeed, SRF and ERKs both appeared to interfere with the interaction of AR with ELK1. SRF knockdown may release ELK1 from immediate early gene promoters, which are unresponsive to androgen (246). Similarly, ELK1 recruits ERKs directly to a subset of target genes (308) suggesting that ERK competes directly with AR for ELK1 binding. Indeed SPR confirmed binding between ELK1 and AR with a relatively high affinity (K_d , 1.9×10^{-8} M), strongly supporting the premise that the transcriptional synergy between ELK1 and AR is due to direct binding. Loss of this binding upon mutational disruption of the ERK docking sites in ELK1 equates the ELK1 motifs required for functional association with AR with those required for direct binding of AR to ELK1.

ETS elements are commonly enriched at or in the vicinity of AR binding sites in the chromatin (269, 309) and indeed physical association of AR has been suggested with ETV1 (310) and ETS1 (309). However, in neither case has the structural binding

elements in either AR or the ETS protein been elucidated. Among the known DNA binding proteins that have been suggested to recruit AR, the interactions of AR with HoxB13 and C/EBPa are perhaps the best studied. HoxB13 interacts with the DNA binding domain of AR (242) whereas C/EBPa did not show a strong AR domain selectivity for interaction and its association with AR involved multiple AR domains (245). Relatively little is known about the structural basis for non-genomic interactions of AR and other nuclear receptors with signaling pathways involving MAPK, PI3K/Akt, PKC, PLC and GPCR (275). Notable exceptions include the direct or indirect associations of NRs with the Src SH2 or SH3 domains where proline-rich motifs in AR and the progesterone receptor or LXXL motifs in the estrogen receptor are required (311-314). The relatively large size and multi-domain structure of NRs appears to offer a diversity of binding motifs for interactions with co-activators and DNA binding transcription factors.

To our knowledge the functional interaction of AR with ELK1 is the first demonstration of a nuclear receptor co-opting protein kinase docking sites to regulate or constitutively activate a signaling pathway. The finding that ERK docking motifs can recruit AR suggests that AR may adopt similar modes of interaction in its crosstalk with other signaling molecules. Certainly, by mimicking ERK interactions with docking motifs, AR may interact with additional substrates of ERK, of which there are over fifty (298). There is much crosstalk between AR genomic and non-genomic pathways in prostate cancer. The canonical pathway for AR signaling requires nuclear translocation of the ligand bound receptor to activate transcription and induce proliferation in PCa cells. Activation of the MAPK phosphorylation cascade can be induced through non-genomic

pathways of AR signaling and stimulate cell proliferation. Activated ERK can phosphorylate AR and its coactivators, and therefore this feedback loop of the non-genomic AR signaling may induce genomic AR signaling in prostate cancer (315, 316). These are pathways that are well known in the literature pertaining to PCa; however these classical genomic and non-genomic AR signaling pathways are independent of the AR tethering mechanism and the ability of AR to co-opt the ERK docking sites in ELK1 to activate transcription.

Overexpression of an ELK1 docking site mutant in which the ability to associate with AR was disrupted without disrupting the DNA binding domain, had a dominant-negative effect on androgen-stimulated growth in PCa cells. This was unrelated to loss of ERK binding in the mutant ELK1 as the cells were insensitive to MEK inhibition. As the discrete DNA binding domain in the mutant ELK1 was not compromised, the mutant presumably still bound to ELK1 elements in the DNA; however, because the D-box was deleted in the mutant ELK1, our mapping data would predict that AR would not bind to it. The dominant-negative effect of the mutant ELK1 on androgen-stimulated growth is therefore consistent with this prediction. These observations provide an additional functional link between recruitment of AR by ELK1 and growth signaling by AR in PCa cells. The characterization of such discrete AR interacting motifs should enable development of small molecule drugs that bind to those sites and selectively target dysregulated growth signaling in prostate cancer, while avoiding the global side effects of androgen ablation.

CHAPTER 4- Tumor Selective Disruption of Androgen Receptor function in Prostate Cancer

The information on the high throughput screening methodology and small molecule inhibitors of ELK1-AR interactions described in this chapter comprise intellectual property of Wayne State University and is covered by provisional patents filed by the university.

4.1 Introduction

A unique feature of prostate oncogenesis is its dependence on androgen, which acts by binding to and activating transcriptional signaling by the androgen receptor (AR). Both early stage and advanced prostate tumors are generally dependent on AR for growth (272-274, 279-281). Following initial surgery or radiation treatment, residual or recurrent prostate cancer (PC) is commonly treated by suppressing testicular androgen synthesis, typically by disruption of the pituitary hypothalamus axis (chemical castration) (107, 110). In addition, androgen antagonists or an androgen synthesis inhibitor may be used to inhibit AR activation via intratumoral testosterone synthesis (317). Unfortunately, the initial responders to androgen deprivation therapy (ADT) tend to develop hormone refractory disease, referred to as castration resistant PC (CRPC), which nevertheless continues to depend on AR (192, 214, 290, 291, 318, 319). Growth signaling may be sustained in CRPC largely through amplification of AR (291) or expression of its splice variants. Splice variants of AR lack the ligand binding domain but are localized in the nucleus of CRPC cells (289). AR splice variants are frequently co-expressed with full length AR with which they heterodimerize and translocate to the nuclear compartment in a ligand-independent manner (220). AR splice variants, in

collaboration with full length AR, confer optimal hormone-independent growth and insensitivity to anti-androgens and their expression is both functionally and clinically linked to tumor progression (210, 221, 319, 320). Resistance mechanisms also include hormone-independent cross-talk between AR and certain signaling pathways and alterations in the AR co-regulator complement or mutation of AR (291).

Adverse effects associated with ADT are both acute (fatigue, hot flashes, flares) and long-term (hyperlipidemia, insulin resistance, cardiovascular disease, anemia, osteoporosis, sexual dysfunction and cognitive defects) and include loss of the feeling of well-being (107, 111, 112). The high affinity androgen antagonist enzalutamide, used to treat CRPC, inactivates AR by blocking its nuclear entry and impairing its transcriptional activity (321) but it necessarily also abrogates AR signaling in normal tissues (322) and is ineffective against AR splice variants or highly overexpressed AR (221, 323-325). The recurrent and metastatic disease is then treated by chemotherapy, which is typically non-curative and has adverse side effects. Newer types of chemotherapy, immunotherapy and radiation therapy offer valuable, but limited, improvements (112, 121-123, 125, 126, 321, 322). Experimental drugs that block co-activator protein binding to AR have been developed via high throughput small molecule screening. They are effective against AR splice variants (234, 236, 326, 327) but they may also be expected to impair AR function in normal tissues.

Thus the current clinical paradigm for long-term treatment of advanced PC is ubiquitous attenuation of AR signaling (328). However, these approaches have two major limitations: 1. ineffectiveness against advanced tumors in which functional AR has been restored through any of the aforementioned mechanisms; and 2. the need to

deprive the patient of androgen or AR function in all tissues and the consequent multiple long-term side effects noted above. A strategic approach to addressing the dual limitation of ADT is to identify and disrupt a functional arm of AR that (i) is preserved as a crucial mechanism for supporting growth in CRPC and (ii) is necessary for tumor growth, but not for the physiological role of androgen in differentiated normal tissues. Mechanisms of growth signaling by AR that are tumor-specific could potentially offer a highly sensitive point of attack, even in cells that have acquired resistance to ADT and anti-androgen therapies.

As androgen plays a major role in all physiological aspects of the normal prostate epithelium including development, differentiation, maintenance and function (329), malignant prostate epithelial cells must selectively support mechanisms that redirect androgen/AR signaling to strongly support growth. In the classical model of gene regulation by AR the receptor requires bound ligand to homo-dimerize, enter the nucleus and bind to DNA at well-characterized androgen response elements (AREs) associated with target genes (58-60, 284, 285). When the bound ligand is an agonist, AR then recruits co-activators; in contrast, when bound to antagonists, co-repressors are preferentially recruited (59, 60). AR contains sites of co-regulator binding that are either ligand-dependent or -independent. However, in PC cells that are adapted to grow in the absence of hormone, the AR apo-protein is localized in the nucleus, where it is transcriptionally active even in the absence of hormone (210, 221, 245, 267, 289). AR cannot optimally bind to AREs without androgen; nevertheless, both ligand-bound and -unbound AR will still activate a large set of growth supporting genes and support growth through associations with chromatin via putative tethering proteins (267). We have

previously reported that ELK1 is an AR tethering protein that is obligatory for androgen/AR-dependent malignant growth in a variety of well-established PC/CRPC models (246, 268).

ELK1 is a downstream effector of the MAPK signaling pathway and belongs to the ternary complex factor (TCF) sub-family of the ETS family of transcription factors. ELK1 characteristically binds to purine-rich GGA core sequences (295) and is in a repressive association with many cell growth genes. Phosphorylation by ERK transiently stimulates ELK1 to activate its target genes including association with serum response factor (SRF) for activation of immediate early genes (261, 262, 295-297, 308). ELK1 was at least partially required for a substantial proportion (~ 27 percent) of all gene activation by androgen in PC cells (246). The activation of AR target growth genes through ELK1 is mechanistically distinct from the mode of activation of immediate early genes by ELK1 in that it does not require hyper-phosphorylation by ERK; the phosphorylation state of ELK1 is unaltered in the context of the ELK1-AR synergy (246). Tethering of AR by ELK1 in PC/CRPC cells enables constitutive activation of a crucial set of growth genes by AR. In the normal differentiated prostate epithelium and in other normal differentiated AR+ tissues, where growth genes are not activated, it is possible that ELK1 is displaced in the chromatin by related members of the large ETS family that do not associate with AR. Alternatively, at the relatively low AR levels in normal tissues, the receptor could be sequestered by preferential binding to AREs associated with genes unrelated to growth. The N-terminal A/B domain of AR [AR(A/B)], which lacks the ligand binding site, is adequate for interaction with ELK1 (246), in contrast to other known AR tethering proteins (242, 245). AR splice variants, which have C-terminal

deletions and lack the ligand binding domain (LBD), also synergize with ELK1 and support growth (268).

The goal of this study is to establish the feasibility of developing a new class of small molecule drugs that could selectively suppress growth signaling by AR or its variants required by PC/CRPC without affecting other actions of the receptor. To accomplish this, we undertook an unbiased cell-based screen to search for small molecules that could block the association of AR with ELK1 and further derived a lead molecule from an initial hit. Here we report on this small molecule discovery including a detailed evaluation of its mechanism of action and selectivity and efficacy as an inhibitor of the growth of PC/CRPC cells and tumors.

4.2 Materials and Methods

4.2.1 Cell Culture and Reagents

LNCaP, CWR22Rv1, VCaP, DU145, HEK293, H1650 and HeLa cell lines were from the American Type Culture Collection (Manassas, VA); 293FT cells were from Invitrogen. LNCaP, CWR22Rv1 and H1650 cells were routinely grown at 37°C in 5% CO₂ in RPMI 1640 medium supplemented with 10% FBS (Invitrogen), 100 units/ml penicillin, 100 µg/ml streptomycin, 2mM L-glutamine mixture (Invitrogen), with the exception that sodium pyruvate (1mM) (Invitrogen) was included in the LNCaP culture media alone. VCaP, HEK293, DU145 and HeLa cells were grown in DMEM medium supplemented with 10% FBS (Invitrogen), 100 units/ml penicillin, 100 µg/ml streptomycin, 2mM L-glutamine mixture (Invitrogen) or for hormone depletion, LNCaP cells were grown in phenol-red free RPMI 1640 medium supplemented with 10% heat-inactivated and charcoal-stripped FBS (Sigma) and 100 units/ml penicillin, 100µg/ml

streptomycin, and 2mM L-glutamine mixture for 96 hours before each experiment. Affinity-purified rabbit anti-human antibody to AR (sc-7305) and mouse antibody to GAPDH (sc-47724) were purchased from Santa Cruz Biotechnology (Santa Cruz, CA). Rabbit monoclonal anti-human antibody to ELK1 (ab32106) was from Abcam (Cambridge, MA). Testosterone was from Sigma-Aldrich. Lipofectamine™ 2000 was purchased from Thermo Scientific (product number 78410). 5,7,3',4'-Tetrahydroxyflavone was from Selleckchem (S2320); 5,7,3',4'-Tetrahydroxyisoflavone was from BOC Sciences (480-23-9). The following compounds were from INDOFINE Chemical Company: 5,7,3',4'-Tetrahydroxyflavanone (021111S); 5,3',4'-Tetrahydroxyflavone (T-406); 5,3'-Dihydroxyflavone (D-409); 7,4'-Dihydroxyflavone (D-412); 5-Hydroxyflavone (H-025); 3'-Hydroxyflavone (H-410); 5,3'-Dihydroxy-6,7,4'-trimethoxyflavone (D-123). The following compounds were from Extrasynthase: 3',4',7-Trihydroxyflavone (1223); 5,7-Dihydroxyflavone (1362S); 3',4'-Dihydroxyflavone (1204); 4',5,7-Trihydroxy-3'-methoxyflavone (1104S); 3',4',5,7-Tetrahydroxyflavone-3-methoxyflavone (1342); and 3',4',5,7-Tetramethoxyflavone (1204). The following compounds were from Cayman Chemical: 4',5,7-Trihydroxyflavone (10010275) and 5,7,3'-Trihydroxy-4'-methoxyflavone (18649). 7,3'-Dihydroxyflavone was from Sigma-Aldrich (CDS06791). 4',5-Dihydroxyflavone was from Santa Cruz (sc-267859). shRNAs targeting AR and ELK1 and non-targeting control shRNA in the lentiviral expression vector pLKO.1-puro were purchased from Sigma-Aldrich. The pLVX-AR-V7 plasmid and pLVX control plasmid were a kind gift from Dr. Yan Dong from Tulane University (New Orleans, LA).

4.2.2 Generation of recombinant cell lines for high throughput screening and counter screening of small molecule libraries

The recombinant cells used for primary screening were generated from HeLa HLR cells, kindly provided by Dr. Johann Hofman (Innsbruck Medical University), which were originally designed to serve as a cell-based assay system to measure modulation of MAPK activity. HeLa HLR cells have a stably integrated minimal promoter-luciferase reporter containing five upstream Gal4 elements (Gal4-TATA-Luc) and also constitutively express a Gal4-ELK1 fusion protein in which the Gal4 DNA binding domain is substituted for the ETS DNA binding domain of ELK1. We stably transduced these cells with a vector expressing the full-length AR. The full length AR was subcloned from the pCMV expression vector (Origene) into the pCDH-CMV-MCS-EF1-Puro cDNA Cloning and Expression Vector (System Biosciences) at NheI (upstream) and BamHI (downstream) sites. The lentiviral vector expressing full length AR was then packaged in lentivirus and the HeLa HLR cells were infected as described below in the sub-section '*Lentivirus-mediated-Transduction*'. After 72h of infection, 2 ug/mL of puromycin was added to the culture media to select for the transduced cells. The cells were plated at low density for colony formation (20 -40 colonies) in a 100 mm dish. Clonal cells were isolated using cloning cylinders from CORNING (Cat. #3166-8). The selected clones were further expanded and then tested for luciferase induction by testosterone. The clone that gave the greatest luciferase signal to noise ratio in response to testosterone treatment was then chosen for use in the primary screening assay for high throughput small molecule screening.

The cells generated for counter screening comprise HeLa cells stably transduced with a lentiviral plasmid construct containing a minimal promoter-luciferase reporter and an upstream androgen response element (ARE) sequence. The cells were also transduced with a lentiviral expression plasmid for the full-length AR. These constructs were made as follows. Custom synthesized PCR primers were used to amplify and clone the ARE sequence from the pG5luc vector into the pGreenFire1™ -mCMV-EF1-Neo (Plasmid) at SpeI (upstream) and BamHI (downstream) sites. The lentiviral vector expressing ARE-luciferase reporter was then packaged in lentivirus and parental HeLa cells were infected as described below under the sub-section '*Lentivirus-mediated-Transduction*'. After 72h of infection, 400 ug/mL of Geneticin was added to the culture media to select for the transduced cells. These cells were then infected with the lentivirus containing the full length AR expression plasmid described above. After 72h of infection, 2 ug/mL of Puromycin was added to the culture media to select for the transduced cells. Clonal cells harboring both the ARE-promoter-luciferase reporter and also stably expressing AR were then isolated using cloning cylinders as described above. The selected clones were further expanded and then tested for luciferase induction by testosterone. The clone that gave the greatest luciferase signal to noise ratio in response to testosterone treatment was then chosen for use in the counter screening assay for high throughput small molecule screening. All of the plasmid constructs generated above were sent to either the Plant-Microbe Genomics Facility for DNA Sequencing at The Ohio State University (Columbus, OH) or to Genewiz (South Plainfield, NJ) to verify DNA sequences before the constructs were used in the studies.

The recombinant HeLa cells generated above were routinely grown in DMEM supplemented with 10% FBS and 100 units/ml penicillin, 100µg/ml streptomycin, 2mM L-glutamine mixture (Invitrogen) and the appropriate selection antibiotics. The antibiotics used in the culture media for the primary screening cells included 100µg/ml Hygromycin (Invitrogen) (to maintain Gal4-ELK1), 100µg /ml Geneticin (Invitrogen) (to maintain Gal4-TATA-Luc) and 2 µg /ml Puromycin (Sigma-Aldrich) (to maintain AR). The antibiotics used in the culture media for the counter screening cells included 400 µg/ml Geneticin (Invitrogen) (to maintain ARE-TATA-Luc) 2 µg /ml Puromycin (Sigma-Aldrich) (to maintain AR).

4.2.3 High Throughput Screening

The high throughput screening was conducted at University of Michigan's Center for Chemical Genomics Screening facility under the guidance of its Director, Martha Larsen. Recombinant primary screening cells were first depleted of hormone by growing them for 24h in media in which the serum used was heat-inactivated and charcoal-stripped. The cells were then plated in 384-well white flat bottom plates (5,000 cells/well) (Corning Product #3570) using a Multidrop (Thermo Fisher Scientific, Waltham, MA). The plates were then incubated for 24h prior to adding compounds. The following day compounds from the LOPAC, Prestwick, or Maybridge Hitfinder libraries were added precisely in a 0.2 µL volume in the test wells using a Biomek FX liquid handler (Beckman Coulter, Break, CA) to achieve final media concentration of 10 µM of each compound. Using the same technique, testosterone was added in addition to the compounds to achieve a final media concentration of 10 nM. As the compounds were re-constituted from powder stocks using dimethyl sulfoxide (DMSO) as the solvent, the

final media concentration of DMSO was 0.4% v/v. For the assay negative control on each plate, one row of wells on each plate contained 10 nM testosterone and 0.4% v/v of DMSO. For the assay positive control on each plate, one row of wells on each plate contained 10 nM testosterone and 10 μ M enzalutamide dissolved in DMSO (0.4% v/v of DMSO in the wells). The plates were incubated for 24h at 37°C in 5% CO₂. The medium was then aspirated leaving a residual volume 10 μ l using an Elx 405-plate washer (Bio Tek U.S.). Then, 10 μ L of the assay reagent Bright-Glo (Promega Corp., Madison WI) was added to each well. Luciferase activities in the wells were then measured using a Biomek FX dual head (Beckman) plate reader. A total of 18,270 compounds were tested in the primary screen. A 'hit' was initially defined using relatively low stringency criteria as a compound able to reduce luciferase activity in the test well \geq 3 standard deviations below the negative control wells or to a level \geq 40% of the enzalutamide control wells. For the primary assay this definition produced 1613 hits for an overall hit rate of 8.8%. The 1613 compounds were then tested again in the primary screening assay in parallel with the counter screening assay in triplicate. A hit was now redefined as a compound able to reduce luciferase activity in the test wells \geq 3 standard deviations below the negative control wells and that was unable to reduce luciferase activity \geq 50% in the counter screen. By this definition, 92 hits were obtained. Compounds were further triaged based on their ability to inhibit in the primary screen by \geq 80% and produced no inhibition in the counter screen. One of the top hits was prioritized for this study.

4.2.4 Purified Proteins

Full length human AR expressed in insect cells and purified to >95% by affinity chromatography and FPLC chromatography (ab82609) was purchased from Abcam (Cambridge MA). Recombinant his-tagged ELK1 expressed from baculovirus infected Sf9 cells was purified using nickel agarose affinity chromatography as previously described by us (268). The proteins were eluted with 200mM imidazole and dialysed against 20 mM HEPES, pH 7.9 containing 10% glycerol, 20mM KCl, 2mM MgCl₂, 0.2 mM EDTA, 0.5mM benzamidine and 0.5mM DTT. Purity of the proteins was estimated to be > 85% by SDS-polyacrylamide gel electrophoresis.

4.2.5 Surface Plasmon Resonance

Amine Coupling Kit, CM5 sensor chip and HBS-N buffer (GE Healthcare) were used for surface plasmon resonance (SPR) analysis. The rate and equilibrium binding constants of the interaction of AR with KCI807 was determined using Biacore 3000 (Biacore, Piscataway, NJ). Depending on the experimental plan, affinity-purified AR or ELK1 polypeptide (ligand) was immobilized on a CM5 research grade sensor chip by an amine coupling method (302). The immobilization involved activation of carboxymethyl groups on a dextran-coated chip by reaction with *N*-hydroxysuccinimide, followed by covalent bonding of the ligand (AR) to the chip surface via amide linkages. Reference surfaces were prepared in the same manner but blocked with ethanolamine and thus contained no ligand. To examine binding of KCI807 or enzalutamide, kinetic binding analysis was carried out, by injecting the compound (analyte) at different concentrations (0-320 nM for KCI807 or 0-200 nM for enzalutamide) into the flow cells (ligand and reference cell). The interaction (response units, RU) between analyte and ligand was recorded as the ligand RU minus the reference RU. Kinetic values were determined

using BIAevaluation software (Biacore), and the data were fitted with the model showing closest match (303, 304). A 1:1 Langmuir binding model was generally selected, in which all the sensorgrams representing the different analyte concentrations were fitted simultaneously with the wide window of association and dissociation phases. Individual concentration curves were also evaluated to confirm the fitting data. The equilibrium dissociation constant (K_d) was calculated by $K_d = k_{off}/k_{on}$. In all cases, baseline was established in the presence of the vehicle used for the compounds (DMSO) appropriately diluted in HBS-N buffer.

Competition binding experiments were executed on the Biacore 3000 system at a flow rate of 5-10 $\mu\text{l}/\text{min}$ in HBS-N buffer (330, 331). A fixed concentration (200 nM) of AR in the presence of increasing concentrations of KCl807 or enzalutamide was passed over a covalently stabilized ELK1 sensor surface for 5 min at 50 $\mu\text{l min}^{-1}$. The sensor surface was regenerated between experiments by dissociating any formed complex in HBS-N buffer for 30 min, followed by a further 30-min stabilization period. After regeneration, the SPR signal returned to the original level (baseline). In all cases, baseline was established in the presence of the vehicle used for the compounds (DMSO) appropriately diluted in HBS-N buffer. The binding curves were analyzed using the heterogeneous analyte competition model. The kinetic curves were analyzed for a one-to-one Langmuir fitting model provided by with the Biacore 3000 instrument software.

4.2.6 Transfections and Reporter Luciferase Assays

Hela Cells were plated in a 24-well plate at a concentration of 75,000 cells/well in antibiotic-free red DMEM. The following day the cells were transfected with a total of

300 ng of plasmid DNA/well using Lipofectamine 2000. The cells were incubated for 24h then lysed using luciferase assay lysis buffer 5X (REF: E291A) from Promega. The luciferase activity of the cell lysates were measured using firefly substrate from Promega and a luminometer (Lumat LB9501, Berthold, Wildbad, Germany).

4.2.7 Lentivirus-mediated-Transduction

shRNAs for ELK1, AR, and non-targeting control shRNA were packaged in 293FT cells. The lentiviral particles were generated using lipofectamine and three plasmids, pMD2G, pMDLg/RRE, and pRSV/Rev which all code for essential elements of the virus. The virus containing supernatant was harvested at 48 and 72 h after transfection. Cells were plated in 6-well poly-D-lysine coated plates (BD Falcon) in phenol red-free medium supplemented with 10% heat-inactivated charcoal-stripped FBS and 2mM L-glutamine. The following day cells were infected with control shRNA, ELK1 shRNA, or AR shRNA lentivirus with Polybrene (8µg/ml) for a 5 h duration, followed by an additional 5h. After infection, the virus was replaced with fresh phenol red-free growth medium.

4.2.8 Colony Growth Assay

Cells were trypsinized, and 1000 cells/well were seeded in poly-D-lysine coated 6-well plates in phenol red-free regular growth media. The cells were treated with the indicated concentration of KCI807, which was replenished every 48h. The cells were grown at 37°C in 5 % CO₂ for 10 days until colonies grew to the desired size in the untreated control wells. Colonies were fixed with methanol and stained with crystal violet. Each treatment was conducted in triplicate and the number of colonies was counted using the GelCount™ colony counter and a 350 size cutoff.

4.2.9 Cell Monolayer Growth Assay

Cells were trypsinized and 3000-4000 cells/well were seeded in 96-well plates coated with poly-D-lysine. The cells were seeded in phenol red-free medium supplemented with 10% FBS, 100units/ml penicillin, 100 µg/ml streptomycin, 2mM L-glutamine mixture and sodium pyruvate (1mM) for LNCaP cells and phenol red-free medium supplemented with 10% FBS, 100units/ml penicillin, 100 µg/ml streptomycin and 2mM L-glutamine mixture for VCaP, 22Rv1, DU145, HeLa, HEK293 and H1650 cells. The cells were grown at 37°C in 5% CO₂. Twenty four hours after seeding in the 96-well plates, the cells were treated with the indicated concentration of KCI807 or DMSO (vehicle). The cells were re-treated on Day 3 by removing half the volume of medium and replacing it with fresh treated medium. Cell viability was determined using the MTT assay from day zero until day five. MTT (10µL, 5mg/mL) was added to each well and incubated for 2h at 37°C. The formazan crystal sediments were dissolved in 100µL of DMSO, and the absorbance at 570nm was measured using the BioTek Synergy 2 Microplate Reader (BioTek, Winooski, VT). The assay was conducted in sextuplicate wells and values were normalized to day zero.

4.2.10 Western Blot Analysis

The treated cells were washed once with phosphate buffered saline (PBS) and then lysed with RIPA buffer (150mM NaCl, 1% Nonidet P-40, 0.5% sodium deoxycholate, 0.1% SDS, 50mM Tris of pH 8.0) containing a protease inhibitor cocktail (Pierce, Thermo Fisher Scientific). The cell lysates were then incubated on ice for 40 minutes and vortexed every 10 minutes. Total protein concentrations were estimated using the Bradford Assay (Bio-Rad). Ten micrograms of each protein sample was

heated at 95°C for 5 minutes and resolved by electrophoresis on 8% polyacrylamide-SDS gels and electrophoretically transferred to PVDF membranes (Millipore, Billerica, MA). The membranes were then probed overnight at 4°C with the appropriate primary antibody followed by the appropriate horseradish peroxidase-conjugated secondary antibody. The blots were then developed to visualize the protein bands using the HyGLO Chemiluminescent HRP Antibody Detection Reagent (Denville Scientific, Metuchen, NJ) (332) (332) (332) (332) (331) (331) (331) (75) (74).

4.2.11 RNA isolation, Reverse Transcription, and Real Time PCR.

Total RNA was isolated from cells using the RNeasy Mini Kit (Qiagen). Reverse transcription PCR was then performed using 500 ng of total RNA with random primers and using the high-capacity complementary DNA Archive kit (Applied Biosystems). The complementary DNA from this reaction was measured using quantitative real time PCR using the StepONE Plus Real Time PCR system (Life Technologies Corporation, Carlsbad, CA). All reactions were performed in triplicate and normalized to glyceraldehyde-3-phosphate-dehydrogenase values in the same samples. All primers and Taqman probes were purchased from the applied Biosystems inventory (Invitrogen)

4.2.12 Measurement of intracellular and serum levels of compounds

4.2.12.1 Chromatographic and mass-spectrometric conditions

Instrumentation

All LC-MS/MS analyses were performed on an AB SCIEX (Foster City, CA) QTRAP 6500 LC-MS/MS system, which consists of a SHIMADZU (Kyoto, Japan) Nexera ultra-high performance liquid chromatography (UPLC) coupled with a hybrid triple quadrupole / linear ion trap mass spectrometer. The UPLC system is equipped with two X2 LC-

30AD pumps, an X2 SIL-30AC autosampler, a CBM-20A communication bus module, an X2 CTO-30A column oven, and two DGU-20A degassing units. Analyst[®]1.6 software was used for system control and data acquisition, and MultiQuant 3.0 software was used for data processing and quantitation.

Liquid chromatography

Chromatographic separation was achieved on a Waters XBridge C18 (2.1 × 50 mm, 3.5 μm) column using an optimized gradient elution consisting of mobile phase A (0.1% formic acid in water) and mobile phase B (0.1% formic acid in acetonitrile), at a flow rate of 0.3 mL/min. The elution gradient program was as follows [shown as the time (min), (% mobile phase B)]: 0 – 2.5 min, 40%; 2.5 – 4.5 min, 40 – 55%; 4.5 – 5 min, 55 – 100%; 5 – 6 min, 100%; 6 – 6.5 min, 100 - 40%; and 6.5 – 10 min, 40%. Column oven temperature was maintained at 40°C. To minimize the carryover, external and internal washes were implemented prior to and post the injection for both the auto-sampler syringe and injection port, as follows: 50% methanol (for R3) was used for external wash with one second rinse dip and 500 μL volume, and the mixture of IPA:MeOH:Acetonitrile:H₂O 1:1:1:1 (for R1) and 40% acetonitrile (R0) was used in the internal wash with sequence R1 to R0.

Mass spectrometry (MS)

The QTRAP 6500 mass spectrometer was operated in electrospray positive ionization using multiple reaction monitoring mode (MRM). The MS parameters were optimized to obtain the most sensitive and specific MS transitions for 5, 3'-dihydroxyflavone, 5, 3', 4'-trihydroxyflavone, and 5, 7, 3', 4'- tetrahydroxyflavone by direct infusion 0.5 μM of the standard solutions into the ion source with a syringe pump.

The Turbo ion-spray voltage was set at 4500 V and the source temperature was set at 500 °C. Collision gas was optimized at medium level with curtain gas, ion source gas 1 and ion source gas 2 delivered at 20, 30 and 30 psi, respectively. The dwell time was set for 50 ms. For each compound, four most sensitive MS transitions were selected and the corresponding decluttering potential, collision energy, collision cell exit potential, and entrance potential were optimized as shown in table below.

Q1 (m/z)	Q3 (m/z)	Time (ms)	ID	DP (Voltage)	CE (Voltage)	CXP (Voltage)
255	137.1	50	5,3-dihydroxyflavone_1	130	41.5	23.3
255	152	50	5,3-dihydroxyflavone_2	130	61.9	25.8
255	181	50	5,3-dihydroxyflavone_3	130	43.5	16.9
255	155	50	5,3-dihydroxyflavone_4	130	54.1	25
271.3	117.1	50	5, 3', 4'-trihydroxyflavone_1	99.7	46.2	13.8
271.3	135	50	5, 3', 4'-trihydroxyflavone_2	99.1	39.1	11.9
271.3	137.1	50	5, 3', 4'-trihydroxyflavone_3	97	39.7	12.3
271.3	225.1	50	5, 3', 4'-trihydroxyflavone_4	97.4	41.8	13.6
287.5	135	50	5, 7, 3', 4'-tetrahydroxyflavone_1	118.9	39.2	15.7
287.5	153	50	5, 7, 3', 4'-tetrahydroxyflavone_2	120	41.8	13.9
287.5	160.9	50	5, 7, 3', 4'-tetrahydroxyflavone_3	112.4	44.9	22.1
287.5	241	50	5, 7, 3', 4'-tetrahydroxyflavone_4	82.3	41	13.9

DP: Decluttering Potential

CE: Collision Energy

CXP: Collision Cell Exit Potential

4.2.12.2 Sample Preparation

Stock solutions, calibration standards, and quality control (QC) samples

The stock solutions were prepared in DMSO at a final concentration of 5 mM, and stored in brown glass vials at -20°C . The working solutions were prepared freshly by serial dilutions of the stock solution with DMSO on each day of analysis. For the concentration determination in mouse serum or cell samples, the calibration standards were prepared by spiking 5 μL of working solution into 95 μL of blank human plasma or untreated cell lysate, respectively. All standards were prepared fresh daily.

Mouse serum samples for the determination of serum concentrations of 5,3-dihydroxyflavone

Frozen serum samples were thawed at room temperature. An aliquot of 100 μL serum was transferred into a micro centrifuge tube, and 1000 μL ethyl acetate was added. The mixture was vortex-mixed for 15 minutes and centrifuged at 14000 rpm at 4°C for 15 min, 950 μL of the supernatant was transferred to a new 1.7 mL centrifuge tube, and dried under a steam of nitrogen at room temperature. The sample was then reconstituted with 100 μL 40% acetonitrile, and 5 μL was injected into the LC-MS/MS system.

Cell samples for the determination of intracellular concentrations of 5,3-dihydroxyflavone, 5, 3', 4'-trihydroxyflavone, or 5, 7, 3', 4'-tetrahydroxyflavone

The suspended cells were sonicated to generate a cell lysate, and then 1000 μL ethyl acetate was added. The mixture was vortex-mixed for 15 minutes and centrifuged at 14000 rpm at 4°C for 15 min, 950 μL of the supernatant was transferred to a new 1.7 mL centrifuge tube, and dried under a steam of nitrogen at room temperature. The sample was then reconstituted with 100 μL 40% acetonitrile, and 5 μL was injected into

the LC-MS/MS system. Measured concentrations were normalized to cell protein concentrations.

4.2.13 Tumor xenograft model studies

The 22Rv1 human CRPC xenograft model was established subcutaneous implant of 22Rv1 cells (10,000,000 cells) and serial passaging of the tumors in male SCID mice. 5,3'-Dihydroxyflavone was administered by ip injection (formulation: 1% carboxymethyl cellulose, 5% DMSO, and 0.5% NaHCO₃). For preliminary dose determinations, mice were tested for immediate post-injection toxicity by monitoring weight and behavior following daily ip injection of 3 doses of the compound (100, 150 and 250 mg/kg body weight) for a duration of 7 days. As the mice were asymptomatic at all doses, the highest dose of 250mg/kg body weight was used for anti-tumor efficacy studies of the compound. Plasma levels of unmetabolized compound for this dose regimen were determined by LCMS at our institutional Pharmacology Core Services as described in a separate sub-section. Male SCID mice were implanted bilaterally SC with 30-50 mg tumor fragments by 12 gauge trocar, and randomly distributed to various treatment and vehicle control groups. Treatment typically began 5 days post-implant (early stage disease) to determine antitumor efficacies and to further evaluate potential cumulative toxicities. Tumors were measured with a caliper 3 times/week and tumor masses (in mg) estimated by the formula, $mg = (a \times b^2)/2$, where "a" and "b" are tumor length and width in mm, respectively. Mice were sacrificed when cumulative tumor burdens reached 5-10% of body weight (1-2g).

4.3 Results

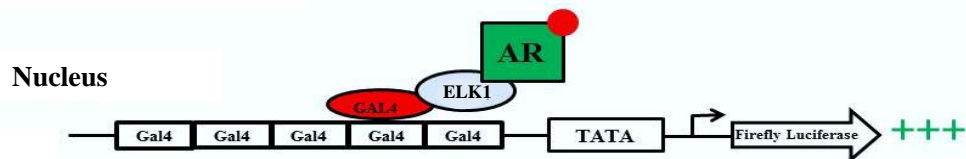
4.3.1 Discovery of the lead compound

For initial discovery of small molecules that selectively blocked the binding of ELK1 and AR, we developed a stringent and methodical system for high throughput screening (HTS) of a high diversity compound library. We expected a relatively high probability of success because we were screening for molecules that could bind at any one of a minimum of four target sites, considering the two AR docking sites on ELK1 and the corresponding binding sites in AR. Therefore, we screened a diversity library of ~ 20,000 small molecules based on conventional wisdom at our facility that the primary hit rate for a single target in cell-based HTS by moderately stringent criteria is 1-2 %.

For the primary screen, we used recombinant AR+ HeLa cells harboring a Gal4 promoter-luciferase reporter as well as a Gal4-ELK1 fusion protein gene. When these cells are treated with testosterone AR translocates to the nucleus where it binds to Gal4-ELK1 and activates the reporter gene. The cells for counter screening were identical to the primary screening cells with the exception that an androgen response element (ARE) sequence replaced Gal4 in the promoter and Gal4-ELK1 was absent. Compounds of interest should only suppress the signal in the primary screening assay, as the only difference between these two assays is AR recruitment to the promoter via ELK1 binding vs. direct DNA binding (Illustrative schematic in Figure 4.1). The Z-factor for the primary screening assay was 0.734 and for the counter screening assay it was 0.711. In both assays enzalutamide, which does not allow nuclear translocation of AR, completely suppressed the signal (Figure 4.2a, 4.2b). We initially screened two pilot sets of compound libraries, LOPAC and Prestwick, and then the Maybridge Hit Finder library, all of which are diversity sets, at a compound concentration of 10 μ M. A hit in the primary screen was defined as a compound able to reduce luciferase reporter activity \geq

a.

Primary Screen



b.

Counter Screen

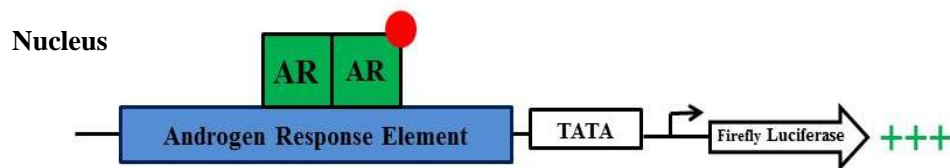


Figure 4.1 Schematic of HTS screening system (a) Schematic of the reporter system for the primary screening assay. Recombinant HeLa cells used in this assay harbor the Gal4-TATA-luc promoter-reporter, and express a Gal4-ELK1 fusion protein as well as the androgen receptor (AR). Gal4-ELK1 is bound to the Gal4 elements in the promoter. In the absence of testosterone (red circle), AR is localized in the cytoplasm. When testosterone is present it binds to AR causing AR to translocate to the nucleus where it then binds to Gal4-ELK1 and activates the downstream luciferase reporter. (b) Schematic of the reporter system for the counter screening assay. Recombinant HeLa cells used in this assay are identical to the primary screening cells except for the absence of Gal4-ELK1 and substitution of the Gal4 elements in the promoter with a canonical ARE. In this case, testosterone causes cytosolic AR to translocate to the nucleus and bind as a dimer to the ARE in the promoter resulting in activation of the luciferase reporter.

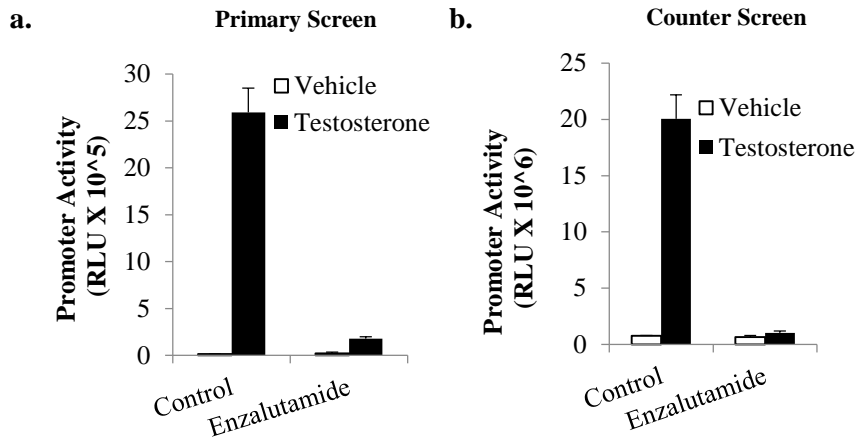


Figure 4.2 Testing recombinant HeLa cells for HTS. Recombinant HeLa cells used in the primary screen (**a**) and in the counter screen (**b**) were treated with either vehicle (ethanol) or 10 nM testosterone together with 10uM of Enzalutamide or vehicle (DMSO) control. Cells were harvested and luciferase assay was performed 24 h post-treatment.

3 standard deviations below the negative control or to a level $\geq 40\%$ of the enzalutamide control. This definition produced 1613 hits. Elimination of false positives by counter-screening resulted in 15 compounds with variable potencies (40% - 100% inhibition) in the primary screen. We chose 5,7,3',4'-tetrahydroxyflavone (Hit 1), one of our top hits in terms of potency of inhibition in the primary screen (80% - 100% in < 6 hours) and virtual absence of an effect in the counter screen (Figure 4.3a). This hit was prioritized for further studies because it is a natural dietary product and could potentially be introduced relatively rapidly in the clinic in an appropriately modified form.

Hit1 is itself highly unstable (easily oxidized) *in vitro* and rapidly metabolized *in vivo* because of its multiple phenolic hydroxyl groups including hydroxyls on adjacent carbon atoms (333, 334); hence its reported anti-inflammatory, neuroprotective and other physiological effects (335, 336) may be related to its metabolites rather than its original structure. In order to identify the essential structural elements required for selective activity against the ELK1-AR complex, we conducted structure-activity analysis using the same *in vitro* assay as in the primary screening. First, we tested the effect of substituting the flavone scaffold in Hit 1 with the closely related flavanone and isoflavone scaffolds. Hit 1 was unable to affect either ELK1-dependent or ARE-dependent promoter activation by AR upon scaffold substitution (Figure 4.3b, 4.3c). Further structure-activity analysis using derivatives of Hit 1 in which individual or pairs of hydroxyl groups were substituted by hydrogen indicated that only the hydroxyls at the 5 and 3' positions are necessary for inhibition of the ELK1-AR synergy (Table 4.1). However, the hydroxyl group at either position alone had no activity (Table 4.1). Substitution of all four hydroxyl groups with methoxy groups or substitution at the 3'

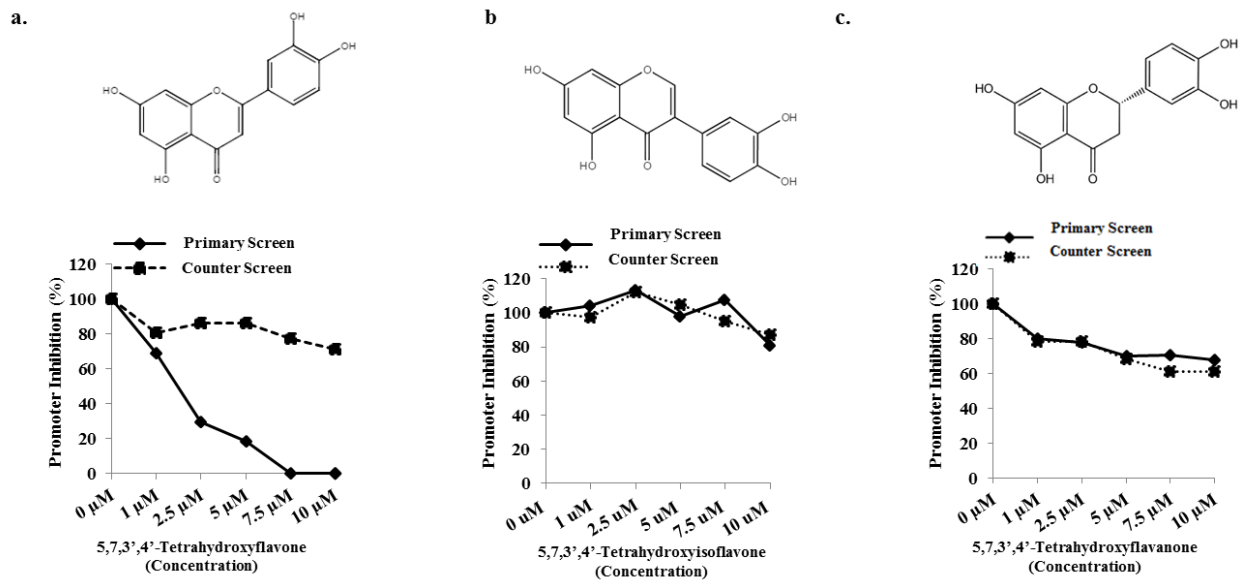
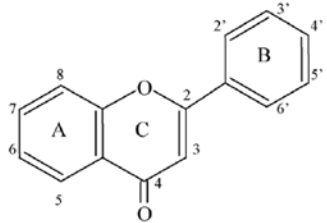


Figure 4.3 Hit1 (5,7,3',4'-Tetrahydroxyflavone) selectively inhibits ELK1-dependent promoter activation by AR and the compound scaffold is obligatory. Dose response curve for (a) 5,7,3',4'-Tetrahydroxyflavone (b) 5,7,3',4'-Tetrahydroxyisoflavone (c) 5,7,3',4'-Tetrahydroxyflavanone for inhibition of promoter activation by testosterone in the primary screening assay (ELK1-dependent promoter activation by AR) compared with the counter screening assay (ARE-dependent promoter activation by AR). The cells were simultaneously treated with compound and testosterone for 6h and promoter activity was measured in terms of reporter luciferase activity.

Structure	Flavonoid	-R ₃	-R ₅	-R ₆	-R ₇	-R _{3'}	-R _{4'}	IC ₅₀
	5,7,3',4'-Tetrahydroxyflavone	H	OH	H	OH	OH	OH	2.7
	5,3',4'-Trihydroxyflavone	H	OH	H	H	OH	OH	1.8
	4',5,7-Trihydroxyflavone	H	OH	H	OH	H	OH	No effect
	3',4',7-Trihydroxyflavone	H	H	H	OH	OH	OH	No effect
	5,7-Dihydroxyflavone	H	OH	H	OH	H	H	>10
	3',4'-Dihydroxyflavone	H	H	H	H	OH	OH	No effect
	7,3'-Dihydroxyflavone	H	H	H	OH	OH	H	No effect
	4',5-Dihydroxyflavone	H	OH	H	H	H	OH	>10
	5,3'-Dihydroxyflavone	H	OH	H	H	OH	H	1.3
	7,4'-Dihydroxyflavone	H	H	H	OH	H	OH	No effect
	5-Hydroxyflavone	H	OH	H	H	H	H	No effect
	3'-Hydroxyflavone	H	H	H	H	OH	H	No effect
	5,3'-Dihydroxy-6,7,4'-trimethoxyflavone	H	OH	OCH ₃	OCH ₃	OH	OCH ₃	4.5
	4',5,7-Trihydroxy-3'-methoxyflavone	H	OH	H	OH	OCH ₃	OH	No effect
	5,7,3'-Trihydroxy-4'-methoxyflavone	H	OH	H	OH	OH	OCH ₃	7.5
	3',4',5,7-Tetrahydroxy-3-methoxyflavone	OCH ₃	OH	H	OH	OH	OH	No effect
	3',4',5,7-Tetramethoxyflavone	H	OCH ₃	H	OCH ₃	OCH ₃	OCH ₃	No effect

In Table 1, R₈, R_{2'}, R_{5'} and R_{6'} comprise H in all cases

Table 4.1 Structure-activity relationships for inhibition of ELK1-dependent promoter activation by AR. The primary screening assay (ELK1-dependent promoter activation by AR) was used to determine the IC₅₀ values for Hit1 and its various derivatives as indicated, using a compound dose range of 1-10μM.

position alone with a methoxy group abolished activity (Table 4.1). Further, methoxy substitutions on carbons at positions 4', 6 and 7 were tolerated although the derivatives had sub-optimal activity (Table 4.1). Finally, methoxy substitution on the carbon at position 3 was not tolerated (Table 4.1), predicting possible steric hindrance from any bulky substitutions at this position.

To test the relative stability of 5,3'-dihydroxyflavone, we compared the intracellular concentrations of 5,3'-dihydroxyflavone, 5,3',4'-trihydroxyflavone and 5,7,3',4'-tetrahydroxyflavone (Hit 1) following incubation at a media concentration of 2 μ M compound. The intracellular concentration of 5,3'-dihydroxyflavone was unchanged between 1h and 6h in contrast to the tri- and tetra-hydroxy compounds whose concentrations rapidly declined during this period, indicating that removal of hydroxyl groups at the 7 and 4' positions in Hit 1 conferred stability without compromising effectiveness against the target (Figure 4.4).

As a secondary test of target selectivity, we examined the effect of 5,3'-dihydroxyflavone on activation of ELK1 by MEK/ERK using recombinant HeLa cells harboring the Gal4 promoter-luciferase reporter and expressing the Gal4-ELK1 fusion protein. In these cells, activation of the luciferase reporter by transduction with a constitutively active mutant form of MEK was completely inhibited by the MEK inhibitor trametinib but 5,3'-dihydroxyflavone did not inhibit the promoter activation (Figure 4.5).

To conclude, 5,3'-dihydroxyflavone, which is much more stable and predictably bioavailable than Hit 1, is the minimal structure that is fully and selectively active against the target ELK1-AR interaction. We name this lead compound KCI807.

4.3.2 Binding of KCI807 to AR and disruption of ELK1 binding

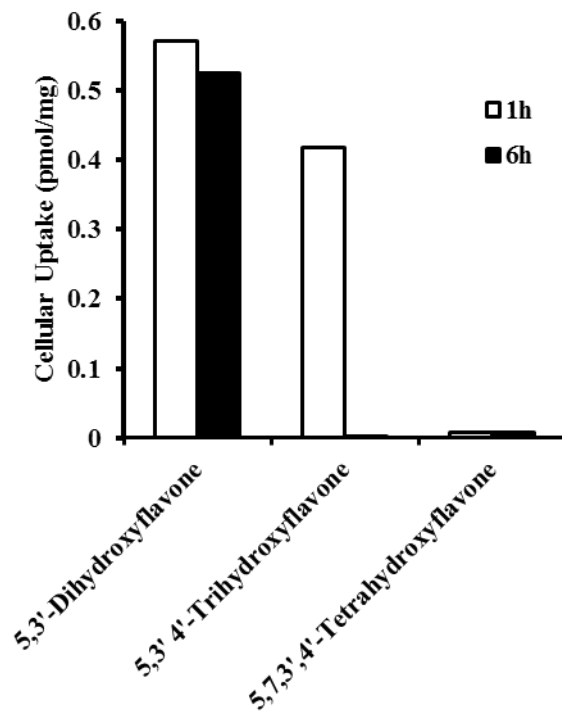


Figure 4.4 Cellular uptake in HeLa cells for active compounds. HeLa cells were treated with 2 μM of each compound and incubated for 1h or 6h. At the end of the incubation the cells were washed 3x with cold PBS and scraped in molecular grade H_2O . The compounds were extracted and then quantified using LCMS.

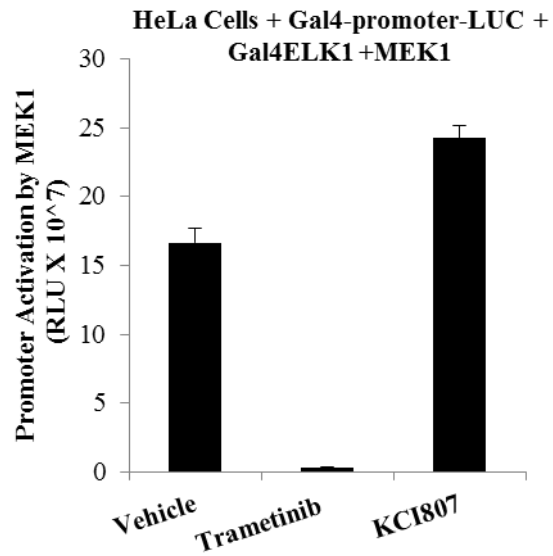


Figure 4.5 KCI807 does not inhibit ERK1/2 activation of ELK1. HeLa cells were co-transfected with the Gal4 promoter-luciferase reporter construct and the expression plasmid for the Gal4-ELK1 fusion protein gene. In addition the cells were transfected with an expression plasmid for a constitutively active MEK1 protein. The cells were then treated with the MEK1 inhibitor, trametinib (1 μ M), KCI807 (20 μ M), or vehicle (DMSO). Cells were harvested 48h post transfection and luciferase activity was measured.

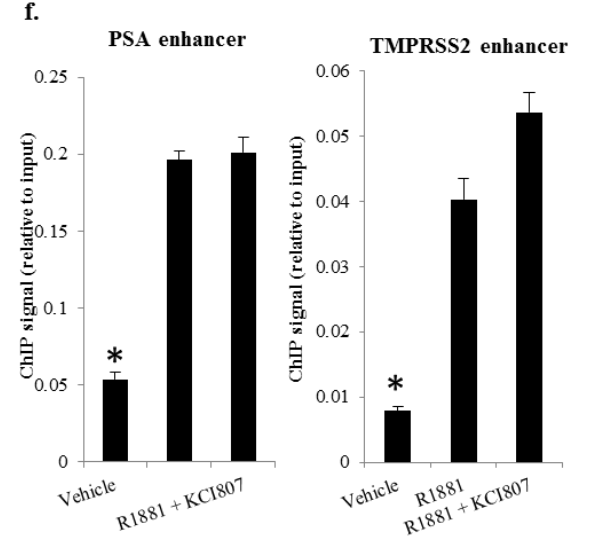
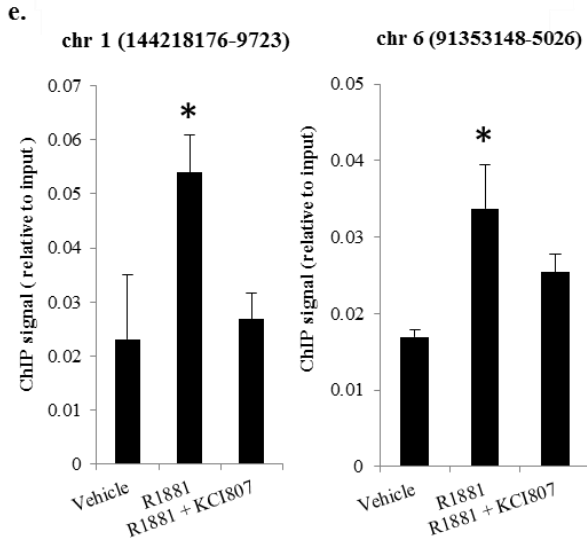
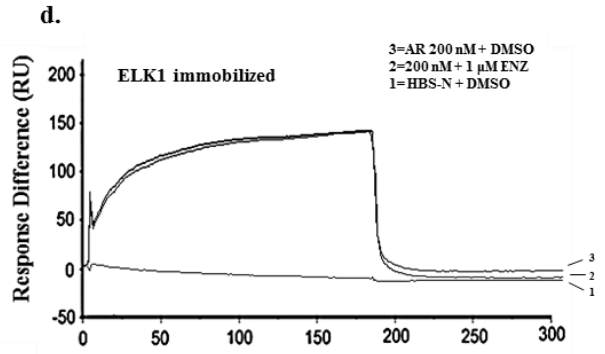
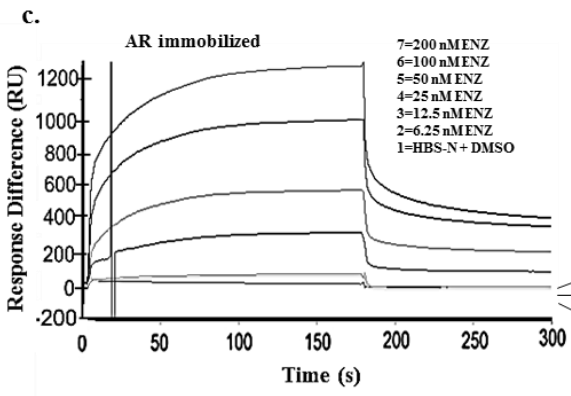
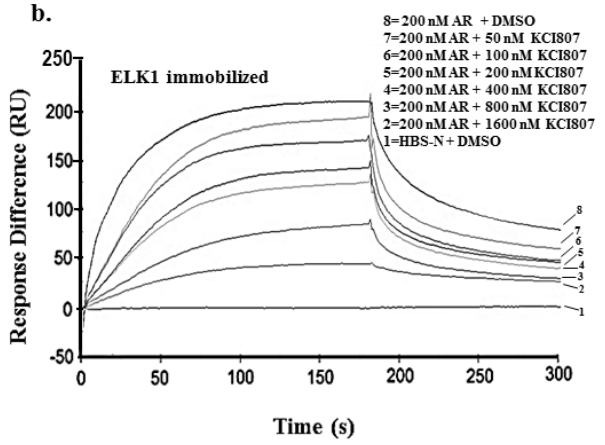
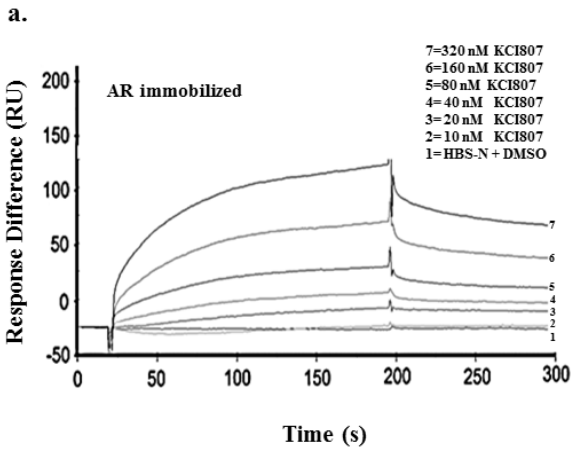


Figure 4.6 KCI807 binds to purified AR and blocks ELK1 binding. (a) Surface plasmon resonance (SPR) kinetic curves for quantitative analyses of KCI807 binding to AR. AR was immobilized and KCI807 (analyte) was diluted in a series (0, 10, 20, 40, 80, 1600, and 320nM). (b) SPR kinetic curves for quantitative analyses inhibition of binding of AR (used as analyte) to immobilized ELK1 by KCI807. A fixed concentration of AR (200 nM) was combined with KCI807 diluted in a series (0, 50, 100, 200, 400, 800, and 1600 nM). (c) SPR kinetic curves for quantitative analyses of enzalutamide binding to AR. AR was immobilized and enzalutamide (analyte) was diluted in a series (0, 6.25, 12.5, 25, 50, 100, 200nM). (d) SPR kinetic curves to test for inhibition of binding of AR (used as analyte) to immobilized ELK1 by enzalutamide. AR (200 nM) was combined with enzalutamide (0 uM or 1 uM). (e) and (f) Chromatin immunoprecipitation using anti-AR antibody and LNCaP cells treated with R1881 (10nM), R1881 (10nM) + KCI807 (20uM), or vehicle for 2h. The target sites for the ChIP assay included previously established sites in the chromatin at which ELK1 recruits AR (e) or the canonical ARE enhancer sites associated with the PSA or theTMPRSS2 gene.

It was determined by surface plasmon resonance (SPR) that KCI807 binds to purified immobilized AR with a dissociation constant of 7×10^{-8} M (Figure 4.6a). In contrast, KCI807 did not bind to immobilized ELK1 (Figure 4.6b). SPR analysis demonstrated that KCI807 blocked binding of purified AR (used as analyte) to purified immobilized ELK1 progressively with increasing molar ratios relative to AR (Figure 4.6b). In contrast, although SPR analysis could demonstrate the binding of enzalutamide to AR with a dissociation constant of 1.7×10^{-9} M (Figure 4.6c), enzalutamide was unable to block the binding of AR to ELK1 (Figure 4.6d).

We then tested the ability of KCI807 to selectively block recruitment of AR by ELK1 to chromatin *in situ*. Chromatin immunoprecipitation (ChIP) assays showed that in LNCaP PC cells, KCI807 prevented association of AR with two previously (246) established sites in the chromatin at which ELK1 recruits AR (Figure 4.6e). In contrast, KCI807 did not affect AR recruitment at the well-established canonical ARE enhancer sites associated with the PSA or TMPRSS2 gene (Figure 4.6f).

The set of complementary results described above establish that KCI807 directly binds to AR and selectively blocks its physical association with ELK1, inhibiting ELK1-dependent transcriptional activity of AR.

4.3.3 Narrow genotropic effects of KCI807 in AR-V7 expressing CRPC cells

KCI807 also inhibited hormone-independent promoter activation by the splice variant AR-V7 (Figure 4.7a). The relatively higher concentrations of the compound required for this inhibition is likely because AR-V7 was overexpressed in the assay system.

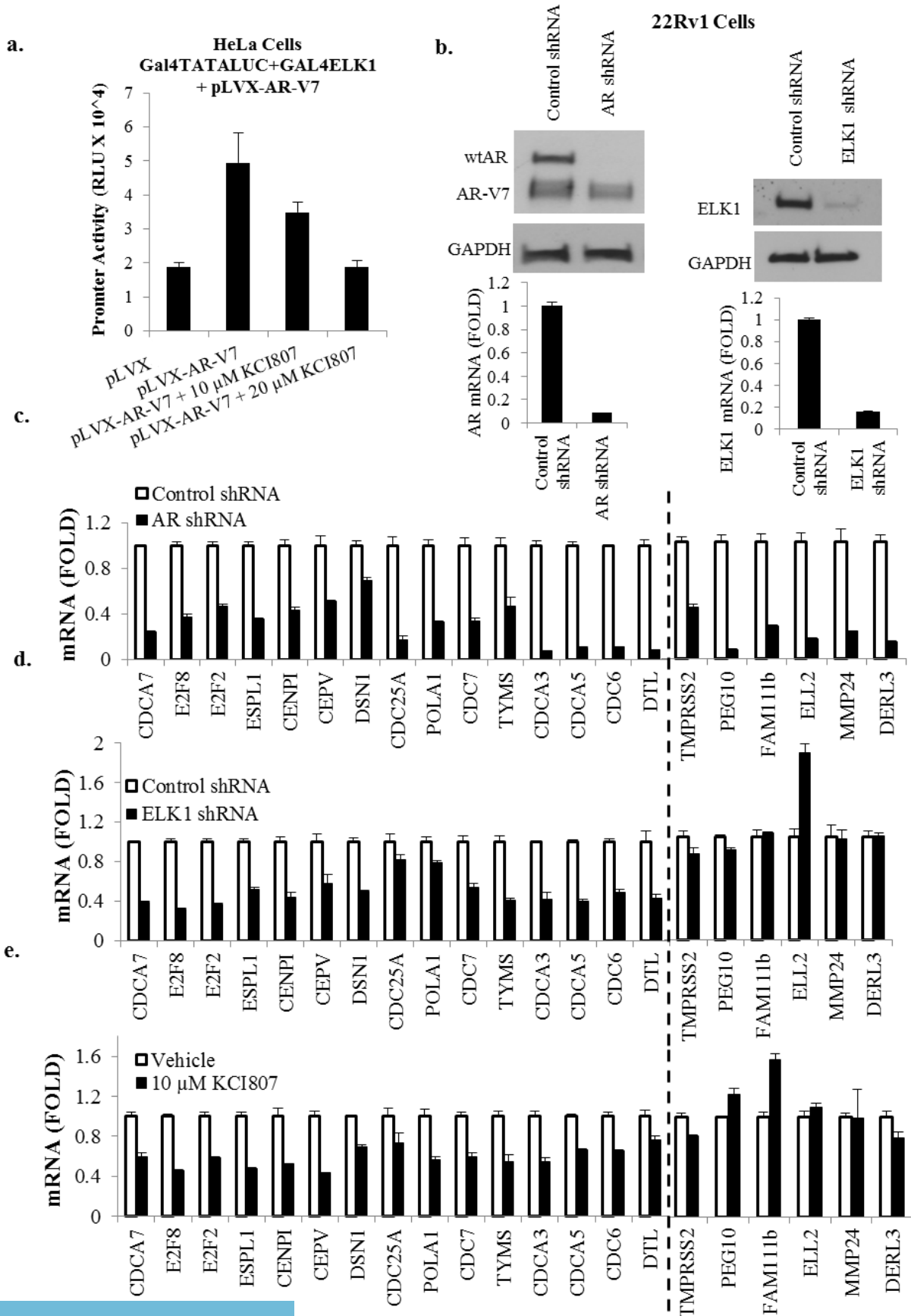


Figure 4.7 Transcriptional targets of KCI807. (a) HeLa cells were co-transfected with the Gal4 promoter-luciferase reporter construct and the Gal4-ELK1 fusion protein expression plasmid. In addition the cells were transfected with either the AR-V7 expression plasmid or the corresponding vector plasmid (pLVX). At the time of transfection with AR-V7, the cells were also treated in parallel with KCI807 (10 μ M and 20 μ M) or with the vehicle control. Promoter activity was measured in terms of reporter luciferase activity. (b) 22Rv1 cells were infected with lentivirus expressing shRNA selective for full length AR or ELK1 shRNA or control shRNA. The cell lysates were analyzed by western blot to confirm knockdown of full length AR (top left panel) or ELK1 (top right panel). Real time PCR was used to confirm depletion of mRNA for full length AR (bottom left panel) or ELK1 mRNA (bottom right panel). (c) In the 22Rv1 cells in which full length AR was depleted, the mRNAs for the indicated panel of genes were measured by real time PCR. (d) In the 22Rv1 cells in which ELK1 was depleted, the mRNAs for the same panel of genes were measured by real time PCR. (e) 22Rv1 cells were treated with 10 μ M of KCI807 for 72h and real time PCR was used to measure mRNAs for the indicated panel of genes tested in c and d.

To test the selectivity of KCI807 for ELK1-dependent gene activation by AR vs. other target genes of the receptor, we examined 22Rv1 CRPC cells, which are dependent on both full length AR and AR-V7 for hormone-independent growth. In these cells, depletion of full length AR using lentiviral shRNA (Figure 4.7b, left) led to reduction in mRNA levels of representative AR target genes previously (246) shown to be activated by AR in either an ELK1-dependent or -independent manner (Figure 4.7c). Depletion of ELK1 using lentiviral shRNA (Figure 4.7b, right) caused reduction only in the mRNAs for genes previously reported to be ELK1-dependent for regulation by AR (Figure 4.7d, left of the dashed line). Treatment of the cells with KCI807 decreased expression of only the genes supported by ELK1 (Figure 4.7e). The results demonstrate selectivity of KCI807 for AR target genes that are synergistically activated by ELK1 and AR, which are typically strongly associated with cell cycle progression and mitosis.

4.3.4 Selective *in vitro* growth inhibition by KCI807 and comparison with enzalutamide

KCI807 inhibited both androgen-dependent and androgen-independent *in vitro* growth of standard AR-dependent PC/CRPC cell line models. After initiation of colony formation of the enzalutamide-resistant (191) 22Rv1 CRPC cells, further colony growth was virtually completely inhibited by KCI807 beyond 125nM compound, with an IC_{50} of 33.12 nM. With respect to dose response of the cell growth inhibition by the MTT viability assay, KCI807 was more effective than enzalutamide in LNCaP (androgen-dependent) and 22Rv1 (androgen-independent) cells; moreover, KCI807 completely inhibited cell growth whereas enzalutamide only showed partial effects even at a

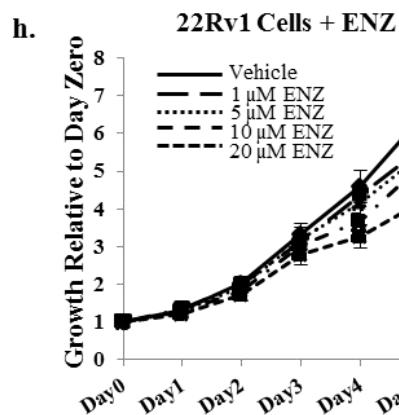
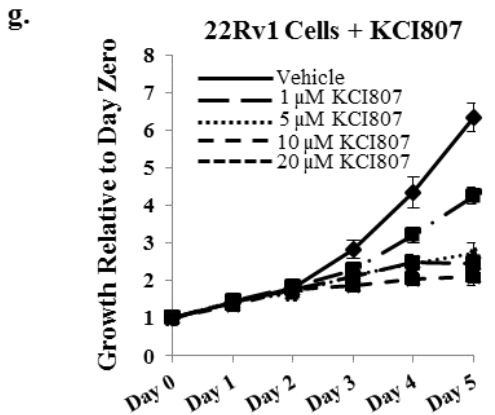
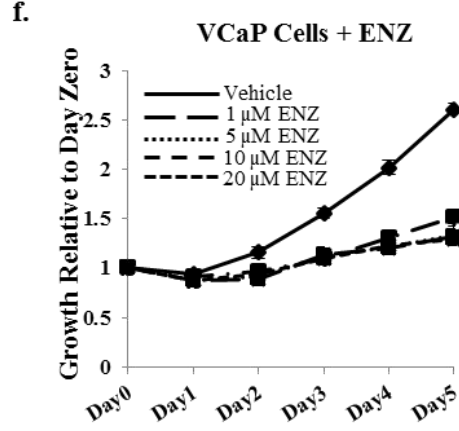
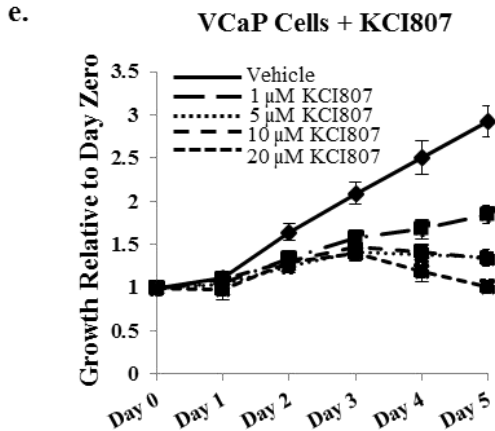
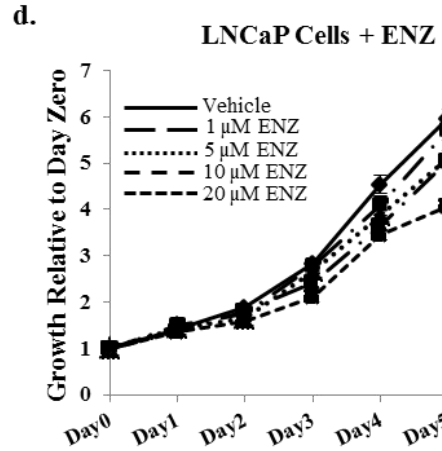
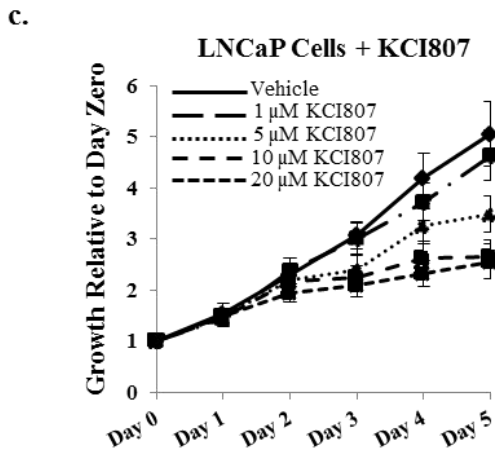
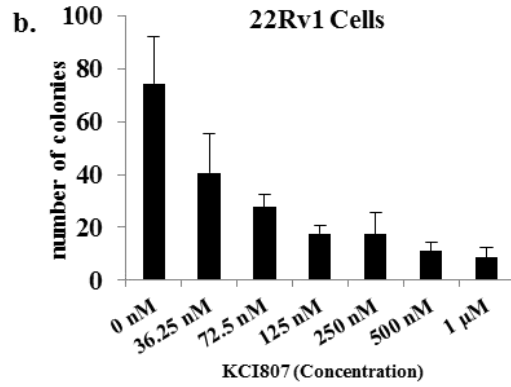
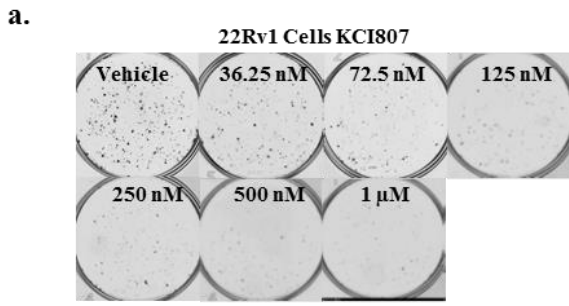
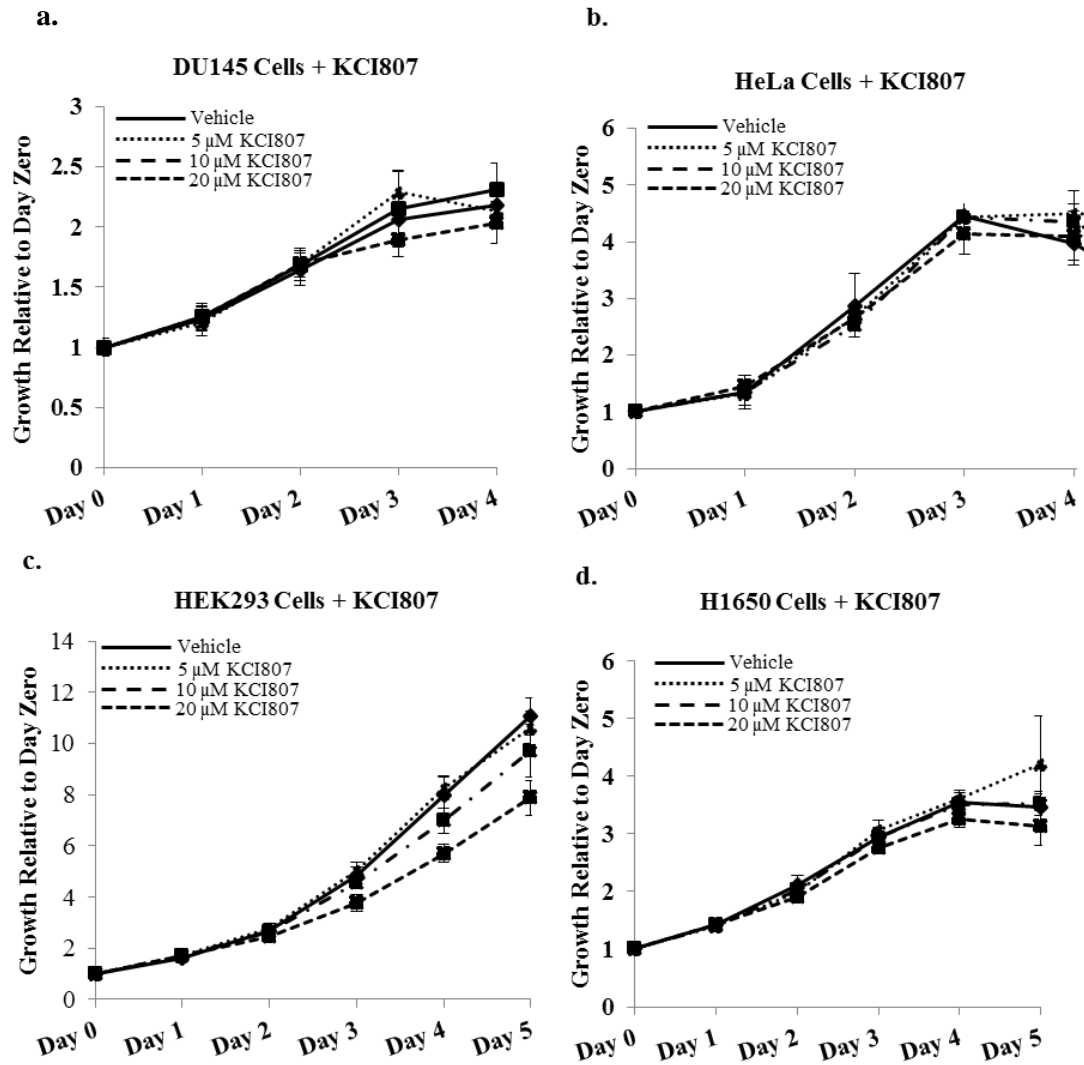


Figure 4.8 Inhibition of AR-dependent PC/CRPC clonogenic survival and cell growth by KCI807 and comparison with enzalutamide. (a) 22Rv1 cells were seeded in triplicate wells in phenol red-free growth media and treated with the indicated concentrations of KCI807 with replenishment of the treatments every 48h. Colonies were stained with crystal violet, 10 days later. The left panel shows representative images of the stained wells. The colony counts were determined using a size cutoff and average values from replicate wells are plotted in the right panel. (b) - (g) The growth inhibitory effects of KCI807 were compared with that of enzalutamide using the MTT assay. Twenty four hours after plating the cells, they were treated with the indicated concentrations of each compound. (b) LNCaP Cells + KCI807 (c) LNCaP Cells + enzalutamide (d) VCaP Cells + KCI807 (e) VCaP Cells + enzalutamide (f) 22Rv1 cells + KCI807 (g) 22Rv1 cells + enzalutamide.



Supplementary Figure 4.9 Effect of KCI807 on *in vitro* growth of AR-negative cancer cell lines was measured by the MTT assay. All values were normalized to the Day zero value for each cell line. (a) Du145 Cells (b) HeLa Cells (c) HEK293 Cells (d) H1650 Cells

concentration of 20 μM (Figure 4.8). VCaP cells (androgen-dependent) were the most sensitive to KCI807 as well as enzalutamide at comparable doses (Figure 4.8). KCI807 did not appreciably affect the growth of AR-negative cell lines including DU145 (PC cells), HeLa (cervical cancer cells), HEK293 (adenovirus transformed kidney fibroblasts) and H1650 (lung adenocarcinoma cells) (Figure 4.9). The growth inhibitory effect of KCI 807 is thus selective for PC cells that are dependent on AR and/or AR-V7 and further this compound shows a better growth inhibitory profile than enzalutamide in well-established cell line models.

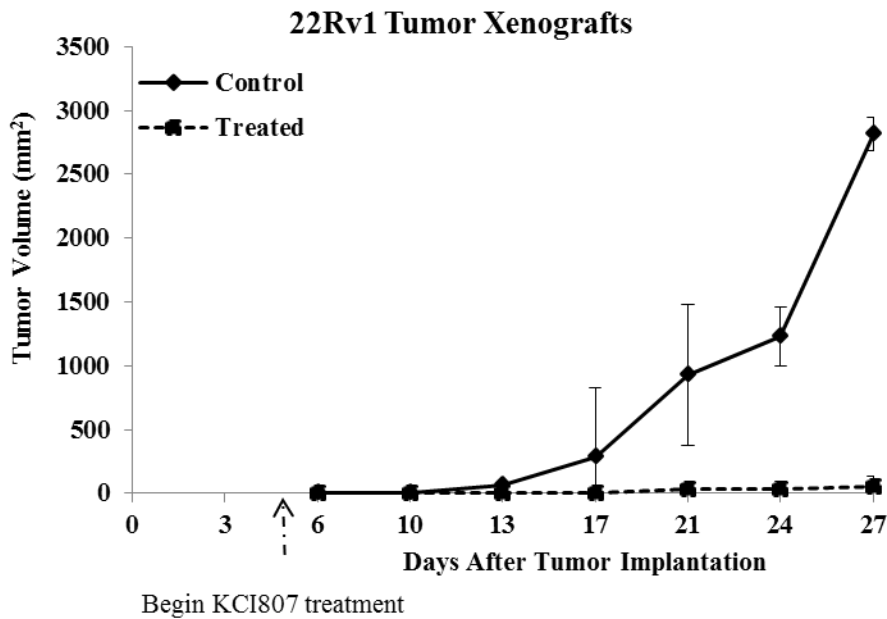
4.3.5 Suppression of CRPC growth *in vivo* by KCI807

The *in vivo* anti-tumor efficacy of KCI807 was tested using the 22Rv1 cell line xenograft model in male SCID mice. Tumor xenografts of 22Rv1 cells were implanted into male SCID mice in the two flanks. Following growth of implanted tumors to ~100 mg, the compound was administered (begin treatment on Day 5) intraperitoneally on alternate days at a dose of 250 mg/kg. for 18 days, reaching a total dose of 4.5 g/Kg. Tumor growth was completely inhibited up until the time the experiment was terminated when the tumor burden in the placebo group reached 5-10% of body weight (Figure 4.10a). The mice treated with KCI807 did not show appreciable weight loss or obvious physical or behavioral abnormalities (Figure 4.10b). The serum concentration of unmetabolized KCI807 24h following the final injection was 0.56 μM .

4.4 Discussion

Current and experimental modalities of therapeutic targeting of the AR signaling axis in prostate cancer, including inhibition of testosterone synthesis and antagonists that bind to either the ligand binding pocket of AR or to the amino-terminal hormone-

a.



b.

Days After Tumor Implantation	0	3	6	10	13	17	21	24	27
Control % body weight lost/gained	0	0	-4	0	0	0	0	0	+2
Treated % body weight lost/gained	0	0	-3.8	-7.7	-7.7	-3.8	-3.8	-3.8	0

Figure 4.10 Inhibition of in vivo CRPC tumor growth by KCI807. Tumor xenografts of 22Rv1 cells were implanted into male SCID mice in the two flanks. On Day 5 after implantation, mice were administered 250mg/Kg of KCI807 or vehicle control, intraperitoneally, every other day for 18 days, reaching a total dose of 4.5 g/Kg. (a) Tumor volumes were measured every 3 days. (b) Changes in body weight of the mice administered either KCI807 or the vehicle control were recorded.

independent activation functions of AR, entail global disruption of androgen/AR actions (337). This study was undertaken to prove the concept that a critical growth signaling arm of AR could be selectively disrupted by small molecule drug candidates that could also circumvent resistance to current treatments from restoration of AR function. Using an unbiased HTS approach combined with SAR studies, we have discovered and characterized a flavonoid molecule (KCI807) that directly binds to AR, blocks binding of ELK1 to AR and also prevents recruitment of AR to chromatin by ELK1. As a result, KCI807 selectively inhibits transcriptional activity of AR mediated by ELK1 binding DNA elements vs. canonical AREs. This is reflected by selective inhibition by KCI807 of ELK1-dependent activation of endogenous genes by AR. As target genes of ELK1-dependent transcriptional activation by AR are critical for cell cycle progression and mitosis, KCI807 selectively inhibits AR-dependent prostate cancer cell growth *in vitro* and tumor growth *in vivo*. As ELK1 binds to the amino-terminal domain of AR, KCI807 is also able to inhibit ELK1-dependent transcriptional activity of the major AR splice variant, AR-V7 and to inhibit growth of AR-V7 expressing cells and tumors.

Similar to other nuclear receptors, including steroid receptors, the amino-terminal domain of AR is intrinsically disordered (338). This is a major obstacle for structure-based design of small molecule drugs targeting functional motifs within this region of the receptor. Nevertheless, it has been previously demonstrated by the empirical approach of small molecule screening and structure-activity studies that small molecules including certain bis-phenols (EPI) (237) and Sintokamide A (239) can bind selectively to this domain of AR with profound inhibitory effects on co-activator binding. Mutational and binding analysis indicates that for binding to ELK1, the amino-terminal domain of AR

precisely only requires the two ERK docking sites in ELK1 (268). Based on our structure-activity studies, the structure of KCI807 only retains the minimal features of the initial hit from our HTS that are required for disrupting the interaction of AR with ELK1, i.e., a flavone scaffold and two hydroxyl groups at specific positions (5 and 3'). Notably, removal of hydroxyl groups at positions 7 and 4' results in a more stable molecule and also prevents rapid metabolism *in vivo* as observed in the mouse model. This relatively small molecule binds to AR with a dissociation constant that is only ~ 3 times that for the binding of ELK1 to AR (268) presumably by binding to a substructure required for the formation the recognition site for one of the two AR docking sites on ELK1. Nevertheless, KCI807 did not interfere with the activation of ELK1 by ERK. Indeed, it has not been possible to identify structures within the amino-terminal region of AR that are similar to the two docking site recognition sites in ERK previously identified using substrate peptides for hydrogen exchange mass spectrometry and X-ray crystallography (339, 340). Therefore, there appears to be some degree of conformational flexibility that enables AR to bind to ELK1. By extension of this principle, it may be possible to identify other small molecules that selectively disrupt the AR-ELK1 complex by binding to other sites on AR or to either one of its two docking sites on ELK1.

From pharmacological and clinical perspectives, the results of this study establish that the ELK1-AR interaction is a drugable target. In the mouse tumor xenograft model, complete suppression of CRPC tumor growth and as well a relatively high level of unmetabolized compound were achieved. This is encouraging because even rapidly metabolized dietary flavonoids, reach quite high (5 - 10 μ M) plasma levels

in humans after continuous dietary supplementation (341). KCI807 was generally a better inhibitor of androgen/AR-dependent PC/CRPC cell growth *in vitro* when compared with enzalutamide in the same dose range using standard cell line models. KCI807 showed no apparent toxicity in the mouse xenograft tumor model of AR-V7 expressing CRPC while showing profound anti-tumor activity. As KCI807 did not interfere with the classical ARE-dependent promoter and gene activation by AR, it is clear that it does not affect co-activator recruitment by the amino-terminal domain of AR, in contrast to current experimental drugs (237, 239) targeting the amino terminal domain that affect a broader range of transcriptional activities of AR. However, the possibility exists that KCI807 may interfere with binding of AR to a yet unidentified tethering protein(s) although this would likely have a much narrower range of effects than systemic testosterone suppression.

Disruption of ELK1-dependent gene activation by KCI807 could in turn affect the expression of certain indirect target genes. Notably, although the PSA encoding gene (KLK3) is regulated by AR via canonical AREs, it is also known to be activated by the protein products of genes such as HIST1H4D (342) and H2AFX (343) which we have found to be synergistically activated by ELK1 and AR. Therefore PSA, which is a biomarker of prostate tumor response to conventional anti-androgen treatments, may also serve as a biomarker of response to KCI807.

In conclusion, our studies demonstrate that the ELK1-dependent arm of androgen/AR signaling is a drugable and functionally tumor selective target in the spectrum of prostate tumors including CRPC and one that predictably obviates the need for systemic testosterone suppression.

CHAPTER 5- Hybrid Enzalutamide Derivatives with Histone Deacetylase Inhibitor Activity Decrease HSP90 and the Androgen Receptor Levels and Inhibit Viability in Enzalutamide Resistant C4-2 Prostate Cancer Cells

Reprinted with permission of the American Society for Pharmacology and Experimental Therapeutics. All rights reserved.

MOLECULAR PHARMACOLOGY Mol Pharmacol 90:225–237, September 2016
Copyright ©2016 by The American Society for Pharmacology and Experimental Therapeutics

5.1 Introduction

Prostate cancer (PCa) is the second leading cause of cancer-related deaths in men in the United States (344). PCa is initially managed with surgery, radiation, androgen antagonists (e.g., bicalutamide) and surgical or chemical castration. However, the relapsed or metastatic disease post-castration (castration-recurrent prostate cancer or CRPC) has poor prognosis with most patients dying within 2 years (345). Innovative treatment approaches are urgently needed to treat CRPC patients.

Androgen receptor (AR) signaling is a major driving force in all stages of PCa (114). CRPC cells evolve mechanisms to re-activate AR signaling under androgen deprivation conditions (346); these mechanisms include overexpression and gain-of-function mutations of AR (347, 348), overexpression of AR splice variants (AR-Vs) (210), compensatory cross-talk between AR and other signaling pathways (349) and enhanced intra-tumoral androgen biosynthesis (350). Enzalutamide (Enz) is a newly FDA approved AR antagonist that prolongs survival of CRPC patients (351, 352). Enz competitively binds to AR with 5-8 fold higher affinity than bicalutamide and, in contrast to bicalutamide, does not promote AR nuclear translocation (321). Nevertheless, acquired resistance to Enz typically develops within months and is associated with a relatively short-lived patient survival benefit. Indeed, *in vivo* generated CRPC cell line

models that vastly overexpress AR (e.g., C4-2 cells), presumably in combination with changes in other cellular signaling pathways, are completely resistant to Enz in conditioned media while remaining addicted to AR (191).

A possible strategy to overcome resistance to androgen depletion is to induce destabilization and degradation of AR and its associated proteins in CRPC cells. AR is stabilized in the cytosol by its interaction with heat shock protein 90 (HSP90) and other chaperone proteins. HSP90 is commonly overexpressed in many types of cancer cells and has been explored as a drug target for cancer treatment, including PCa (353, 354). HSP90 is an ATP-dependent molecular chaperone that aids the folding and stability of a number of client proteins, such as steroid receptors, protein kinases, transcription factors and proteins involved in regulating cell survival. Therefore, inhibition of HSP90 leads to degradation of its client proteins via the ubiquitin-proteasome pathway. Association of the AR apo-protein with HSP90 is critical for stabilizing AR in a conformation that allows androgen binding (355, 356). In PCa cells, HSP90 inhibitors induce AR degradation and impair AR nuclear translocation while simultaneously reducing the levels of other oncogenic client proteins, such as p-AKT/AKT, EGFR and IGF-IR and survivin (357-360). Simultaneous disruption of AR and other aberrant growth/survival networks via HSP90 inhibition is an advantageous treatment strategy for CRPC as this would silence potentially mutually compensatory oncogenic signaling pathways. Despite this attractive scientific rationale, clinical development of HSP90 inhibitors for PCa treatment were disappointing (361-364) and was also limited by adverse toxicity to non-target tissues.

One of the actions of histone deacetylase (HDAC) inhibitors (HDACi) is to disrupt HSP90 activity. HDACs remove acetyl groups from lysine residues of histone and non-histone proteins. Eighteen HDACs categorized into four classes have been identified in mammalian cells. Among them, HDAC6 is a zinc-dependent, class-IIb HDAC and is localized in the cytoplasm (365). HDAC6 deacetylates HSP90 (366, 367). Inhibition of HDAC6 could result in hyper-acetylation of HSP90, loss of ATP binding and dissociation and degradation of its client proteins, including AR. The HDACi LAQ-824 (368), PDX-101 (i.e. Belinostat) (369), suberoylanilide hydroxamic acid (SAHA or vorinostat) (370, 371) and natural products sulforaphane (372) and genistein (373) have all been reported to reduce AR protein levels in PCa cells by disrupting the HDAC6-HSP90 chaperone function.

Clinical use of HDACi is now confined to hematological malignancies. Although nuclear HDACs (e.g., HDAC1 and HDAC3) are indispensable for AR transcriptional activity (374) and increased HDAC levels have been reported in clinical CRPC samples and positively correlated to Gleason scores (375, 376), they are not likely to serve as effective drug targets to treat PCa. HDACi, such as vorinostat (SAHA) (377), romidepsin (FK-228) (378), panobinostat (LBH-589) (379) and pracinostat (SB-939) (380) have been tested in CRPC patients but have resulted in modest outcomes. Toxicities associated with their pleiotropic effects could contribute to the ineffectiveness of HDACi in PCa treatment. Moreover, recent studies have associated the pleiotropic effects of HDACi, particularly epigenetic modifications of chromatin-associated proteins, with induction of epithelial to mesenchymal transition (EMT) in prostate, endometrial and nasopharyngeal cancer cells (381-384). Therefore clinical translation of the extensive

and promising pre-clinical findings of the efficacies of HDACi in treating solid tumors must address the issue of toxicities that prevent application of effective HDACi treatment regimens in the clinic.

We sought to develop enzalutamide derivatives armed with HDACi activity to antagonize AR and HSP90 actions in AR-overexpressing and enzalutamide resistant CRPC cells with reduced pleiotropic effects typical of strong HDACis. Accordingly, we have designed, synthesized and tested the prototype compounds **2-75** and **1005**. The **2-75** and **1005** chemical scaffolds are designed to retain AR binding affinity. The compounds are also designed to have lower intrinsic HDACi activity compared to SAHA, thus reducing the HDACi activity against non-target proteins. Nevertheless, the HDACi activity is expected to produce effective disruption of AR as well as other HSP90 client proteins, resulting in loss of viability in Enz-resistant CRPC cells.

5.2 Materials and Methods

5.2.1 Compound Synthesis

Detailed procedures for the synthesis of compounds **2-75**, **1005**, **3-52** and **1002** are described in (385). The chemical identities of the compounds were confirmed by using ^1H , ^{13}C -NMR and high resolution mass spectrometry. All chemical compounds (**2-75**, **1005**, **3-52** and **1002**) listed were synthesized by Dr. Zhihui Qin's laboratory.

5.2.2 HDAC activity assay

In *vitro* HDAC inhibition was measured by using the HDAC fluorimetric assay/drug discovery Kit (Enzo Life Sciences, BML-AK500) and the HDAC6 fluorimetric drug discovery kit (Enzo Life Sciences, BML-AK516) following the

manufacturer's protocols and instructions. IC_{50} values were calculated from nonlinear aggression plots using GraphPad Prism5 software.

5.2.3 Cell Culture and Reagents

LNCaP and PC3 cell lines were from American Type Culture Collection (Manassas, Va). LNCaP and C4-2 cells were routinely grown at 37°C in 5% CO₂ in RPMI 1640 medium supplemented with 10% FBS (Invitrogen); 100units/ml penicillin, 100 µg/ml streptomycin, 2mM L-glutamine mixture (Invitrogen); and sodium pyruvate (1mM) (Invitrogen). PC3 cells were grown in RPMI 1640 medium supplemented with 10% FBS (Invitrogen); 100units/ml penicillin, 100 µg/ml streptomycin, and 2mM L-glutamine mixture (Invitrogen). Affinity-purified rabbit anti-human antibody to AR (sc-816), mouse anti-human antibody to GAPDH (sc-47724) and affinity-purified mouse anti-human antibody to alpha tubulin (sc-8035) were purchased from Santa Cruz Biotechnology (Santa Cruz, CA). Affinity-purified rabbit anti-human antibody to HSP90 (C45G5) #4877, rabbit anti-human antibody to acetylated lysine #9441, and affinity-purified rabbit anti-human antibody to p21 Waf1/Cip1 #2947S were purchased from Cell Signaling Technology. Affinity-purified rabbit anti-human antibody to acetyl-tubulin (#ABT241), acetyl Histone H4 (#07-328), acetyl Histone H3 (#ABE18) were purchased from Millipore. R1881 was kindly provided by Dr. Stephan Patrick (Karmanos Cancer Institute). Cycloheximide was from Sigma. All experiments were conducted using phenol-red free growth media. For hormone depletion, cells were grown in phenol-red free RPMI 1640 medium supplemented with 10% charcoal stripped FBS (Sigma-Aldrich) which was heat inactivated at 56°C for thirty minutes, and a mixture of 100units/ml penicillin, 100 µg/ml streptomycin and 2 mM L-glutamine for 96 h.

5.2.4 Cell Viability Assay

Cells were trypsinized and 6000 cells/well were seeded in 96-well plates coated with poly-D-lysine. The cells were seeded in phenol red-free medium supplemented with 10% FBS, 100units/ml penicillin, 100 µg/ml streptomycin, 2mM L-glutamine mixture and sodium pyruvate (1mM) for C4-2 cells and phenol red-free medium supplemented with 10% FBS, 100units/ml penicillin, 100 µg/ml streptomycin and 2mM L-glutamine mixture for PC3 cells. The cells were grown at 37°C in 5% CO₂. Twenty four hours after seeding in the 96-well plates, the cells were treated with indicated compound or DMSO (vehicle). The culture medium was not changed during the time course of the assay. On day zero and on day 3, cell viability was determined using the MTT assay. MTT (10µL, 5mg/mL) was added to each well and incubated for 2h at 37°C. The formazan crystal sediments were dissolved in 100µL of DMSO, and the absorbance at 570nm was measured using the BioTek Synergy 2 Microplate Reader (BioTek, Winooski, VT). The assay was conducted in sextuplicate wells and values were normalized to day zero (386). IC₅₀ values were calculated from nonlinear aggression plots using GraphPad Prism5 software.

5.2.5 Western Blot Analysis

Cells were washed once with phosphate buffered saline (PBS) and then lysed with RIPA buffer (150mM NaCl, 1% Nonidet P-40, 0.5% sodium deoxycholate, 0.1% SDS, 50mM Tris of pH 8.0) containing a protease inhibitor cocktail (Pierce, Thermo Fisher Scientific). The cell lysates were then incubated on ice for 40 minutes. Total protein concentrations were estimated using the Bradford Assay (Bio-Rad). Protein samples (10-40 µg) were heated at 95°C for 5 minutes and resolved by electrophoresis

on 8% polyacrylamide-SDS gels and electrophoretically transferred to PVDF membranes (Millipore, Billerica, MA). The membranes were then probed overnight at 4°C with the appropriate primary antibody followed by the appropriate horseradish peroxidase-conjugated secondary antibody. The blots were then developed to visualize the protein bands using the HyGLO Chemiluminescent HRP Antibody Detection Reagent (Denville Scientific, Metuchen, NJ) (332).

5.2.6 RNA isolation, Reverse Transcription, and Real Time PCR

Total RNA was isolated from cells using the RNeasy Mini Kit (Qiagen). Reverse transcription PCR was then performed using 500 ng of total RNA with random primers and using the high-capacity complementary DNA Archive kit (Applied Biosystems). The complementary DNA from this reaction was measured using quantitative real time PCR using the StepONE Plus Real Time PCR system (Life Technologies Corporation, Carlsbad, CA). All reactions were performed in triplicate and normalized to glyceraldehyde-3-phosphate-dehydrogenase values in the same samples. All primers and Taqman probes were purchased from the applied Biosystems inventory (Invitrogen) (387).

5.2.7 Chromatin Immunoprecipitation (ChIP)

C4-2 cells were treated with either vehicle, R1881 (1 nM or 10 nM), or 10uM of each indicated compound for 2 h and then subjected to ChIP using anti-AR antibody (sc-816 from Santa Cruz, CA). The ChIP assay was performed using the EX ChIP chromatin immunoprecipitation kit (catalogue number 17-371 from Millipore, Temecula, CA) according to the vendor's protocol. The ChIP signals were measured by

quantitative real time PCR analysis of the immunoprecipitated products. Each sample was tested in triplicate (246).

5.2.8 Statistical Analysis

All experiments were performed in triplicate groups and repeated at least three times. The error bars in all graphs represent the standard deviation. Statistical analysis was performed using one-way ANOVA with post-hoc and LSD (Least Square Differences) and/or T-test (388) using GraphPad v.6.0 software.

5.3 Results

5.3.1 Design and synthesis of compounds 2-75 and 1005 with partial chemical scaffolds of Enz and SAHA.

Compounds **2-75** and **1005** were designed to retain partial functional scaffolds of Enz and SAHA (Figure 5.1A). Upon binding to AR, the cyano group of Enz/Enz derivatives forms a critical hydrogen bond with Arg752, and the conformationally restricted thiohydantoin ring in the middle forces the rest of the molecule to the “H11 pocket”, a region near the C terminus of helix 11 and the loop connecting helices 11 and 12 (389). To design derivatives with both AR-binding and HDACi activities, different linkers connecting Enz and a zinc binding group (ZBG) were introduced to retain the above structural features that are required for AR binding in an antagonist-related conformation. **1005** is a cinnamyl hydroxamic acid derivative with a three-carbon linker. A relatively longer carbon chain in **2-75** was used to more closely mimic the chemical structure of SAHA. Compound **7 (3-52)**, a close structural analogue of **2-75** using methyl ester to replace ZBG was synthesized as a control compound without an HDACi functional group (Figure 5.1B). Compound **7 (3-52)** and synthetic intermediate

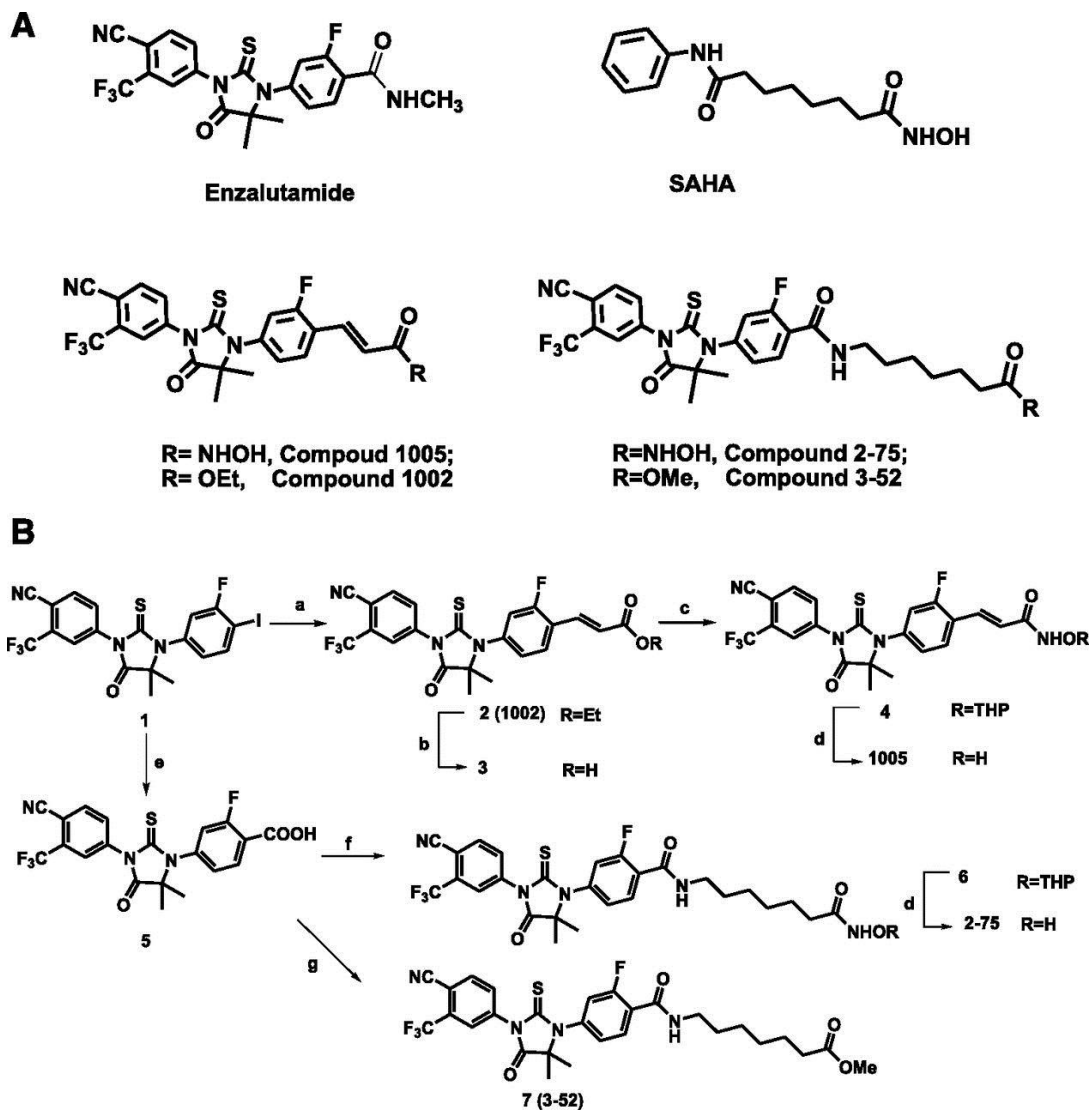


Figure 5.1 Compound structures and synthetic schemes. (A) Chemical structures of Enz, SAHA, 1005, 2-75, 1002, and 3-52. (B) Synthesis of 1005, 2-75, 1002, and 3-52. Reagents and conditions are as follows: (a) ethyl acrylate, Pd(OAc)₂, P(*o*-tolyl)₃, DIPEA, DMF, 80°C, 75%; (b) 37% HCl (aq), acetonitrile, reflux, 91%; (c) NH₂OTHP, BOP, DIPEA, DMF, 51%; (d) HCl (4 N in dioxane), MeOH, 60% for 1005, 32% for 2-75; (e) HCOOLi, Ac₂O, Pd₂(dba)₃, LiCl, DMF, 80°C, 92%; (f) 7-amino-*N*-(tetrahydro-2*H*-pyran-2-yl)oxy heptanamide, HBTU, DIPEA, DMF, 30%; and (g) methyl 7-aminoheptanoate hydrochloride, HBTU, DIPEA, DMF, 47%. BOP, benzotriazol-1-yl-oxy-tris-(dimethylamino)phosphonium hexa-fluorophosphate; DIPEA, *N,N*-Diisopropylethylamine; DMF, *N,N*-Dimethylformamide; HBTU, 2-(1*H*-benzotriazol-1-yl)-1,1,3,3-tetramethyluronium hexafluorophosphate; THP, tetrahydropyranyl. *Reprinted with permission of the American Society for Pharmacology and Experimental Therapeutics. All rights reserved.*

compound **2** (i.e. **1002**, an ethyl ester analogue of **1005**, Figure 5.1A, B) were used to investigate AR antagonist properties of **2-75** and **1005** scaffold, respectively.

Both **2-75** and **1005** were synthesized from a 4'-iodo substituted intermediate (Figure 5.1B) **1**. Acrylate linker of **1005** was introduced via Pd(OAc)₂-catalyzed Heck reaction to afford compound **2**, followed by hydrolysis of ethyl ester, coupling to THP (tetrahydropyranyl acetal)-protected hydroxylamine and the final acidic deprotection. To synthesize **2-75**, carboxylation of aryl iodine **1** was performed using a palladium-catalyzed carboxylation reaction (390), the resulted carboxylic acid then coupled with primary amines to attach the alkyl chain with protected hydroxamic acid (compound **6**) or methyl ester (compound **7**). Removal of THP protecting group gave the final product **2-75**. The detailed synthetic procedures are described in the Supplemental Material.

5.3.2 Compounds 2-75 and 1005 possess intrinsically weak inhibitor activity against nuclear HDACs and cytosolic HDAC6

To measure HDAC inhibitory activities of **2-75** and **1005**, cell-free enzymatic assays were performed against a nuclear extract of HeLa cells and also against human recombinant HDAC6. HDAC1 and HDAC2 are enriched in nuclear extracts whereas HDAC6 is a cytosolic enzyme that is the principal modulator of the acetylation status of HSP90. The HeLa cell nuclear extract was used to evaluate inhibitory activity against nuclear HDACs. **2-75** and **1005** dose-dependently inhibited HDACs enriched in the HeLa nuclear extract with IC₅₀ values of 1.08 μM and 2.41 μM compared to a value of 0.30 μM for SAHA (Figure 5.2A). In contrast, compounds **3-52** and **1002**, which share the chemical scaffolds of **2-75** and **1005** respectively, but lack the HDACi functional group, did not inhibit nuclear HDAC activity even up to a concentration of 25 μM (Figure 5.2B).

As expected, Enz also lacked any HDACi activity in contrast to a pan-HDACi, trichostatin A (TSA), which was used as a positive control (Figure 5.2B). **2-75** and **1005** were also weaker inhibitors of recombinant HDAC6, with IC_{50} values of 2.0 μ M and 6.93 μ M, respectively compared with the IC_{50} of 0.85 μ M for SAHA (Figure 5.2C). As expected, the negative control compounds **3-52** and **1002** as well as Enz did not show significant inhibitory activity against HDAC6 even at a concentration of 25 μ M (Figure 5.2D). Again, TSA served as the positive control in Figure 5.2D.

The HDACi activities of **2-75** and **1005** were also compared with those of their parent compounds *in situ* in both LNCaP and C4-2 prostate cancer cells using activation of the DLC1 tumor suppressor gene as the readout. SAHA induces histone acetylation at the DLC1 promoter and effectively increases DLC1 mRNA expression in prostate cancer cells (391). Accordingly, DLC1 mRNA was strongly up-regulated by SAHA in both LNCaP cells (Figure 5.2E) and in C4-2 cells (Figure 5.2F). As expected from the fact that DLC1 is not an AR-regulated gene, Enz had no effect on DLC1 mRNA expression. Consistent with the results of the cell-free HDACi assays above, compounds **2-75** and **1005** were poor inducers of DLC1 mRNA compared with SAHA, both in LNCaP cells and in C4-2 cells (Figure 5.2E and 5.2F). Further, similar to the results from cell-free assays, **1005** was a much weaker HDACi than **2-75** in the *in situ* assays (Figure 5.2E and 5.2F). Taken together, the results indicate that compounds **2-75** and, to a greater degree, **1005** have much less potent HDACi activity in the cellular context reflecting their intrinsically weak inhibitor activities compared with SAHA.

5.3.3 The partial Enz chemical scaffold confers AR targeted antagonist activity without ligand-induced chromatin association of AR

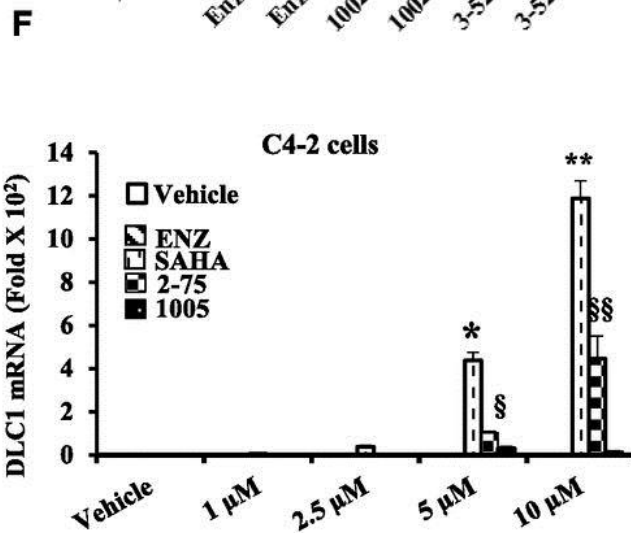
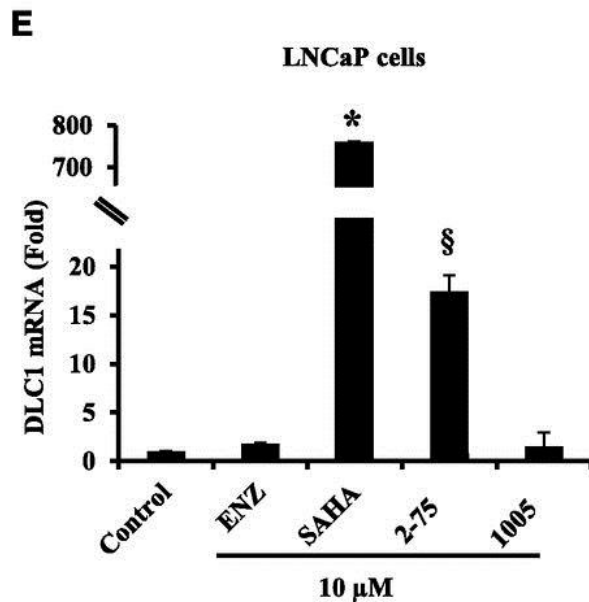
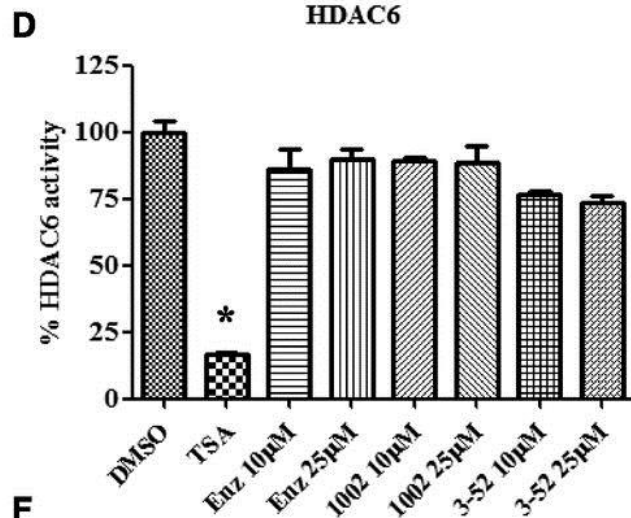
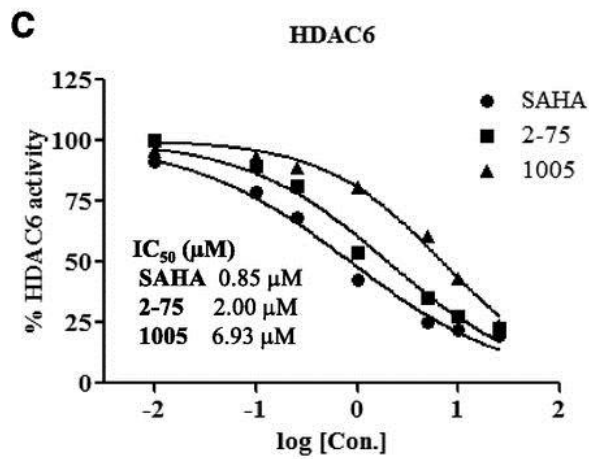
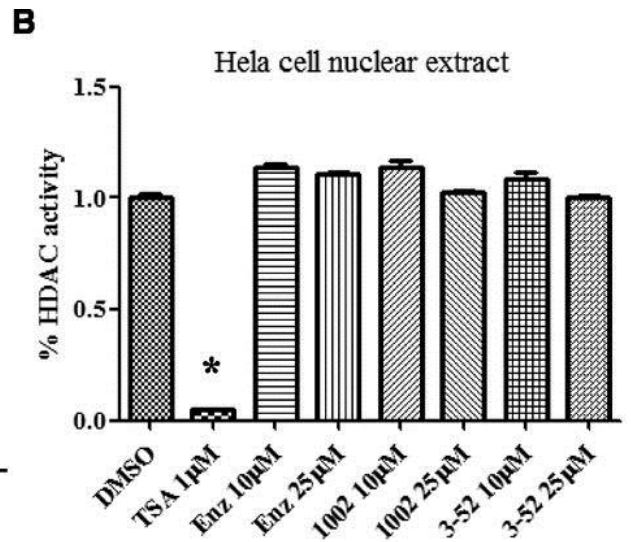
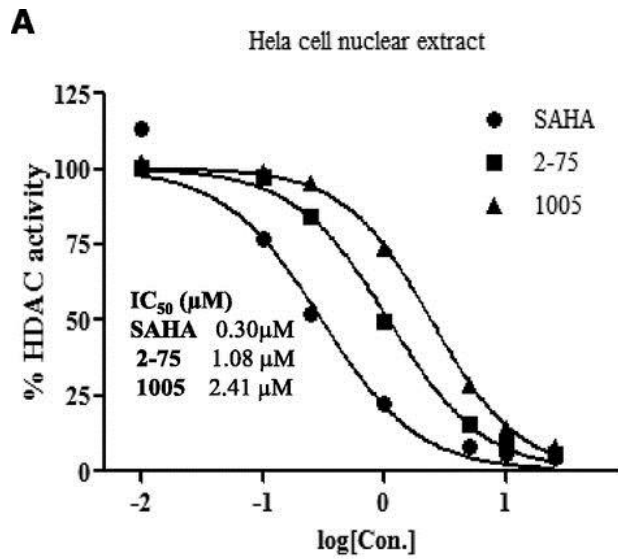


Figure 5.2 Measurement of intrinsic and in situ HDACI activities. (A) Dose-dependent inhibition of HDACs from HeLa cell nuclear extract by 2-75, 1005, and SAHA. HeLa cell nuclear extract was incubated with each drug at the indicated concentrations. IC_{50} values were calculated from nonlinear regression plots using GraphPad Prism5 software. (B) Enz, 1002, and 3-52 were tested against HeLa cell nuclear extract at 10 μ M and 25 μ M and TSA (1 μ M) was used as a positive control. (C) Dose-dependent inhibition of recombinant HDAC6 by 2-75, 1005, and SAHA. Recombinant HDAC6 was incubated with each drug at the indicated concentrations. IC_{50} values were calculated from nonlinear regression plots using GraphPad Prism5 software. (D) Enz, 1002, and 3-52 were tested against recombinant HDAC6 at 10 μ M and 25 μ M and TSA (1 μ M) was used as a positive control. (E) LNCaP cells were treated with the indicated compounds (10 μ M) or vehicle (DMSO) for 48 hours. Cells were then harvested to quantify mRNA for DLC1 and values were normalized to the values for GAPDH mRNA. (F) C4-2 cells were treated with the indicated concentrations of Enz, SAHA, 2-75, or 1005 or vehicle (DMSO) for 48 hours. Cells were then harvested to quantify mRNA for DLC1 and values were normalized to the values for GAPDH mRNA. In all panels, the error bars represent the standard deviation of experimental triplicates. Where indicated *, **, §, §§, $P < 0.05$. DMSO, dimethylsulfoxide; TSA, trichostatin A. *Reprinted with permission of the American Society for Pharmacology and Experimental Therapeutics. All rights reserved.*

Although C4-2 cells are not growth-inhibited by Enz due to hormone-independent actions of AR, the canonical androgen target genes KLK3 and TMPRSS2 are activated by androgen and their activation is inhibited by androgen antagonists (241). HDACi are also potent inhibitors of the androgen signaling axis as they cause degradation of AR in the cytosol in addition to other cellular effects (368, 369, 392). To test whether the Enz moiety could enable **2-75** and **1005** to target to AR, we tested the ability of compound **3-52** to inhibit activation of KLK3 and TMPRSS2 by androgen. Compound **3-52** shares the chemical scaffold of **2-75** but lacks the HDACi functional group; therefore **3-52** should depend on the partial Enz chemical scaffold to antagonize gene activation by androgen. SAHA partially inhibited activation of KLK3 (Figure 5.3A) and TMPRSS2 (Figure 5.3B) by the synthetic androgen R1881 in C4-2 cells whereas Enz showed progressive inhibition at higher doses. Compounds **2-75** and **1005** were both better inhibitors of gene activation by androgen compared with either Enz or SAHA (Figure 5.3A and 5.3B). On the other hand, compound **3-52** inhibited activation of KLK3 and TMPRSS2 to a degree that was comparable to Enz suggesting that the partial Enz chemical scaffold in compounds **2-75** and **1005** retained an Enz-like AR binding property. The superior androgen antagonist activities of **2-75** and **1005** compared with Enz may be explained by their additional HDACi activities.

AR ligands including agonists and classical androgen antagonists such as bicalutamide promote nuclear translocation of AR and the binding of AR to canonical hormone (androgen) response elements associated with androgen-regulated genes. In contrast, Enz does not stimulate AR nuclear translocation and DNA binding (321, 393). To test whether the partial Enz chemical scaffold would mobilize AR to the chromatin,

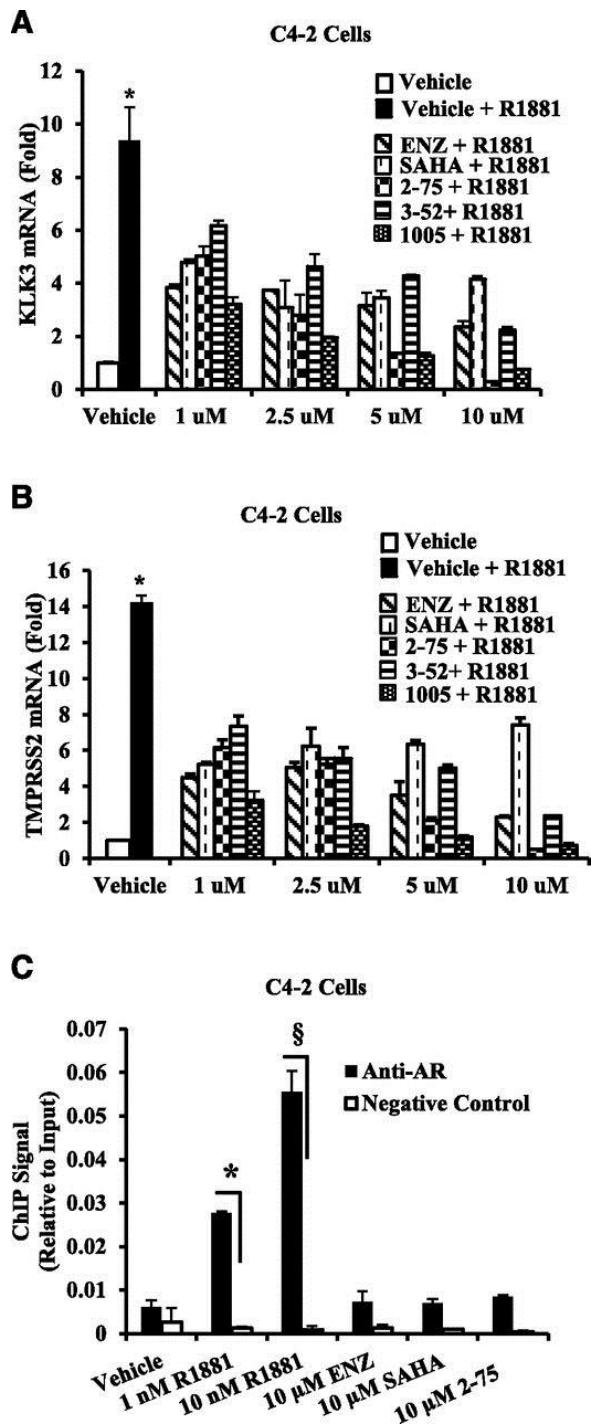


Figure 5.3 Testing the ability of compounds to interact with AR and to induce chromatin association of AR. (A and B) Data obtained using C4-2 cells are shown. After 96 hours of hormone depletion, cells were treated with R1881 (1 nM) and 1 μ M, 2.5 μ M, 5 μ M, or 10 μ M of the indicated compound or vehicle (DMSO) for 48 hours. Cells were then harvested to purify total RNA. The mRNAs for KLK3 and TMPRSS2 were quantified by normalizing to the values for GAPDH mRNA. In all panels, the error bars represent the standard deviation of experimental triplicates. (C) C4-2 cells plated in hormone-depleted medium were treated with vehicle, R1881, or the indicated compound for 2 hours. Cells were harvested and subjected to ChIP using AR antibody. TaqMan probes targeting androgen response element enhancer elements associated with the KLK3 gene were used to quantify the immunoprecipitated chromatin. In all panels, the error bars represent the standard deviation of experimental triplicates. Where indicated, * and §, $P < 0.01$. Reprinted with permission of the American Society for Pharmacology and Experimental Therapeutics. All rights reserved.

we employed chromatin immunoprecipitation using C4-2 cells treated with androgen, Enz, SAHA and compound **2-75**. As a target site for the ChIP assay, we chose the well-established AR binding enhancer elements located 4kb upstream of the transcription initiation site of the KLK3 gene. As seen in Figure 5.3C, androgen treatment strongly stimulated chromatin association of AR whereas Enz, SAHA and compound **2-75** all gave the basal ChIP signal corresponding to the vehicle treatment control. These results suggest that the new compounds must antagonize AR in the cytosolic rather than in the nuclear compartment.

5.3.4 Compounds 2-75 and 1005 induce enhanced degradation of AR and HSP90 and hyper-acetylation in a putative 55 KDa HSP90 fragment

Previous observations using potent non-targeted HDACi have shown that the compounds directly affect the AR signaling axis by hyper-acetylation of the AR chaperone complex, through inhibition of HDAC6, leading to degradation of HSP90 as well as release and degradation of AR. We therefore hypothesized that despite their intrinsically weak HDACi activities, the Enz moiety may enable compounds **2-75** and **1005** to more effectively target AR in its chaperone complex, leading to relatively efficient degradation of AR. To test this possibility, we treated C4-2 cells with Enz, SAHA, **1005** and **2-75** at doses ranging from 1 μ M to 10 μ M for 24h. Western blots of the cell lysates were probed for AR and GAPDH (loading control) and the AR band intensities relative to GAPDH were quantified using ImageJ software (Figure 5.4A). Whereas Enz did not cause an appreciable change in the AR protein level, SAHA did cause a decrease in AR level in a dose-dependent manner (Figure 5.4A). Compared to SAHA, both **2-75** and **1005** decreased the AR level to a greater extent with **2-75** being

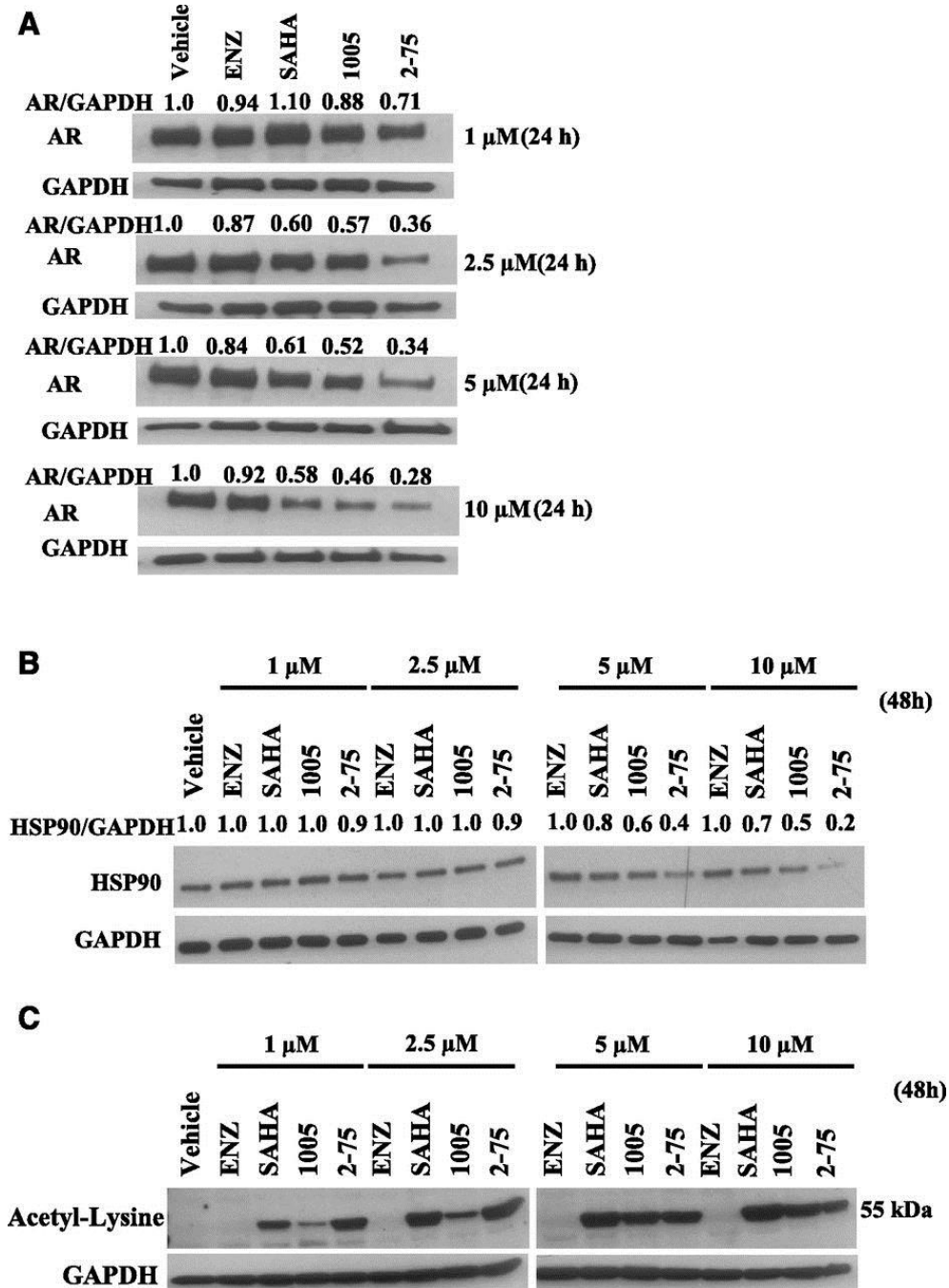


Figure 5.4 Modulation of protein levels and hyperacetylation. C4-2 cells were treated with the indicated concentrations of Enz, SAHA, 1005, or 2-75 or with vehicle (dimethylsulfoxide) for the time indicated. Cells were then harvested for Western blot analysis using antibody to AR (A), HSP90 (B), acetyl lysine (C), or GAPDH (loading control). ImageJ software was used to determine the intensities of the bands relative to the vehicle control for each protein. The values were then divided by the values for GAPDH within the same samples. *Reprinted with permission of the American Society for Pharmacology and Experimental Therapeutics. All rights reserved.*

more effective than **1005** at each dose (Figure 5.4A). To determine whether the decrease in AR was due to increase in the rate of AR degradation we tested the effects of the compounds after blocking *de novo* protein synthesis using cycloheximide. We monitored degradation of p21 to confirm the activity of cycloheximide. As expected there was a rapid decrease in p21 upon treatment with cycloheximide confirming that the treatment efficiently blocked *de novo* protein synthesis (Figure 5.5). In the presence of cycloheximide the AR protein level was decreased by approximately half at the end of 24h indicating a relatively slow turnover of the AR protein. Under these conditions treatment with SAHA, 1005 and 2-75 all caused greater declines in the AR level with 2-75 showing the strongest effect (Figure 5.5). The results indicate that the decrease in AR caused by 1005 and 2-75 is due to increased degradation of AR. The extent of degradation of AR in C4-2 cells appeared adequate to offset the high level of overexpression of AR that is necessary to support growth in these cells.

To explore a possible link between decreased AR levels and effects of the compounds on the AR chaperone complex, we examined whether compounds **2-75** and **1005** decreased the level of HSP90. Probing of the lysates from the treated cells (48h treatment) for HSP90 by western blot and quantification of HSP90 was conducted by procedures similar to that used above for AR. Enz had no effect on the level of HSP90 whereas in the SAHA-treated cells, a decrease in HSP90 was evident at the higher doses (5 μ M and 10 μ M) (Figure 5.4B). On the other hand, cells treated with **1005** and **2-75** showed more marked reduction in HSP90, with **2-75** being more efficient than **1005**. Probing identical western blots with an antibody against acetylated lysine showed that SAHA as well as **1005** and **2-75**, but not Enz, showed hyper-acetylation of a ~55 kDa

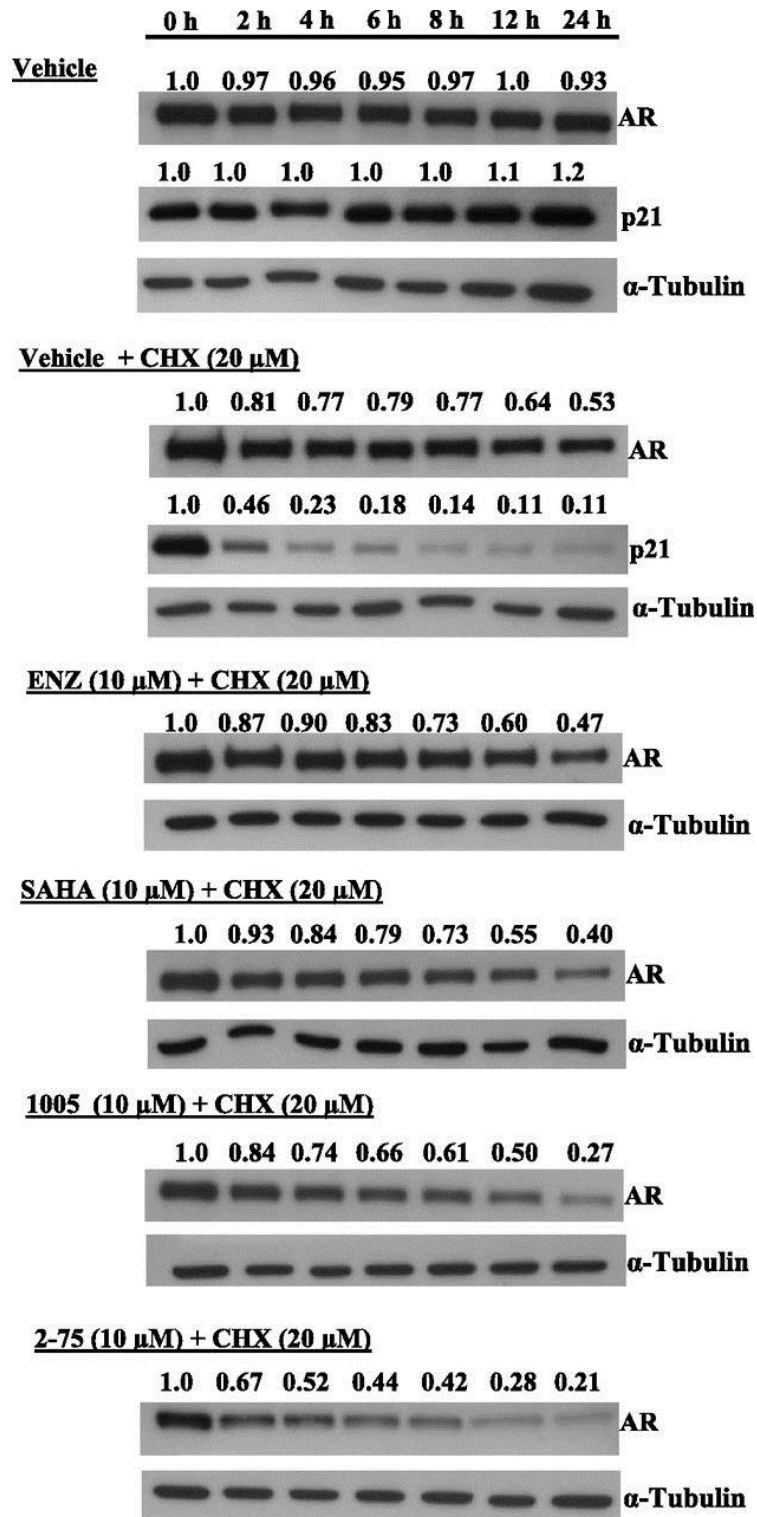


Figure 5.5 Induction of AR degradation. C4-2 cells were pretreated with cycloheximide (20 μ M) or with vehicle for 2 hours, followed by the introduction of Enz (10 μ M), SAHA (10 μ M), 1005 (10 μ M), 2-75 (10 μ M), or vehicle for the indicated durations. Cells were then harvested for Western blot analysis and probed with antibody to AR, p21, or α -tubulin (loading control). ImageJ software was used to determine the intensities of the bands relative to the 0-hour time point for each treatment. CHX, cycloheximide. *Reprinted with permission of the American Society for Pharmacology and Experimental Therapeutics. All rights reserved.*

polypeptide (Figure 5.4C), similar to one that has previously been identified as a fragment HSP90 produced by SAHA treatment (394). Taken together, the above results are consistent with the view that the ability of the compounds to induce acetylation and reduction of HSP90, and consequently AR degradation, underlies the ability of the compounds to attenuate AR signaling.

5.3.5 The hybrid molecules selectively inhibit cytosolic HDAC6 *in situ*

As HSP90 in the AR chaperone complex is a target of the cytosolic HDAC6, the hyper-acetylation of degradation of HSP90 induced by **2-75** and **1005** is likely to occur through inhibition of HDAC6. If this were the case, we may expect that **2-75** and **1005** would also induce hyper-acetylation of α -tubulin which is diagnostic of HDAC6 inhibition. To test this possibility, we treated C4-2 cells with Enz, SAHA, **1005** and **2-75** at doses ranging from 2.5 μ M to 10 μ M for 24h. Western blots of the cell lysates were probed for acetyl-tubulin, as well as total α -tubulin. The band intensities for acetyl-tubulin relative to total α -tubulin were quantified using ImageJ software (Figure 5.6). **2-75** induced a greater degree of hyper-acetylation of α -tubulin (relative to total tubulin) compared to SAHA, whereas 1005 produced a similar effect albeit to a somewhat lesser degree than SAHA (Figure 5.6). When the same cell lysates were probed using antibodies against acetylated histones H3 and H4, it was clear that SAHA alone induced a strong induction of histone acetylation (Figure 5.6). The results clearly demonstrate strong and selective *in situ* activity of **2-75** and **1005** on cytosolic HDAC6.

5.3.6 Compounds **2-75** and **1005** up-regulate p21 and inhibit viability of Enz-resistant prostate cancer cells

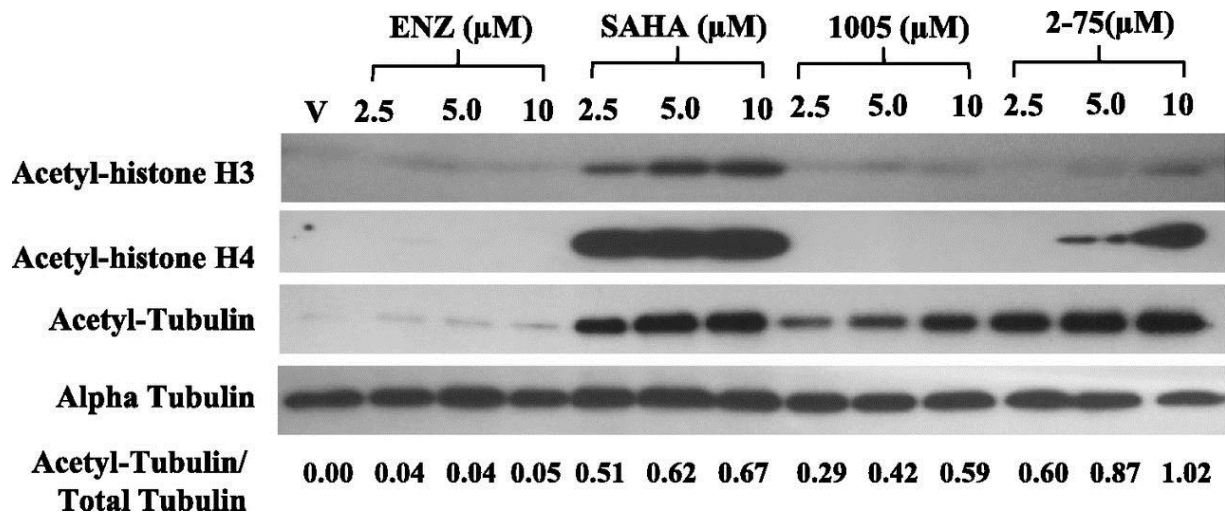


Figure 5.6 Hyperacetylation of α -tubulin and histones H3 and H4. C4-2 cells were treated with Enz, SAHA, 1005, or 2-75 (2.5 μM , 5 μM , or 10 μM) or vehicle for 24 hours. Cells were then harvested for Western blot analysis and probed with antibody to acetyl histone H3, acetyl histone H4, acetyl tubulin, or α -tubulin. ImageJ software was used to determine the intensities of the bands of acetyl tubulin relative to the total amount of tubulin for each treatment. The ratio of acetyl tubulin to total tubulin in each sample is indicated. *Reprinted with permission of the American Society for Pharmacology and Experimental Therapeutics. All rights reserved.*

HDACis activate transcription of p21. However, as compounds **2-75** and **1005** exhibited weak intrinsic HDACi activity against nuclear HDACs and as their apparent major cellular HDACi activity was related to targeting of the AR axis within the cytosolic compartment, it was of interest to examine their ability to induce p21.

Enz had no effect on p21 mRNA expression in either the Enz-sensitive LNCaP cells (Figure 5.7A) or in the Enz-insensitive C4-2 cells (Figure 5.7B), whereas SAHA induced p21 mRNA in both cell lines (Figure 5.7A and 5.7B). Compounds **2-75** and **1005** both induced p21 to a greater extent than SAHA in the two cell lines (Figure 5.7A and 5.7B). Moreover, combined treatment with equimolar concentrations of Enz and SAHA did not induce p21 to a greater extent than SAHA alone, indicating the importance of the hybrid scaffold of **2-75** and **1005** (Figure 5.7C).

To expect therapeutic effects from **2-75** and **1005**, it is important to establish that, similar to SAHA, they can induce loss of viability in Enz-resistant CRPC cells, rather than mere growth inhibition. Therefore, the effects of **2-75**, **1005** and SAHA on cell viability were assessed in the well-established C4-2 model of Enz-resistant CRPC.

In C4-2 cells Enz could not appreciably affect viability even at a concentration of 10 μ M, whereas SAHA caused loss of viability in a dose dependent manner (Figure 5.8A). Compounds **2-75** and **1005** both caused greater loss of viability compared with SAHA with compound **2-75** being more effective than **1005** (Figure 5.8A). As a control, compound **1002**, which has a chemical scaffold similar to **1005** but lacks the HDACi activity (Figure 5.2B and 5.2D), was unable to affect C4-2 cell viability (Figure 5.8A). As another experimental control, at the lower drug concentration (2.5 μ M) although SAHA, **2-75** and **1005** caused growth inhibition, combining Enz with SAHA (each at 2.5 μ M) did

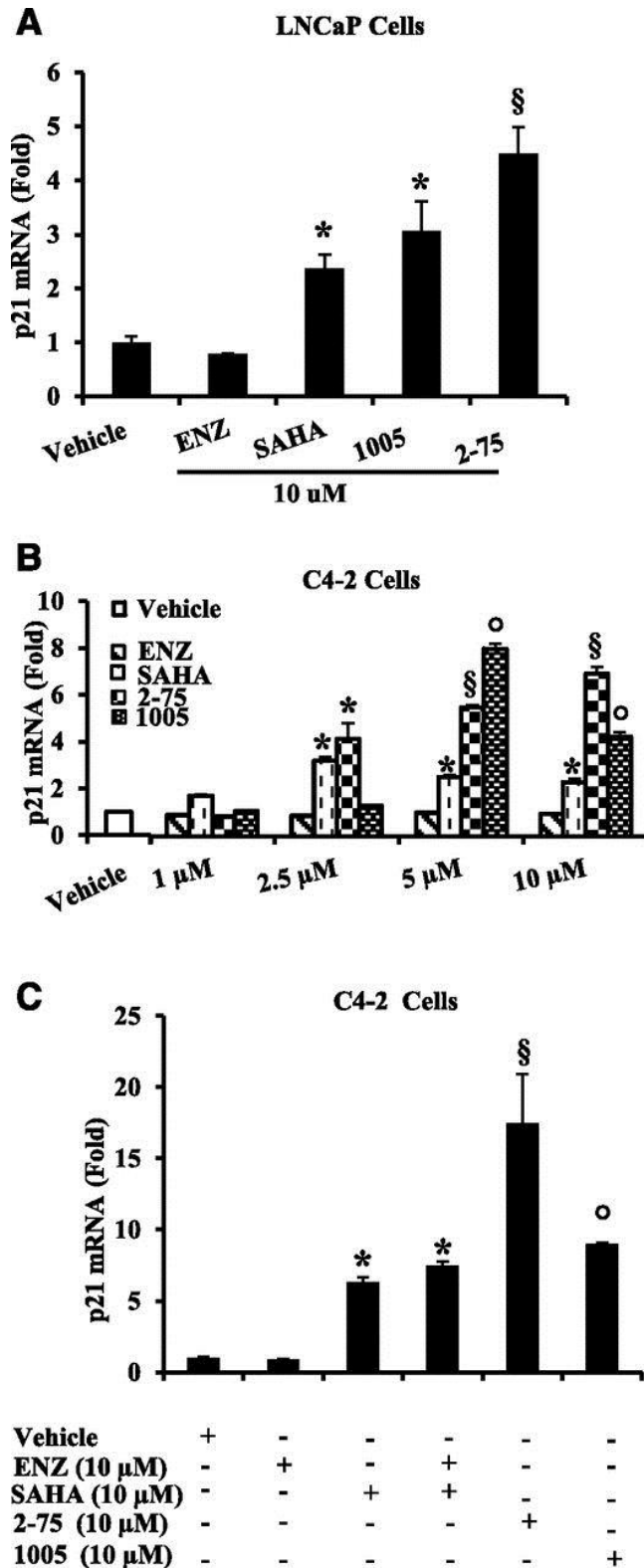


Figure 5.7 Induction of p21 mRNA.

(A) LNCaP cells were treated with Enz, SAHA, 1005, or 2-75 at a concentration of 10 μ M or with vehicle (dimethylsulfoxide) for 48 hours. Cells were then harvested to quantify p21 mRNA and the values were normalized to those for GAPDH mRNA. (B) C4-2 cells were treated with Enz, SAHA, 1005, or 2-75 at the indicated concentrations or with vehicle (dimethylsulfoxide) for 48 hours. Cells were then harvested to quantify p21 mRNA and the values were normalized to those for GAPDH mRNA. (C) C4-2 cells were treated with either Enz (10 μ M) or SAHA (10 μ M), an equimolar (10 μ M each) mixture of Enz and SAHA, 2-75 (10 μ M), or 1005 (10 μ M). Cells were then harvested to quantify p21 mRNA and the values were normalized to those for GAPDH mRNA. In all panels, the error bars represent the standard deviation of experimental triplicates. Where indicated, *, §, ° $P < 0.05$. Reprinted with permission of the American Society for Pharmacology and Experimental Therapeutics. All rights reserved.

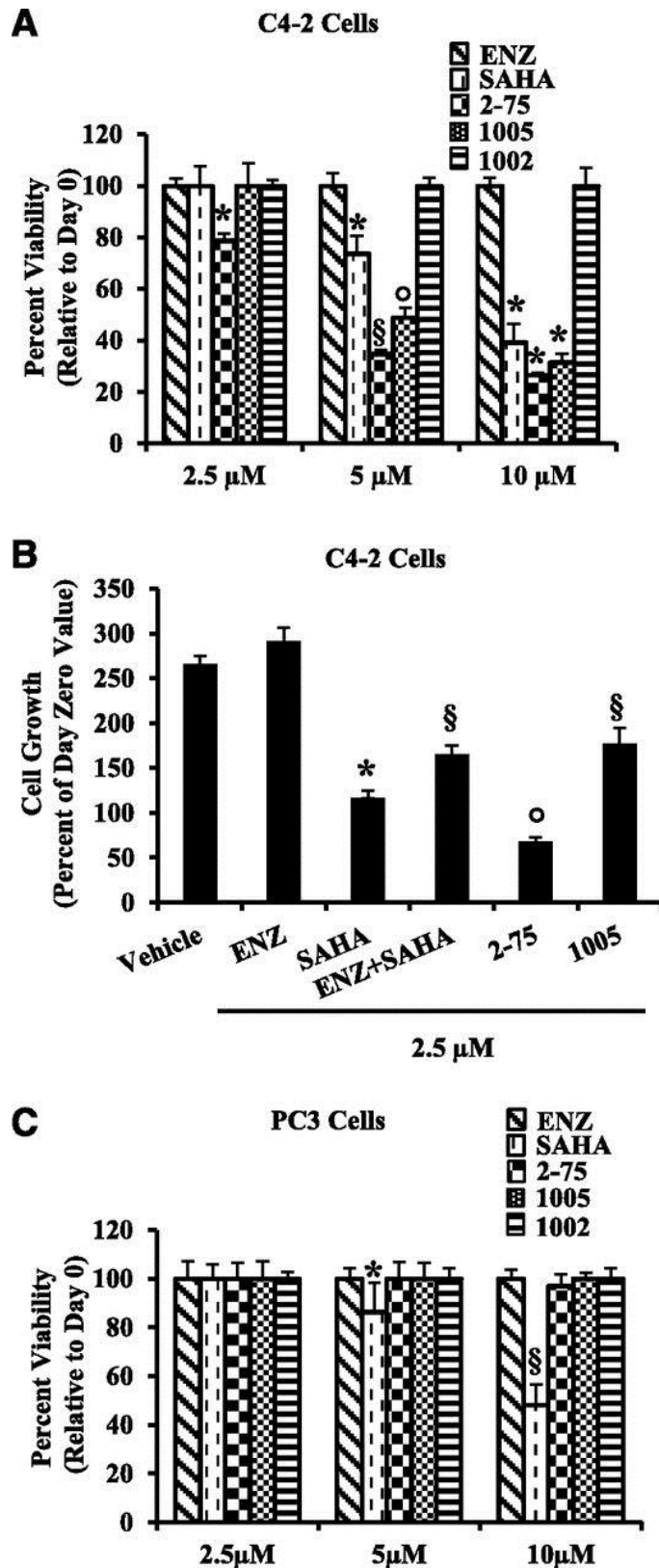


Figure 5.8 Effects on cell viability in Enz-resistant CRPC cells. (A) C4-2 cells were seeded in 96-well plates and 24 hours later, they were treated with the indicated compounds (2.5 μ M, 5 μ M, or 10 μ M) or with vehicle (dimethylsulfoxide). Cell density was measured by the MTT assay on days 0 and 3 of treatment. Values equal to or above that on day 0 were considered to represent 100% viability. (B) C4-2 cells were seeded and treated 24 hours later with Enz (2.5 μ M), SAHA (2.5 μ M), an equimolar mixture of Enz and SAHA (each compound at 2.5 μ M), 2-75 (2.5 μ M), 1005 (2.5 μ M), or vehicle (dimethylsulfoxide). Cell density was measured by the MTT assay on days 0 and 3 of treatment. The y-axis shows percent cell growth on day 3 relative to the cell density on day 0. (C) PC3 cells were seeded in 96-well plates and 24 hours later, they were treated with the indicated compounds (2.5 μ M, 5 μ M, or 10 μ M) or with vehicle (dimethylsulfoxide). Cell density was measured by the MTT assay on days 0 and 3 of treatment. Values equal to or above that on day 0 were considered to represent 100% viability. In all panels, the error bars represent the standard deviation of experimental sextuplicate samples. Where indicated, *, §, ° $P < 0.05$. MTT, 3-(4,5-dimethylthiazol-2-yl)-2,5-diphenyltetrazolium bromide. Reprinted with permission of the American Society for Pharmacology and Experimental Therapeutics. All rights reserved.

not enhance the ability of SAHA to inhibit cell growth (Figure 5.8B). In the AR-negative PC3 PCa cells, SAHA induced loss of viability in a dose-dependent manner (Figure 5.8C). However, in contrast to C4-2 cells, neither **2-75** nor **1005** affected viability of PC3 cells within the duration of the assay (Figure 5.8C). As expected, the AR-positive and hormone-dependent LNCaP cells were sensitive to SAHA, **2-75** and **1005** as well as Enz (Figure 5.9).

The results indicate that despite the weaker inherent HDACi activities of **2-75** and **1005** compared with SAHA, the compounds could be as good or better at reducing viability of Enz-resistant and AR-overexpressing PCa cells.

5.4 Discussion

The success of clinical interventions in prostate cancer, including surgical or chemical castration and treatment with androgen antagonists and androgen synthesis inhibitors support the view that the majority of prostate tumors are addicted to AR to support PCa growth and progression (273). Nevertheless, the current interventions that target androgen/AR signaling are circumvented by the tumors, most commonly through mechanisms that restore functional AR (395, 396), resulting in short-lived clinical benefit from the treatments. The goal of this study was to develop a class of compounds that may overcome this manner of resistance to the conventional treatments by efficiently disrupting both AR and HSP90 in the AR-HSP90 complex with minimal effects on most other cellular targets. To accomplish this, we synthesized compounds that would incorporate properties of two well-known drugs, an HDACi (SAHA) that efficiently modifies and disrupts the cytosolic AR chaperone complex and an AR ligand (Enz), which is a high affinity AR antagonist. We additionally sought to substantially weaken

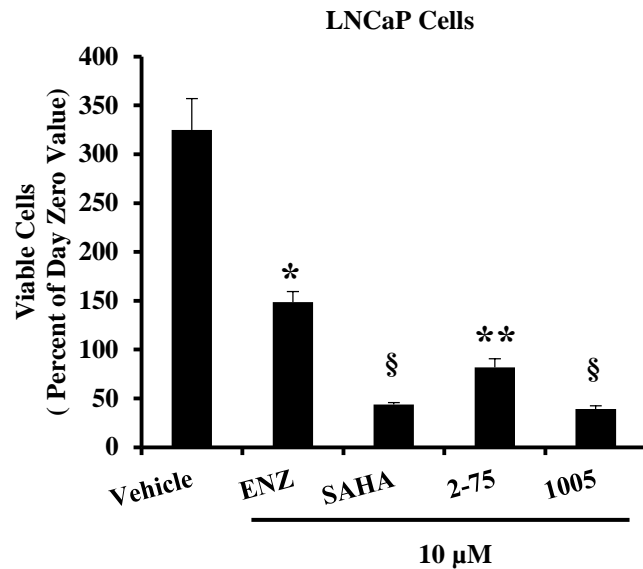


Figure 5.9: Effects on cell viability in androgen-sensitive cells.

LNCaP cells were seeded in 96-well plates and 24h later, they were treated with the indicated compounds (10 μM) or with vehicle (DMSO). Cell density was measured by the MTT assay on Days 0 and 3 of treatment. The error bars represent standard deviation of experimental sextuplicate samples. Where indicated, $P < 0.05$ Reprinted with permission of the American Society for Pharmacology and Experimental Therapeutics. All rights reserved.

the intrinsic HDACi activity of the drug to minimize its ability to affect many targets. The studies described above suggest that compounds **2-75** and **1005** may be prototype molecules that fit this paradigm.

The HDACi functional groups in **2-75** and **1005** conferred only weak HDACi activity in cell-free assays using either nuclear HDACs or the cytosolic HDAC6 compared with SAHA; the shorter carbon chain in **1005** resulted in even weaker HDACi activity than **2-75**. The relative potencies of HDACi inhibition of **2-75** and **1005** was clearly reflected in their relatively poor ability to induce DLC1, an established nuclear target gene of HDACi (391, 397, 398), that is strongly induced by SAHA. **2-75** and **1005** were also poor modulators of histone acetylation *in situ* compared with SAHA. Therefore, the new molecules may have less toxic effects than those associated with the potent pan-HDACi activity of SAHA (377).

SAHA partially inhibited gene activation by androgen but did not produce a further dose-dependent inhibition between 1 μ M and 10 μ M concentrations. At this time, we do not have a clear explanation for why this effect of SAHA was only partial except that it may be related to the pleiotropic cellular effects of SAHA including its effects on cross-talking molecular pathways. More important, **2-75** and **1005** produced a dose-dependent inhibition of gene activation by androgen similar to Enz. The stronger inhibition observed for the compounds compared to Enz may be attributed to their HDACi moieties. However, the close parallel between the control compound **3-52** and Enz in their dose-dependent antagonism of gene activation by androgen, despite the lack of a HDACi functional group in **3-52**, indicates that the Enz moiety in **2-75** and **1005** is functional in enabling binding to AR. Additionally, CHIP analysis showed that the

modified Enz scaffold retained the inability of Enz to mobilize AR to its chromatin binding sites in the nucleus in contrast to conventional androgen antagonists.

In the context of targeted delivery to AR via their Enz moiety, the weak intrinsic HDACi activities of **2-75** and **1005** were adequate to mimic or surpass the effects of SAHA on AR protein levels. The efficiency of degradation of AR by **1005** was comparable to SAHA but **2-75** clearly induced AR degradation to a greater degree at each dose. This difference between **2-75** and **1005** may be related to the fact that the HDACi activity of **1005** was less than that of **2-75**, despite their common Enz moiety. To test the mechanism by which **2-75** and **1005** may cause AR degradation, we relied on literature reports that HDACi destabilize and degrade AR by hyper-acetylation and inducing degradation of the cytosolic AR chaperone protein, HSP90 (368, 369, 392). It has also been reported that the hyper-acetylation and degradation of HSP90 coincides with the appearance of a ~55 KDa HSP90 polypeptide fragment. As a diagnostic test of this mechanism, we observed that similar to SAHA, **2-75** and **1005** did indeed cause a decrease in HSP90, with **2-75** being more efficient than either SAHA or **1005**. We were able to observe the predicted ~55KDa fragment in cells treated with SAHA, **2-75** or **1005** using an antibody against acetylated lysine; however our antibody against HSP90 was unable to detect this fragment, possibly because the levels of the cleaved HSP90 fragment were too low to be in the detectable range of the antibody. Nevertheless, all indications point to the AR chaperone complex in the cytosol as the mediating the action of **2-75** and **1005**. Consistent with this view HDAC6 which is associated with the AR-HSP90 complex was more strongly and selectively inhibited *in situ* by **2-75** compared to

SAHA. Indeed **1005** which had weaker intrinsic HDACi activity than **2-75** also strongly inhibited HDAC6 *in situ* with virtually no effect on histone acetylation.

An increase in the expression of the cyclin-dependent kinase inhibitor p21 (399) is a hall mark of the antiproliferative effects of HDACi (400, 401). Potent inhibition of the nuclear HDAC1 at the promoter of the p21 gene is associated with induction of p21 by HDACi (402). Inhibitors of HSP90 also increase p21 expression in PCa cells (368). Therefore it is significant that p21 mRNA was induced by both **2-75** and **1005** more strongly than SAHA and that combination with Enz did not further increase p21 induction by SAHA. The inability of Enz to induce p21 in the hormone-dependent LNCaP cells despite the sensitivity of the AR signaling in these cells to Enz suggests that induction of p21 by **2-75** and **1005** may not be directly related to disruption of AR; rather, it may be due to their effects on additional HSP90 client proteins through AR-mediated targeting of HDACi activity to HSP90. Notably, AKT and GR are also HSP90 client proteins and upregulated AKT or GR signaling were reported to result in Enz resistance (403-406). Therefore, these pathways could be involved in the loss of viability induced by the compounds.

HDACi pharmacophores have previously been linked to a chemical scaffold of cyanonilutamide, which is another nonsteroidal AR antagonist (392). However, the antiproliferative effects of cyanonilutamide-HDACi were related to their ability to induce AR nuclear localization, enabling elevated local concentrations of HDACi activities in the nucleus. In contrast, our prototype drug molecules were designed to limit nuclear HDACi activities as an approach to limiting toxicity. Our working model that would need further testing is that in C4-2 cells, **2-75** and **1005** bind to cytosolic AR and inhibit

HDAC6 associated with the AR chaperone complex, resulting in HSP90 acetylation and degradation, AR degradation, suppression of ligand-insensitive gene activation by AR and inhibition HSP90 interactions with additional client proteins (Schematic in Figure 5.10). We propose that this mechanism may address some of the limitations of strong pan-HDAC inhibitors related to toxicity.

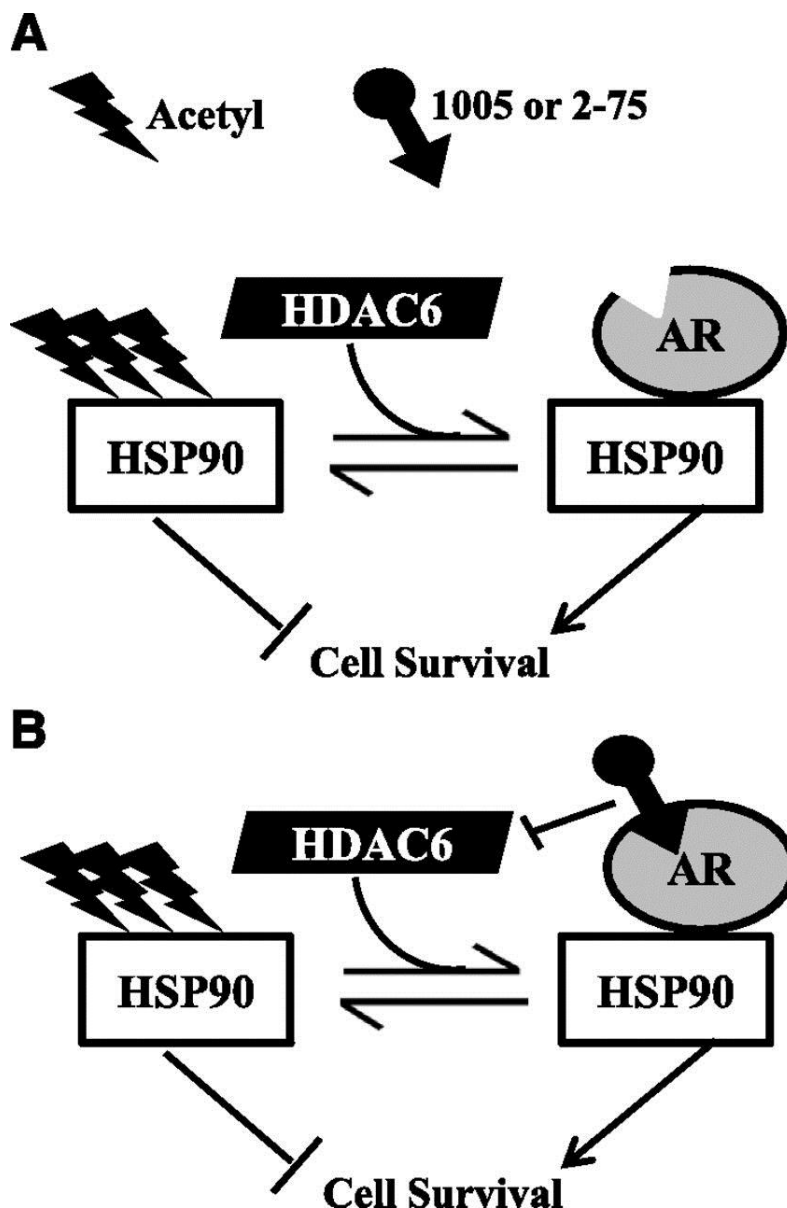


Figure 5.10 Mechanistic model for the actions of compounds 1005 and 2-75. (A) In the absence of bound ligand, AR is in a stable complex with HSP90, which is maintained in a hypoacetylated state by HDAC6. Hypoacetylated HSP90 stabilizes AR and also supports cell survival through regulation of its other client proteins. When 2-75 or 1005 bind to AR in the chaperone complex, their HDACI moieties inhibit HDAC6 that associates with the complex. Despite their relatively weak intrinsic HDACI activities, the efficiency of HDAC6 inhibition by the hybrid molecules is enhanced by their localized effect in the chaperone complex. (B) This results in hyperacetylation of HSP90, leading to destabilization of AR and also loss of cell survival through deregulation of other HSP90 client proteins. *Reprinted with permission of the American Society for Pharmacology and Experimental Therapeutics. All rights reserved.*

CHAPTER 6- CONCLUSIONS

The goal of this dissertation work was to use new mechanistic concepts and approaches for the development of small molecule drug candidates to treat prostate cancer. Using complementary methods, we discovered that the amino-terminal domain of AR utilizes the two ERK docking sites on ELK1 to directly bind to ELK1, inducing constitutive activation of genes essential for prostate cancer growth even in cells that are insensitive to androgen and resistant to enzalutamide (Chapter 3). Through the development of a strategic cell-based screening assay and further tertiary tests and structure-activity studies, we have identified a lead small molecule drug candidate that binds directly to AR, disrupts its interaction with ELK1 to selectively block ELK1-dependent gene activation by AR and suppresses growth of AR positive PC/CRPC cells and tumors (Chapter 4). Finally, as an alternative approach we developed hybrid small molecule drugs containing partial structural scaffolds derived from enzalutamide and SAHA, two therapeutics currently in the clinic. By weakening the pan HDAC inhibitor activity of SAHA and using enzalutamide to direct the HDAC inhibitor activity, we could more selectively disrupt the growth of AR overexpressing prostate cancer cells (Chapter 5).

Because of the dependence of early stage and advanced prostate tumors on AR, testosterone suppression is a mainstay in the treatment of prostate cancer. Prostate cancer progresses to become resistant to ADT by restoring functional AR.. ADT is also associated with many major undesirable side effects on normal tissues. Our lab has previously discovered that tethering of AR by ELK1 in PC/CRPC cells enables constitutive activation of a crucial set of growth genes by AR. In this study, we have discovered a lead compound, KCI807 that disrupts the ELK1-AR interaction and

selectively suppress growth signaling by AR in PC/CRPC cells. KCI807 represents a new functional class of potential small molecule drugs that offers the dual benefit of obviating the need for testosterone suppression and being effective against a broader spectrum of prostate tumors.

In our second approach, we reduced the potency of histone deacetylase activity of SAHA while generating a hybrid molecule that would enable targeting of this activity to the Hsp90-AR complex. These studies resulted in a prototype compound that has the potential to circumvent the pan activity of currently used HDAC inhibiting drugs that is associated with toxicity. Furthermore, this prototype drug should be more selective for AR positive prostate cancer cells.

Together, these studies have addressed two separate goals to prove the principle that small molecules can be developed for prostate cancer that 1.) can be functionally tumor selective in both early stage and advanced disease and that do not require androgen ablation and 2.) that have the capability of being active in enzalutamide-resistant prostate cancer cells. For these reasons, such molecules should serve as superior therapeutics compared with conventional hormonal therapies for prostate cancer.

APPENDIX- INTELLECUTAL PROPERTY

The information on the high throughput screening methodology and small molecule inhibitors of ELK1-AR interactions described in chapter four comprise intellectual property of Wayne State University and is covered by provisional patents filed by the university.

REFERENCES

1. Rosati R, Patki M, Chari V, Dakshnamurthy S, McFall T, Saxton J, Kidder BL, Shaw PE, Ratnam M. The Amino-terminal Domain of the Androgen Receptor Co-opts ERK Docking Sites in ELK1 to Induce Sustained Gene Activation that Supports Prostate Cancer Cell Growth. *The Journal of biological chemistry*. 2016. Epub 2016/10/30. doi: 10.1074/jbc.M116.745596. PubMed PMID: 27793987.
2. Foundation PC. Prostate Cancer Risk Factors 2017 [cited 2017 May 7]. Available from: <https://www.pcf.org/c/prostate-cancer-risk-factors/>.
3. American_Cancer_Society. Key Statistics for Prostate Cancer 2017 [cited 2017 May 5]. Available from: <https://www.cancer.org/cancer/prostate-cancer/about/key-statistics.html>.
4. Packer JR, Maitland NJ. The molecular and cellular origin of human prostate cancer. *Biochimica et biophysica acta*. 2016;1863(6 Pt A):1238-60. Epub 2016/02/28. doi: 10.1016/j.bbamcr.2016.02.016. PubMed PMID: 26921821.
5. The_Editors_of_Encyclopedia_Britannica. Prostate Gland: Encyclopædia Britannica, inc.; 2017 [cited 2017 May 7]. Available from: <https://www.britannica.com/science/prostate-gland>.
6. Kumar V, Majumder P. Prostate gland: structure, functions and regulation. *International urology and nephrology*. 1995;27(3):231-43.
7. Isaacs J. Testosterone and the prostate. *Testosterone: action, deficiency, substitution*. 2004;3:347-74.

8. Mann T, Lutwak-Mann C. Male reproductive function and the composition of semen: general considerations. *Male Reproductive Function and Semen*: Springer; 1981. p. 1-37.
9. Aitken RJ, Buckingham DW, Carreras A, Irvine DS. Superoxide dismutase in human sperm suspensions: relationship with cellular composition, oxidative stress, and sperm function. *Free Radical Biology and Medicine*. 1996;21(4):495-504.
10. Mann T. Secretory function of the prostate, seminal vesicle and other male accessory organs of reproduction. *Journal of reproduction and fertility*. 1974;37(1):179-88.
11. Pennefather J, Lau W, Mitchelson F, Ventura S. The autonomic and sensory innervation of the smooth muscle of the prostate gland: a review of pharmacological and histological studies. *Journal of autonomic pharmacology*. 2000;20(4):193-206.
12. Torrens M, Morrison JF. *The physiology of the lower urinary tract*: Springer Science & Business Media; 2012.
13. Cunha GR, Ricke W, Thomson A, Marker PC, Risbridger G, Hayward SW, Wang Y, Donjacour AA, Kurita T. Hormonal, cellular, and molecular regulation of normal and neoplastic prostatic development. *The Journal of steroid biochemistry and molecular biology*. 2004;92(4):221-36.
14. Aumüller G. *Prostate gland and seminal vesicles*: Springer Science & Business Media; 2012.
15. Cleveland_Clinic. *The Male Reproductive System 1995-2017* [cited 2017 May 11]. Available from: <https://my.clevelandclinic.org/health/articles/the-male-reproductive-system>.

16. Kaiho Y, Nakagawa H, Saito H, Ito A, Ishidoya S, Saito S, Arai Y. Nerves at the ventral prostatic capsule contribute to erectile function: initial electrophysiological assessment in humans. *European urology*. 2009;55(1):148-55.
17. Franz MC, Anderle P, Burzle M, Suzuki Y, Freeman MR, Hediger MA, Kovacs G. Zinc transporters in prostate cancer. *Molecular aspects of medicine*. 2013;34(2-3):735-41. Epub 2013/03/20. doi: 10.1016/j.mam.2012.11.007. PubMed PMID: 23506906; PubMed Central PMCID: PMC4046638.
18. American_Cancer_Society. Can Prostate Cancer Be Found Early? 2017 [cited 2017 May 11]. Available from: <https://www.cancer.org/cancer/prostate-cancer/detection-diagnosis-staging/detection.html>.
19. McNeal JE, Redwine EA, Freiha FS, Stamey TA. Zonal distribution of prostatic adenocarcinoma: correlation with histologic pattern and direction of spread. *The American journal of surgical pathology*. 1988;12(12):897-906.
20. Martini FH, Timmons, M. J., & Tallitsch, R. B. . *Human Anatomy*. (7th Edition). San Francisco: : Pearson Benjamin Cummings; 2012.
21. Shier D, Butler, J., & Lewis, R. . *Hole's Essentials of Human Anatomy and Physiology*. Boston: WCB McGraw-Hill; 1998.
22. Wei JT, Calhoun E, Jacobsen SJ. Urologic diseases in america project: benign prostatic hyperplasia. *The Journal of urology*. 2008;179(5 Suppl):S75-80. Epub 2008/04/25. doi: 10.1016/j.juro.2008.03.141. PubMed PMID: 18405761.
23. Li SH, Yang QF, Zuo PY, Liu YW, Liao YH, Liu CY. Prostate volume growth rate changes over time: Results from men 18 to 92 years old in a longitudinal community-based study. *Journal of Huazhong University of Science and Technology Medical*

sciences = Hua zhong ke ji da xue xue bao Yi xue Ying De wen ban = Huazhong keji daxue xuebao Yixue Yingdewen ban. 2016;36(6):796-800. Epub 2016/12/08. doi: 10.1007/s11596-016-1664-x. PubMed PMID: 27924517.

24. McNeal JE. The zonal anatomy of the prostate. *The prostate*. 1981;2(1):35-49.

25. Lubahn DB, Joseph DR, Sar M, Tan J-a, Higgs HN, Larson RE, French FS, Wilson EM. The human androgen receptor: complementary deoxyribonucleic acid cloning, sequence analysis and gene expression in prostate. *Molecular Endocrinology*. 1988;2(12):1265-75.

26. Gelmann EP. Molecular biology of the androgen receptor. *Journal of Clinical Oncology*. 2002;20(13):3001-15.

27. Mangelsdorf DJ, Thummel C, Beato M, Herrlich P, Schütz G, Umesono K, Blumberg B, Kastner P, Mark M, Chambon P. The nuclear receptor superfamily: the second decade. *Cell*. 1995;83(6):835-9.

28. Kempainen JA, Lane MV, Sar M, Wilson EM. Androgen receptor phosphorylation, turnover, nuclear transport, and transcriptional activation. Specificity for steroids and antihormones. *Journal of Biological Chemistry*. 1992;267(2):968-74.

29. Simental JA, Sar M, Lane MV, French FS, Wilson EM. Transcriptional activation and nuclear targeting signals of the human androgen receptor. *Journal of Biological Chemistry*. 1991;266(1):510-8.

30. Brown C, Goss S, Lubahn D, Joseph D, Wilson EM, French FS, Willard H. Androgen receptor locus on the human X chromosome: regional localization to Xq11-12 and description of a DNA polymorphism. *American journal of human genetics*. 1989;44(2):264.

31. Lubahn DB, Joseph DR, Sullivan PM, Willard HF, French FS, Wilson EM. Cloning of human androgen receptor complementary DNA and localization to the X chromosome. *Science*. 1988;240(4850):327.
32. Simental JA, Sar M, Lane MV, French FS, Wilson EM. Transcriptional activation and nuclear targeting signals of the human androgen receptor. *The Journal of biological chemistry*. 1991;266(1):510-8. Epub 1991/01/05. PubMed PMID: 1985913.
33. Brinkmann A, Blok L, De Ruiter P, Doesburg P, Steketee K, Berrevoets C, Trapman J. Mechanisms of androgen receptor activation and function. *The Journal of steroid biochemistry and molecular biology*. 1999;69(1):307-13.
34. McEwan IJ. Intrinsic disorder in the androgen receptor: identification, characterisation and drugability. *Molecular bioSystems*. 2012;8(1):82-90.
35. Hsu WL, Oldfield CJ, Xue B, Meng J, Huang F, Romero P, Uversky VN, Dunker AK. Exploring the binding diversity of intrinsically disordered proteins involved in one-to-many binding. *Protein Science*. 2013;22(3):258-73.
36. Hilser VJ, Thompson EB. Structural dynamics, intrinsic disorder, and allostery in nuclear receptors as transcription factors. *Journal of Biological Chemistry*. 2011;286(46):39675-82.
37. Ueda T, Mawji NR, Bruchofsky N, Sadar MD. Ligand-independent activation of the androgen receptor by interleukin-6 and the role of steroid receptor coactivator-1 in prostate cancer cells. *J Biol Chem*. 2002;277(41):38087-94. Epub 2002/08/07. doi: 10.1074/jbc.M203313200. PubMed PMID: 12163482.
38. Dehm SM, Regan KM, Schmidt LJ, Tindall DJ. Selective role of an NH2-terminal WxxLF motif for aberrant androgen receptor activation in androgen depletion

independent prostate cancer cells. *Cancer research*. 2007;67(20):10067-77. Epub 2007/10/19. doi: 10.1158/0008-5472.can-07-1267. PubMed PMID: 17942941.

39. Tan MH, Li J, Xu HE, Melcher K, Yong EL. Androgen receptor: structure, role in prostate cancer and drug discovery. *Acta pharmacologica Sinica*. 2015;36(1):3-23. Epub 2014/06/10. doi: 10.1038/aps.2014.18. PubMed PMID: 24909511; PubMed Central PMCID: PMC4571323.

40. Jenster G, van der Korput HA, Trapman J, Brinkmann AO. Identification of two transcription activation units in the N-terminal domain of the human androgen receptor. *The Journal of biological chemistry*. 1995;270(13):7341-6. Epub 1995/03/31. PubMed PMID: 7706276.

41. He B, Kemppainen JA, Voegel JJ, Gronemeyer H, Wilson EM. Activation function 2 in the human androgen receptor ligand binding domain mediates interdomain communication with the NH₂-terminal domain. *Journal of Biological Chemistry*. 1999;274(52):37219-25.

42. Schoenmakers E, Alen P, Verrijdt G, Peeters B, Verhoeven G, Rombauts W, Claessens F. Differential DNA binding by the androgen and glucocorticoid receptors involves the second Zn-finger and a C-terminal extension of the DNA-binding domains. *The Biochemical journal*. 1999;341 (Pt 3):515-21. Epub 1999/07/27. PubMed PMID: 10417312; PubMed Central PMCID: PMC4571323.

43. Berrevoets CA, Doesburg P, Steketeer K, Trapman J, Brinkmann AO. Functional interactions of the AF-2 activation domain core region of the human androgen receptor with the amino-terminal domain and with the transcriptional coactivator TIF2 (transcriptional intermediary factor 2). *Molecular Endocrinology*. 1998;12(8):1172-83.

44. Veldscholte J, Berrevoets CA, Ris-Stalpers C, Kuiper GG, Jenster G, Trapman J, Brinkmann AO, Mulder E. The androgen receptor in LNCaP cells contains a mutation in the ligand binding domain which affects steroid binding characteristics and response to antiandrogens. *The Journal of steroid biochemistry and molecular biology*. 1992;41(3-8):665-9. Epub 1992/03/01. PubMed PMID: 1562539.
45. Clinckemalie L, Vanderschueren D, Boonen S, Claessens F. The hinge region in androgen receptor control. *Molecular and cellular endocrinology*. 2012;358(1):1-8. Epub 2012/03/13. doi: 10.1016/j.mce.2012.02.019. PubMed PMID: 22406839.
46. Quigley CA, De Bellis A, Marschke KB, el-Awady MK, Wilson EM, French FS. Androgen receptor defects: historical, clinical, and molecular perspectives. *Endocrine reviews*. 1995;16(3):271-321. Epub 1995/06/01. doi: 10.1210/edrv-16-3-271. PubMed PMID: 7671849.
47. Heinlein CA, Chang C. Androgen receptor (AR) coregulators: an overview. *Endocrine reviews*. 2002;23(2):175-200. Epub 2002/04/12. doi: 10.1210/edrv.23.2.0460. PubMed PMID: 11943742.
48. Zhou ZX, Lane MV, Kempainen JA, French FS, Wilson EM. Specificity of ligand-dependent androgen receptor stabilization: receptor domain interactions influence ligand dissociation and receptor stability. *Molecular Endocrinology*. 1995;9(2):208-18.
49. Dehm SM, Tindall DJ. Androgen receptor structural and functional elements: role and regulation in prostate cancer. *Molecular endocrinology (Baltimore, Md)*. 2007;21(12):2855-63. Epub 2007/07/20. doi: 10.1210/me.2007-0223. PubMed PMID: 17636035.

50. Wilson JD. Role of dihydrotestosterone in androgen action. *The Prostate*. 1996;29(S6):88-92.
51. Isaacs JT, Coffey DS. Changes in dihydrotestosterone metabolism associated with the development of canine benign prostatic hyperplasia. *Endocrinology*. 1981;108(2):445-53. Epub 1981/02/01. doi: 10.1210/endo-108-2-445. PubMed PMID: 6161001.
52. Bruchoovsky N, Sadar MD, Akakura K, Goldenberg SL, Matsuoka K, Rennie PS. Characterization of 5alpha-reductase gene expression in stroma and epithelium of human prostate. *J Steroid Biochem Mol Biol*. 1996;59(5-6):397-404. Epub 1996/12/01. PubMed PMID: 9010345.
53. Silver RI, Wiley EL, Davis DL, Thigpen AE, Russell DW, McConnell JD. Expression and regulation of steroid 5 alpha-reductase 2 in prostate disease. *The Journal of urology*. 1994;152(2 Pt 1):433-7. Epub 1994/08/01. PubMed PMID: 7516976.
54. Nadal M, Prekovic S, Gallastegui N, Helsen C, Abella M, Zielinska K, Gay M, Vilaseca M, Taules M, Houtsmuller AB, van Royen ME, Claessens F, Fuentes-Prior P, Estebanez-Perpina E. Structure of the homodimeric androgen receptor ligand-binding domain. *Nature communications*. 2017;8:14388. Epub 2017/02/07. doi: 10.1038/ncomms14388. PubMed PMID: 28165461; PubMed Central PMCID: PMC5303882.
55. Cutress ML, Whitaker HC, Mills IG, Stewart M, Neal DE. Structural basis for the nuclear import of the human androgen receptor. *Journal of cell science*. 2008;121(7):957-68.

56. Claessens F, Clinckemalie L, Christine H, Spans L, Dubois V, Laurent M, Boonen S, Vanderschueren D. Selective and classical androgen response elements in androgen-regulated gene expression. *Androgen-Responsive Genes in Prostate Cancer*: Springer; 2013. p. 13-27.
57. Kang Z, Janne OA, Palvimo JJ. Coregulator recruitment and histone modifications in transcriptional regulation by the androgen receptor. *Molecular endocrinology* (Baltimore, Md). 2004;18(11):2633-48. Epub 2004/08/17. doi: 10.1210/me.2004-0245. PubMed PMID: 15308689.
58. Beato M, Herrlich P, Schutz G. Steroid hormone receptors: many actors in search of a plot. *Cell*. 1995;83(6):851-7. PubMed PMID: 8521509.
59. Glass CK, Rosenfeld MG. The coregulator exchange in transcriptional functions of nuclear receptors. *Genes & development*. 2000;14(2):121-41. PubMed PMID: 10652267.
60. McKenna NJ, O'Malley BW. Combinatorial control of gene expression by nuclear receptors and coregulators. *Cell*. 2002;108(4):465-74. PubMed PMID: 11909518.
61. Wen S, Chang HC, Tian J, Shang Z, Niu Y, Chang C. Stromal androgen receptor roles in the development of normal prostate, benign prostate hyperplasia, and prostate cancer. *The American journal of pathology*. 2015;185(2):293-301. Epub 2014/11/29. doi: 10.1016/j.ajpath.2014.10.012. PubMed PMID: 25432062; PubMed Central PMCID: PMC4305176.
62. Chung LW, Baseman A, Assikis V, Zhau HE. Molecular insights into prostate cancer progression: the missing link of tumor microenvironment. *The Journal of urology*. 2005;173(1):10-20.

63. Marker PC, Donjacour AA, Dahiya R, Cunha GR. Hormonal, cellular, and molecular control of prostatic development. *Developmental biology*. 2003;253(2):165-74.
64. Isaacs JT, Isaacs WB. Androgen receptor outwits prostate cancer drugs. *Nature medicine*. 2004;10(1):26-7. Epub 2004/01/02. doi: 10.1038/nm0104-26. PubMed PMID: 14702629.
65. Niu YN, Xia SJ. Stroma-epithelium crosstalk in prostate cancer. *Asian journal of andrology*. 2009;11(1):28-35. Epub 2008/12/23. doi: 10.1038/aja.2008.39. PubMed PMID: 19098934; PubMed Central PMCID: PMCPCmc3735213.
66. Taylor RA, Risbridger GP. Prostatic tumor stroma: a key player in cancer progression. *Current cancer drug targets*. 2008;8(6):490-7. Epub 2008/09/11. PubMed PMID: 18781895.
67. Goldstein AS. A symbiotic relationship between epithelial and stromal stem cells. *Proceedings of the National Academy of Sciences of the United States of America*. 2013;110(51):20356-7. Epub 2013/11/29. doi: 10.1073/pnas.1320032110. PubMed PMID: 24284171; PubMed Central PMCID: PMCPCmc3870754.
68. D'Antonio JM, Vander Griend DJ, Isaacs JT. DNA licensing as a novel androgen receptor mediated therapeutic target for prostate cancer. *Endocrine-related cancer*. 2009;16(2):325-32. Epub 2009/02/26. doi: 10.1677/erc-08-0205. PubMed PMID: 19240183; PubMed Central PMCID: PMCPCmc3072142.
69. Litvinov IV, De Marzo AM, Isaacs JT. Is the Achilles' heel for prostate cancer therapy a gain of function in androgen receptor signaling? *The Journal of clinical*

endocrinology and metabolism. 2003;88(7):2972-82. Epub 2003/07/05. doi: 10.1210/jc.2002-022038. PubMed PMID: 12843129.

70. Gao J, Arnold JT, Isaacs JT. Conversion from a paracrine to an autocrine mechanism of androgen-stimulated growth during malignant transformation of prostatic epithelial cells. *Cancer research*. 2001;61(13):5038-44.

71. Litvinov IV, De Marzo AM, Isaacs JT. Is the Achilles' heel for prostate cancer therapy a gain of function in androgen receptor signaling? *The Journal of Clinical Endocrinology & Metabolism*. 2003;88(7):2972-82.

72. Krieger JN, Nyberg Jr L, Nickel JC. NIH consensus definition and classification of prostatitis. *Jama*. 1999;282(3):236-7.

73. Collins MM, Stafford RS, O'leary MP, Barry MJ. How common is prostatitis? A national survey of physician visits. *The Journal of urology*. 1998;159(4):1224-8.

74. Mobley D. Bacterial prostatitis: treatment with carbenicillin indanyl sodium. *Investigative urology*. 1981;19(1):31-3.

75. Barbalias GA, Nikiforidis G, Liatsikos EN. Alpha-blockers for the treatment of chronic prostatitis in combination with antibiotics. *The Journal of urology*. 1998;159(3):883-7.

76. Thorpe A, Neal D. Benign prostatic hyperplasia. *The Lancet*. 2003;361(9366):1359-67.

77. Isaacs JT, Bartsch G. Benign prostatic hyperplasia. *Current Opinion in Urology*. 1992;2(1):1-2.

78. Berry SJ, Coffey DS, Walsh PC, Ewing LL. The development of human benign prostatic hyperplasia with age. *The Journal of urology*. 1984;132(3):474-9.

79. Kirby RS, McConnell JD, Fitzpatrick JM, Roehrborn CG, Boyle P. Textbook of benign prostatic hyperplasia: CRC Press; 2004.
80. Schauer IG, Rowley DR. The functional role of reactive stroma in benign prostatic hyperplasia. *Differentiation; research in biological diversity*. 2011;82(4-5):200-10. Epub 2011/06/15. doi: 10.1016/j.diff.2011.05.007. PubMed PMID: 21664759; PubMed Central PMCID: PMC3179838.
81. Chughtai B, Lee R, Te A, Kaplan S. Role of inflammation in benign prostatic hyperplasia. *Rev Urol*. 2011;13(3):147-50.
82. Bartsch G, Muller HR, Oberholzer M, Rohr HP. Light microscopic stereological analysis of the normal human prostate and of benign prostatic hyperplasia. *The Journal of urology*. 1979;122(4):487-91. Epub 1979/10/01. PubMed PMID: 90177.
83. National_Institute_of_Health. Benign Prostatic Hyperplasia 2017 [cited 2017 May 12]. Available from: <https://www.niddk.nih.gov/health-information/urologic-diseases/prostate-problems/prostate-enlargement-benign-prostatic-hyperplasia>.
84. Brawer MK, Adams G, Epstein H. Terazosin in the treatment of benign prostatic hyperplasia. Terazosin Benign Prostatic Hyperplasia Study Group. *Archives of family medicine*. 1993;2(9):929-35. Epub 1993/09/01. PubMed PMID: 7509243.
85. Lepor H. Alpha blockers for the treatment of benign prostatic hyperplasia. *Reviews in urology*. 2007;9(4):181.
86. Roehrborn CG. Male lower urinary tract symptoms (LUTS) and benign prostatic hyperplasia (BPH). *The Medical clinics of North America*. 2011;95(1):87-100. Epub 2010/11/26. doi: 10.1016/j.mcna.2010.08.013. PubMed PMID: 21095413.

87. Auffenberg GB, Helfand BT, McVary KT. Established medical therapy for benign prostatic hyperplasia. *The Urologic clinics of North America*. 2009;36(4):443-59, v-vi. Epub 2009/11/28. doi: 10.1016/j.ucl.2009.07.004. PubMed PMID: 19942044.
88. Shen MM, Abate-Shen C. Molecular genetics of prostate cancer: new prospects for old challenges. *Genes & development*. 2010;24(18):1967-2000. Epub 2010/09/17. doi: 10.1101/gad.1965810. PubMed PMID: 20844012; PubMed Central PMCID: PMC2939361.
89. Adamczyk P, Wolski Z, Butkiewicz R, Nussbeutel J, Drewa T. Significance of atypical small acinar proliferation and extensive high-grade prostatic intraepithelial neoplasm in clinical practice. *Central European journal of urology*. 2014;67(2):136-41. Epub 2014/08/21. doi: 10.5173/ceju.2014.02.art4. PubMed PMID: 25140226; PubMed Central PMCID: PMC4132590.
90. Meiers I, Kahane H, Bostwick DG. Atypical small acinar proliferation in the prostate. *AJSP: Reviews & Reports*. 2008;13(4):129-34.
91. Bostwick DG, Meiers I. Atypical small acinar proliferation in the prostate: clinical significance in 2006. *Archives of pathology & laboratory medicine*. 2006;130(7):952-7.
92. Epstein JI, Herawi M. Prostate needle biopsies containing prostatic intraepithelial neoplasia or atypical foci suspicious for carcinoma: implications for patient care. *The Journal of urology*. 2006;175(3 Pt 1):820-34. Epub 2006/02/14. doi: 10.1016/s0022-5347(05)00337-x. PubMed PMID: 16469560.
93. Gokden N, Roehl KA, Catalona WJ, Humphrey PA. High-grade prostatic intraepithelial neoplasia in needle biopsy as risk factor for detection of adenocarcinoma:

current level of risk in screening population. *Urology*. 2005;65(3):538-42. Epub 2005/03/23. doi: 10.1016/j.urology.2004.10.010. PubMed PMID: 15780372.

94. Lilja H, Abrahamsson PA. Three predominant proteins secreted by the human prostate gland. *The Prostate*. 1988;12(1):29-38. Epub 1988/01/01. PubMed PMID: 3347596.

95. Lilja H. Structure, function, and regulation of the enzyme activity of prostate-specific antigen. *World journal of urology*. 1993;11(4):188-91.

96. Dunn MW. Prostate Cancer Screening. *Seminars in oncology nursing*. 2017;33(2):156-64. Epub 2017/03/28. doi: 10.1016/j.soncn.2017.02.003. PubMed PMID: 28343840.

97. Tosoian JJ, Druskin SC, Andreas D, Mullane P, Chappidi M, Joo S, Ghabili K, Agostino J, Macura KJ, Carter HB, Schaeffer EM, Partin AW, Sokoll LJ, Ross AE. Use of the Prostate Health Index for detection of prostate cancer: results from a large academic practice. *Prostate cancer and prostatic diseases*. 2017. Epub 2017/01/25. doi: 10.1038/pcan.2016.72. PubMed PMID: 28117387.

98. Prostate_Cancer_Foundation. PSA & DRE Screening 2017 [cited 2017 May 17]. Available from: <https://www.pcf.org/c/psa-dre-screening/>.

99. Madu CO, Lu Y. Novel diagnostic biomarkers for prostate cancer. *Journal of Cancer*. 2010;1:150-77. Epub 2010/10/27. PubMed PMID: 20975847; PubMed Central PMCID: PMCPmc2962426.

100. Sobin LH, editor. TNM: evolution and relation to other prognostic factors. *Seminars in surgical oncology*; 2003: Wiley Online Library.

101. Schröder F, Hermanek P, Denis L, Fair W, Gospodarowicz M, Pavone-Macaluso M. The TNM classification of prostate cancer. *The Prostate*. 1992;21(S4):129-38.
102. Partin AW, Kattan MW, Subong EN, Walsh PC, Wojno KJ, Oesterling JE, Scardino PT, Pearson J. Combination of prostate-specific antigen, clinical stage, and Gleason score to predict pathological stage of localized prostate cancer: a multi-institutional update. *Jama*. 1997;277(18):1445-51.
103. Prostate_Cancer_Foundation. Staging the Disease 2017 [cited 2017 May 17]. Available from: <https://www.pcf.org/c/staging-the-disease/>.
104. Sharifi N, Gulley JL, Dahut WL. Androgen deprivation therapy for prostate cancer. *Jama*. 2005;294(2):238-44.
105. D'amico AV, Whittington R, Malkowicz SB, Schultz D, Blank K, Broderick GA, Tomaszewski JE, Renshaw AA, Kaplan I, Beard CJ. Biochemical outcome after radical prostatectomy, external beam radiation therapy, or interstitial radiation therapy for clinically localized prostate cancer. *Jama*. 1998;280(11):969-74.
106. Heidenreich A, Bellmunt J, Bolla M, Joniau S, Mason M, Matveev V, Mottet N, Schmid H-P, van der Kwast T, Wiegel T. EAU guidelines on prostate cancer. Part 1: screening, diagnosis, and treatment of clinically localised disease. *European urology*. 2011;59(1):61-71.
107. Dunn MW, Kazer MW. Prostate cancer overview. *Seminars in oncology nursing*. 2011;27(4):241-50. doi: 10.1016/j.soncn.2011.07.002. PubMed PMID: 22018403.
108. Gelet A, Chapelon JY, Poissonnier L, Bouvier R, Rouviere O, Curiel L, Janier M, Vallancien G. Local recurrence of prostate cancer after external beam radiotherapy:

early experience of salvage therapy using high-intensity focused ultrasonography. *Urology*. 2004;63(4):625-9.

109. Moul JW, Wu H, Sun L, McLeod DG, Amling C, Donahue T, Kusuda L, Sexton W, O'reilly K, Hernandez J. Early versus delayed hormonal therapy for prostate specific antigen only recurrence of prostate cancer after radical prostatectomy. *The Journal of urology*. 2004;171(3):1141-7.

110. Loblaw DA, Virgo KS, Nam R, Somerfield MR, Ben-Josef E, Mendelson DS, Middleton R, Sharp SA, Smith TJ, Talcott J, Taplin M, Vogelzang NJ, Wade JL, 3rd, Bennett CL, Scher HI. Initial hormonal management of androgen-sensitive metastatic, recurrent, or progressive prostate cancer: 2006 update of an American Society of Clinical Oncology practice guideline. *Journal of clinical oncology : official journal of the American Society of Clinical Oncology*. 2007;25(12):1596-605. Epub 2007/04/04. doi: 10.1200/jco.2006.10.1949. PubMed PMID: 17404365.

111. Myklak K, Wilson S. An update on the changing indications for androgen deprivation therapy for prostate cancer. *Prostate cancer*. 2011;2011:419174. Epub 2011/11/24. doi: 10.1155/2011/419174. PubMed PMID: 22110986; PubMed Central PMCID: PMC3216006.

112. Holzbeierlein JM, McLaughlin MD, Thrasher JB. Complications of androgen deprivation therapy for prostate cancer. *Current opinion in urology*. 2004;14(3):177-83. Epub 2004/04/08. PubMed PMID: 15069309.

113. Pienta KJ, Bradley D. Mechanisms underlying the development of androgen-independent prostate cancer. *Clinical cancer research : an official journal of the*

American Association for Cancer Research. 2006;12(6):1665-71. Epub 2006/03/23. doi: 10.1158/1078-0432.ccr-06-0067. PubMed PMID: 16551847.

114. Chen Y, Clegg NJ, Scher HI. Anti-androgens and androgen-depleting therapies in prostate cancer: new agents for an established target. *The lancet oncology*. 2009;10(10):981-91. Epub 2009/10/03. doi: 10.1016/s1470-2045(09)70229-3. PubMed PMID: 19796750; PubMed Central PMCID: PMC2935850.

115. Lam MS, Ignoffo RJ. A guide to clinically relevant drug interactions in oncology. *Journal of Oncology Pharmacy Practice*. 2003;9(2-3):45-85.

116. Sweat GT. Guiding prostate cancer treatment choices: Early detection means more options for more men. *Postgraduate medicine*. 2005;117(4):45-50.

117. Dreicer R, Bajorin DF, McLeod DG, Petrylak DP, Moul JW. New data, new paradigms for treating prostate cancer patients—VI: novel hormonal therapy approaches. *Urology*. 2011;78(5):S494-S8.

118. Bahl A. Metastatic castration-resistant prostate cancer. Part 1: the challenges of the disease and its treatment. *European journal of oncology nursing : the official journal of European Oncology Nursing Society*. 2013;17 Suppl 1:S1-6. Epub 2014/01/28. doi: 10.1016/s1462-3889(14)70002-x. PubMed PMID: 24461207.

119. Cai C, Balk SP. Intratumoral androgen biosynthesis in prostate cancer pathogenesis and response to therapy. *Endocrine-related cancer*. 2011;18(5):R175-R82.

120. Cai C, Chen S, Ng P, Bublely GJ, Nelson PS, Mostaghel EA, Marck B, Matsumoto AM, Simon NI, Wang H, Balk SP. Intratumoral de novo steroid synthesis activates androgen receptor in castration-resistant prostate cancer and is upregulated

by treatment with CYP17A1 inhibitors. *Cancer research*. 2011;71(20):6503-13. Epub 2011/08/27. doi: 0008-5472.CAN-11-0532 [pii]

10.1158/0008-5472.CAN-11-0532. PubMed PMID: 21868758; PubMed Central PMCID: PMC3209585.

121. de Bono JS, Oudard S, Ozguroglu M, Hansen S, Machiels JP, Kocak I, Gravis G, Bodrogi I, Mackenzie MJ, Shen L, Roessner M, Gupta S, Sartor AO. Prednisone plus cabazitaxel or mitoxantrone for metastatic castration-resistant prostate cancer progressing after docetaxel treatment: a randomised open-label trial. *Lancet*. 2010;376(9747):1147-54. Epub 2010/10/05. doi: 10.1016/s0140-6736(10)61389-x. PubMed PMID: 20888992.

122. Nilsson S, Franzen L, Parker C, Tyrrell C, Blom R, Tennvall J, Lennernas B, Petersson U, Johannessen DC, Sokal M, Pigott K, Yachnin J, Garkavij M, Strang P, Harmenberg J, Bolstad B, Bruland OS. Bone-targeted radium-223 in symptomatic, hormone-refractory prostate cancer: a randomised, multicentre, placebo-controlled phase II study. *The lancet oncology*. 2007;8(7):587-94. Epub 2007/06/05. doi: 10.1016/s1470-2045(07)70147-x. PubMed PMID: 17544845.

123. de Bono JS, Logothetis CJ, Molina A, Fizazi K, North S, Chu L, Chi KN, Jones RJ, Goodman OB, Jr., Saad F, Staffurth JN, Mainwaring P, Harland S, Flaig TW, Hutson TE, Cheng T, Patterson H, Hainsworth JD, Ryan CJ, Sternberg CN, Ellard SL, Flechon A, Saleh M, Scholz M, Efstathiou E, Zivi A, Bianchini D, Loriot Y, Chieffo N, Kheoh T, Haqq CM, Scher HI. Abiraterone and increased survival in metastatic prostate cancer. *The New England journal of medicine*. 2011;364(21):1995-2005. Epub

2011/05/27. doi: 10.1056/NEJMoa1014618. PubMed PMID: 21612468; PubMed Central PMCID: PMCPmc3471149.

124. Hoffman-Censits J, Kelly WK. Practical guide to the use of enzalutamide. The Canadian journal of urology. 2014;21(2 Supp 1):64-9. Epub 2014/04/30. PubMed PMID: 24775726.

125. Fizazi K, Carducci M, Smith M, Damiao R, Brown J, Karsh L, Milecki P, Shore N, Rader M, Wang H, Jiang Q, Tadros S, Dansey R, Goessl C. Denosumab versus zoledronic acid for treatment of bone metastases in men with castration-resistant prostate cancer: a randomised, double-blind study. Lancet. 2011;377(9768):813-22. Epub 2011/03/01. doi: 10.1016/s0140-6736(10)62344-6. PubMed PMID: 21353695; PubMed Central PMCID: PMCPmc3090685.

126. Kantoff PW, Higano CS, Shore ND, Berger ER, Small EJ, Penson DF, Redfern CH, Ferrari AC, Dreicer R, Sims RB, Xu Y, Frohlich MW, Schellhammer PF. Sipuleucel-T immunotherapy for castration-resistant prostate cancer. The New England journal of medicine. 2010;363(5):411-22. Epub 2010/09/08. doi: 10.1056/NEJMoa1001294. PubMed PMID: 20818862.

127. Jones JM, Kohli M, Loprinzi CL. Androgen deprivation therapy-associated vasomotor symptoms. Asian journal of andrology. 2012;14(2):193-7. Epub 2012/01/31. doi: 10.1038/aja.2011.101. PubMed PMID: 22286861; PubMed Central PMCID: PMCPmc3338189.

128. Kouriefs C, Georgiou M, Ravi R. Hot flushes and prostate cancer: pathogenesis and treatment. BJU international. 2002;89(4):379-83.

129. Smith Jr J. A prospective comparison of treatments for symptomatic hot flushes following endocrine therapy for carcinoma of the prostate. *The Journal of urology*. 1994;152(1):132-4.
130. Khan A, Lewis R, Hughes S. Managing hot flushes in men receiving androgen deprivation therapy for prostate cancer. *Trends in Urology & Men's Health*. 2014;5(1):31-3.
131. Naoe M, Ogawa Y, Shichijo T, Fuji K, Fukagai T, Yoshida H. Pilot evaluation of selective serotonin reuptake inhibitor antidepressants in hot flash patients under androgen-deprivation therapy for prostate cancer. *Prostate cancer and prostatic diseases*. 2006;9(3):275-8. Epub 2006/06/21. doi: 10.1038/sj.pcan.4500891. PubMed PMID: 16786037.
132. Frisk J. Managing hot flushes in men after prostate cancer—a systematic review. *Maturitas*. 2010;65(1):15-22.
133. Haffner SM, Mykkanen L, Valdez RA, Katz MS. Relationship of sex hormones to lipids and lipoproteins in nondiabetic men. *The Journal of clinical endocrinology and metabolism*. 1993;77(6):1610-5. Epub 1993/12/01. doi: 10.1210/jcem.77.6.8263149. PubMed PMID: 8263149.
134. Solomon KR, Freeman MR. The complex interplay between cholesterol and prostate malignancy. *Urologic Clinics of North America*. 2011;38(3):243-59.
135. Braga-Basaria M, Muller DC, Carducci MA, Dobs AS, Basaria S. Lipoprotein profile in men with prostate cancer undergoing androgen deprivation therapy. *International journal of impotence research*. 2006;18(5):494-8. Epub 2006/04/18. doi: 10.1038/sj.ijir.3901471. PubMed PMID: 16617314.

136. Shahani S, Braga-Basaria M, Basaria S. Androgen deprivation therapy in prostate cancer and metabolic risk for atherosclerosis. *The Journal of Clinical Endocrinology & Metabolism*. 2008;93(6):2042-9.
137. Mostaghel EA, Solomon KR, Pelton K, Freeman MR, Montgomery RB. Impact of circulating cholesterol levels on growth and intratumoral androgen concentration of prostate tumors. *PloS one*. 2012;7(1):e30062.
138. Kollmeier MA, Katz MS, Mak K, Yamada Y, Feder DJ, Zhang Z, Jia X, Shi W, Zelefsky MJ. Improved biochemical outcomes with statin use in patients with high-risk localized prostate cancer treated with radiotherapy. *International Journal of Radiation Oncology* Biology* Physics*. 2011;79(3):713-8.
139. Higano CS. Side effects of androgen deprivation therapy: monitoring and minimizing toxicity. *Urology*. 2003;61(2):32-8.
140. Aversa A, Isidori A, De Martino M, Caprio M, Fabbrini E, Rocchietti-March M, Frajese G, Fabbri A. Androgens and penile erection: evidence for a direct relationship between free testosterone and cavernous vasodilation in men with erectile dysfunction. *Clinical endocrinology*. 2000;53(4):517-22.
141. Chamness SL, Ricker DD, Crone JK, Dembeck CL, Maguire MP, Burnett AL, Chang TS. The effect of androgen on nitric oxide synthase in the male reproductive tract of the rat. *Fertility and sterility*. 1995;63(5):1101-7. Epub 1995/05/01. PubMed PMID: 7536692.
142. Chou TM, Sudhir K, Hutchison SJ, Ko E, Amidon TM, Collins P, Chatterjee K. Testosterone induces dilation of canine coronary conductance and resistance arteries in vivo. *Circulation*. 1996;94(10):2614-9. Epub 1996/11/15. PubMed PMID: 8921808.

143. Oefelein MG, Feng A, Scolieri MJ, Ricchiutti D, Resnick MI. Reassessment of the definition of castrate levels of testosterone: implications for clinical decision making. *Urology*. 2000;56(6):1021-4. Epub 2000/01/11. PubMed PMID: 11113751.
144. Traish AM, Toselli P, Jeong SJ, Kim NN. Adipocyte accumulation in penile corpus cavernosum of the orchietomized rabbit: A potential mechanism for veno-occlusive dysfunction in androgen deficiency. *Journal of Andrology*. 2005;26(2):242-8.
145. Traish AM, Munarriz R, O'Connell L, Choi S, Kim SW, Kim NN, Huang YH, Goldstein I. Effects of medical or surgical castration on erectile function in an animal model. *J Androl*. 2003;24(3):381-7. Epub 2003/05/02. PubMed PMID: 12721214.
146. Elliott S, Latini DM, Walker LM, Wassersug R, Robinson JW. Androgen deprivation therapy for prostate cancer: recommendations to improve patient and partner quality of life. *The journal of sexual medicine*. 2010;7(9):2996-3010.
147. Higano CS. Sexuality and intimacy after definitive treatment and subsequent androgen deprivation therapy for prostate cancer. *Journal of Clinical Oncology*. 2012;30(30):3720-5.
148. Green HJ, Pakenham KI, Headley BC, Yaxley J, Nicol DL, Mactaggart PN, Swanson CE, Watson RB, Gardiner RA. Quality of life compared during pharmacological treatments and clinical monitoring for non-localized prostate cancer: a randomized controlled trial. *BJU international*. 2004;93(7):975-9. Epub 2004/05/15. doi: 10.1111/j.1464-410X.2004.04763.x. PubMed PMID: 15142146.
149. Schroder FH, Collette L, de Reijke TM, Whelan P. Prostate cancer treated by anti-androgens: is sexual function preserved? EORTC Genitourinary Group. European Organization for Research and Treatment of Cancer. *British journal of cancer*.

2000;82(2):283-90. Epub 2000/01/26. doi: 10.1054/bjoc.1999.0916. PubMed PMID: 10646878; PubMed Central PMCID: PMCPmc2363280.

150. Basaria S, Dobs AS. Androgens and the hematopoietic system. *Androgens in Health and Disease*: Springer; 2003. p. 233-42.

151. Perlmutter MA, Lepor H. Androgen deprivation therapy in the treatment of advanced prostate cancer. *Reviews in urology*. 2007;9:S3.

152. Shahani S, Braga-Basaria M, Maggio M, Basaria S. Androgens and erythropoiesis: past and present. *Journal of endocrinological investigation*. 2009;32(8):704-16.

153. Curtis KK, Adam TJ, Chen S-C, Pruthi RK, Gornet MK. Anaemia following initiation of androgen deprivation therapy for metastatic prostate cancer: a retrospective chart review. *The Aging Male*. 2008;11(4):157-61.

154. Michaelson MD, Cotter SE, Gargollo PC, Zietman AL, Dahl DM, Smith MR. Management of complications of prostate cancer treatment. *CA: a cancer journal for clinicians*. 2008;58(4):196-213.

155. Diamond TH, Higano CS, Smith MR, Guise TA, Singer FR. Osteoporosis in men with prostate carcinoma receiving androgen-deprivation therapy. *Cancer*. 2004;100(5):892-9.

156. Kiratli BJ, Srinivas S, Perkash I, Terris MK. Progressive decrease in bone density over 10 years of androgen deprivation therapy in patients with prostate cancer. *Urology*. 2001;57(1):127-32.

157. Smith MR. Osteoporosis during androgen deprivation therapy for prostate cancer. *Urology*. 2002;60(3):79-85.

158. Saylor P, Smith M. Bone health and prostate cancer. Prostate cancer and prostatic diseases. 2010;13(1):20-7.
159. Clarke BL, Khosla S. Androgens and bone. Steroids. 2009;74(3):296-305.
160. van der Eerden BC, van Til NP, Brinkmann AO, Lowik CW, Wit JM, Karperien M. Gender differences in expression of androgen receptor in tibial growth plate and metaphyseal bone of the rat. Bone. 2002;30(6):891-6. Epub 2002/06/08. PubMed PMID: 12052459.
161. Sinnesael M, Claessens F, Laurent M, Dubois V, Boonen S, Deboel L, Vanderschueren D. Androgen receptor (AR) in osteocytes is important for the maintenance of male skeletal integrity: evidence from targeted AR disruption in mouse osteocytes. Journal of bone and mineral research : the official journal of the American Society for Bone and Mineral Research. 2012;27(12):2535-43. Epub 2012/07/28. doi: 10.1002/jbmr.1713. PubMed PMID: 22836391.
162. Kasperk C, Helmboldt A, Borcsok I, Heuthe S, Cloos O, Niethard F, Ziegler R. Skeletal site-dependent expression of the androgen receptor in human osteoblastic cell populations. Calcified tissue international. 1997;61(6):464-73. Epub 1998/02/12. PubMed PMID: 9383273.
163. Vanderschueren D, Vandenput L, Boonen S, Lindberg MK, Bouillon R, Ohlsson C. Androgens and bone. Endocrine reviews. 2004;25(3):389-425. Epub 2004/06/08. doi: 10.1210/er.2003-0003. PubMed PMID: 15180950.
164. Hadjidakis DJ, Androulakis II. Bone remodeling. Annals of the New York Academy of Sciences. 2006;1092(1):385-96.

165. Sountoulides P, Rountos T. Adverse effects of androgen deprivation therapy for prostate cancer: prevention and management. *ISRN urology*. 2013;2013.
166. Ross RW, Small EJ. Osteoporosis in men treated with androgen deprivation therapy for prostate cancer. *The Journal of urology*. 2002;167(5):1952-6.
167. Alibhai SM, Yun L, Cheung AM, Paszat L. Screening for osteoporosis in men receiving androgen deprivation therapy. *Jama*. 2012;307(3):255-6.
168. Berenson JR, Rosen LS, Howell A, Porter L, Coleman RE, Morley W, Dreicer R, Kuross SA, Lipton A, Seaman JJ. Zoledronic acid reduces skeletal-related events in patients with osteolytic metastases. *Cancer*. 2001;91(7):1191-200.
169. Smith MR, Egerdie B, Toriz NH, Feldman R, Tammela TL, Saad F, Heracek J, Szwedowski M, Ke C, Kupic A. Denosumab in men receiving androgen-deprivation therapy for prostate cancer. *New England Journal of Medicine*. 2009;361(8):745-55.
170. Boyle WJ, Simonet WS, Lacey DL. Osteoclast differentiation and activation. *Nature*. 2003;423(6937):337-42.
171. Smith MR, Saad F, Egerdie B, Szwedowski M, Tammela TL, Ke C, Leder BZ, Goessl C. Effects of denosumab on bone mineral density in men receiving androgen deprivation therapy for prostate cancer. *The Journal of urology*. 2009;182(6):2670-6.
172. Miller K. [Cardiovascular risks of androgen deprivation therapy for prostate cancer]. *Der Urologe Ausg A*. 2016;55(5):627-31. Epub 2016/03/24. doi: 10.1007/s00120-015-0021-1. PubMed PMID: 27003571.
173. Zareba P, Duivenvoorden W, Leong DP, Pinthus JH. Androgen deprivation therapy and cardiovascular disease: what is the linking mechanism? *Therapeutic advances in urology*. 2016;8(2):118-29. Epub 2016/04/02. doi:

10.1177/1756287215617872. PubMed PMID: 27034724; PubMed Central PMCID: PMCPmc4772356.

174. Keating NL, O'Malley AJ, Smith MR. Diabetes and cardiovascular disease during androgen deprivation therapy for prostate cancer. *Journal of clinical oncology : official journal of the American Society of Clinical Oncology*. 2006;24(27):4448-56. Epub 2006/09/20. doi: 10.1200/jco.2006.06.2497. PubMed PMID: 16983113.

175. Saylor PJ, Smith MR. Metabolic complications of androgen deprivation therapy for prostate cancer. *The Journal of urology*. 2009;181(5):1998-2008.

176. Braga-Basaria M, Dobs AS, Muller DC, Carducci MA, John M, Egan J, Basaria S. Metabolic syndrome in men with prostate cancer undergoing long-term androgen-deprivation therapy. *Journal of Clinical Oncology*. 2006;24(24):3979-83.

177. Traish AM, Abdou R, Kypreos KE. Androgen deficiency and atherosclerosis: The lipid link. *Vascular pharmacology*. 2009;51(5):303-13.

178. Beyenburg S, Watzka M, Clusmann H, Blümcke I, Bidlingmaier F, Elger CE, Stoffel-Wagner B. Androgen receptor mRNA expression in the human hippocampus. *Neuroscience letters*. 2000;294(1):25-8.

179. Lavranos G, Angelopoulou R, Manolakou P, Balla M. Hormonal and meta-hormonal determinants of sexual dimorphism. *Collegium antropologicum*. 2006;30(3):659-63.

180. Nunez J, Huppenbauer CB, McAbee M, Juraska J, DonCarlos LL. Androgen receptor expression in the developing male and female rat visual and prefrontal cortex. *Developmental Neurobiology*. 2003;56(3):293-302.

181. Preston AR, Eichenbaum H. Interplay of hippocampus and prefrontal cortex in memory. *Current Biology*. 2013;23(17):R764-R73.
182. Wu LM, Diefenbach MA, Gordon WA, Cantor JB, Cherrier MM. Cognitive problems in patients on androgen deprivation therapy: a qualitative pilot study. *Urologic oncology*. 2013;31(8):1533-8. Epub 2012/09/15. doi: 10.1016/j.urolonc.2012.07.003. PubMed PMID: 22975107; PubMed Central PMCID: PMC3720684.
183. Holland J, Bandelow S, Hogervorst E. Testosterone levels and cognition in elderly men: a review. *Maturitas*. 2011;69(4):322-37.
184. Bennett G, Badger TA, editors. Depression in men with prostate cancer. *Oncology Nursing Forum-Oncology Nursing Society*; 2005: [Pittsburgh, PA, etc.] Oncology Nursing Society.
185. Pirl WF. Evidence report on the occurrence, assessment, and treatment of depression in cancer patients. *Monographs-National Cancer Institute*. 2004;32:32-9.
186. Mehnert A, Lehmann C, Graefen M, Huland H, Koch U. Depression, anxiety, post-traumatic stress disorder and health-related quality of life and its association with social support in ambulatory prostate cancer patients. *European journal of cancer care*. 2010;19(6):736-45.
187. Armandari I, Hamid AR, Verhaegh G, Schalken J. Intratumoral steroidogenesis in castration-resistant prostate cancer: a target for therapy. *Prostate international*. 2014;2(3):105-13.
188. Ishizaki F, Nishiyama T, Kawasaki T, Miyashiro Y, Hara N, Takizawa I, Naito M, Takahashi K. Androgen deprivation promotes intratumoral synthesis of

dihydrotestosterone from androgen metabolites in prostate cancer. *Scientific reports*. 2013;3:1528.

189. Ferraldeschi R, Sharifi N, Auchus RJ, Attard G. Molecular pathways: inhibiting steroid biosynthesis in prostate cancer. *Clinical cancer research*. 2013;19(13):3353-9.

190. Edwards J, Krishna NS, Grigor KM, Bartlett JM. Androgen receptor gene amplification and protein expression in hormone refractory prostate cancer. *British journal of cancer*. 2003;89(3):552-6. Epub 2003/07/31. doi: 10.1038/sj.bjc.6601127. PubMed PMID: 12888829; PubMed Central PMCID: PMC12394367.

191. Patki M, Huang Y, Ratnam M. Restoration of the cellular secretory milieu overrides androgen dependence of in vivo generated castration resistant prostate cancer cells overexpressing the androgen receptor. *Biochemical and biophysical research communications*. 2016;476(2):69-74. Epub 2016/05/18. doi: 10.1016/j.bbrc.2016.05.058. PubMed PMID: 27179779.

192. Chen CD, Welsbie DS, Tran C, Baek SH, Chen R, Vessella R, Rosenfeld MG, Sawyers CL. Molecular determinants of resistance to antiandrogen therapy. *Nature medicine*. 2004;10(1):33-9. Epub 2004/01/02. doi: 10.1038/nm972. PubMed PMID: 14702632.

193. Heemers HV, Tindall DJ. Androgen receptor (AR) coregulators: a diversity of functions converging on and regulating the AR transcriptional complex. *Endocrine reviews*. 2007;28(7):778-808.

194. Horwitz K, Jackson T, Bain D, Richer J, Takimoto G, Tung L. Nuclear receptor coactivators and corepressors. *Molecular Endocrinology*. 1996;10(10):1167-77.

195. Hur E, Pfaff SJ, Payne ES, Grøn H, Buehrer BM, Fletterick RJ. Recognition and accommodation at the androgen receptor coactivator binding interface. *PLoS Biol.* 2004;2(9):e274.
196. Shang Y, Myers M, Brown M. Formation of the androgen receptor transcription complex. *Molecular cell.* 2002;9(3):601-10. Epub 2002/04/05. PubMed PMID: 11931767.
197. Wang L, Hsu CL, Chang C. Androgen receptor corepressors: an overview. *The Prostate.* 2005;63(2):117-30.
198. Jenster G. Coactivators and corepressors as mediators of nuclear receptor function: an update. *Molecular and cellular endocrinology.* 1998;143(1-2):1-7. Epub 1998/11/07. PubMed PMID: 9806345.
199. Edwards DP. The role of coactivators and corepressors in the biology and mechanism of action of steroid hormone receptors. *Journal of mammary gland biology and neoplasia.* 2000;5(3):307-24. Epub 2004/02/20. PubMed PMID: 14973393.
200. Brooke GN, Parker M, Bevan C. Mechanisms of androgen receptor activation in advanced prostate cancer: differential co-activator recruitment and gene expression. *Oncogene.* 2008;27(21):2941-50.
201. Li P, Yu X, Ge K, Melamed J, Roeder RG, Wang Z. Heterogeneous expression and functions of androgen receptor co-factors in primary prostate cancer. *The American journal of pathology.* 2002;161(4):1467-74. Epub 2002/10/09. doi: 10.1016/s0002-9440(10)64422-7. PubMed PMID: 12368219; PubMed Central PMCID: PMC1867282.

202. Ueda T, Bruchofsky N, Sadar MD. Activation of the androgen receptor N-terminal domain by interleukin-6 via MAPK and STAT3 signal transduction pathways. *Journal of Biological Chemistry*. 2002;277(9):7076-85.
203. Hobisch A, Eder IE, Putz T, Horninger W, Bartsch G, Klocker H, Culig Z. Interleukin-6 regulates prostate-specific protein expression in prostate carcinoma cells by activation of the androgen receptor. *Cancer research*. 1998;58(20):4640-5.
204. Jenster G. Ligand-independent activation of the androgen receptor in prostate cancer by growth factors and cytokines. *The Journal of pathology*. 2000;191(3):227-8.
205. Yeh S, Lin HK, Kang HY, Thin TH, Lin MF, Chang C. From HER2/Neu signal cascade to androgen receptor and its coactivators: a novel pathway by induction of androgen target genes through MAP kinase in prostate cancer cells. *Proceedings of the National Academy of Sciences of the United States of America*. 1999;96(10):5458-63. Epub 1999/05/13. PubMed PMID: 10318905; PubMed Central PMCID: PMC21881.
206. Marcelli M, Ittmann M, Mariani S, Sutherland R, Nigam R, Murthy L, Zhao Y, DiConcini D, Puxeddu E, Esen A, Eastham J, Weigel NL, Lamb DJ. Androgen receptor mutations in prostate cancer. *Cancer research*. 2000;60(4):944-9. Epub 2000/03/08. PubMed PMID: 10706109.
207. Tilley WD, Buchanan G, Hickey TE, Bentel JM. Mutations in the androgen receptor gene are associated with progression of human prostate cancer to androgen independence. *Clinical cancer research : an official journal of the American Association for Cancer Research*. 1996;2(2):277-85. Epub 1996/02/01. PubMed PMID: 9816170.
208. Cao S, Zhan Y, Dong Y. Emerging data on androgen receptor splice variants in prostate cancer. *Endocrine-related cancer*. 2016;23(12):T199-t210. Epub 2016/10/22.

doi: 10.1530/erc-16-0298. PubMed PMID: 27702752; PubMed Central PMCID: PMCPmc5107136.

209. Haile S, Sadar MD. Androgen receptor and its splice variants in prostate cancer. Cellular and Molecular Life Sciences. 2011;68(24):3971-81.

210. Li Y, Chan SC, Brand LJ, Hwang TH, Silverstein KA, Dehm SM. Androgen receptor splice variants mediate enzalutamide resistance in castration-resistant prostate cancer cell lines. Cancer research. 2013;73(2):483-9. Epub 2012/11/03. doi: 10.1158/0008-5472.CAN-12-3630. PubMed PMID: 23117885; PubMed Central PMCID: PMC3549016.

211. Guo Z, Yang X, Sun F, Jiang R, Linn DE, Chen H, Kong X, Melamed J, Tepper CG, Kung HJ, Brodie AM, Edwards J, Qiu Y. A novel androgen receptor splice variant is up-regulated during prostate cancer progression and promotes androgen depletion-resistant growth. Cancer research. 2009;69(6):2305-13. Epub 2009/02/27. doi: 10.1158/0008-5472.CAN-08-3795. PubMed PMID: 19244107; PubMed Central PMCID: PMC2672822.

212. Dehm SM, Schmidt LJ, Heemers HV, Vessella RL, Tindall DJ. Splicing of a novel androgen receptor exon generates a constitutively active androgen receptor that mediates prostate cancer therapy resistance. Cancer research. 2008;68(13):5469-77.

213. Hu R, Lu C, Mostaghel EA, Yegnasubramanian S, Gurel M, Tannahill C, Edwards J, Isaacs WB, Nelson PS, Bluemn E, Plymate SR, Luo J. Distinct transcriptional programs mediated by the ligand-dependent full-length androgen receptor and its splice variants in castration-resistant prostate cancer. Cancer research.

2012;72(14):3457-62. Epub 2012/06/20. doi: 10.1158/0008-5472.can-11-3892. PubMed PMID: 22710436; PubMed Central PMCID: PMCPmc3415705.

214. Hu R, Dunn TA, Wei S, Isharwal S, Veltri RW, Humphreys E, Han M, Partin AW, Vessella RL, Isaacs WB, Bova GS, Luo J. Ligand-independent androgen receptor variants derived from splicing of cryptic exons signify hormone-refractory prostate cancer. *Cancer research*. 2009;69(1):16-22. Epub 2009/01/02. doi: 10.1158/0008-5472.can-08-2764. PubMed PMID: 19117982; PubMed Central PMCID: PMCPmc2614301.

215. Hornberg E, Ylitalo EB, Crnalic S, Antti H, Stattin P, Widmark A, Bergh A, Wikstrom P. Expression of androgen receptor splice variants in prostate cancer bone metastases is associated with castration-resistance and short survival. *PloS one*. 2011;6(4):e19059. Epub 2011/05/10. doi: 10.1371/journal.pone.0019059. PubMed PMID: 21552559; PubMed Central PMCID: PMCPmc3084247.

216. Gillis JL, Selth LA, Centenera MM, Townley SL, Sun S, Plymate SR, Tilley WD, Butler LM. Constitutively-active androgen receptor variants function independently of the HSP90 chaperone but do not confer resistance to HSP90 inhibitors. *Oncotarget*. 2013;4(5):691.

217. Egan A, Dong Y, Zhang H, Qi Y, Balk SP, Sartor O. Castration-resistant prostate cancer: adaptive responses in the androgen axis. *Cancer treatment reviews*. 2014;40(3):426-33.

218. Schaufele F, Carbonell X, Guerbador M, Borngraeber S, Chapman MS, Ma AAK, Miner JN, Diamond MI. The structural basis of androgen receptor activation:

intramolecular and intermolecular amino–carboxy interactions. Proceedings of the National Academy of Sciences of the United States of America. 2005;102(28):9802-7.

219. Xu D, Zhan Y, Qi Y, Cao B, Bai S, Xu W, Gambhir SS, Lee P, Sartor O, Flemington EK, Zhang H, Hu CD, Dong Y. Androgen Receptor Splice Variants Dimerize to Transactivate Target Genes. Cancer research. 2015;75(17):3663-71. Epub 2015/06/11. doi: 10.1158/0008-5472.can-15-0381. PubMed PMID: 26060018; PubMed Central PMCID: PMCPmc4558376.

220. Cao B, Qi Y, Zhang G, Xu D, Zhan Y, Alvarez X, Guo Z, Fu X, Plymate SR, Sartor O, Zhang H, Dong Y. Androgen receptor splice variants activating the full-length receptor in mediating resistance to androgen-directed therapy. Oncotarget. 2014;5(6):1646-56. Epub 2014/04/12. doi: 10.18632/oncotarget.1802. PubMed PMID: 24722067; PubMed Central PMCID: PMCPmc4039237.

221. Sun S, Sprenger CC, Vessella RL, Haugk K, Soriano K, Mostaghel EA, Page ST, Coleman IM, Nguyen HM, Sun H, Nelson PS, Plymate SR. Castration resistance in human prostate cancer is conferred by a frequently occurring androgen receptor splice variant. The Journal of clinical investigation. 2010;120(8):2715-30. Epub 2010/07/21. doi: 10.1172/jci41824. PubMed PMID: 20644256; PubMed Central PMCID: PMCPmc2912187.

222. Zhan Y, Zhang G, Wang X, Qi Y, Bai S, Li D, Ma T, Sartor O, Flemington EK, Zhang H, Lee P, Dong Y. Interplay between Cytoplasmic and Nuclear Androgen Receptor Splice Variants Mediates Castration Resistance. Molecular cancer research : MCR. 2017;15(1):59-68. Epub 2016/09/28. doi: 10.1158/1541-7786.mcr-16-0236. PubMed PMID: 27671337; PubMed Central PMCID: PMCPmc5215946.

223. Hu R, Lu C, Mostaghel EA, Yegnasubramanian S, Gurel M, Tannahill C, Edwards J, Isaacs WB, Nelson PS, Bluemn E. Distinct transcriptional programs mediated by the ligand-dependent full-length androgen receptor and its splice variants in castration-resistant prostate cancer. *Cancer research*. 2012;72(14):3457-62.
224. Hu R, Isaacs WB, Luo J. A snapshot of the expression signature of androgen receptor splicing variants and their distinctive transcriptional activities. *The Prostate*. 2011;71(15):1656-67.
225. Helin K, Dhanak D. Chromatin proteins and modifications as drug targets. *Nature*. 2013;502(7472):480-8.
226. Dey A, Chitsaz F, Abbasi A, Misteli T, Ozato K. The double bromodomain protein Brd4 binds to acetylated chromatin during interphase and mitosis. *Proceedings of the National Academy of Sciences*. 2003;100(15):8758-63.
227. Wu S-Y, Chiang C-M. The double bromodomain-containing chromatin adaptor Brd4 and transcriptional regulation. *Journal of Biological Chemistry*. 2007;282(18):13141-5.
228. Itzen F, Greifenberg AK, Bösken CA, Geyer M. Brd4 activates P-TEFb for RNA polymerase II CTD phosphorylation. *Nucleic acids research*. 2014;42(12):7577-90.
229. Asangani IA, Dommeti VL, Wang X, Malik R, Cieslik M, Yang R, Escara-Wilke J, Wilder-Romans K, Dhanireddy S, Engelke C, Iyer MK, Jing X, Wu YM, Cao X, Qin ZS, Wang S, Feng FY, Chinnaiyan AM. Therapeutic targeting of BET bromodomain proteins in castration-resistant prostate cancer. *Nature*. 2014;510(7504):278-82. Epub 2014/04/25. doi: 10.1038/nature13229. PubMed PMID: 24759320; PubMed Central PMCID: PMC4075966.

230. Lin TH, Izumi K, Lee SO, Lin WJ, Yeh S, Chang C. Anti-androgen receptor ASC-J9 versus anti-androgens MDV3100 (Enzalutamide) or Casodex (Bicalutamide) leads to opposite effects on prostate cancer metastasis via differential modulation of macrophage infiltration and STAT3-CCL2 signaling. *Cell death & disease*. 2013;4:e764. Epub 2013/08/10. doi: 10.1038/cddis.2013.270. PubMed PMID: 23928703; PubMed Central PMCID: PMCPmc3763432.
231. Asangani IA, Wilder-Romans K, Dommeti VL, Krishnamurthy PM, Apel IJ, Escara-Wilke J, Plymate SR, Navone NM, Wang S, Feng FY, Chinnaiyan AM. BET Bromodomain Inhibitors Enhance Efficacy and Disrupt Resistance to AR Antagonists in the Treatment of Prostate Cancer. *Molecular cancer research : MCR*. 2016;14(4):324-31. Epub 2016/01/23. doi: 10.1158/1541-7786.mcr-15-0472. PubMed PMID: 26792867; PubMed Central PMCID: PMCPmc4834259.
232. Blee AM, Liu S, Wang L, Huang H. BET bromodomain-mediated interaction between ERG and BRD4 promotes prostate cancer cell invasion. *Oncotarget*. 2016;7(25):38319-32. Epub 2016/10/23. doi: 10.18632/oncotarget.9513. PubMed PMID: 27223260; PubMed Central PMCID: PMCPmc5122392.
233. Chan SC, Selth LA, Li Y, Nyquist MD, Miao L, Bradner JE, Raj GV, Tilley WD, Dehm SM. Targeting chromatin binding regulation of constitutively active AR variants to overcome prostate cancer resistance to endocrine-based therapies. *Nucleic acids research*. 2015;43(12):5880-97. Epub 2015/04/25. doi: 10.1093/nar/gkv262. PubMed PMID: 25908785; PubMed Central PMCID: PMCPmc4499120.
234. Andersen RJ, Mawji NR, Wang J, Wang G, Haile S, Myung JK, Watt K, Tam T, Yang YC, Banuelos CA, Williams DE, McEwan IJ, Wang Y, Sadar MD. Regression of

castrate-recurrent prostate cancer by a small-molecule inhibitor of the amino-terminus domain of the androgen receptor. *Cancer cell*. 2010;17(6):535-46. Epub 2010/06/15. doi: 10.1016/j.ccr.2010.04.027. PubMed PMID: 20541699.

235. De Mol E, Fenwick RB, Phang CT, Buzon V, Szulc E, de la Fuente A, Escobedo A, Garcia J, Bertoncini CW, Estebanez-Perpina E, McEwan IJ, Riera A, Salvatella X. EPI-001, A Compound Active against Castration-Resistant Prostate Cancer, Targets Transactivation Unit 5 of the Androgen Receptor. *ACS chemical biology*. 2016;11(9):2499-505. Epub 2016/06/30. doi: 10.1021/acscchembio.6b00182. PubMed PMID: 27356095; PubMed Central PMCID: PMCPmc5027137.

236. Myung JK, Banuelos CA, Fernandez JG, Mawji NR, Wang J, Tien AH, Yang YC, Tavakoli I, Haile S, Watt K, McEwan IJ, Plymate S, Andersen RJ, Sadar MD. An androgen receptor N-terminal domain antagonist for treating prostate cancer. *The Journal of clinical investigation*. 2013;123(7):2948-60. Epub 2013/06/01. doi: 10.1172/JCI66398. PubMed PMID: 23722902; PubMed Central PMCID: PMC3696543.

237. Yang YC, Banuelos CA, Mawji NR, Wang J, Kato M, Haile S, McEwan IJ, Plymate S, Sadar MD. Targeting Androgen Receptor Activation Function-1 with EPI to Overcome Resistance Mechanisms in Castration-Resistant Prostate Cancer. *Clinical cancer research : an official journal of the American Association for Cancer Research*. 2016;22(17):4466-77. Epub 2016/05/04. doi: 10.1158/1078-0432.ccr-15-2901. PubMed PMID: 27140928; PubMed Central PMCID: PMCPmc5010454.

238. Sadar MD, Williams DE, Mawji NR, Patrick BO, Wikanta T, Chasanah E, Irianto HE, Soest RV, Andersen RJ. Sintokamides A to E, chlorinated peptides from the sponge *Dysidea* sp. that inhibit transactivation of the N-terminus of the androgen

receptor in prostate cancer cells. *Organic letters*. 2008;10(21):4947-50. Epub 2008/10/07. doi: 10.1021/ol802021w. PubMed PMID: 18834139.

239. Banuelos CA, Tavakoli I, Tien AH, Caley DP, Mawji NR, Li Z, Wang J, Yang YC, Imamura Y, Yan L, Wen JG, Andersen RJ, Sadar MD. Sintokamide A Is a Novel Antagonist of Androgen Receptor That Uniquely Binds Activation Function-1 in Its Amino-terminal Domain. *The Journal of biological chemistry*. 2016;291(42):22231-43. Epub 2016/09/01. doi: 10.1074/jbc.M116.734475. PubMed PMID: 27576691; PubMed Central PMCID: PMCPmc5064002.

240. Goicochea NL, Garnovskaya M, Blanton M, Chan G, Weisbart R, Lilly M. Abstract 642: Cell-penetrating bispecific antibodies for targeting androgen receptor signaling in advanced prostate cancer. *Cancer research*. 2015;75(15 Supplement):642-. doi: 10.1158/1538-7445.am2015-642.

241. Ratnam M, Patki M, Gonit M, Trumbly R. Mechanisms of ARE-Independent Gene Activation by the Androgen Receptor in Prostate Cancer Cells: Potential Targets for Better Intervention Strategies. In: Wang Z, editor. *Androgen-Responsive Genes in Prostate Cancer*: Springer New York; 2013. p. 85-100.

242. Norris JD, Chang CY, Wittmann BM, Kunder RS, Cui H, Fan D, Joseph JD, McDonnell DP. The homeodomain protein HOXB13 regulates the cellular response to androgens. *Molecular cell*. 2009;36(3):405-16. Epub 2009/11/18. doi: 10.1016/j.molcel.2009.10.020. PubMed PMID: 19917249; PubMed Central PMCID: PMCPmc2788777.

243. Sivakumaran S, Zhang J, Kelley KM, Gonit M, Hao H, Ratnam M. Androgen activation of the folate receptor alpha gene through partial tethering of the androgen

receptor by C/EBPalpha. The Journal of steroid biochemistry and molecular biology. 2010;122(5):333-40. Epub 2010/09/08. doi: 10.1016/j.jsbmb.2010.08.008. PubMed PMID: 20817090; PubMed Central PMCID: PMCPmc2964422.

244. Zhang J, Wilkinson JE, Gonit M, Keck R, Selman S, Ratnam M. Expression and sub-cellular localization of the CCAAT/enhancer binding protein alpha in relation to postnatal development and malignancy of the prostate. The Prostate. 2008;68(11):1206-14. Epub 2008/05/16. doi: 10.1002/pros.20779. PubMed PMID: 18481268; PubMed Central PMCID: PMCPmc3911780.

245. Zhang J, Gonit M, Salazar MD, Shatnawi A, Shemshedini L, Trumbly R, Ratnam M. C/EBPalpha redirects androgen receptor signaling through a unique bimodal interaction. Oncogene. 2010;29(5):723-38. Epub 2009/11/11. doi: 10.1038/onc.2009.373. PubMed PMID: 19901962.

246. Patki M, Chari V, Sivakumaran S, Gonit M, Trumbly R, Ratnam M. The ETS domain transcription factor ELK1 directs a critical component of growth signaling by the androgen receptor in prostate cancer cells. The Journal of biological chemistry. 2013;288(16):11047-65. Epub 2013/02/22. doi: 10.1074/jbc.M112.438473. PubMed PMID: 23426362; PubMed Central PMCID: PMCPmc3630885.

247. Podlasek CA, Clemens JQ, Bushman W. Hoxa-13 gene mutation results in abnormal seminal vesicle and prostate development. The Journal of urology. 1999;161(5):1655-61. Epub 1999/04/21. PubMed PMID: 10210434.

248. Huang L, Pu Y, Hepps D, Danielpour D, Prins GS. Posterior Hox gene expression and differential androgen regulation in the developing and adult rat prostate

lobes. *Endocrinology*. 2007;148(3):1235-45. Epub 2006/12/02. doi: 10.1210/en.2006-1250. PubMed PMID: 17138648; PubMed Central PMCID: PMC2276874.

249. Jung C, Kim RS, Zhang HJ, Lee SJ, Jeng MH. HOXB13 induces growth suppression of prostate cancer cells as a repressor of hormone-activated androgen receptor signaling. *Cancer research*. 2004;64(24):9185-92. Epub 2004/12/18. doi: 10.1158/0008-5472.CAN-04-1330. PubMed PMID: 15604291.

250. Ramji DP, Foka P. CCAAT/enhancer-binding proteins: structure, function and regulation. *The Biochemical journal*. 2002;365(Pt 3):561-75. Epub 2002/05/15. doi: 10.1042/BJ20020508. PubMed PMID: 12006103; PubMed Central PMCID: PMC1222736.

251. Umek RM, Friedman AD, McKnight SL. CCAAT-enhancer binding protein: a component of a differentiation switch. *Science*. 1991;251(4991):288-92. Epub 1991/01/18. PubMed PMID: 1987644.

252. Hendricks-Taylor LR, Darlington GJ. Inhibition of cell proliferation by C/EBP alpha occurs in many cell types, does not require the presence of p53 or Rb, and is not affected by large T-antigen. *Nucleic acids research*. 1995;23(22):4726-33. Epub 1995/11/25. PubMed PMID: 8524667; PubMed Central PMCID: PMC307450.

253. Watkins PJ, Condreay JP, Huber BE, Jacobs SJ, Adams DJ. Impaired proliferation and tumorigenicity induced by CCAAT/enhancer-binding protein. *Cancer research*. 1996;56(5):1063-7. Epub 1996/03/01. PubMed PMID: 8640762.

254. Timchenko NA, Wilde M, Nakanishi M, Smith JR, Darlington GJ. CCAAT/enhancer-binding protein alpha (C/EBP alpha) inhibits cell proliferation through

the p21 (WAF-1/CIP-1/SDI-1) protein. *Genes & development*. 1996;10(7):804-15. Epub 1996/04/01. PubMed PMID: 8846917.

255. Timchenko NA, Harris TE, Wilde M, Bilyeu TA, Burgess-Beusse BL, Finegold MJ, Darlington GJ. CCAAT/enhancer binding protein alpha regulates p21 protein and hepatocyte proliferation in newborn mice. *Molecular and cellular biology*. 1997;17(12):7353-61. Epub 1997/12/31. PubMed PMID: 9372966; PubMed Central PMCID: PMC232591.

256. Wang GL, Iakova P, Wilde M, Awad S, Timchenko NA. Liver tumors escape negative control of proliferation via PI3K/Akt-mediated block of C/EBP alpha growth inhibitory activity. *Genes & development*. 2004;18(8):912-25. Epub 2004/04/27. doi: 10.1101/gad.1183304. PubMed PMID: 15107404; PubMed Central PMCID: PMC395850.

257. Wang GL, Timchenko NA. Dephosphorylated C/EBPalpha accelerates cell proliferation through sequestering retinoblastoma protein. *Molecular and cellular biology*. 2005;25(4):1325-38. Epub 2005/02/03. doi: 10.1128/MCB.25.4.1325-1338.2005. PubMed PMID: 15684384; PubMed Central PMCID: PMC548025.

258. Chattopadhyay S, Gong EY, Hwang M, Park E, Lee HJ, Hong CY, Choi HS, Cheong JH, Kwon HB, Lee K. The CCAAT enhancer-binding protein-alpha negatively regulates the transactivation of androgen receptor in prostate cancer cells. *Mol Endocrinol*. 2006;20(5):984-95. Epub 2006/02/04. doi: 10.1210/me.2005-0240. PubMed PMID: 16455820.

259. Buchwalter G, Gross C, Wasylyk B. Ets ternary complex transcription factors. *Gene*. 2004;324:1-14. Epub 2003/12/25. PubMed PMID: 14693367.

260. Sharrocks AD. Complexities in ETS-domain transcription factor function and regulation: lessons from the TCF (ternary complex factor) subfamily. The Colworth Medal Lecture. Biochemical Society transactions. 2002;30(2):1-9. Epub 2002/05/25. doi: 10.1042/. PubMed PMID: 12023815.
261. Shaw PE, Frasch S, Nordheim A. Repression of c-fos transcription is mediated through p67SRF bound to the SRE. The EMBO journal. 1989;8(9):2567-74. Epub 1989/09/01. PubMed PMID: 2511007; PubMed Central PMCID: PMCPmc401258.
262. Sharrocks AD. The ETS-domain transcription factor family. Nature reviews Molecular cell biology. 2001;2(11):827-37. Epub 2001/11/21. doi: 10.1038/35099076. PubMed PMID: 11715049.
263. Yang SH, Vickers E, Brehm A, Kouzarides T, Sharrocks AD. Temporal recruitment of the mSin3A-histone deacetylase corepressor complex to the ETS domain transcription factor Elk-1. Molecular and cellular biology. 2001;21(8):2802-14. Epub 2001/04/03. doi: 10.1128/mcb.21.8.2802-2814.2001. PubMed PMID: 11283259; PubMed Central PMCID: PMCPmc86910.
264. Shore P, Sharrocks AD. The transcription factors Elk-1 and serum response factor interact by direct protein-protein contacts mediated by a short region of Elk-1. Molecular and cellular biology. 1994;14(5):3283-91. Epub 1994/05/01. PubMed PMID: 8164681; PubMed Central PMCID: PMCPmc358695.
265. Cesari F, Rennekampff V, Vintersten K, Vuong LG, Seibler J, Bode J, Wiebel FF, Nordheim A. Elk-1 knock-out mice engineered by Flp recombinase-mediated cassette exchange. Genesis. 2004;38(2):87-92. doi: 10.1002/gene.20003. PubMed PMID: 14994271.

266. Singh D, Febbo PG, Ross K, Jackson DG, Manola J, Ladd C, Tamayo P, Renshaw AA, D'Amico AV, Richie JP, Lander ES, Loda M, Kantoff PW, Golub TR, Sellers WR. Gene expression correlates of clinical prostate cancer behavior. *Cancer cell*. 2002;1(2):203-9. Epub 2002/06/28. PubMed PMID: 12086878.
267. Gonit M, Zhang J, Salazar M, Cui H, Shatnawi A, Trumbly R, Ratnam M. Hormone depletion-insensitivity of prostate cancer cells is supported by the AR without binding to classical response elements. *Mol Endocrinol*. 2011;25(4):621-34. Epub 2011/02/19. doi: me.2010-0409 [pii] 10.1210/me.2010-0409. PubMed PMID: 21330406; PubMed Central PMCID: PMC3063083.
268. Rosati R, Patki M, Chari V, Dakshnamurthy S, McFall T, Saxton J, Kidder BL, Shaw PE, Ratnam M. The Amino-terminal Domain of the Androgen Receptor Co-opts Extracellular Signal-regulated Kinase (ERK) Docking Sites in ELK1 Protein to Induce Sustained Gene Activation That Supports Prostate Cancer Cell Growth. *Journal of Biological Chemistry*. 2016;291(50):25983-+. doi: 10.1074/jbc.M116.745596. PubMed PMID: WOS:000390345200019.
269. Urbanucci A, Sahu B, Seppala J, Larjo A, Latonen LM, Waltering KK, Tammela TL, Vessella RL, Lahdesmaki H, Janne OA, Visakorpi T. Overexpression of androgen receptor enhances the binding of the receptor to the chromatin in prostate cancer. *Oncogene*. 2012;31(17):2153-63. Epub 2011/09/13. doi: 10.1038/onc.2011.401. PubMed PMID: 21909140.
270. Goodwin JF, Kothari V, Drake JM, Zhao S, Dylgjeri E, Dean JL, Schiewer MJ, McNair C, Jones JK, Aytes A, Magee MS, Snook AE, Zhu Z, Den RB, Birbe RC,

Gomella LG, Graham NA, Vashisht AA, Wohlschlegel JA, Graeber TG, Karnes RJ, Takhar M, Davicioni E, Tomlins SA, Abate-Shen C, Sharifi N, Witte ON, Feng FY, Knudsen KE. DNA-PKcs-Mediated Transcriptional Regulation Drives Prostate Cancer Progression and Metastasis. *Cancer cell*. 2015;28(1):97-113. Epub 2015/07/16. doi: 10.1016/j.ccell.2015.06.004. PubMed PMID: 26175416; PubMed Central PMCID: PMC4531387.

271. Ruizeveld de Winter JA, Janssen PJ, Sleddens HM, Verleun-Mooijman MC, Trapman J, Brinkmann AO, Santerse AB, Schroder FH, van der Kwast TH. Androgen receptor status in localized and locally progressive hormone refractory human prostate cancer. *The American journal of pathology*. 1994;144(4):735-46. Epub 1994/04/01. PubMed PMID: 7512791; PubMed Central PMCID: PMC4531387.

272. Linja MJ, Savinainen KJ, Saramaki OR, Tammela TL, Vessella RL, Visakorpi T. Amplification and overexpression of androgen receptor gene in hormone-refractory prostate cancer. *Cancer research*. 2001;61(9):3550-5. Epub 2001/04/28. PubMed PMID: 11325816.

273. Zegarra-Moro OL, Schmidt LJ, Huang H, Tindall DJ. Disruption of androgen receptor function inhibits proliferation of androgen-refractory prostate cancer cells. *Cancer research*. 2002;62(4):1008-13. PubMed PMID: 11861374.

274. Li TH, Zhao H, Peng Y, Beliakoff J, Brooks JD, Sun Z. A promoting role of androgen receptor in androgen-sensitive and -insensitive prostate cancer cells. *Nucleic acids research*. 2007;35(8):2767-76. Epub 2007/04/12. doi: 10.1093/nar/gkm198. PubMed PMID: 17426117; PubMed Central PMCID: PMC4531387.

275. Zarif JC, Miranti CK. The importance of non-nuclear AR signaling in prostate cancer progression and therapeutic resistance. *Cellular signalling*. 2016;28(5):348-56. Epub 2016/02/02. doi: 10.1016/j.cellsig.2016.01.013. PubMed PMID: 26829214; PubMed Central PMCID: PMCPmc4788534.
276. Kousteni S, Bellido T, Plotkin LI, O'Brien CA, Bodenner DL, Han L, Han K, DiGregorio GB, Katzenellenbogen JA, Katzenellenbogen BS, Roberson PK, Weinstein RS, Jilka RL, Manolagas SC. Nongenotropic, sex-nonspecific signaling through the estrogen or androgen receptors: dissociation from transcriptional activity. *Cell*. 2001;104(5):719-30. Epub 2001/03/21. PubMed PMID: 11257226.
277. Falkenstein E, Tillmann HC, Christ M, Feuring M, Wehling M. Multiple actions of steroid hormones--a focus on rapid, nongenomic effects. *Pharmacological reviews*. 2000;52(4):513-56. Epub 2000/12/21. PubMed PMID: 11121509.
278. Lonard DM, O'Malley BW. Nuclear receptor coregulators: modulators of pathology and therapeutic targets. *Nature reviews Endocrinology*. 2012;8(10):598-604. Epub 2012/06/27. doi: 10.1038/nrendo.2012.100. PubMed PMID: 22733267; PubMed Central PMCID: PMCPmc3564250.
279. Snoek R, Cheng H, Margiotti K, Wafa LA, Wong CA, Wong EC, Fazli L, Nelson CC, Gleave ME, Rennie PS. In vivo knockdown of the androgen receptor results in growth inhibition and regression of well-established, castration-resistant prostate tumors. *Clinical cancer research : an official journal of the American Association for Cancer Research*. 2009;15(1):39-47. doi: 10.1158/1078-0432.CCR-08-1726. PubMed PMID: 19118031.

280. Massard C, Fizazi K. Targeting continued androgen receptor signaling in prostate cancer. *Clinical cancer research : an official journal of the American Association for Cancer Research*. 2011;17(12):3876-83. Epub 2011/06/18. doi: 10.1158/1078-0432.ccr-10-2815. PubMed PMID: 21680543.
281. Ryan CJ, Tindall DJ. Androgen receptor rediscovered: the new biology and targeting the androgen receptor therapeutically. *Journal of clinical oncology : official journal of the American Society of Clinical Oncology*. 2011;29(27):3651-8. doi: 10.1200/JCO.2011.35.2005. PubMed PMID: 21859989.
282. Gelmann EP. Molecular biology of the androgen receptor. *Journal of clinical oncology : official journal of the American Society of Clinical Oncology*. 2002;20(13):3001-15. PubMed PMID: 12089231.
283. Zhou ZX, Lane MV, Kempainen JA, French FS, Wilson EM. Specificity of ligand-dependent androgen receptor stabilization: receptor domain interactions influence ligand dissociation and receptor stability. *Molecular endocrinology*. 1995;9(2):208-18. Epub 1995/02/01. doi: 10.1210/mend.9.2.7776971. PubMed PMID: 7776971.
284. Pratt WB, Toft DO. Steroid receptor interactions with heat shock protein and immunophilin chaperones. *Endocrine reviews*. 1997;18(3):306-60. Epub 1997/06/01. doi: 10.1210/edrv.18.3.0303. PubMed PMID: 9183567.
285. Shaffer PL, Jivan A, Dollins DE, Claessens F, Gewirth DT. Structural basis of androgen receptor binding to selective androgen response elements. *Proceedings of the National Academy of Sciences of the United States of America*. 2004;101(14):4758-63. Epub 2004/03/24. doi: 10.1073/pnas.0401123101

0401123101 [pii]. PubMed PMID: 15037741; PubMed Central PMCID: PMC387321.

286. Visakorpi T, Hyytinen E, Koivisto P, Tanner M, Keinänen R, Palmberg C, Palotie A, Tammela T, Isola J, Kallioniemi OP. In vivo amplification of the androgen receptor gene and progression of human prostate cancer. *Nature genetics*. 1995;9(4):401-6. Epub 1995/04/01. doi: 10.1038/ng0495-401. PubMed PMID: 7795646.

287. Toren P, Zoubeidi A. Targeting the PI3K/Akt pathway in prostate cancer: challenges and opportunities (review). *International journal of oncology*. 2014;45(5):1793-801. Epub 2014/08/15. doi: 10.3892/ijo.2014.2601. PubMed PMID: 25120209.

288. Xin L, Teitell MA, Lawson DA, Kwon A, Mellinghoff IK, Witte ON. Progression of prostate cancer by synergy of AKT with genotropic and nongenotropic actions of the androgen receptor. *Proceedings of the National Academy of Sciences of the United States of America*. 2006;103(20):7789-94. Epub 2006/05/10. doi: 10.1073/pnas.0602567103. PubMed PMID: 16682621; PubMed Central PMCID: PMC1458510.

289. Chan SC, Li Y, Dehm SM. Androgen receptor splice variants activate androgen receptor target genes and support aberrant prostate cancer cell growth independent of canonical androgen receptor nuclear localization signal. *The Journal of biological chemistry*. 2012;287(23):19736-49. Epub 2012/04/26. doi: 10.1074/jbc.M112.352930. PubMed PMID: 22532567; PubMed Central PMCID: PMC3366007.

290. Chang KH, Li R, Papari-Zareei M, Watumull L, Zhao YD, Auchus RJ, Sharifi N. Dihydrotestosterone synthesis bypasses testosterone to drive castration-resistant prostate cancer. *Proceedings of the National Academy of Sciences of the United States*

of America. 2011;108(33):13728-33. Epub 2011/07/29. doi: 10.1073/pnas.1107898108. PubMed PMID: 21795608; PubMed Central PMCID: PMC3158152.

291. Lamont KR, Tindall DJ. Minireview: Alternative activation pathways for the androgen receptor in prostate cancer. *Molecular endocrinology (Baltimore, Md)*. 2011;25(6):897-907. Epub 2011/03/26. doi: 10.1210/me.2010-0469. PubMed PMID: 21436259; PubMed Central PMCID: PMCPmc3100605.

292. Kawahara T, Ide H, Kashiwagi E, Patterson JD, Inoue S, Shareef HK, Aljarah AK, Zheng Y, Baras AS, Miyamoto H. Silodosin inhibits the growth of bladder cancer cells and enhances the cytotoxic activity of cisplatin via ELK1 inactivation. *American journal of cancer research*. 2015;5(10):2959-68. Epub 2015/12/23. PubMed PMID: 26693052; PubMed Central PMCID: PMCPmc4656723.

293. Kawahara T, Shareef HK, Aljarah AK, Ide H, Li Y, Kashiwagi E, Netto GJ, Zheng Y, Miyamoto H. ELK1 is up-regulated by androgen in bladder cancer cells and promotes tumor progression. *Oncotarget*. 2015;6(30):29860-76. Epub 2015/09/06. doi: 10.18632/oncotarget.5007. PubMed PMID: 26342199.

294. Yu J, Yu J, Mani RS, Cao Q, Brenner CJ, Cao X, Wang X, Wu L, Li J, Hu M, Gong Y, Cheng H, Laxman B, Vellaichamy A, Shankar S, Li Y, Dhanasekaran SM, Morey R, Barrette T, Lonigro RJ, Tomlins SA, Varambally S, Qin ZS, Chinnaiyan AM. An integrated network of androgen receptor, polycomb, and TMPRSS2-ERG gene fusions in prostate cancer progression. *Cancer cell*. 2010;17(5):443-54. Epub 2010/05/19. doi: 10.1016/j.ccr.2010.03.018. PubMed PMID: 20478527; PubMed Central PMCID: PMCPmc2874722.

295. Shaw PE, Saxton J. Ternary complex factors: prime nuclear targets for mitogen-activated protein kinases. *The international journal of biochemistry & cell biology*. 2003;35(8):1210-26. Epub 2003/05/22. PubMed PMID: 12757758.
296. Gille H, Sharrocks AD, Shaw PE. Phosphorylation of transcription factor p62TCF by MAP kinase stimulates ternary complex formation at c-fos promoter. *Nature*. 1992;358(6385):414-7. Epub 1992/07/30. doi: 10.1038/358414a0. PubMed PMID: 1322499.
297. Gille H, Kortenjann M, Thomae O, Moomaw C, Slaughter C, Cobb MH, Shaw PE. ERK phosphorylation potentiates Elk-1-mediated ternary complex formation and transactivation. *The EMBO journal*. 1995;14(5):951-62. Epub 1995/03/01. PubMed PMID: 7889942; PubMed Central PMCID: PMCPmc398167.
298. Jacobs D, Glossip D, Xing H, Muslin AJ, Kornfeld K. Multiple docking sites on substrate proteins form a modular system that mediates recognition by ERK MAP kinase. *Genes & development*. 1999;13(2):163-75.
299. Tanoue T, Adachi M, Moriguchi T, Nishida E. A conserved docking motif in MAP kinases common to substrates, activators and regulators. *Nature cell biology*. 2000;2(2):110-6. Epub 2000/02/03. doi: 10.1038/35000065. PubMed PMID: 10655591.
300. Tanoue T, Yamamoto T, Nishida E. Modular structure of a docking surface on MAPK phosphatases. *The Journal of biological chemistry*. 2002;277(25):22942-9. Epub 2002/04/16. doi: 10.1074/jbc.M202096200. PubMed PMID: 11953434.
301. Criqui-Filipe P, Ducret C, Maira SM, Wasyluk B. Net, a negative Ras-switchable TCF, contains a second inhibition domain, the CID, that mediates repression through interactions with CtBP and de-acetylation. *The EMBO journal*. 1999;18(12):3392-403.

Epub 1999/06/16. doi: 10.1093/emboj/18.12.3392. PubMed PMID: 10369679; PubMed Central PMCID: PMCPmc1171419.

302. Johnsson B, Lofas S, Lindquist G. Immobilization of proteins to a carboxymethyl-dextran-modified gold surface for biospecific interaction analysis in surface plasmon resonance sensors. *Analytical biochemistry*. 1991;198(2):268-77. Epub 1991/11/01. PubMed PMID: 1724720.

303. Drescher DG, Ramakrishnan NA, Drescher MJ. Surface plasmon resonance (SPR) analysis of binding interactions of proteins in inner-ear sensory epithelia. *Methods in molecular biology (Clifton, NJ)*. 2009;493:323-43. Epub 2008/10/08. doi: 10.1007/978-1-59745-523-7_20. PubMed PMID: 18839357; PubMed Central PMCID: PMCPmc2864718.

304. Selvakumar D, Drescher MJ, Drescher DG. Cyclic nucleotide-gated channel alpha-3 (CNGA3) interacts with stereocilia tip-link cadherin 23 + exon 68 or alternatively with myosin VIIa, two proteins required for hair cell mechanotransduction. *The Journal of biological chemistry*. 2013;288(10):7215-29. Epub 2013/01/19. doi: 10.1074/jbc.M112.443226. PubMed PMID: 23329832; PubMed Central PMCID: PMCPmc3591630.

305. Evans EL, Saxton J, Shelton SJ, Begitt A, Holliday ND, Hipkind RA, Shaw PE. Dimer formation and conformational flexibility ensure cytoplasmic stability and nuclear accumulation of Elk-1. *Nucleic acids research*. 2011;39(15):6390-402. Epub 2011/05/06. doi: 10.1093/nar/gkr266. PubMed PMID: 21543455; PubMed Central PMCID: PMCPmc3159454.

306. Fantz DA, Jacobs D, Glossip D, Kornfeld K. Docking sites on substrate proteins direct extracellular signal-regulated kinase to phosphorylate specific residues. *The Journal of biological chemistry*. 2001;276(29):27256-65. Epub 2001/05/24. doi: 10.1074/jbc.M102512200. PubMed PMID: 11371562.
307. Sharrocks AD, Yang SH, Galanis A. Docking domains and substrate-specificity determination for MAP kinases. *Trends in biochemical sciences*. 2000;25(9):448-53. Epub 2000/09/06. PubMed PMID: 10973059.
308. Zhang HM, Li L, Papadopoulou N, Hodgson G, Evans E, Galbraith M, Dear M, Vouquier S, Saxton J, Shaw PE. Mitogen-induced recruitment of ERK and MSK to SRE promoter complexes by ternary complex factor Elk-1. *Nucleic Acids Res*. 2008;36(8):2594-607. Epub 2008/03/13. doi: 10.1093/nar/gkn099. PubMed PMID: 18334532; PubMed Central PMCID: PMCPmc2377423.
309. Massie CE, Adryan B, Barbosa-Morais NL, Lynch AG, Tran MG, Neal DE, Mills IG. New androgen receptor genomic targets show an interaction with the ETS1 transcription factor. *EMBO reports*. 2007;8(9):871-8. Epub 2007/08/28. doi: 10.1038/sj.embor.7401046. PubMed PMID: 17721441; PubMed Central PMCID: PMCPmc1950328.
310. Shin S, Kim TD, Jin F, van Deursen JM, Dehm SM, Tindall DJ, Grande JP, Munz JM, Vasmatazis G, Janknecht R. Induction of prostatic intraepithelial neoplasia and modulation of androgen receptor by ETS variant 1/ETS-related protein 81. *Cancer research*. 2009;69(20):8102-10. Epub 2009/10/01. doi: 10.1158/0008-5472.can-09-0941. PubMed PMID: 19789348; PubMed Central PMCID: PMCPmc3947560.

311. Migliaccio A, Castoria G, Di Domenico M, de Falco A, Bilancio A, Lombardi M, Barone MV, Ametrano D, Zannini MS, Abbondanza C, Auricchio F. Steroid-induced androgen receptor-oestradiol receptor beta-*Src* complex triggers prostate cancer cell proliferation. *The EMBO journal*. 2000;19(20):5406-17. Epub 2000/10/18. doi: 10.1093/emboj/19.20.5406. PubMed PMID: 11032808; PubMed Central PMCID: PMC314017.
312. Unni E, Sun S, Nan B, McPhaul MJ, Cheskis B, Mancini MA, Marcelli M. Changes in androgen receptor nongenotropic signaling correlate with transition of LNCaP cells to androgen independence. *Cancer research*. 2004;64(19):7156-68. Epub 2004/10/07. doi: 10.1158/0008-5472.can-04-1121. PubMed PMID: 15466214.
313. Boonyaratanakornkit V, Scott MP, Ribon V, Sherman L, Anderson SM, Maller JL, Miller WT, Edwards DP. Progesterone receptor contains a proline-rich motif that directly interacts with SH3 domains and activates c-*Src* family tyrosine kinases. *Molecular cell*. 2001;8(2):269-80. Epub 2001/09/08. PubMed PMID: 11545730.
314. Barletta F, Wong CW, McNally C, Komm BS, Katzenellenbogen B, Cheskis BJ. Characterization of the interactions of estrogen receptor and MNAR in the activation of c-*Src*. *Molecular endocrinology*. 2004;18(5):1096-108. Epub 2004/02/14. doi: 10.1210/me.2003-0335. PubMed PMID: 14963108.
315. Liao RS, Ma S, Miao L, Li R, Yin Y, Raj GV. Androgen receptor-mediated non-genomic regulation of prostate cancer cell proliferation. *Translational andrology and urology*. 2013;2(3):187-96. Epub 2013/09/01. doi: 10.3978/j.issn.2223-4683.2013.09.07. PubMed PMID: 26816736; PubMed Central PMCID: PMC3140176.

316. Peterziel H, Mink S, Schonert A, Becker M, Klocker H, Cato AC. Rapid signalling by androgen receptor in prostate cancer cells. *Oncogene*. 1999;18(46):6322-9. Epub 1999/12/22. doi: 10.1038/sj.onc.1203032. PubMed PMID: 10597231.
317. Yin L, Hu Q. CYP17 inhibitors--abiraterone, C17,20-lyase inhibitors and multi-targeting agents. *Nature reviews Urology*. 2014;11(1):32-42. Epub 2013/11/28. doi: 10.1038/nrurol.2013.274. PubMed PMID: 24276076.
318. Cai C, Chen S, Ng P, Bubley GJ, Nelson PS, Mostaghel EA, Marck B, Matsumoto AM, Simon NI, Wang H, Chen S, Balk SP. Intratumoral de novo steroid synthesis activates androgen receptor in castration-resistant prostate cancer and is upregulated by treatment with CYP17A1 inhibitors. *Cancer research*. 2011;71(20):6503-13. Epub 2011/08/27. doi: 10.1158/0008-5472.can-11-0532. PubMed PMID: 21868758; PubMed Central PMCID: PMC3209585.
319. Guo Z, Yang X, Sun F, Jiang R, Linn DE, Chen H, Chen H, Kong X, Melamed J, Tepper CG, Kung HJ, Brodie AM, Edwards J, Qiu Y. A novel androgen receptor splice variant is up-regulated during prostate cancer progression and promotes androgen depletion-resistant growth. *Cancer research*. 2009;69(6):2305-13. Epub 2009/02/27. doi: 10.1158/0008-5472.can-08-3795. PubMed PMID: 19244107; PubMed Central PMCID: PMC2672822.
320. Li Y, Hwang TH, Oseth LA, Hauge A, Vessella RL, Schmechel SC, Hirsch B, Beckman KB, Silverstein KA, Dehm SM. AR intragenic deletions linked to androgen receptor splice variant expression and activity in models of prostate cancer progression. *Oncogene*. 2012;31(45):4759-67. Epub 2012/01/24. doi: 10.1038/onc.2011.637. PubMed PMID: 22266865; PubMed Central PMCID: PMC3337879.

321. Tran C, Ouk S, Clegg NJ, Chen Y, Watson PA, Arora V, Wongvipat J, Smith-Jones PM, Yoo D, Kwon A, Wasielewska T, Welsbie D, Chen CD, Higano CS, Beer TM, Hung DT, Scher HI, Jung ME, Sawyers CL. Development of a second-generation antiandrogen for treatment of advanced prostate cancer. *Science*. 2009;324(5928):787-90. Epub 2009/04/11. doi: 10.1126/science.1168175
1168175 [pii]. PubMed PMID: 19359544; PubMed Central PMCID: PMC2981508.
322. Evans CP, Lara PN, Jr. Prostate cancer: Predicting response to androgen receptor signalling inhibition. *Nature reviews Urology*. 2014;11(8):433-5. Epub 2014/07/23. doi: 10.1038/nrurol.2014.179. PubMed PMID: 25048863.
323. Antonarakis ES, Lu C, Wang H, Luber B, Nakazawa M, Roeser JC, Chen Y, Mohammad TA, Chen Y, Fedor HL, Lotan TL, Zheng Q, De Marzo AM, Isaacs JT, Isaacs WB, Nadal R, Paller CJ, Denmeade SR, Carducci MA, Eisenberger MA, Luo J. AR-V7 and resistance to enzalutamide and abiraterone in prostate cancer. *N Engl J Med*. 2014;371(11):1028-38. Epub 2014/09/04. doi: 10.1056/NEJMoa1315815. PubMed PMID: 25184630; PubMed Central PMCID: PMCPmc4201502.
324. Nakazawa M, Antonarakis ES, Luo J. Androgen receptor splice variants in the era of enzalutamide and abiraterone. *Hormones & cancer*. 2014;5(5):265-73. Epub 2014/07/23. doi: 10.1007/s12672-014-0190-1. PubMed PMID: 25048254; PubMed Central PMCID: PMC4167475.
325. Sprenger CC, Plymate SR. The link between androgen receptor splice variants and castration-resistant prostate cancer. *Hormones & cancer*. 2014;5(4):207-17. Epub 2014/05/07. doi: 10.1007/s12672-014-0177-y. PubMed PMID: 24798453.

326. Sadar MD. Advances in small molecule inhibitors of androgen receptor for the treatment of advanced prostate cancer. *World J Urol.* 2012;30(3):311-8. Epub 2011/08/13. doi: 10.1007/s00345-011-0745-5. PubMed PMID: 21833557.
327. Sadar MD. Small molecule inhibitors targeting the "achilles' heel" of androgen receptor activity. *Cancer research.* 2011;71(4):1208-13. Epub 2011/02/03. doi: 10.1158/0008-5472.CAN_10-3398
0008-5472.CAN_10-3398 [pii]. PubMed PMID: 21285252; PubMed Central PMCID: PMC3132148.
328. Larsson R, Mongan NP, Johansson M, Shcherbina L, Abrahamsson PA, Gudas LJ, Sterner O, Persson JL. Clinical trial update and novel therapeutic approaches for metastatic prostate cancer. *Curr Med Chem.* 2011;18(29):4440-53. Epub 2011/08/26. doi: BSP/CMC/E-Pub/2011/ 347 [pii]. PubMed PMID: 21864277.
329. Hayward SW, Cunha GR. The prostate: development and physiology. *Radiologic clinics of North America.* 2000;38(1):1-14. Epub 2000/02/09. PubMed PMID: 10664663.
330. Gao Y, Li X, Guo L-H. Development of a label-free competitive ligand binding assay with human serum albumin on a molecularly engineered surface plasmon resonance sensor chip. *Analytical Methods.* 2012;4(11):3718-23.
331. Bahloul A, Michel V, Hardelin JP, Nouaille S, Hoos S, Houdusse A, England P, Petit C. Cadherin-23, myosin VIIa and harmonin, encoded by Usher syndrome type I genes, form a ternary complex and interact with membrane phospholipids. *Human molecular genetics.* 2010;19(18):3557-65. Epub 2010/07/20. doi: 10.1093/hmg/ddq271. PubMed PMID: 20639393; PubMed Central PMCID: PMCPmc2928128.

332. Salazar MD, Ratnam M, Patki M, Kisovic I, Trumbly R, Iman M, Ratnam M. During hormone depletion or tamoxifen treatment of breast cancer cells the estrogen receptor apoprotein supports cell cycling through the retinoic acid receptor alpha1 apoprotein. *Breast cancer research : BCR*. 2011;13(1):R18. Epub 2011/02/09. doi: 10.1186/bcr2827. PubMed PMID: 21299862; PubMed Central PMCID: PMCPmc3109587.
333. Gao S, Hu M. Bioavailability challenges associated with development of anti-cancer phenolics. *Mini reviews in medicinal chemistry*. 2010;10(6):550-67. Epub 2010/04/08. PubMed PMID: 20370701; PubMed Central PMCID: PMCPmc2919492.
334. Ramešová Š, Sokolová R, Tarábek J, Degano I. The oxidation of luteolin, the natural flavonoid dye. *Electrochimica Acta*. 2013;110:646-54.
335. Nabavi SF, Braidy N, Gortzi O, Sobarzo-Sanchez E, Daglia M, Skalicka-Woźniak K, Nabavi SM. Luteolin as an anti-inflammatory and neuroprotective agent: a brief review. *Brain research bulletin*. 2015;119:1-11.
336. Ravishankar D, Watson KA, Boateng SY, Green RJ, Greco F, Osborn HM. Exploring quercetin and luteolin derivatives as antiangiogenic agents. *European journal of medicinal chemistry*. 2015;97:259-74.
337. Crona DJ, Milowsky MI, Whang YE. Androgen receptor targeting drugs in castration-resistant prostate cancer and mechanisms of resistance. *Clinical pharmacology and therapeutics*. 2015;98(6):582-9. Epub 2015/09/04. doi: 10.1002/cpt.256. PubMed PMID: 26331358; PubMed Central PMCID: PMCPmc4715745.

338. McEwan IJ. Intrinsic disorder in the androgen receptor: identification, characterisation and drugability. *Molecular bioSystems*. 2012;8(1):82-90. Epub 2011/08/09. doi: 10.1039/c1mb05249g. PubMed PMID: 21822504.
339. Chang CI, Xu BE, Akella R, Cobb MH, Goldsmith EJ. Crystal structures of MAP kinase p38 complexed to the docking sites on its nuclear substrate MEF2A and activator MKK3b. *Molecular cell*. 2002;9(6):1241-9. Epub 2002/06/28. PubMed PMID: 12086621.
340. Lee T, Hoofnagle AN, Kabuyama Y, Stroud J, Min X, Goldsmith EJ, Chen L, Resing KA, Ahn NG. Docking motif interactions in MAP kinases revealed by hydrogen exchange mass spectrometry. *Molecular cell*. 2004;14(1):43-55. Epub 2004/04/08. PubMed PMID: 15068802.
341. Rice-Evans CA, Packer L. *Flavonoids in health and disease*: CRC Press; 2003.
342. GeneCards. Histone Cluster 1 H4 Family Member D 1996-2017 [cited 2017 May 5]. Available from: <http://www.genecards.org/cgi-bin/carddisp.pl?gene=HIST1H4D>.
343. GeneCards. H2A Histone Family Member X 1996-2017 [cited 2017 May 5]. Available from: <http://www.genecards.org/cgi-bin/carddisp.pl?gene=H2AFX>.
344. Siegel RL, Miller KD, Jemal A. Cancer statistics, 2015. *CA: a cancer journal for clinicians*. 2015;65(1):5-29. doi: 10.3322/caac.21254. PubMed PMID: 25559415.
345. Karantanos T, Evans CP, Tombal B, Thompson TC, Montironi R, Isaacs WB. Understanding the mechanisms of androgen deprivation resistance in prostate cancer at the molecular level. *European urology*. 2015;67(3):470-9. doi: 10.1016/j.eururo.2014.09.049. PubMed PMID: 25306226.

346. Mitsiades N. A road map to comprehensive androgen receptor axis targeting for castration-resistant prostate cancer. *Cancer research*. 2013;73(15):4599-605. doi: 10.1158/0008-5472.CAN-12-4414. PubMed PMID: 23887973.
347. Joseph JD, Lu N, Qian J, Sensintaffar J, Shao G, Brigham D, Moon M, Maneval EC, Chen I, Darimont B, Hager JH. A clinically relevant androgen receptor mutation confers resistance to second-generation antiandrogens enzalutamide and ARN-509. *Cancer discovery*. 2013;3(9):1020-9. doi: 10.1158/2159-8290.CD-13-0226. PubMed PMID: 23779130.
348. Korpai M, Korn JM, Gao X, Rakiec DP, Ruddy DA, Doshi S, Yuan J, Kovats SG, Kim S, Cooke VG, Monahan JE, Stegmeier F, Roberts TM, Sellers WR, Zhou W, Zhu P. An F876L mutation in androgen receptor confers genetic and phenotypic resistance to MDV3100 (enzalutamide). *Cancer discovery*. 2013;3(9):1030-43. doi: 10.1158/2159-8290.CD-13-0142. PubMed PMID: 23842682.
349. Liu C, Zhang Z, Tang H, Jiang Z, You L, Liao Y. Crosstalk between IGF-1R and other tumor promoting pathways. *Current pharmaceutical design*. 2014;20(17):2912-21. Epub 2013/08/16. PubMed PMID: 23944361.
350. Nakamura Y, Suzuki T, Nakabayashi M, Endoh M, Sakamoto K, Mikami Y, Moriya T, Ito A, Takahashi S, Yamada S, Arai Y, Sasano H. In situ androgen producing enzymes in human prostate cancer. *Endocrine-related cancer*. 2005;12(1):101-7. Epub 2005/03/25. doi: 10.1677/erc.1.00914. PubMed PMID: 15788642.
351. Scher HI, Fizazi K, Saad F, Taplin ME, Sternberg CN, Miller K, de Wit R, Mulders P, Chi KN, Shore ND, Armstrong AJ, Flaig TW, Flechon A, Mainwaring P, Fleming M, Hainsworth JD, Hirmand M, Selby B, Seely L, de Bono JS, Investigators A. Increased

survival with enzalutamide in prostate cancer after chemotherapy. *The New England journal of medicine*. 2012;367(13):1187-97. doi: 10.1056/NEJMoa1207506. PubMed PMID: 22894553.

352. Beer TM, Armstrong AJ, Rathkopf DE, Loriot Y, Sternberg CN, Higano CS, Iversen P, Bhattacharya S, Carles J, Chowdhury S, Davis ID, de Bono JS, Evans CP, Fizazi K, Joshua AM, Kim CS, Kimura G, Mainwaring P, Mansbach H, Miller K, Noonberg SB, Perabo F, Phung D, Saad F, Scher HI, Taplin ME, Venner PM, Tombal B, Investigators P. Enzalutamide in metastatic prostate cancer before chemotherapy. *The New England journal of medicine*. 2014;371(5):424-33. doi: 10.1056/NEJMoa1405095. PubMed PMID: 24881730; PubMed Central PMCID: PMC4418931.

353. Bhat R, Tummalapalli SR, Rotella DP. Progress in the discovery and development of heat shock protein 90 (Hsp90) inhibitors. *Journal of medicinal chemistry*. 2014;57(21):8718-28. doi: 10.1021/jm500823a. PubMed PMID: 25141341.

354. Neckers L, Workman P. Hsp90 molecular chaperone inhibitors: are we there yet? *Clinical cancer research : an official journal of the American Association for Cancer Research*. 2012;18(1):64-76. doi: 10.1158/1078-0432.CCR-11-1000. PubMed PMID: 22215907; PubMed Central PMCID: PMC3252205.

355. Veldscholte J, Berrevoets CA, Zegers ND, van der Kwast TH, Grootegoed JA, Mulder E. Hormone-induced dissociation of the androgen receptor-heat-shock protein complex: use of a new monoclonal antibody to distinguish transformed from nontransformed receptors. *Biochemistry*. 1992;31(32):7422-30. PubMed PMID: 1510931.

356. Fang Y, Fliss AE, Robins DM, Caplan AJ. Hsp90 regulates androgen receptor hormone binding affinity in vivo. *The Journal of biological chemistry*. 1996;271(45):28697-702. PubMed PMID: 8910505.
357. He S, Zhang C, Shafi AA, Sequeira M, Acquaviva J, Friedland JC, Sang J, Smith DL, Weigel NL, Wada Y, Proia DA. Potent activity of the Hsp90 inhibitor ganetespib in prostate cancer cells irrespective of androgen receptor status or variant receptor expression. *International journal of oncology*. 2013;42(1):35-43. doi: 10.3892/ijo.2012.1698. PubMed PMID: 23152004; PubMed Central PMCID: PMC3583620.
358. Liu W, Vielhauer GA, Holzbeierlein JM, Zhao H, Ghosh S, Brown D, Lee E, Blagg BS. KU675, a Concomitant Heat-Shock Protein Inhibitor of Hsp90 and Hsc70 that Manifests Isoform Selectivity for Hsp90alpha in Prostate Cancer Cells. *Molecular pharmacology*. 2015;88(1):121-30. doi: 10.1124/mol.114.097303. PubMed PMID: 25939977; PubMed Central PMCID: PMC4468638.
359. Saporita AJ, Ai J, Wang Z. The Hsp90 inhibitor, 17-AAG, prevents the ligand-independent nuclear localization of androgen receptor in refractory prostate cancer cells. *The Prostate*. 2007;67(5):509-20. doi: 10.1002/pros.20541. PubMed PMID: 17221841; PubMed Central PMCID: PMC2810394.
360. Solit DB, Zheng FF, Drobnjak M, Munster PN, Higgins B, Verbel D, Heller G, Tong W, Cordon-Cardo C, Agus DB, Scher HI, Rosen N. 17-Allylamino-17-demethoxygeldanamycin induces the degradation of androgen receptor and HER-2/neu and inhibits the growth of prostate cancer xenografts. *Clinical cancer research : an*

official journal of the American Association for Cancer Research. 2002;8(5):986-93.
PubMed PMID: 12006510.

361. Heath EI, Hillman DW, Vaishampayan U, Sheng S, Sarkar F, Harper F, Gaskins M, Pitot HC, Tan W, Ivy SP, Pili R, Carducci MA, Erlichman C, Liu G. A phase II trial of 17-allylamino-17-demethoxygeldanamycin in patients with hormone-refractory metastatic prostate cancer. *Clinical cancer research : an official journal of the American Association for Cancer Research*. 2008;14(23):7940-6. doi: 10.1158/1078-0432.CCR-08-0221. PubMed PMID: 19047126; PubMed Central PMCID: PMC3085545.

362. Oh WK, Galsky MD, Stadler WM, Srinivas S, Chu F, Bublely G, Goddard J, Dunbar J, Ross RW. Multicenter phase II trial of the heat shock protein 90 inhibitor, retaspimycin hydrochloride (IPI-504), in patients with castration-resistant prostate cancer. *Urology*. 2011;78(3):626-30. doi: 10.1016/j.urology.2011.04.041. PubMed PMID: 21762967; PubMed Central PMCID: PMC3166448.

363. Pacey S, Wilson RH, Walton M, Eatock MM, Hardcastle A, Zetterlund A, Arkenau HT, Moreno-Farre J, Banerji U, Roels B, Peachey H, Aherne W, de Bono JS, Raynaud F, Workman P, Judson I. A phase I study of the heat shock protein 90 inhibitor alvespimycin (17-DMAG) given intravenously to patients with advanced solid tumors. *Clinical cancer research : an official journal of the American Association for Cancer Research*. 2011;17(6):1561-70. doi: 10.1158/1078-0432.CCR-10-1927. PubMed PMID: 21278242; PubMed Central PMCID: PMC3060938.

364. Thakur MK, Heilbrun LK, Sheng S, Stein M, Liu G, Antonarakis ES, Vaishampayan U, Dzinic SH, Li X, Freeman S, Smith D, Heath EI. A phase II trial of ganetespib, a heat shock protein 90 Hsp90) inhibitor, in patients with docetaxel-

pretreated metastatic castrate-resistant prostate cancer (CRPC)-a prostate cancer clinical trials consortium (PCCTC) study. *Investigational new drugs*. 2015. Epub 2015/11/20. doi: 10.1007/s10637-015-0307-6. PubMed PMID: 26581400.

365. Kramer OH, Mahboobi S, Sellmer A. Drugging the HDAC6-HSP90 interplay in malignant cells. *Trends in pharmacological sciences*. 2014;35(10):501-9. doi: 10.1016/j.tips.2014.08.001. PubMed PMID: 25234862.

366. Bali P, Pranpat M, Bradner J, Balasis M, Fiskus W, Guo F, Rocha K, Kumaraswamy S, Boyapalle S, Atadja P, Seto E, Bhalla K. Inhibition of histone deacetylase 6 acetylates and disrupts the chaperone function of heat shock protein 90: a novel basis for antileukemia activity of histone deacetylase inhibitors. *The Journal of biological chemistry*. 2005;280(29):26729-34. doi: 10.1074/jbc.C500186200. PubMed PMID: 15937340.

367. Kovacs JJ, Murphy PJ, Gaillard S, Zhao X, Wu JT, Nicchitta CV, Yoshida M, Toft DO, Pratt WB, Yao TP. HDAC6 regulates Hsp90 acetylation and chaperone-dependent activation of glucocorticoid receptor. *Molecular cell*. 2005;18(5):601-7. doi: 10.1016/j.molcel.2005.04.021. PubMed PMID: 15916966.

368. Chen L, Meng S, Wang H, Bali P, Bai W, Li B, Atadja P, Bhalla KN, Wu J. Chemical ablation of androgen receptor in prostate cancer cells by the histone deacetylase inhibitor LAQ824. *Molecular cancer therapeutics*. 2005;4(9):1311-9. doi: 10.1158/1535-7163.MCT-04-0287. PubMed PMID: 16170022.

369. Gravina GL, Marampon F, Muzi P, Mancini A, Piccolella M, Negri-Cesi P, Motta M, Lenzi A, Di Cesare E, Tombolini V, Jannini EA, Festuccia C. PDX101 potentiates hormonal therapy and prevents the onset of castration-resistant phenotype modulating

androgen receptor, HSP90, and CRM1 in preclinical models of prostate cancer. *Endocrine-related cancer*. 2013;20(3):321-37. doi: 10.1530/ERC-12-0240. PubMed PMID: 23507703.

370. Sato A, Asano T, Ito K, Asano T. Vorinostat and bortezomib synergistically cause ubiquitinated protein accumulation in prostate cancer cells. *The Journal of urology*. 2012;188(6):2410-8. Epub 2012/10/24. doi: 10.1016/j.juro.2012.07.108. PubMed PMID: 23088964.

371. Marrocco DL, Tilley WD, Bianco-Miotto T, Evdokiou A, Scher HI, Rifkind RA, Marks PA, Richon VM, Butler LM. Suberoylanilide hydroxamic acid (vorinostat) represses androgen receptor expression and acts synergistically with an androgen receptor antagonist to inhibit prostate cancer cell proliferation. *Molecular cancer therapeutics*. 2007;6(1):51-60. Epub 2007/01/16. doi: 10.1158/1535-7163.mct-06-0144. PubMed PMID: 17218635.

372. Gibbs A, Schwartzman J, Deng V, Alumkal J. Sulforaphane destabilizes the androgen receptor in prostate cancer cells by inactivating histone deacetylase 6. *Proceedings of the National Academy of Sciences of the United States of America*. 2009;106(39):16663-8. doi: 10.1073/pnas.0908908106. PubMed PMID: 19805354; PubMed Central PMCID: PMC2757849.

373. Basak S, Pookot D, Noonan EJ, Dahiya R. Genistein down-regulates androgen receptor by modulating HDAC6-Hsp90 chaperone function. *Molecular cancer therapeutics*. 2008;7(10):3195-202. doi: 10.1158/1535-7163.MCT-08-0617. PubMed PMID: 18852123.

374. Welsbie DS, Xu J, Chen Y, Borsu L, Scher HI, Rosen N, Sawyers CL. Histone deacetylases are required for androgen receptor function in hormone-sensitive and castrate-resistant prostate cancer. *Cancer research*. 2009;69(3):958-66. doi: 10.1158/0008-5472.CAN-08-2216. PubMed PMID: 19176386; PubMed Central PMCID: PMC3219545.
375. Burdelski C, Ruge OM, Melling N, Koop C, Simon R, Steurer S, Sauter G, Kluth M, Hube-Magg C, Minner S, Wittmer C, Wilczak W, Hinsch A, Lebok P, Izbicki JR, Heinzer H, Graefen M, Huland H, Schlomm T, Krech T. HDAC1 overexpression independently predicts biochemical recurrence and is associated with rapid tumor cell proliferation and genomic instability in prostate cancer. *Experimental and molecular pathology*. 2015;98(3):419-26. doi: 10.1016/j.yexmp.2015.03.024. PubMed PMID: 25794974.
376. Weichert W, Roske A, Gekeler V, Beckers T, Stephan C, Jung K, Fritzsche FR, Niesporek S, Denkert C, Dietel M, Kristiansen G. Histone deacetylases 1, 2 and 3 are highly expressed in prostate cancer and HDAC2 expression is associated with shorter PSA relapse time after radical prostatectomy. *British journal of cancer*. 2008;98(3):604-10. doi: 10.1038/sj.bjc.6604199. PubMed PMID: 18212746; PubMed Central PMCID: PMC2243142.
377. Bradley D, Rathkopf D, Dunn R, Stadler WM, Liu G, Smith DC, Pili R, Zwiebel J, Scher H, Hussain M. Vorinostat in advanced prostate cancer patients progressing on prior chemotherapy (National Cancer Institute Trial 6862): trial results and interleukin-6 analysis: a study by the Department of Defense Prostate Cancer Clinical Trial Consortium and University of Chicago Phase 2 Consortium. *Cancer*.

2009;115(23):5541-9. doi: 10.1002/cncr.24597. PubMed PMID: 19711464; PubMed Central PMCID: PMC2917101.

378. Molife LR, Attard G, Fong PC, Karavasilis V, Reid AH, Patterson S, Riggs CE, Jr., Higano C, Stadler WM, McCulloch W, Dearnaley D, Parker C, de Bono JS. Phase II, two-stage, single-arm trial of the histone deacetylase inhibitor (HDACi) romidepsin in metastatic castration-resistant prostate cancer (CRPC). *Annals of oncology : official journal of the European Society for Medical Oncology / ESMO*. 2010;21(1):109-13. doi: 10.1093/annonc/mdp270. PubMed PMID: 19608618.

379. Rathkopf DE, Picus J, Hussain A, Ellard S, Chi KN, Nydam T, Allen-Freda E, Mishra KK, Porro MG, Scher HI, Wilding G. A phase 2 study of intravenous panobinostat in patients with castration-resistant prostate cancer. *Cancer chemotherapy and pharmacology*. 2013;72(3):537-44. doi: 10.1007/s00280-013-2224-8. PubMed PMID: 23820963; PubMed Central PMCID: PMC3970811.

380. Eigel BJ, North S, Winkquist E, Finch D, Wood L, Sridhar SS, Powers J, Good J, Sharma M, Squire JA, Bazov J, Jamaspishvili T, Cox ME, Bradbury PA, Eisenhauer EA, Chi KN. A phase II study of the HDAC inhibitor SB939 in patients with castration resistant prostate cancer: NCIC clinical trials group study IND195. *Investigational new drugs*. 2015;33(4):969-76. doi: 10.1007/s10637-015-0252-4. PubMed PMID: 25983041.

381. Kong D, Ahmad A, Bao B, Li Y, Banerjee S, Sarkar FH. Histone deacetylase inhibitors induce epithelial-to-mesenchymal transition in prostate cancer cells. *PloS one*. 2012;7(9):e45045. doi: 10.1371/journal.pone.0045045. PubMed PMID: 23024790; PubMed Central PMCID: PMC3443231.

382. Uchida H, Maruyama T, Nishikawa-Uchida S, Oda H, Miyazaki K, Yamasaki A, Yoshimura Y. Studies using an in vitro model show evidence of involvement of epithelial-mesenchymal transition of human endometrial epithelial cells in human embryo implantation. *The Journal of biological chemistry*. 2012;287(7):4441-50. doi: 10.1074/jbc.M111.286138. PubMed PMID: 22174415; PubMed Central PMCID: PMC3281640.
383. Jiang GM, Wang HS, Zhang F, Zhang KS, Liu ZC, Fang R, Wang H, Cai SH, Du J. Histone deacetylase inhibitor induction of epithelial-mesenchymal transitions via up-regulation of Snail facilitates cancer progression. *Biochimica et biophysica acta*. 2013;1833(3):663-71. doi: 10.1016/j.bbamcr.2012.12.002. PubMed PMID: 23246564.
384. Tam WL, Weinberg RA. The epigenetics of epithelial-mesenchymal plasticity in cancer. *Nature medicine*. 2013;19(11):1438-49. doi: 10.1038/nm.3336. PubMed PMID: 24202396; PubMed Central PMCID: PMC4190672.
385. Rosati R, Chen B, Patki M, McFall T, Ou S, Heath E, Ratnam M, Qin Z. Hybrid Enzalutamide Derivatives with Histone Deacetylase Inhibitor Activity Decrease Heat Shock Protein 90 and Androgen Receptor Levels and Inhibit Viability in Enzalutamide-Resistant C4-2 Prostate Cancer Cells. *Molecular pharmacology*. 2016;90(3):225-37. Epub 2016/07/07. doi: 10.1124/mol.116.103416. PubMed PMID: 27382012; PubMed Central PMCID: PMCPmc4998664.
386. Patki M, Gadgeel S, Huang Y, McFall T, Shields AF, Matherly LH, Bepler G, Ratnam M. Glucocorticoid receptor status is a principal determinant of variability in the sensitivity of non-small-cell lung cancer cells to pemetrexed. *Journal of thoracic oncology : official publication of the International Association for the Study of Lung*

Cancer. 2014;9(4):519-26. Epub 2014/04/17. doi: 10.1097/jto.0000000000000111. PubMed PMID: 24736075; PubMed Central PMCID: PMC4075060.

387. Patki M, Salazar M, Trumbly R, Ratnam M. Differential effects of estrogen-dependent transactivation vs. transrepression by the estrogen receptor on invasiveness of HER2 overexpressing breast cancer cells. Biochemical and biophysical research communications. 2015;457(3):404-11. Epub 2015/01/15. doi: 10.1016/j.bbrc.2015.01.004. PubMed PMID: 25582774; PubMed Central PMCID: PMC4334377.

388. McFall T, Patki M, Rosati R, Ratnam M. Role of the short isoform of the progesterone receptor in breast cancer cell invasiveness at estrogen and progesterone levels in the pre- and post-menopausal ranges. Oncotarget. 2015;6(32):33146-64. Epub 2015/09/12. doi: 10.18632/oncotarget.5082. PubMed PMID: 26356672.

389. Balbas MD, Evans MJ, Hosfield DJ, Wongvipat J, Arora VK, Watson PA, Chen Y, Greene GL, Shen Y, Sawyers CL. Overcoming mutation-based resistance to antiandrogens with rational drug design. eLife. 2013;2:e00499. doi: 10.7554/eLife.00499. PubMed PMID: 23580326; PubMed Central PMCID: PMC3622181.

390. Cacchi S, Fabrizi G, Goggiamani A. Palladium-catalyzed hydroxycarbonylation of aryl and vinyl halides or triflates by acetic anhydride and formate anions. Organic letters. 2003;5(23):4269-72. doi: 10.1021/ol0354371. PubMed PMID: 14601977.

391. Zhou X, Yang XY, Popescu NC. Preclinical evaluation of combined antineoplastic effect of DLC1 tumor suppressor protein and suberoylanilide hydroxamic acid on prostate cancer cells. Biochemical and biophysical research communications.

2012;420(2):325-30. doi: 10.1016/j.bbrc.2012.02.158. PubMed PMID: 22425986; PubMed Central PMCID: PMC3322246.

392. Gryder BE, Akbashev MJ, Rood MK, Raftery ED, Meyers WM, Dillard P, Khan S, Oyelere AK. Selectively targeting prostate cancer with antiandrogen equipped histone deacetylase inhibitors. *ACS chemical biology*. 2013;8(11):2550-60. doi: 10.1021/cb400542w. PubMed PMID: 24004176; PubMed Central PMCID: PMC3836611.

393. Guerrero J, Alfaro IE, Gomez F, Protter AA, Bernales S. Enzalutamide, an androgen receptor signaling inhibitor, induces tumor regression in a mouse model of castration-resistant prostate cancer. *The Prostate*. 2013;73(12):1291-305. doi: 10.1002/pros.22674. PubMed PMID: 23765603.

394. Park S, Park JA, Kim YE, Song S, Kwon HJ, Lee Y. Suberoylanilide hydroxamic acid induces ROS-mediated cleavage of HSP90 in leukemia cells. *Cell stress & chaperones*. 2015;20(1):149-57. Epub 2014/08/15. doi: 10.1007/s12192-014-0533-4. PubMed PMID: 25119188; PubMed Central PMCID: PMC4255254.

395. Feldman BJ, Feldman D. The development of androgen-independent prostate cancer. *Nature Reviews Cancer*. 2001;1(1):34-45.

396. Yuan X, Balk SP, editors. Mechanisms mediating androgen receptor reactivation after castration. *Urologic Oncology: Seminars and Original Investigations*; 2009: Elsevier.

397. Zhou X, Yang XY, Popescu NC. Synergistic antineoplastic effect of DLC1 tumor suppressor protein and histone deacetylase inhibitor, suberoylanilide hydroxamic acid

(SAHA), on prostate and liver cancer cells: perspectives for therapeutics. International journal of oncology. 2010;36(4):999-1005. Epub 2010/03/04. PubMed PMID: 20198346.

398. Guan M, Zhou X, Soultzis N, Spandidos DA, Popescu NC. Aberrant methylation and deacetylation of deleted in liver cancer-1 gene in prostate cancer: potential clinical applications. Clinical cancer research : an official journal of the American Association for Cancer Research. 2006;12(5):1412-9. Epub 2006/03/15. doi: 10.1158/1078-0432.ccr-05-1906. PubMed PMID: 16533763.

399. Gartel AL, Tyner AL. The role of the cyclin-dependent kinase inhibitor p21 in apoptosis. Molecular cancer therapeutics. 2002;1(8):639-49. PubMed PMID: 12479224.

400. Marks PA. The mechanism of the anti-tumor activity of the histone deacetylase inhibitor, suberoylanilide hydroxamic acid (SAHA). Cell cycle. 2004;3(5):534-5. PubMed PMID: 15020838.

401. Gui CY, Ngo L, Xu WS, Richon VM, Marks PA. Histone deacetylase (HDAC) inhibitor activation of p21WAF1 involves changes in promoter-associated proteins, including HDAC1. Proceedings of the National Academy of Sciences of the United States of America. 2004;101(5):1241-6. doi: 10.1073/pnas.0307708100. PubMed PMID: 14734806; PubMed Central PMCID: PMC337037.

402. Lagger G, Doetzlhofer A, Schuettengruber B, Haidweger E, Simboeck E, Tischler J, Chiocca S, Suske G, Rotheneder H, Wintersberger E, Seiser C. The tumor suppressor p53 and histone deacetylase 1 are antagonistic regulators of the cyclin-dependent kinase inhibitor p21/WAF1/CIP1 gene. Molecular and cellular biology. 2003;23(8):2669-79. PubMed PMID: 12665570; PubMed Central PMCID: PMC152549.

403. Bitting RL, Armstrong AJ. Targeting the PI3K/Akt/mTOR pathway in castration-resistant prostate cancer. *Endocrine-related cancer*. 2013;20(3):R83-R99.
404. Toren P, Kim S, Cordonnier T, Crafter C, Davies BR, Fazli L, Gleave ME, Zoubeidi A. Combination AZD5363 with enzalutamide significantly delays enzalutamide-resistant prostate cancer in preclinical models. *European urology*. 2015;67(6):986-90.
405. Montgomery B, Kheoh T, Molina A, Li J, Bellmunt J, Tran N, Loriot Y, Efstathiou E, Ryan CJ, Scher HI. Impact of baseline corticosteroids on survival and steroid androgens in metastatic castration-resistant prostate cancer: exploratory analysis from COU-AA-301. *European urology*. 2015;67(5):866-73.
406. Arora VK, Schenkein E, Murali R, Subudhi SK, Wongvipat J, Balbas MD, Shah N, Cai L, Efstathiou E, Logothetis C. Glucocorticoid receptor confers resistance to antiandrogens by bypassing androgen receptor blockade. *Cell*. 2013;155(6):1309-22.

ABSTRACT**NEW MECHANISM BASED APPROACHES FOR TREATING PROSTATE CANCER**

by

RAYNA C. ROSATI**August 2017****Advisor:** Dr. Manohar Ratnam**Major:** Cancer Biology**Degree:** Doctor of Philosophy

Prostate cancer (PC) is generally dependent on the androgen signaling axis for tumor growth. PC is managed by androgen deprivation therapy (ADT). The tumors then frequently progress by restoring ADT-resistant AR signaling through mechanisms such as intratumoral androgen synthesis, overexpression of AR, expression of splice variants of AR and alteration in the balance of AR co-regulators. This stage of progression is termed castrate recurrent prostate cancer (CRPC). Moreover, ADT has many major undesirable acute and chronic side effects on various normal tissues. Therefore a more strategic therapy approach is one that would disrupt a functional arm of AR signaling critical for PC/CRPC growth but not for the essential physiological roles of AR in normal adult tissues. This thesis describes two different mechanism-based approaches to develop small molecule drugs that address the above problems.

The transcription factor ELK1 tethers the androgen receptor (AR) to chromatin, enabling sustained activation of genes critical for growth in prostate cancer cell lines. The N-terminal A/B domain of AR [AR(A/B)], which excludes the ligand binding pocket of AR, is adequate for interaction with ELK1. This is significant because the major splice variants of AR (AR-V7) that lack the ligand binding domain, as well as overexpressed

full length AR, are known to strongly support growth of castration resistant prostate cancer (CRPC). In our first approach to develop small molecule drugs for prostate cancer, we showed that both wtAR and AR-V7 synergize with ELK1 by coopting the two ERK docking sites on ELK1, independent of the classical mechanism of (transient) activation of ELK1 via phosphorylation by ERK. As the association of ELK1 and AR is only required for prostate tumor growth, disrupting this interaction should selectively inhibit the growth of CRPC cells without interfering with the physiological role of androgen in normal tissues. Therefore, small molecules that disrupt binding of AR to ELK1 should inhibit the growth of a broader spectrum of advanced prostate tumors than androgen ablation or conventional anti-androgen therapies without the many acute and chronic side effects associated with those treatments. We have developed and conducted a stringent *in situ* high throughput screen for small molecules that selectively disrupt the ELK1-AR synergy. We initially screened over 18,000 compounds from diversity sets that follow the Lipinski guidelines for “drug-likeness”. Our top hit from the screen inhibited ELK1-dependent promoter activation by androgen in a dose-dependent manner but did not inhibit promoter activation via canonical androgen response elements. Follow up structure-activity studies identified a lead compound that was much more stable than the initial hit. We report discovery of this small molecule (KCI807) that selectively disrupts ELK1-dependent promoter activation by wild-type and variant forms of AR without interfering with ELK1 activation by ERK. KCI807 has an obligatory flavone scaffold and functional hydroxyl groups on C5 and C3'. KCI807 binds to purified AR, blocking ELK1 binding, and selectively blocks recruitment of AR to chromatin by ELK1. KCI807 narrowly affects a subset AR target growth genes and selectively inhibits AR-

dependent growth of PCa cell lines and Enzalutamide-resistant PCa tumor xenografts. The results offer a mechanism-based therapeutic paradigm for disrupting the AR growth signaling axis in the spectrum of prostate tumors while avoiding global attenuation of testosterone actions.

The second approach to developing new small molecule drugs against prostate cancer involved the development of hybrid molecules. Histone deacetylase inhibitors (HDACis) can disrupt androgen signaling through the down regulation of heat shock protein 90 (HSP90). However despite their ineffectiveness in prostate cancer (PCa) cells non-selective toxicities are associated with these molecules. We designed hybrid molecules containing partial scaffolds of the AR targeted drug, enzalutamide, and the HDAC inhibitor, suberoylanilide hydroxamic acid (SAHA), to weaken the intrinsic pan-HDACi activity of the molecule and to selectively target the cytosolic AR-HSP90 complex in AR overexpressing and enzalutamide-resistant PCa cells. These new molecules, 2-75 and 1005, showed reduced potency in intrinsic HDAC inhibitor activity, degraded the HSP90 chaperone protein, induced hyper acetylation of the HDAC6 substrate α tubulin, induced p21, and caused loss of viability of the enz-resistant C4-2 cells all to a greater extent compared to either parent compound alone. These results suggested that these new molecules could be used as prototypes for the development of hybrid HDAC inhibiting drugs with reduced pan HDAC inhibitor activity and increased selectivity for AR overexpressing PC cells.

AUTOBIOGRAPHICAL STATEMENT

EDUCATION

Wayne State University **2012-2017**

Doctor of Philosophy: Cancer Biology

University at Buffalo, State University of New York **2008-2012**

Bachelor of Science in Biology

Concentration: Cellular and Molecular Biology

GRANTS

Rumble Fellowship- Wayne State University **2016-2017**

T-32 Training Grant- National Institute of Health (NIH) **2014-2016**

SELECTED PUBLICATIONS

Rosati R, Patki M, Chari V, Dakshnamurthy S, McFall T, Saxton J, Kidder BL, Shaw PE and Ratnam M. The Amino-terminal Domain of the Androgen Receptor Co-opts ERK Docking Sites in ELK1 to Induce Sustained Gene Activation that Supports Prostate Cancer Cell Growth. The Journal of biological chemistry. 2016. PMID: 27793987

Movassaghian S, Xie Y, Hildebrandt C, **Rosati R**, Li Y, Kim NH, Conti DS, da Rocha SR, Yang ZQ and Merkel OM. Post-Transcriptional Regulation of the GASC1 Oncogene with Active Tumor-Targeted siRNA-Nanoparticles. Molecular pharmaceutics. 2016; 13(8):2605-2621. PMID:27223606

Rosati R, Chen B, Patki M, McFall T, Ou S, Heath E, Ratnam M and Qin Z. Hybrid Enzalutamide Derivatives with Histone Deacetylase Inhibitor Activity Decrease Heat Shock Protein 90 and Androgen Receptor Levels and Inhibit Viability in Enzalutamide-Resistant C4-2 Prostate Cancer Cells. Molecular pharmacology. 2016; 90(3):225-237. PMID:27382012

McFall T, Patki M, **Rosati R** and Ratnam M. Role of the short isoform of the progesterone receptor in breast cancer cell invasiveness at estrogen and progesterone levels in the pre- and post-menopausal ranges. Oncotarget. 2015; 6(32):33146-33164. PMID:26356672

Bullwinkle TJ, Samorodnitsky D, **Rosati RC** and Koudelka GB. Determinants of bacteriophage 933W repressor DNA binding specificity. PloS one. 2012; 7(4):e34563. PMID: 22509323